REPORT NO. FAA-RD-73-27

ARTS III AUGMENTED TRACKING STUDY

UNIVAC
DEFENSE SYSTEMS DIVISION
St. Paul, Minnesota

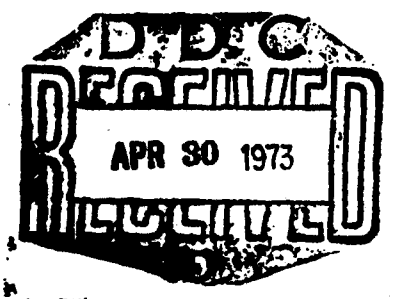

JUNE 1972

FINAL REPORT

DEPARTMENT OF TRANSPORTATION
FEDERAL AVIATION ADMINISTRATION
Systems Research & Development Service
Washington, D.C. 20591

AD-758 886

ARTS-III AUGMENTED TRACKING STUDY

M. Wold, et al

Sperry Rand Corporation

Prepared for:

Federal Aviation Administration

June 1972

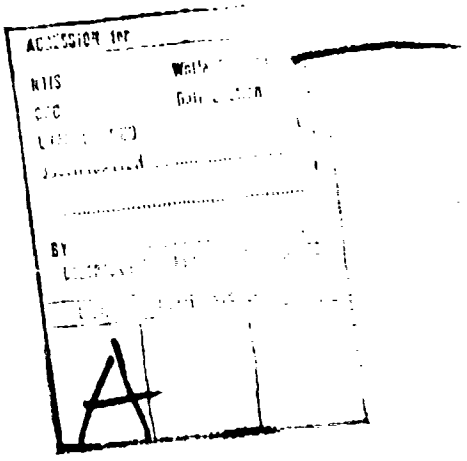

"This report has been prepared by UNIVAC for the Systems Research and Development Service, Federal Aviation Administration, under Contract No. DOT FA70WA-2289. The contents of this report reflect the views of the contractor, who is responsible for the facts and the accuracy of the data presented herein, and do not necessarily reflect the official view or policy of the FAA. This report does not constitute a standard, specification or regulation."

1. DOCUMENT NO.	2. GOVERNMENT ACCESSION NO.	3. RECIPIENT'S CATALOG NO.
FAA-RD-73-27	-	-

4. TITLE AND SUBTITLE	5. REPORT DATE
ARTS-III Augmented Tracking Study	June 1972
	6. PERFORMING ORGANIZATION CODE: -
7. AUTHOR(S) ARCON Corp: B. Smulowicz, R. Sittler UNIVAC: M. Wold, G. Kelly, B. Birkholz, L. Cady	8. PERFORMING ORGANIZATION REPORT NO.: PX 6392
9. PERFORMING ORGANIZATION NAME AND ADDRESS UNIVAC Defense Systems Division St. Paul, Minnesota 55101	10. WORK UNIT NO.: Project No. 19180 11. CONTRACT OR GRANT NO.: DOT FA70WA-2289
12. SPONSORING AGENCY NAME AND ADDRESS Department of Transportation Federal Aviation Administration Systems Research and Development Service Washington, D.C. 20591	13. TYPE OF REPORT AND PERIOD COVERED: Final Report 14. SPONSORING AGENCY CODE
15. SUPPLEMENTARY NOTES -	

16. ABSTRACT

This report is compiled from the results obtained during investigation of methods for improving aircraft tracking techniques within the ARTS-III system. This study recognizes the current tracking level of the Basic Radar Beacon Tracking Level (RBTL) system as the starting point for development. At this level, both radar and beacon target reports from a common sensor site are available for tracking. The work described by this report is an investigation of new methods for utilizing these target reports as well as optimizing and refining existing methods.

In addition to seeking methods for upgrading the tracking function, considerations for improving system performance through integration of the video processing, target detection, and display functions with tracking are also investigated. Numerous alternatives are considered and results of both those which show potential for improvement as well as those which show definite limitations are included. It is anticipated that this may be beneficial for reference in future analysis to discourage rework of areas which have been proved not worthy while stimulating additional development of those with merit.

17. KEY WORDS	18. DISTRIBUTION STATEMENT
ARTS III Aircraft Tracking	- Document is available to the public through the National Technical Information Service, Springfield, Virginia 22151

19. SECURITY CLASSIF. (OF THIS REPORT)	20. SECURITY CLASSIF. (OF THIS PAGE)	21. NO. OF PAGES	22. PRICE
Unclassified	Unclassified	275	

TABLE OF CONTENTS

TABLE OF CONTENTS (continued)

TABLE OF CONTENTS (continued)

LIST OF ILLUSTRATIONS

LIST OF ILLUSTRATIONS (continued)

LIST OF TABLES

SECTION 1
INTRODUCTION

This study is prepared for the Department of Transportation, Federal Aviation Administration, Washington, D. C., in accordance with Contract DOT FA70WA-2289. This document fulfills the requirement for delivery of a final study report as described in section 3.3.2.5.6 of this contract's Statement of Work. The analysis work which is described was performed as a joint effort by Univac and the ARCON Corporation.

1.1 DESCRIPTION AND OBJECTIVES

The study described by this report is an investigation of methods for improving aircraft tracking confidence and accuracy through the use of data available from co-located, synchronously operating radar and beacon systems. This study considers as a baseline the Basic Radar Beacon Tracking Level (RBTL) system which was a first step in expanding the basic ARTS-III Beacon Tracking Level (BTL) system by incorporating a Radar Tracking Level (RTL) add-on package. This initial radar tracking level provided additional tracking capabilities over those realized previously by providing for automatic reporting and tracking of non-beacon equipped aircraft. In addition, for beacon equipped aircraft, it provided reporting backup in the event of beacon failure as well as improved track reliability and tracking accuracy through combined usage of both radar and beacon reports.

The principal objective of the Augmented Tracking Study is that of providing a further improved tracking system through an extensive investigation of the procedures used within tracking. It is felt that the Basic RBTL, because of the "add-on" of radar, is not a completely optimized system, and that by further analysis of the total tracking requirements, significant improvements can be obtained. The objective of this study is not to present a totally defined system for augmented tracking, but rather to provide a detailed analysis of various tracking concepts which will be evaluated and refined in a design effort to follow this present study.

As stated previously, the Basic RBTL is taken as a baseline system and is the starting point for analysis. This provides a level of comparison of new techniques against what is currently available. It will in no way describe the methods to be considered or cause limitations in the development approaches.

In the performance of this study, it was necessary to investigate several tentative tracking system designs in order to evaluate various concepts and data utilization techniques. The analysis was conducted on three distinct levels: conceptual, mathematical, and computer assisted. Strong emphasis was placed on early determination of the suitability of the various techniques to allow the allocation of maximum effort to those which showed most promise.

1.1 (continued)

Among the techniques which received most attention were:

1) Deviation controlled smoothing - a method in which the choice of smoothing constants is influenced by the deviation of the report in the primary bin from the predicted position.

2) Deviation dependent firmness increment - one of several track firmness algorithms investigated.

3) Coast correction - a technique in which the extrapolation of a coasting track is governed by the data pattern encountered on the preceding few scans.

4) Independent choice of tracking parameters in range and in azimuth for each sensor type.

5) Selection of optimum bin sizes for various trajectory and data situations.

6) Bin size determined by recent correlation performance rather than by track firmness.

7) Smoothing constants determined by recent correlation performance rather than by track firmness.

8) Combining of weighted beacon and radar reports prior to tracking.

9) Application of a priori probability distributions of future aircraft positions as an aid in correlation and tracking.

10) Data pattern analysis (pattern history) use in correlation and smoothing.

11) Multistage smoothing algorithm to make better use of simultaneously available beacon and radar reports.

12) Third (or higher order) smoothing methods.

13) Turn detection techniques.

14) Adaptive filtering algorithms.

15) Polynomial regression methods.

16) Track-oriented smoothing methods.

17) Least squares and nearest fit correlation criteria.

18) Feedback of track data for target detection.

1.1 (continued)

Most of these techniques were studied analytically. In addition, extensive computer experiments were performed to test the most promising techniques or those which did not lend themselves to mathematical analysis. These experiments mainly served to determine the general characteristics of selected tracking techniques and to provide valuable insight into their detailed behavior. The experience gained through the computer experiments led to new analytical approaches and suggested new tracking concepts. Occasional negative experiment results were also very helpful by eliminating less promising approaches from further consideration.

1.2 DEFINITION OF SYSTEM AND ENVIRONMENT

Throughout this study, consideration is given to the system and environment in which the tracking operation must function. System information is derived from empirical studies of tracking requirements in the ARTS-III Beacon Tracking Level system, and as such, cannot be interpreted as a firm design., Likewise, environment conditions are derived from published documents including specifications and evaluation reports. In many instances, this data is interpreted and extrapolated as to its application within the ARTS-III environment. As such, the data is representative of the environment and does not suggest firm values. These definitions along with the list of documents used for this data retrieval is given in Appendix A of this study. These values are given as representative of the system requirements to which the Augmented Tracking system will be designed.

1.3 REPORT ORGANIZATION

The report is organized in a number of ordered sections, the first of which describes the requirements of tracking within the expanded ARTS-III system. This section discusses the objectives of tracking and the tasks slated to fulfill these objectives. The second section examines the requirements described in this first section through detailed technical discussion. This includes the analysis method employed, the analysis results obtained, and the basic recommendations. The third section describes the results of the technical discussion section in the form of overall conclusions and final recommendations. The last section includes five appendices which are provided to address topics relevant to tracking development but somewhat independent of the main theme of the report. The first appendix defines the system and environment conditions which are considered throughout this study. The second appendix describes the tracking simulator model used for special case evaluation of tracking concepts, along with the results of several of these concepts. The third appendix contains the results of computer studies of track smoothing, initiation, and termination techniques. The last two appendices describe the detailed problem simulation model and the results of several tracking algorithms which are evaluated using this simulation model.

1.3 (continued)

The level of content in this text assumes that the reader has some background as to the functional requirements of tracking. It is also assumed that the reader has a basic understanding of the total ARTS-III system including the operation and capabilities of the following subsystems: radar and beacon sensors, data acquisition, digital computer, and display. In particular, extensive reference is made to the Basic Radar Beacon Tracking Level (RBTL) system, and it is assumed that the reader is familiar with the concepts applied here. Throughout the report, the analytical methods employed are not discussed extensively, as it is assumed that the reader has sufficient mathematical background to follow the deductions. As a further guideline, the reader should realize that limited consideration is given to the computer's requirements for tracking schemes being considered so as not to discourage continued development of any methods which may significantly improve tracking quality at the cost of additional computer facilities. The trade-off considerations will be pursued in a design effort to follow this study.

SECTION 2
TRACKING REQUIREMENTS

The basic requirement of the tracking function is that of establishing and maintaining track data files of current aircraft position and velocity. For beacon equipped aircraft, this data file will include aircraft identity and altitude when available. This data is provided by tracking for the display subsystem where it is formatted for display as alphanumeric data tags which identify sensor video returns on the controller's display. This data file generation is accomplished through scan-to-scan correlation of radar and beacon target reports. Tracking is accomplished by associating newly acquired radar and beacon target reports with previously established track information, computing the present position and velocity of the aircraft, and predicting where the target should be reported on the subsequent sensor scan. These three basic processes of correlation, track smoothing, and prediction are performed for every track once each sensor scan.

The track correlation process determines which target reports received during the scan are associated with tracked aircraft. Correlation is accomplished primarily on the basis of positional proximity; however, ambiguous situations often occur due to equipment errors, aircraft maneuvers, and tracking compromises which must be resolved. In these instances correlation must extend its scope to consider additional information concerning both report and target track in order to resolve this ambiguity correctly.

Track smoothing is the second phase within tracking which takes place as a result of correlation. This process considers both the reported aircraft position provided by correlation and an internally computed estimate of the position based on the aircraft's past performance, to provide a smoothed best estimate of position and velocity. Since noise errors inherent to the sensor system are propagated in the reported position, and since the estimated position may include errors due to aircraft maneuvers, the track smoothing process consists of an optimum weighting of the two positions to establish a compromise value close to the actual position. This compromise results in the filtering out of the various error components which are present.

The third phase within tracking consists of projecting from the smooth position along the smoothed velocity to predict the position of the aircraft for the next sensor scan. This prediction corresponds to the estimated position referred to in the track smoothing phase.

These three phases as described represent only the basics of tracking, and each can be accomplished with many variations. It is the task of this study to consider each of these phases in detail and to develop optimum methods within each, which, when combined, will provide superior tracking capabilities.

Section 2 (continued)

An additional requirement within the tracking function is that of establishing track files on newly acquired aircraft as well as terminating those tracks which become defunct. This area of tracking is investigated for methods of providing an automatic initiation and termination sequence which will provide for the automatic tracking of all aircraft.

Methods of expanding the tracking function to provide interface with other system functions are also considered. The first of these topics considers the use of track history as established within tracking to aid the target detection function in the declaration of targets when uncertain conditions are encountered. A second topic considers the interaction of tracking with the controller in the areas of display formats for track data and improved keyboard entry sequences.

The tracking requirements summarized here are those addressed in the following technical discussions section. The divisions within this section are provided for ease in organizing the study results: it must be kept in mind that these divisions have total interdependence and must be combined into a single tracking system during operational deployment.

SECTION 3
TRACKING DEVELOPMENT

This section reports the results of study of tracking techniques intended for use in the enhanced ARTS-III system. The technical discussion presented here is mainly concerned with the design and evaluation of alternative methods of multisensor data utilization in the augmented ARTS-III configuration consisting of a single beacon and a single radar sensor located on the same pedestal.

Before further discussion of study results, it is first desirable to again define the terms describing the principal components of the tracking function. Tracking in a track-while-scan system is a general term commonly used to denote all operations applied to the discrete data reports in order to produce continuous tracks. Logically, tracking consists of two distinct processes. The first process sorts the data reports and selects those which are to be associated with the individual tracks to maintain their continuity. In what follows, we shall refer to this process as track correlation. The second process uses the selected data reports to obtain the best estimates of current aircraft position and velocity. We define the operations contained in the second process as track smoothing.

In principle, these two processes should be treated in a single analysis. It has been a particular weakness of previous work in surveillance theory that the problems related to track correlation and smoothing have been isolated and fragmented in order to obtain manageable mathematical models. In general, the correlation and smoothing processes form an interdependent system, and the algorithms for these processes cannot be designed separately. For instance, in most recursive track-while-scan systems, the criteria used in the selection of reports during the correlation process depend on the current estimates of position and velocity obtained by the smoothing process in the course of the immediately preceding scan.

For these reasons, the design and analysis of the correlation and smoothing algorithms comprising the tracking techniques considered in this project have been carried out in a single unified study. However, for the purposes of convenience and the ease of assessment of the data processing requirements, the results of this study have been separated, and the correlation and the track smoothing algorithms have been individually described in following paragraphs within this section.

3.1 CORRELATION

3.1.1 Introduction

The purpose of this section is to present the results of the study of correlation techniques applicable to the augmented configuration of the Enhanced ARTS-III system. The augmented configuration obtains its tracking data from a single site consisting of one Airport Surveillance Radar (ASR) and one

3.1.1 (continued)

beacon sensor located on a common pedestal. This is perhaps the simplest configuration utilizing multisensor data. The radar and beacon antennas are assumed to be fixed with respect to each other and to revolve together at a fixed rate of 15 rpm. Thus, the complex geometrical and asynchronous scanning problems characterizing larger sensor networks need not be considered. Nevertheless, the study of the augmented system reported here has anticipated the need to extend its results to more general multisensor configurations, and has given preference to the tracking techniques which have the desired growth capability. Accordingly, the correlation algorithm selected in this study phase and described in a later part of this section permits a logical extension to noncolocated sensor networks and, in fact, can be regarded as a special case of a more general solution to the problem of correlation of reports generated by such networks.

The correlation algorithm described in this report is intended for further experimentation and testing in a simulation facility and, ultimately, on the Enhanced ARTS-III test bed in St. Paul, Minnesota. In its present form, it is sufficiently flexible to make full use of the content of the available data, such as code identity, mode C, validation and radar hit count, and to take into account the significant characteristics of beacon and radar data and of track type and status. However, because of the fundamental limitations of theoretical analysis of the dynamic behavior of complex mathematical models, several parameters controlling the operation of the algorithm have not been completely specified. The mathematical analysis supplied the basic criteria for the performance of the algorithm and established its fundamental structure. Furthermore, it provided vital insight into the sensitivity relationships between the performance measures and the data characteristics, allowing certain tradeoffs to be made in algorithm optimization. Additional support was given by limited computer experiments carried out to validate the analytical conclusions and to test the performance of intuitively obtained tracking techniques. However, it is believed that the actual operational values of several important algorithm parameters must be eventually obtained through elaborate simulation exercises realistically representing the system environment or, better still, through live experiments on the test bed at St. Paul. This is necessary even in the case of fundamental parameters, such as search bin sizes and weighting coefficients applied to report deviations from the predicted positions. In this case, the analysis can supply only approximate parameter values due to several limiting factors, particularly to the unpredictable nature of aircraft trajectories. It is even more necessary in the case of the parameters controlling the relative effects of validation, hit count, identity and mode C indications on the operation of the algorithm. Traditionally, these effects have been determined by judgment based on qualitative considerations. The analysis can provide a range of reasonable values and initial settings of these parameters for experimentation in a realistic environment.

The basic purpose of using multisensor data in the tracking process is to improve the quality of the resultant tracks. Track quality in this context implies two distinct but not independent attributes: reliability and accuracy.

3.1.1 (continued)

By reliability we ordinarily mean track continuity exhibited by the tenacity of the tracking algorithm in following the track under most circumstances, as well as trustworthiness of the identity maintained in the track file. Accuracy, on the other hand, is a measure of the fidelity of the estimates generated by the track smoothing process. Thus, accuracy is not really defined, unless a track is maintained. From this point of view, therefore, accuracy may be regarded as a secondary attribute. Track reliability is the most essential single attribute of a successful tracking system.

Track reliability and accuracy are usually regarded as separate attributes of the correlation and the smoothing processes respectively. As already mentioned, however, correlation and smoothing processes are closely interdependent and cannot be studied separately. For the same reason, it is not possible to optimize track reliability in the design of a recursive tracking algorithm without stressing its accuracy. In fact, it can be shown that the most reliable tracking algorithm must also be the most accurate.

Analysis of the tracking difficulties encountered in the operation of several terminal area automatic tracking systems using beacon data indicates that the overall tracking reliability is not adequate. This conclusion is supported by the opinions of FAA personnel experienced in terminal area operations. A particular difficulty is caused by the fading of beacon replies usually associated with an aircraft turn or a particular attitude. This type of fading is mostly caused by the shielding of the transponder antenna, and it tends to persist for several scans. Additional difficulties are caused by reflections from ground structures, by reply garbles and by fruit. As a result of missing or spurious beacon reports, the correlation process cannot function properly, tracks are lost, and the overall reliability suffers.

It is reasonable to expect that independent sensor data, represented by radar reports in the augmented ARTS-III system, will improve track reliability by filling the gaps caused by fade sequences and by reinforcing available beacon reports. This, indeed, is possible and has, to some extent, been achieved in the RBTL system. The maximum improvement in track reliability which can be achieved in this manner is basically limited by the imperfections in the available data. The radar data used by the tracking algorithm is characterized by low blip-scan ratio and considerable clutter. Both of these effects tend to limit the usefulness of radar data for tracking. In a multisensor tracking system, low blip-scan ratio can be tolerated since, at worst, it will produce no improvement in performance. However, radar clutter can be highly detrimental and actually cause a degradation in track reliability. For these reasons, radar data must be used with caution, and the tracking algorithm must be judiciously designed to permit satisfactory operation in the presence of clutter.

In the following paragraphs, we present a brief discussion of the basic correlation problem and the design considerations motivating our selection of the correlation algorithm. Finally, we describe the proposed algorithm and discuss its characteristics.

3.1.2 The Correlation Problem

In its most general form, the correlation process performs associations among points in space-time, selecting those groups which are most likely to represent paths of moving objects. The criteria used in each selection are based on assumed models of path dynamics and on data characteristics. In principle, the entire association process must be repeated each time a new data point arrives. Obviously, this procedure leads to immense computational requirements, since all possible group combinations must be considered before an association decision can be made.

Considerably less demanding is the correlation process needed to maintain a set of already established tracks. The rule in this case is that only associations with newly arrived data points are tried, and that previously made association decisions are inviolate. Thus, firm associations must frequently be made on the basis of insufficient information and cannot be revised when further data becomes available. It is clear that, in this case, computational economy is achieved at the expense of degradation in performance. Nevertheless, most recursive correlation algorithms operate in this manner. Even in this case, however, the computational requirements can be substantial, since great many data points must be considered as candidates for association with each track. An obvious remedy for this problem is some form of space partitioning and sorting of data points to limit the selection process to only those regions in the vicinity of each track in which legitimate associations can be performed.

In a recursive correlation algorithm suitable for the ARTS-III system, the required space partitioning is obtained through the use of search bins placed around the predicted positions. As explained below in further detail, the minimum size of the search bins is limited by basic system uncertainties, resulting in frequent bin overlaps, particularly in congested areas. In effect, several tracks often compete for the same reports, and the correlation algorithm must find an optimum solution to a joint association problem in which all tracks and all reports within the appropriate bins are simultaneously considered. Such a joint association process cannot be carried out by a noniterative sequential procedure making unique assignments to one track at a time. Thus, the computational requirements still remain considerable, unless a sub-optimum solution to the joint association problem can be found acceptable.

A simple sub-optimum solution may use a first-come-first-served basis. In this case, the resultant association pattern is clearly dependent on the order in which tracks and reports are processed. A modification of this approach using a two-pass procedure is employed by the RBTL correlation algorithm. The two-pass procedure helps to resolve ambiguous assignments and reduces somewhat the probability of track swapping. Obviously, many sub-optimum solutions to the joint association problem can be proposed, depending mainly on the complexity and the computational requirements which can be tolerated. In general, the complexity and the computational requirements increase rapidly as the performance of the algorithm approaches that of the optimum joint association process. Therefore, the design of the correlation algorithm must carefully consider tradeoffs between track reliability and computer requirements. We believe that the correlation algorithm described below will result in a significant improvement in track reliability when compared with the RBTL system, and

3.1.2 (continued)

at a reasonably modest cost. The proposed algorithm carries the sub-optimization one step further by analyzing the ambiguous assignment situations in somewhat greater detail. This hopefully will increase resistance to track swapping and improve track reliability. Through judicious use of the radar search bin, the algorithm is also expected to improve radar data utilization and result in better clutter rejection.

3.1.3 Design Considerations

In the augmented ARTS-III configuration, the beacon and radar data available to the tracking system are assumed, in general, to contain the following information:

1) Position (range and azimuth).

2) Code identity (discrete and nondiscrete beacon).

3) Mode C (indication of presence and altitude for beacon aircraft).

4) Validation (discrete and nondiscrete beacon).

5) Hit count (radar).

In addition, the tracking system has available to it clutter and track maps, as well as the type and current status of the maintained tracks. Also available and potentially useful is *a priori* information concerning future aircraft behavior, including updated flight plans, pilot intent known to the controller, and geographical aspects of the air route structure.

The task of the correlation process is to make best use of this information in assigning reports to the existing tracks, in order to improve the overall track reliability. Ideally, a wide variety of operational situations must be covered in the study to determine the effectiveness of the selected correlation algorithm. It has been shown, however, that most tracking difficulties arise as a consequence of a few data and trajectory situations. These include:

1) Turning trajectory.

2) Parallel or crossing trajectories.

3) Beacon fading.

4) Radar clutter.

Naturally, the greatest difficulties are caused by several of these situations occurring simultaneously. The most common example is given by beacon fading occurring during aircraft turns. Accordingly, the procedure used in the selection of a practical correlation algorithm involved detailed consideration of various combinations in which the data and trajectory situations may arise,

3.1.3 (continued)

and an evaluation of the response of proposed association techniques.

To prevent undue bias in the results in favor of existing systems, it was desired not to exclude from consideration certain promising approaches merely on the basis of their apparent complexity. However, as already mentioned, the computational requirements grow very rapidly as the number of alternative associations compared by the algorithm is increased and as the performance of the optimum joint association process is approached. For this reason, the selection of correlation algorithms was limited to those whose computational requirements were considered reasonable for application in the Enhanced ARTS-III system. Furthermore, emphasis was placed on that design philosophy and logical structure of the algorithm which were compatible with the architecture of the basic ARTS-III and RBTL systems. It is believed that this emphasis has not resulted in a significant restriction on the performance of the proposed algorithm.

The following are the basic features of the RBTL system which are retained in the proposed algorithm:

1) The main structure of the track store is unchanged; the store is divided into 11.25^{o} sectors.

2) The report store is essentially unchanged, with reports arranged in approximately increasing azimuth.

3) The categories of initial, normal, parent, parent trial, turning and turning trial tracks are similarly defined.

4) The secondary bin logic and its use to search for beacon and radar reports for subsequent correlation are retained.

Also retained is the ability to correlate across sector boundaries. The new system also has the additional capability to resolve across sector boundaries (as well as within sectors) those association conflicts in which two tracks compete for the same reports.

The design of the correlation algorithm for the augmented configuration regards it as a special case of a more general multisensor system. In the augmented system, the radar and beacon antennas revolve together on the same pedestal, generating synchronous data. In a general multisensor system, the sensors are remote from each other and operate independently, producing data at arbitrary instants of time. Thus, the augmented configuration can be viewed as a special case of a general system, with a zero time delay between beacon and radar reports. This approach leads to a more equitable treatment of both types of data, regarding radar as another full-fledged sensor, and not merely as an adjunct for the reinforcement of beacon reports. The resultant algorithm achieves better radar data utilization, preventing the introduction of a bias inherent in the so-called radar-to-beacon correlation. It can also be readily extended to a more general multisensor case, a desirable design goal.

3.1.4 The Correlation Algorithm

We now present a functional description of the proposed correlation algorithm. As already mentioned, the structure and much of the processing mechanism of the RBTL system are retained. The primary/secondary correlation routine is modified to allow the introduction of the proposed changes. The secondary part of this routine is essentially unchanged, except that it will no longer be depended upon to resolve ambiguous situations left over from the first correlation pass. The primary part of the correlation routine, however, is completely replaced by the algorithm discussed below. In effect, as long as successful associations are made within the primary bin, the processing will be entirely governed by the new algorithm. Whenever the primary correlation fails, further track processing will be carried out by the RBTL secondary correlation system.

The general flow of operations in the primary correlation of a beacon track is described by the following sequence:

1) Obtain estimates of position and velocity generated by the smoothing algorithm on the previous scan.

2) By linear extrapolation, compute the predicted track position for the current scan.

3) Select the size of the primary search bin and center it on the predicted position.

4) For each beacon report found in the primary bin, compute the radar search position. The radar search position is defined as an intermediate point on a straight line segment joining the predicted position and the beacon report. The ratio, p, of the distance of this point from the predicted position to the length of the segment is a function of the smoothing constants. If there are no beacon reports in the primary bin, the radar search position is defined to coincide with the predicted position.

5) Select the size of the radar search bin and center it on the radar search position.

6) For each radar report found in the radar bin of each beacon report, compute the association measure. The association measure is defined as a function of the report geometry, of the track and report type and identity, and of report quality (such as validation or hit count).

7) Select the beacon/radar report pair with the smallest association measure. If two tracks compete for the same reports, attempt to find selections which minimize the sum of the respective association measures.

3.1.4 (continued)

The steps in the maintenance of a radar track involve a similar, though somewhat simpler, procedure. As is evident from this description, the association measure constitutes the main mechanism through which association decisions are made. For this purpose, the association measure is defined as a suitably weighted sum of terms individually representing the various aspects of the data relevant to the decision process. For convenience, these terms can be divided into two distinct groups, the first group expressing the impact of report geometry, and the second group summarizing the contributions of the remaining data descriptors. We shall refer to these terms as geometric and qualifying, respectively.

The two geometric terms of the association measure are:

1) The square of the deviation of the beacon report from the predicted track position, and,

2) The square of the deviation of the radar report from the radar search position.

These two terms are multiplied by weighting coefficients, m_1 and m_2 respectively, taking into account the errors in the predicted position and in the current beacon and radar reports. More specifically, the ratio of m_1 to m_2 should be equal to the ratio of the variance of the deviation of the radar report from the radar search position to the variance of the deviation of the beacon report from the predicted track position. However, when properly designed, the areas of the two search bins must be proportional to the corresponding variances. Thus, we conclude that m_1 and m_2 should be inversely proportional to the areas of the corresponding search bins. A slight departure from this relationship may be caused by the designer requiring the size of the radar search bin to be somewhat smaller to provide better clutter rejection with some sacrifice in radar data utilization. The total range of reasonable values of the ratio of m_2 to m_1 lies between 1.5 and 4. For initial experimentation, a value of 2 is recommended.

The qualifying terms comprising the remaining part of the association measure are summarized in table 3-1. Except for the functions of validation and hit count, the qualifying terms are assumed to be constants.

The choice of an assignment process minimizing the value of the association measure has been dictated by analytical considerations assuming a maximum likelihood criterion. Originally applied to the spatial coordinates, this approach has been extended in the form of a generalized nearest fit to include other data dimensions as well. It can be shown that the generalized nearest fit will produce near-optimum solutions to the association problem under a wide range of assumptions.

TABLE 3-1. QUALIFYING TERMS OF THE ASSOCIATION MEASURE

DATA TYPE	TRACK TYPE				
	BEACON				RADAR
	DISCRETE		NON-DISCRETE		
	Mode C	No Mode C	Mode C	No Mode C	
RBC = ABC	$-K_1$	$-K_1$	$-K_7$	$-K_7$	
RBC = LGC	$-K_2$	$-K_2$	$-K_8$	$-K_8$	
No Mode C	K_3	K_4	K_9	K_{10}	
Mode C not within limits	K_5	∞	K_{11}	∞	
Mode C within limits	$-K_6$	∞	$-K_{12}$	∞	
Validation	$-f_1(v)$	$-f_1(v)$	$-f_2(v)$	$-f_2(v)$	
Hit Count					$-f_3(h)$

3.1.4 (continued)

The beacon and radar search bins (both primary and secondary) sort data reports in order to exclude from further processing those regions of space in which candidates for legitimate associations with given tracks are not likely to be found. The basic purpose of the search bins is threefold:

1) To minimize the effects of spurious beacon reports and radar clutter on track reliability.

2) To reduce the probability of miscorrelation with reports from other aircraft and the resultant track swapping.

3) To reduce the computational requirements.

Ideally, the search bins should be as small as possible. The lower bound on the size of the search bins is determined by the deviations of the data reports from the point on which the bin is centered. These deviations are caused by errors in the predicted track position, including the effects of aircraft maneuvers, and by errors in the current data reports. Further discussion of bin determination is presented in section 3.2.

The use of the radar search position by the proposed algorithm to track beacon targets must now be explained. The optimum location for centering the radar bin is the best estimate of the aircraft position available at the time. This estimate must be based on both the track predicted position and on the beacon report being processed. Therefore, the optimum center of the radar bin is some intermediate point on the line joining the predicted position and the beacon report. The location of this point along the line is determined by the ratio of the track prediction errors to the beacon report errors.

Centering the radar bin on the beacon report would result in poorer radar data utilization by not making full use of the available information. Furthermore, such procedure would inevitably introduce harmful bias into the tracking system through unwarranted reinforcement of beacon reports by radar clutter. In this connection, it should be noted that radar errors are measured with respect to the actual aircraft position and not with respect to the location of the beacon report.

The functional flow chart in figure 3-1 describes the operation of the proposed algorithm. Sheets 4 through 7 explain the procedure for processing beacon tracks. The beacon/radar report selection routine (shown in sheets 5 and 6) selects all qualifying pairs of beacon and radar reports and computes and stores in a temporary table their corresponding association measures. The algorithm then attempts to find a selection with the lowest value of this measure. If either or both reports in the tenatively selected pair are already assigned to a previous track, a comparison is performed between two joint associations:

1) The best selection for the present track, combined with the second best selection available for the previous track.

3.1.4 (continued)

2) The second best selection for the present track, combined with the best (previously assigned) selection for the previous track.

In each case, the best selection is synonymous with the lowest association measure. The second best implies a selection of a pair of as yet unassigned reports with the next higher association measure. It is assumed that both the best and the second best selections, if available, are stored by this algorithm with each track in the track file, together with the corresponding values of the association measure. It is believed that the required increase in the size of the track file will not be great since, on the average, not many tracks will have a second best selection available. An alternative to this procedure would have to repeat the association processing for the previous track on demand.

Having compared the two combinations of assignments (1 and 2 above), the algorithm then chooses that one for which the sum of the association measures is smaller. (cf. figure 3-1, sheet 4) As explained above, this procedure is dictated by the maximum likelihood criterion. Obviously, the results will fall short of optimum association performance, since the process is truncated after a single attempt to exchange locally best and second best solutions. Nevertheless, it is believed that the performance of this algorithm will be significantly superior to that of a "first-come-first-served" method. It will be noticed that the algorithm does not alter previous associations in the case when the beacon and radar reports have been assigned to two different tracks.

The procedure for the primary correlation of radar tracks is illustrated by the flow charts in figure 3-1, sheets 2 and 3. In this case, a selection obviously consists of a single radar report. Radar reports previously assigned to a beacon track are not considered for assignments. Otherwise, the procedure is the same as that used for beacon tracks.

A simple example will help to illustrate the behavior of the algorithm. Figure 3-2 shows beacon and radar reports in the primary search bin of a nondiscrete track. The predicted track position is at A. Also shown are dashed lines joining the predicted position with the beacon reports, and the radar bins centered on the respective radar search positions. The performance measure of the beacon/radar combination on the right is superior to that of the single beacon report on the left.

Figure 3-3 illustrates a potential correlation conflict between two radar tracks.* The predicted track positions are at A and B respectively.

---

* The radar track case was chosen to illustrate the assignment logic. The beacon assignment process is similar, but the required complexity of the data pattern would obscure the argument and make interpretation of the figure difficult.

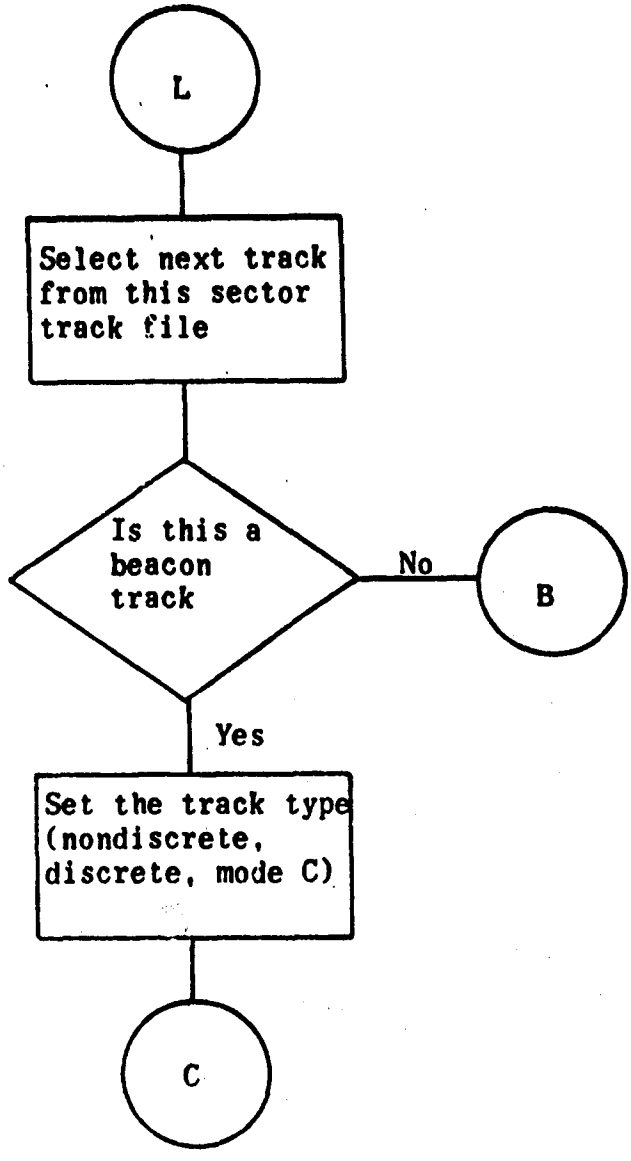

Figure 3-1. Functional Flowchart of The Correlation Algorithm (Sheet 1 of 8)

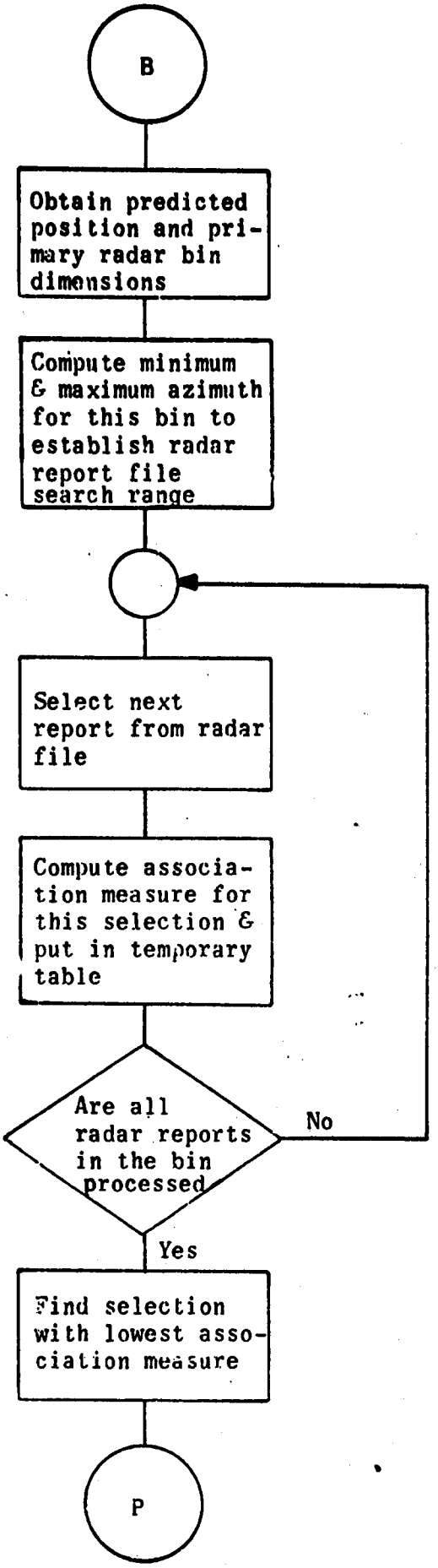

Figure 3-1. Functional Flowchart of The Correlation Algorithm (Sheet 2 of 8)

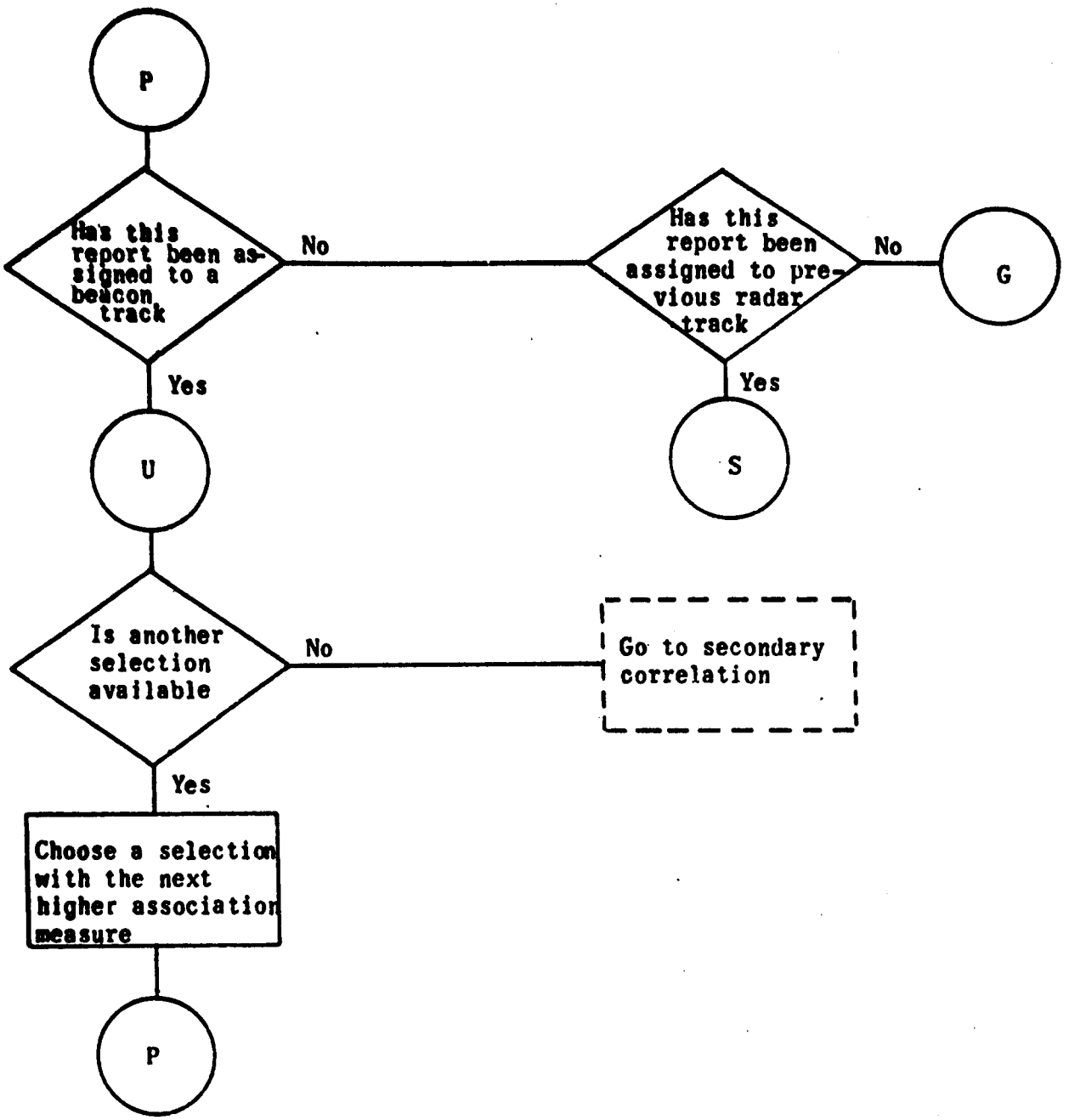

Figure 3-1. Functional Flowchart of The Correlation Algorithm (Sheet 3 of 8)

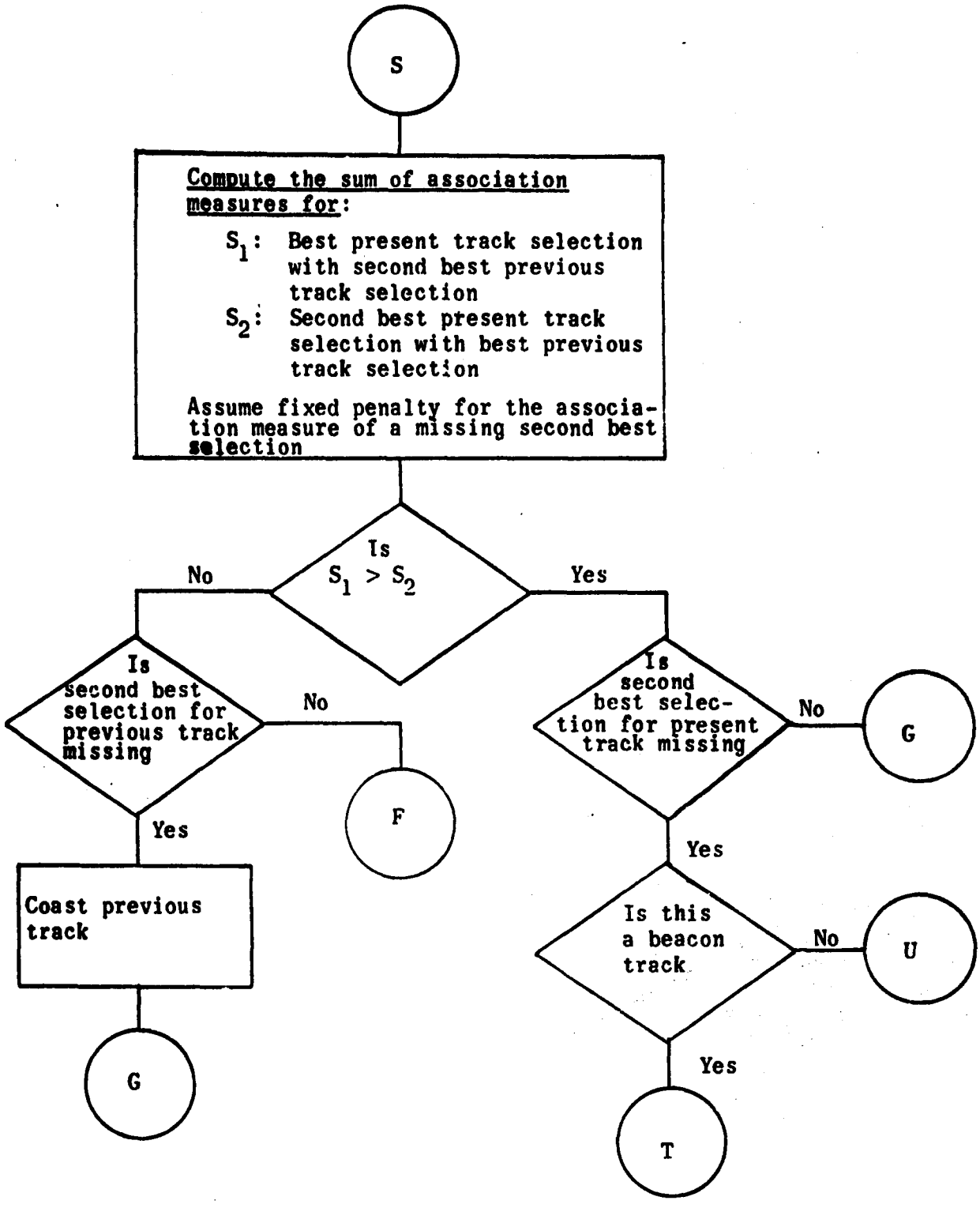

Figure 3-1. Functional Flowchart of The Correlation Algorithm (Sheet 4 of 8)

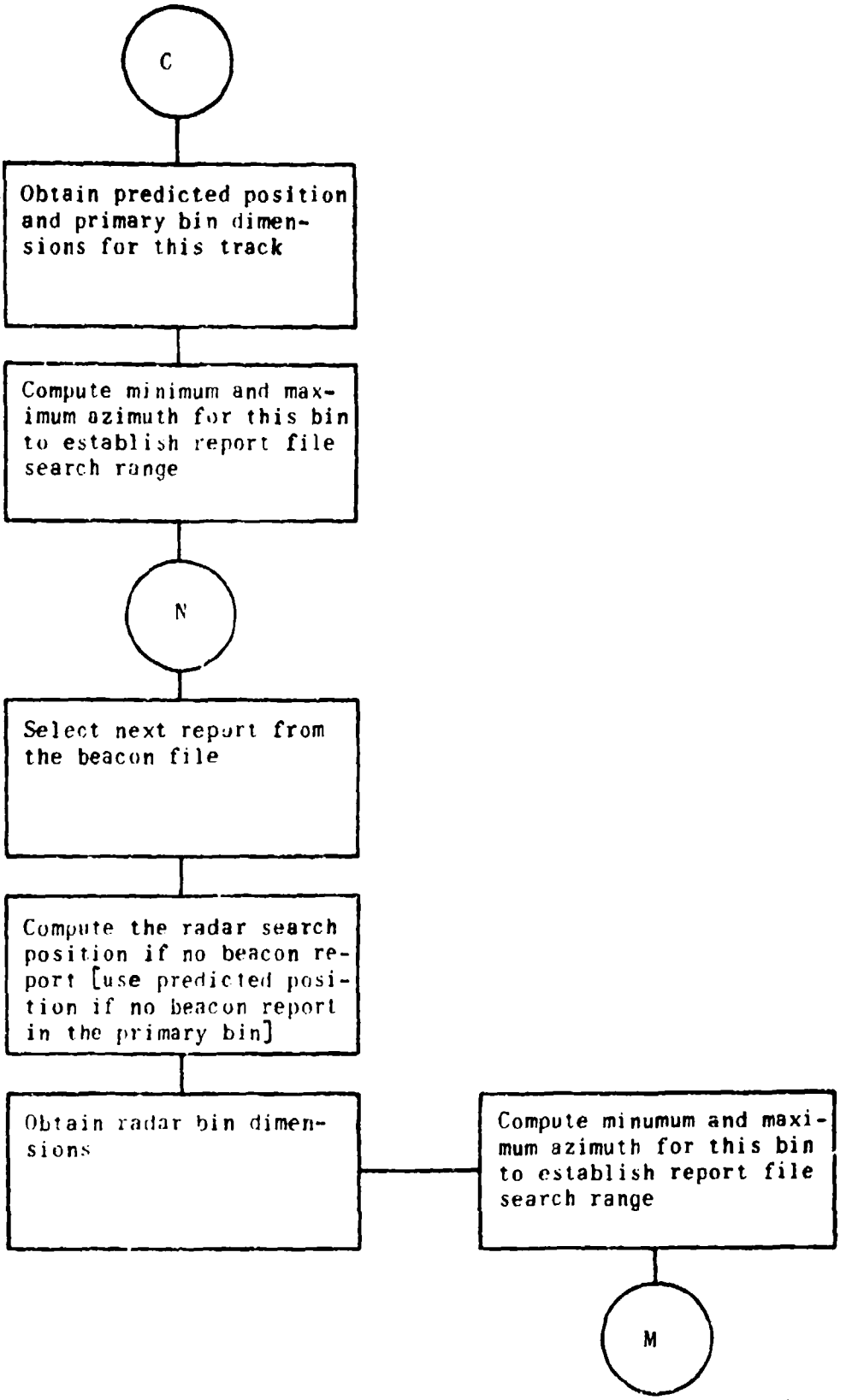

Figure 3-1. Functional Flow Chart of the Correlation Algorithm (Sheet 5 of 8)

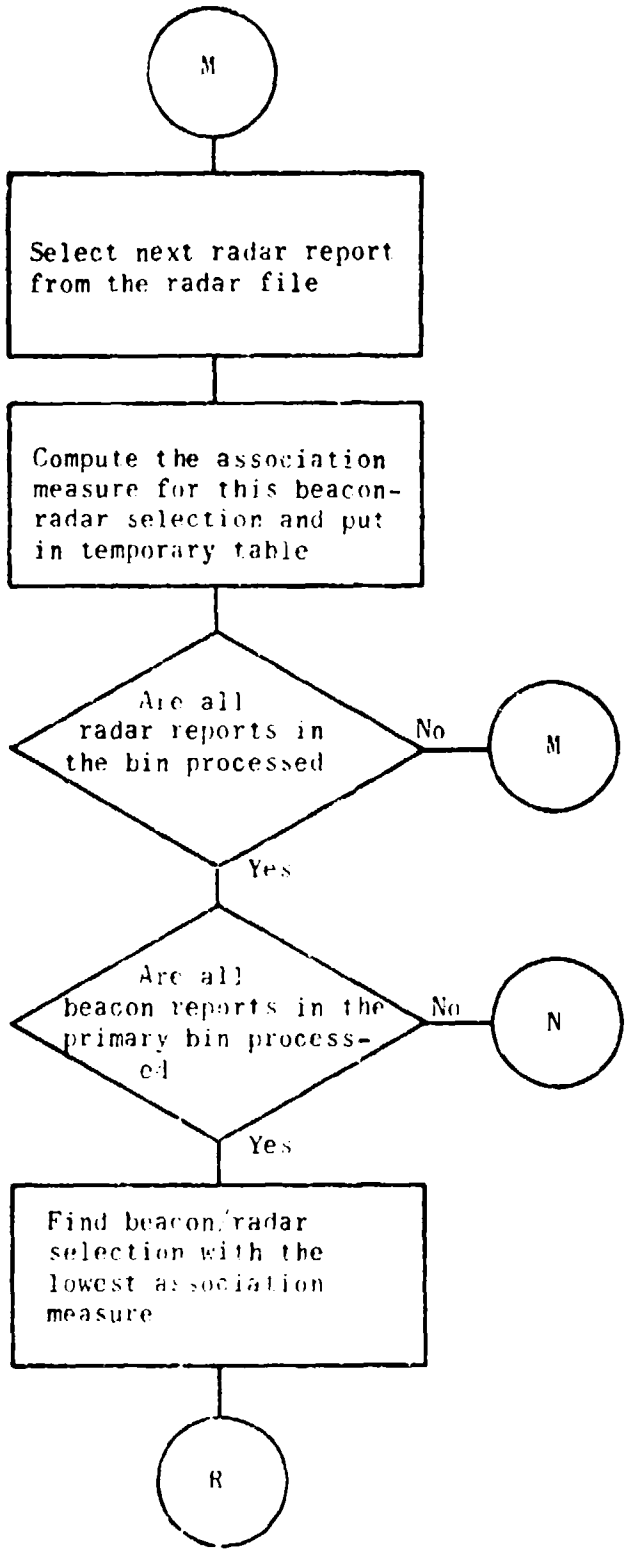

Figure 3-1. Functional Flow Chart of the Correlation Algorithm (Sheet 6 of 8)

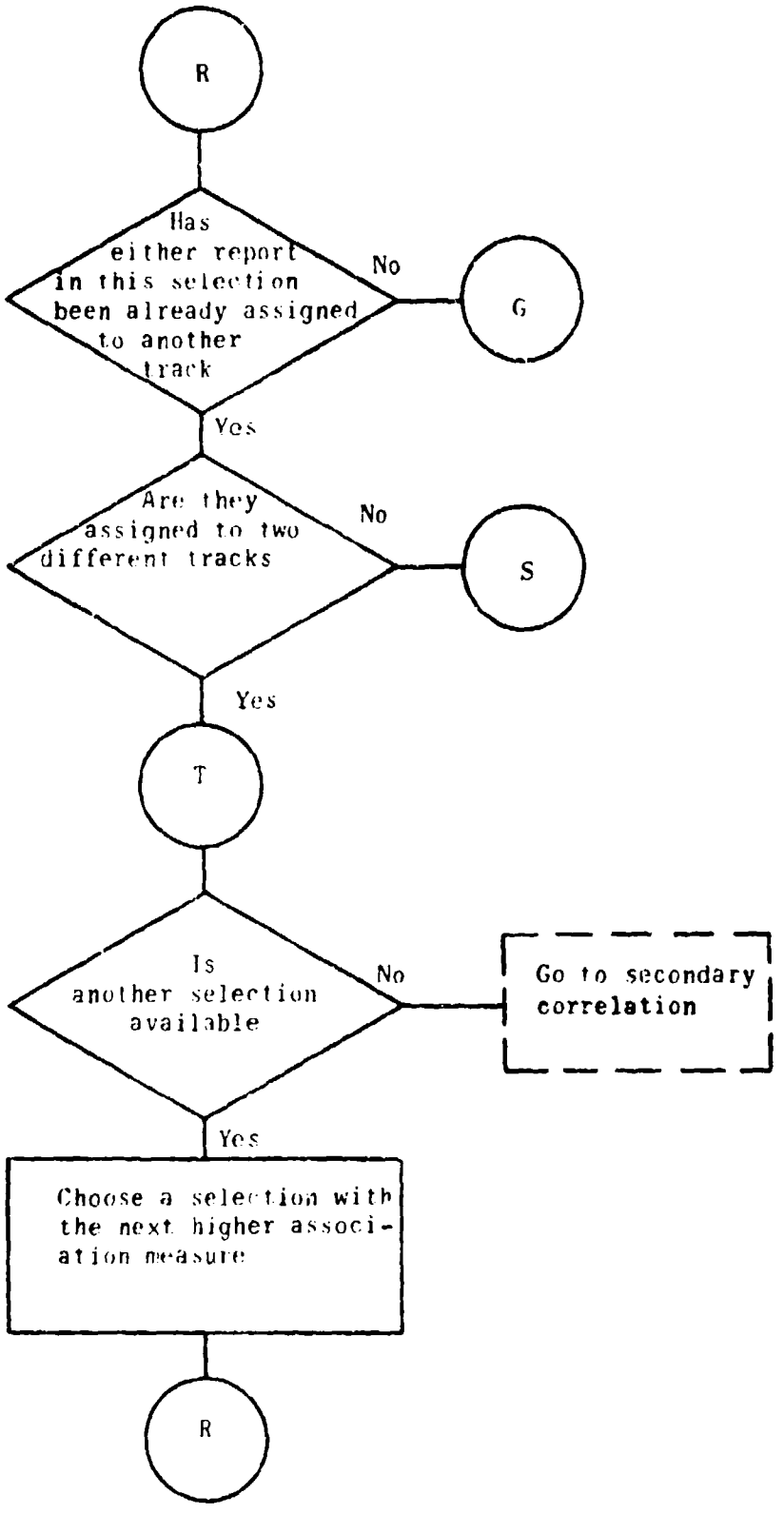

Figure 3-1. Functional Flow Chart of the Correlation Algorithm (Sheet 7 of 8)

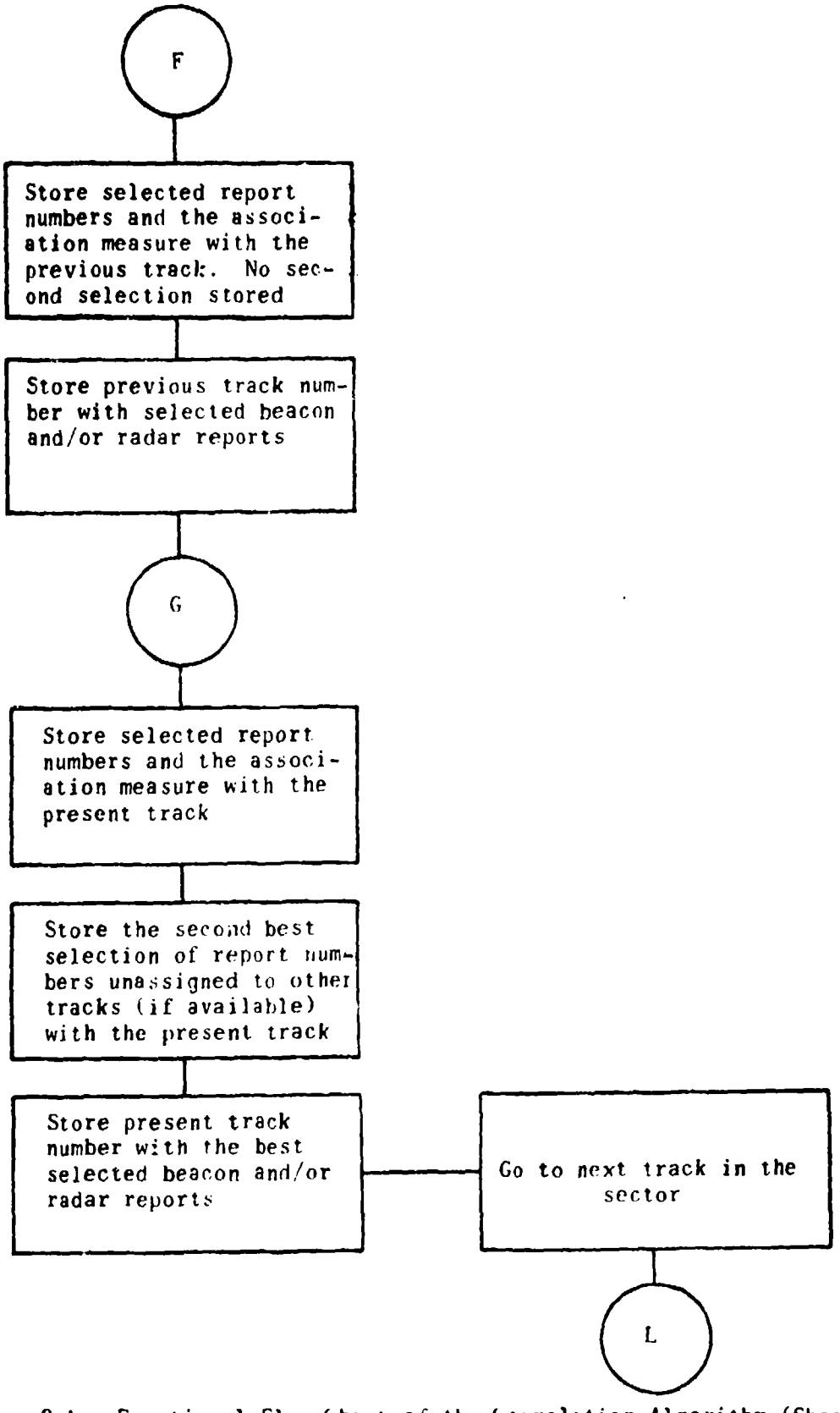

Figure 3-1. Functional Flow Chart of the Correlation Algorithm (Sheet 8 of 8)

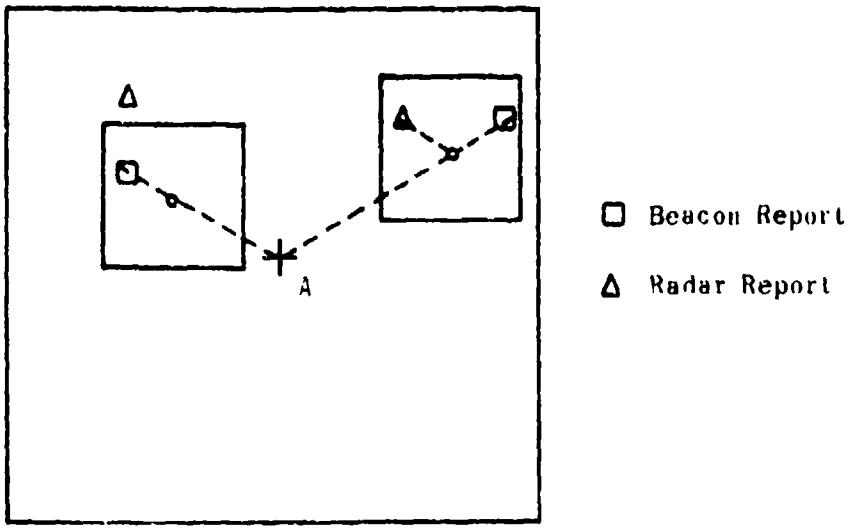

Figure 3-2. Beacon/Radar Report Selection

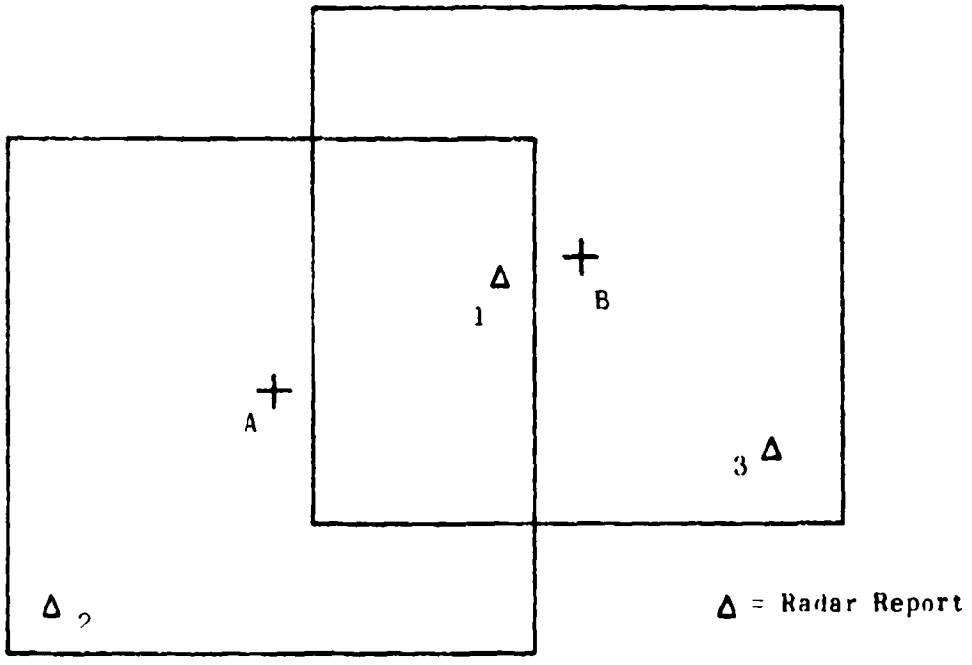

Figure 3-3. Two-Track Assignment Ambiguity

3.1.4 (continued)

Let us first assume that only a single radar report appears at (1). The outcome is then dependent on the relative value of this report to the two tracks and does not depend on the order of processing. Let us next assume that radar reports appear only at (1) and (2). If track A is processed first, it will be initially assigned report (1). When track B is processed next, the situation will be reviewed: track B will probably get report (1), while track A will get report (2). This seems to be a desirable solution. If the tracks are processed in a reversed order, the outcome will be the same.

We now add a radar report at (3) and repeat the procedure. If track A is processed first, it will again receive report (1). When track B is processed next, a complete trade-off among assignments will be performed. The two possible solutions are: A with (1) and B with (3), or A with (2) and B with (1). The algorithm will choose the solution with a superior association measure.

We may now compare these results with the outcome of the RBTL primary correlation logic applied to the same situations:

1) When only a single radar report at (1) is present, the outcome of the RBTL logic will be no correlation decision and both tracks will be coasted.

2) When both reports (1) and (2) are present, the two-pass RBTL Primary/Secondary correlation will assign (2) to A and (1) to B. The result is the same as that of the proposed algorithm.

3) With all three radar reports present, the Primary RBTL correlation will fail, and the tracks will be coasted.

Thus, the proposed algorithm will deal with the situation illustrated in figure 3-3 more effectively than the RBTL primary/secondary correlation. It is difficult to generalize these conclusions because the outcome in each case is critically dependent on the pattern of data in the vicinity of the predicted track positions. It appears, however, that in most situations examined in the study, the proposed algorithm shows a significant improvement over the RBTL logic.

It is emphasized that the behavior of the correlation algorithm in ambiguous data situations is very important. The example in figure 3-3 illustrates one of many possible situations occurring when two tracks approach or cross each other, resulting in a possibility of track swap, one of the main weaknesses of the RBTL logic. Perhaps the most critical is the case of two nondiscrete beacon or radar tracks closely parallelling each other* for an extended period of time. Prolonged exposure creates many opportunities for miscorrelation, making this case particularly vulnerable to track swapping. Another type of ambiguous data situation arises when clutter interferes with the correlation of a radar track. In such cases, clutter may seriously affect correlation performance, particularly when the blip-scan ratio in low. Thus, it can be seen

---

* Not necessarily at the same altitude.

3.1.4 (continued)

that even a small improvement in correlation performance in ambiguous data situations will have a significant effect on track reliability.

3.2 TRACK SMOOTHING AND PREDICTION

3.2.1 Introduction

Track smoothing and prediction (S & P) is a process of statistical estimation in which the data (target reports) attributed to each aircraft by the correlation process are used to determine parameters which describe the motion of each aircraft. It is understood that only data correlated with a given aircraft affect that aircraft's parameters, so that we can proceed on an individual aircraft basis. In the RBTL system, data for a particular aircraft are received once per scan (every four seconds) from a coaligned set of beacon/radar antennas. These data (individual sweep returns) undergo beacon and radar video processing, and target reports are produced. These target reports are associated with the aircraft by the correlation program. Thus, the track S & P routines are faced with four possible data situations for this track: no reports, beacon report only, radar report only, or beacon and radar reports.

The dynamic parameters which describe the motion of an aircraft change in time, so that their estimates must be modified continually with each scan as new data are received. The smoothed values of such parameters are produced just after the receipt of data and are designed to be "best" estimates of the parameters at that time, given all data up to and including that scan. Then the smoothed estimates are extrapolated to the next scan time to provide "best" prediction estimates of parameters before receipt of the next data. These prediction estimates determine the centering of search bins for the next scan correlation process, so that the processes of track-data correlation and track S & P are insolubly linked, being applied alternately to produce a time series of track estimates.

In order that optimal track S & P may be performed, it is necessary that the parameter description of track motion be complete; i.e., as many parameters must be included as are estimable from the data. But the parameter description must not include unobservable superfluous variables lest the accuracy of remaining ones suffers. In what follows, we consider only the problem of aircraft tracking in two horizontal dimensions (as on a PPI presentation). How to select parameters in such a framework is a problem of some importance.

The most general known technique for handling estimation problems with an underlying dynamic evaluation is the Kalman formalism. This technique is capable of accommodating without exception the effects of nonstationary statistics and an arbitrary sequence of data including any combinations of missing reports. In view of its generality and success in practical application to many tracking problems (the α, β tracker is a special example), we adopt the Kalman approach to our work.

3.2.1 (continued)

The methods of analysis for the work of this section includes mathematical study and computer experiments. These are sufficient, when tempered by judgment, to suggest the structure of track S & P algorithms and, in many cases, to suggest appropriate values for algorithm parameters. However, in order to optimize any resulting algorithms for the real world, much more extensive tune-up via simulation and/or live testing will be necessary.

Two aspects of tracking performance are frequently identified as being of importance: track S & P accuracy and track reliability. Reliability has two facets: track lifetime, and tendency to swap with adjacent tracks.

One question frequently arises in S & P problems: is there a tradeoff in estimate accuracy between smoothing and prediction, or between short vs. long range prediction, or between individual parameters of a track parameter set? The answer to all these is in the negative. The optimal method of estimation simultaneously maximizes the accuracy of all these quantities. There is no tradeoff.

Thus, for example, a method which produces a best smoothed track position estimate also produces a most accurate smoothed velocity. Attempts to further reduce velocity fluctuations, if introduced into the track S & P iteration, will only produce less accurate positions and velocities. Of course, the output of the track S & P may be subjected to further smoothing for cosmetic purposes of display, etc., but these changes do not represent a real improvement of the accuracy of the estimate. Only the rate of fluctuation is reduced; the amplitude is increased. Such modified estimates must not be reintroduced into the track S & P loop.

Again, the accuracy requirements on smoothing, one-scan, or multi-scan predictions do not conflict. An optimal method of S & P for the purpose of on-going tracking is directly extensible to provide most accurate long range prediction estimates. Conversely, an improved method of long range prediction would immediately have application to the tracking operation, where better accuracy would also be obtained. A second class of questions is concerned with the possibility of S & P design tradeoff among the various aspects of reliability vs. accuracy. Here the answer is less categorical, but experience to date as well as some analyses indicate no conflict. That is, the problem of optimizing tracking S & P for accuracy is essentially the same as that of maximizing track life and minimizing the tendency to swap. No obvious tradeoffs exist.

As an example, we preview the results of section 3.2.4.1, where analysis of an idealized model indicates a very strong dependence of the mean track life under random maneuver and data noise conditions on the ratio of search bin size to rms position prediction error. Slight reduction of this error causes much greater improvement in track life than a similar variation in other aspects of performance (e.g., the rate of fluctuation of the estimates). Thus, tracking accuracy and life essentially vary together in a one-to-one fashion and are optimized simultaneously. In a clutter environment, reduced prediction error makes reduction of the search bin size possible, thus improving clutter

3.2.1 (continued)

rejection. Further, use of a nearest fit type of correlation logic under reduced error decreases the chances of a successful clutter correlation. Again, improved accuracy improves track life.

Using some simple considerations, we can also make plausible a direct connection between track accuracy and tendency to swap. These considerations are valid in the context of nearest fit correlation logics (which we shall assume throughout). Note the simple situations in figure 3-4 representing two straight tracks perfectly timed for a cross. If the angle of crossing is not too small, it is easy to convince oneself that the first scan after the cross is the most critical for swaps; before this point a likely result of miscorrelation is loss of track. No swap occurs if the two track vectors are in the same relation as the true paths, for then the nearest fit correlated data will keep the two track estimates properly diverging. On the other hand, if fluctuations of the velocity estimates are such that the track vectors are crossed in the improper order, then this improper order will be reinforced by the new data and that relation will persist as the aircraft separate. The tracks then are permanently swapped.

For a given crossing angle, then, the tendency to swap is reduced with a reduction in the size of the one-scan prediction errors and vice versa.

All of these arguments lead to one conclusion. There is basically one problem of tracking S & P system design: the optimization of S & P accuracy. Since it is immaterial which aspect of accuracy we select, we choose most often to work in terms of the one-scan prediction estimates of aircraft position. These are most natural since they are related directly to the requirements of search bin sizes and other aspects of correlation design.

If the various possible measures of tracking performance do not conflict, then what is the major design difficulty? The central difficulty in the design of an optimal tracker is the decision as to what track population to optimize it for. There exists a basic conflict in design for straight, non-maneuvering tracks vs. tracks in maneuver. In the former case, emphasis is placed on smoothing the fluctuations caused by data measurement error; in the latter, on following the twists and turns of the maneuvering track. No one tracker can be optimized simultaneously for both classes of track.

Two approaches to this dilemma are possible. First, we may design the track S & P to be optimal in the sense of average performance over a specified population mix of track types. Secondly, we may attempt to design an adaptive tracker, one which identifies the type of track it is dealing with and adjusts itself accordingly. We shall see later that adaptive methods for the RBTL system appear to have rather marginal capabilities, so that we cannot really avoid the obligation to design for a track population mix.

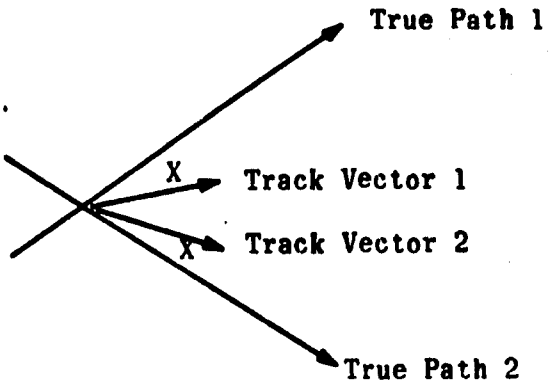

No Swap

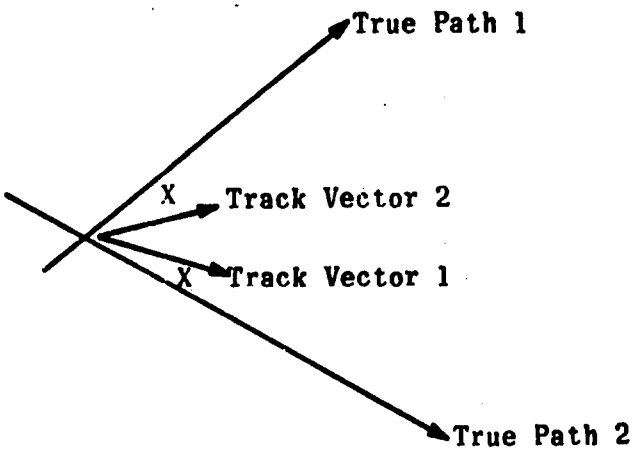

Swap

Figure 3-4. Swap Situations

3.2.2 Model Selection

3.2.2.1 Basic Model and Extensions

Underlying the recursive process of track estimation in a Kalman model is the basic notion of the state (column) vector $\underline{x}$. The state vector has, as components, all of the quantities which describe the dynamic evolution of the system and which, if known exactly, completely summarize the effect of past history on the future development. The equation of state, a set of vector difference equations, describes the evolution mathematically.

$$\underline{x}(n+1) = \Phi(n)\,\underline{x}(n) + \underline{w}(n) \quad . \tag{1}$$

Here $\underline{x}(n)$ is the (true) value of the state vector on scan n. $\Phi(n)$ is a square transition matrix specifying the dynamic connection. $\underline{w}(n)$ is a vector of random driving terms. $\underline{w}$ has components of zero mean, which are serially uncorrelated. However, for any given n, the elements of $\underline{w}$ may be correlated with each other according to a specified covariance matrix Q(n).*

$$E[\underline{w}(n)] = 0 \qquad Q(n) = E[\underline{w}(n)\underline{w}'(n)] \quad . \tag{2}$$

As an example, take the following notion of aircraft motion in the x, y plane. State variables are x, y, $\dot{x}$, and y (position and velocity components). The motion is assumed independent in each coordinate, so that we need to treat only one dimension at a time. Set, therefore, at the scan n,

$$\underline{x}(n) = \begin{bmatrix} x(n) \\ \dot{x}(n) \end{bmatrix} \quad . \tag{3}$$

Assume that the motion is driven by random, serially uncorrelated, zero mean accelerations, a(n), which are held <u>constant</u> through each scan period, Δt. Thus, from the laws of uniformly accelerated motion,

$$x(n+1) = x(n) + \Delta t\dot{x}(n) + \frac{1}{2}\,a(n)(\Delta t)^2 \tag{4}$$

$$\dot{x}(n+1) = \dot{x}(n) + a(n)\Delta t \quad .$$

We identify (4) with the equation of state (1)

---

*Matrix transpose is indicated by an apostrophe. Expectations (mean values) are indicated by the notation E[ ]. Subscripts indicate matrix components.

3.2.2.1 (continued)

where

$$\Phi(n) = \begin{bmatrix} 1 & \Delta t \\ 0 & 1 \end{bmatrix} \qquad \underline{w}(n) = \begin{bmatrix} \frac{1}{2} a(n)(\Delta t)^2 \\ a(n)\Delta t \end{bmatrix} . \tag{5}$$

We assume the acceleration perturbations, a(n), to all have a known common variance a^2. Then,

$$Q(n) = \begin{bmatrix} \frac{1}{4} a^2(\Delta t)^4 & \frac{1}{2} a^2(\Delta t)^3 \\ \frac{1}{2} a^2(\Delta t)^3 & a^2(\Delta t)^2 \end{bmatrix} . \tag{6}$$

With the additional assumption of uncorrelated x, y data errors, this dynamic model leads directly to an α, β tracker of the type used in RBTL. Indeed, it underlies all α, β trackers. If we believe in the correctness of the dynamic assumption which motivates this model, viz., that successive accelerations on each scan are not correlated and that x and y motions are independent and similar, then we are inevitably driven to the α, β tracker, with α, β applied equally to x and y coordinates. By questioning these assumptions, we are led to suitable improvements of the dynamic model and, thus, eventually, to better track estimate accuracy.

Several points of attack are thus presented. Are x and y motions independent and of similar character? Not really, since, if the aircraft is progressing in the x direction, lateral or y accelerations would normally be larger in a maneuver than x or longitudinal accelerations. In fact, the natural coordinate system to use for a more exact description of motion would be oriented in the direction of motion. This presents some problems in practice when used as the basis of track S & P, since the orientation is not only constantly changing, but must be inferred exactly from the velocity estimates themselves. We shall pursue this subject later. The evidence indicates a positive improvement in S & P using track oriented operations.

Are successive accelerations serially uncorrelated? Not exactly. When an aircraft turns a 90^0 turn at 3^0/sec., for example, accelerations are held consistently for 7-8 scans. The problem here is to determine whether such accelerations are large enough and last long enough to be reliably determined from the data before the maneuver is nearly completed. Unless such acceleration runs can be detected in a <u>timely</u> fashion from the data, it avails us little to include them in the motion model. The evidence on this point is negative; accelerations can not be so estimated and track S & P algorithms (α, β, γ trackers) based on their inclusion, are inferior to α, β trackers (i.e., $\gamma = 0$ is

3.2.2.1 (continued)

optimal.) It should be noted, however, that the negative answer is somewhat marginal and depends on the data conditions. If either the data rate or data accuracy were to improve substantially, then acceleration estimation would become feasible.

Is the acceleration variance, a^2, known? No. Specification of the acceleration variance is equivalent to a specification of the track population for which the tracker is optimized. For any given track we really do not know what value of a^2 to assume. In fact, a^2 may change from point to point on the track. Such change can be accommodated in the model through Q(n), but the sequence of values must be known. According to our previous discussion of track populations, we may select a compromise a^2 which then leads to a design which is optimal on the average for that mixed class of tracks.

Attempts to estimate a^2 "on the fly" and thus produce an adaptive filter can be shown to be ineffective, except in extreme cases (i.e., only extreme differences in a^2 can be sensed). Thus, the adaptive feature is not as effective as one might suppose and can serve only to trigger an emergency mode when a straight track suddenly maneuvers and almost escapes from the search bin. This feature is discussed later under "deviation controlled smoothing". This result should not be unexpected in view of the general difficulty of estimating the accelerations themselves, even if sustained, as noted above.

Other variations of the model are also possible. For example, we can reformulate the equations in terms of polar coordinates instead of rectangular coordinates. This reformulation allows one to handle the effect of unequal range and azimuth data errors more handily, but it introduces other complications to be described later.

3.2.2.2 Measurements

The general measurement at scan n for a track whose dynamics are described by (1) is given by the vector $\underline{z}(n)$. The components of $\underline{z}$ represent each individual measurement value. In the Kalman model, $\underline{z}(n)$ is expressed as a linear function of the state vector $\underline{x}(n)$ plus noise $\underline{c}(n)$.

$$\underline{z}(n) = H(n)\,\underline{x}(n) + \underline{c}(n) \quad . \tag{7}$$

The observation matrix H describes the geometry of the measurements, while the added data error $\underline{c}$ has zero mean components, serially uncorrelated in time. The noise variance is described by the covariance matrix, R(n).

$$E[\underline{c}(n)] = 0 \qquad R(n) = E[\underline{c}(n)\underline{c}'(n)] \quad . \tag{8}$$

3.2.2.2 (continued)

As an example, suppose that $\underline{z}$ represents an x, y measurement of the position of an aircraft moving in the x, y plane. Then if the x, y data errors are equal and uncorrelated, each component measurement may be treated separately. Corresponding to the one-component dynamics model (3) through (6), we have the measurement equation

$$\underline{z}(n) = x(n) + c(n) \quad , \tag{9}$$

where

$$H(n) = [1, 0] \qquad R(n) = c^2 \quad . \tag{10}$$

This measurement model, together with the previous example dynamics model, leads to the α, β tracker.

When both radar and beacon data are received on a given scan, there are several statistically equivalent ways to proceed. They may be collected to form a vector observation $\underline{z}$; they may be combined by optimal weighting to form a single measurement, or they may be treated in sequence. For the purposes of track S & P, the precombination approach is the most suitable. However, it should be noted that when S & P is performed, track data has already been selected by the correlation process. For correlation purposes, the sequential approach is required. Thus, the problem of data combination is handled differently for these two tasks. (In reporting some of our computer experiments, the sequential approach was used throughout for convenience.)

Radar and beacon data are weighted together in each component inversely as to their respective noise variances, c_r^2, c_b^2, to produce a combined z.

$$z_{comb} = \frac{\frac{1}{c_b^2} z_b + \frac{1}{c_r^2} z_r}{\frac{1}{c_b^2} + \frac{1}{c_r^2}} \tag{11}$$

$$= kz_b + (1 - k)z_r \quad . \qquad 0 < k < 1 \quad .$$

The equivalent noise variance of the combined measurements is,

$$c_{comb}^2 = \frac{1}{\frac{1}{c_b^2} + \frac{1}{c_r^2}} = kc_b^2 \quad . \tag{12}$$

A typical value of k is $\frac{1}{3}$.

3.2.2.2 (continued)

Therefore, when combined beacon and radar data are obtained on a scan, (9) is used with an appropriate value of reduced noise, c^2.

Missing data (both radar and beacon) can be accommodated by the model through the formal device of setting H = 0. The datum z then obtained consists of pure noise and will be rejected by any optimal S & P filter.

3.2.2.3 Estimation

Let $\hat{\underline{x}}(n)$ be the optimal smoothed estimate of the state vector $\underline{x}(n)$, given the data up to and including scan n. Let $\hat{\hat{\underline{x}}}(n)$ be the optimal prediction estimate of $\underline{x}(n)$ based on data up to but not including $\underline{z}(n)$. Using the general Kalman model, one finds the following optimal (minimum mean square error) S & P operations.

Smoothing: (13)

$$\hat{\underline{x}}(n) = \hat{\hat{\underline{x}}}(n) + K(n)\,[\underline{z}(n) - H(n)\,\hat{\hat{\underline{x}}}(n)]$$

Prediction:

$$\hat{\hat{\underline{x}}}(n+1) = \Phi(n)\,\hat{\underline{x}}(n).$$

K(n) is an optimal weighting matrix which is related to $\Sigma(n)$, the covariance estimate of the prediction errors.

$$K(n) = \Sigma(n)H'(n)[H(n)\Sigma(n)H'(n) + R(n)]^{-1} \tag{14}$$

The prediction error covariance matrices, $\Sigma(n)$, are themselves calculated by a matrix recursion,

$$\Sigma(n+1) = Q(n) + \Phi(n)\{\Sigma(n) - \Sigma(n)H'(n)[H(n)\Sigma(n)H'(n) + R(n)]^{-1} \cdot H(n)\Sigma(n)\}\Phi'(n) \tag{15}$$

As an example, let us set up the S & P system for the dynamics model (4), (5), (6) and measurements model (9), (10). We define the components

$$\Sigma = \begin{bmatrix} \sigma_{xx} & \sigma_{x\dot{x}} \\ \sigma_{x\dot{x}} & \sigma_{\dot{x}\dot{x}} \end{bmatrix} \qquad K = \begin{bmatrix} \alpha \\ \beta \end{bmatrix} \tag{16}$$

3.2.2.3 (continued)

and find:

Smoothing:

$$\hat{x}(n) = \hat{x}(n) + \alpha(n)[z(n) - \hat{x}(n)] \tag{17}$$

$$\hat{\dot{x}}(n) = \overset{\wedge}{\dot{x}}(n) + \beta(n)[z(n) - \hat{x}(n)]$$

(if data is missing set $z(n) = \hat{x}(n)$).

Prediction

$$\hat{x}(n+1) = \hat{x}(n) + \Delta t\hat{\dot{x}}(n)$$

$$\overset{\wedge}{\dot{x}}(n+1) = \hat{\dot{x}}(n)$$

Optimal weighting matrix

(18)

$$\alpha(n) = \frac{\sigma_{xx}(n)}{\sigma_{xx}(n) + c^2}$$

$$\beta(n) = \frac{\sigma_{x\dot{x}}(n)}{\sigma_{xx}(n) + c^2}$$

Covariance recursion

(19)

$$\sigma_{xx}(n+1) = \frac{1}{4} a^2(\Delta t)^4 + \sigma_{xx}(n) + 2\Delta t\sigma_{x\dot{x}}(n) + (\Delta t)^2\sigma_{\dot{x}\dot{x}}(n)$$

$$- h(n) \frac{(\sigma_{xx}(n) + \Delta t\sigma_{x\dot{x}}(n))^2}{\sigma_{xx}(n) + c^2}$$

$$\sigma_{x\dot{x}}(n+1) = \frac{1}{2} a^2(\Delta t)^3 + \sigma_{x\dot{x}}(n) + \Delta t\sigma_{\dot{x}\dot{x}}(n)$$

$$-h(n) \frac{\sigma_{x\dot{x}}(n)(\sigma_{xx}(n) + \Delta t\sigma_{x\dot{x}}(n))}{\sigma_{xx}(n) + c^2}$$

3.2.2.3 (continued)

$$\sigma_{\dot{x}\dot{x}}(n+1) = a^2(\Delta t)^2 + \sigma_{\dot{x}\dot{x}}(n) - h(n)\,\frac{(\sigma_{x\dot{x}}(n))^2}{\sigma_{xx}(n) + c^2} \quad . \tag{19}$$

where we set h(n) = 1 if data are received on scan n and h(n) = 0 if no data are received.

Thus, we have derived an α, β tracker. It can be shown further, if the dynamics model is changed so that the accelerations are no longer random (serially uncorrelated) but are built up from third derivatives of motion which are random, then the state vector has an additional $\dddot{x}$ component, and the α, β tracker is extended to an α, β, γ tracker. The corresponding S & P equations take the form:

Smoothing (20)

$$\hat{x}(n) = \hat{\hat{x}}(n) + \alpha(n)[z(n) - \hat{\hat{x}}(n)]$$

$$\hat{\dot{x}}(n) = \hat{\dot{x}}(n) + \beta(n)[z(n) - \hat{\hat{x}}(n)]$$

$$\hat{\ddot{x}}(n) = \hat{\ddot{x}}(n) + \gamma(n)[z(n) - \hat{\hat{x}}(n)] \quad .$$

Prediction

$$\hat{x}(n+1) = \hat{x}(n) + \Delta t\,\hat{\dot{x}}(n) + \frac{1}{2}(\Delta t)^2\hat{\ddot{x}}(n)$$

$$\hat{\dot{x}}(n+1) = \hat{\dot{x}}(n) + \Delta t\,\hat{\ddot{x}}(n)$$

$$\hat{\ddot{x}}(n+1) = \hat{\ddot{x}}(n) \quad .$$

Of course, the covariance recursion controlling the selection of optimal α, β, γ now is considerably more complex, containing six component relationships.

3.2.2.4 Track-Oriented Smoothing

If the motion and measurement processes do not permit a decomposition of the model into two independent dimensions, then the S & P equations and, particularly, the covariance recursions become quite complex. Extension of the simple α, β tracker to allow general treatment increases the number of independent smoothing constants from 2 to 8. There are then 10 separate equations comprising the covariance recursion. Thus, the cost of departing from independent component operations is quite steep.

3.2.2.4 (continued)

The condition which allows this decomposition on an x, y component basis is that the x and y maneuver acceleration components are not correlated and the x and y data error components are not correlated (both acceleration and data error covariance ellipses are aligned along the x, y axes). A slightly more general condition occurs when one of these ellipses is circular and the other is not aligned with the coordinate axes. Then a rotation of coordinates will bring about the aligned condition and decomposition may be applied.

There are two possibilities. If the maneuver accelerations are assumed isotropic, but the data errors have noncircular distributions which are range-azimuth oriented, then a rotation of coordinates along the local range-azimuth grid directions will uncouple the estimation problem and permit separate c^2 noise variance values to be applied in each direction with a corresponding α, β tracker. If, on the other hand, the accelerations along and transverse to the track directions are assumed different, but the error distribution is circular, then the coordinate system may be rotated in line with the track direction (assuming that it can be accurately estimated). Then separate α, β smoothing can be applied along and across the track direction using appropriate different values of a^2.

If, however, both the data error and maneuver acceleration ellipse are skew oriented with respect to x, y, we have the general configuration, and no decomposition is possible. Careful control of the 8 smoothing parameters would then almost demand a covariance recursion of 10 equations. In the current system we can fairly well reject this possibility as too expensive of computer time and storage for the improvement of performance it might engender. (Some approximations are possible, however, so that we may save some of the information in the skewed distributions. See below.)

The approach we propose (which has been confirmed by some computer experiments) is to orient the smoothing operations to the estimated track direction. This is motivated by the knowledge that aircraft normally move in such a way that transverse accelerations are larger than longitudinal accelerations.

In order to construct track oriented smoothing equations, refer to figure 3-5. The track vector with predicted velocity components, $\hat{\dot{x}}$, $\hat{\dot{y}}$ makes an angle φ with the x axis. The predicted position at $\hat{x}$, $\hat{y}$ and data at z_x, z_y form a data difference vector $\underline{D}$. The longitudinal axis is in the direction of track motion; the transverse axis is perpendicular and positive on the right side. Resolving $\underline{D}$ along the L and T axes in terms of their x, y components, we obtain:

$$D_L = D_x \cos\varphi + D_y \sin\varphi \qquad (21)$$

$$= \frac{D_x \hat{\dot{x}}}{s} + \frac{D_y \hat{\dot{y}}}{s}$$

3.2.2.4 (continued)

$$D_T = D_x \sin\varphi - D_y \cos\varphi \qquad (21)$$

$$= \frac{D_x \hat{\dot{y}}}{s} - \frac{D_y \hat{\dot{x}}}{s}$$

$$s^2 = \hat{\dot{x}}^2 + \hat{\dot{y}}^2 \quad .$$

These differences now provide the longitudinal and transverse corrections to the predicted positions by multiplying by the respective smoothing constants α_L, α_T. But we may describe this process just as easily in the original x, y system. Thus (see figure 3-6) $\hat{x}$ is corrected by adding α_L times the resolution of D_L on the x axis plus α_T times the resolution of D_T on the x axis. Similar results hold for the y direction. At scan n,

$$\hat{x} = \hat{x} + \alpha_L D_L \cos\varphi + \alpha_T D_T \sin\varphi \qquad (22)$$

$$\hat{y} = \hat{y} + \alpha_L D_L \sin\varphi - \alpha_T D_T \cos\varphi \quad .$$

Using (21) we find

$$\hat{x} = \hat{x} + \alpha_L \frac{u\hat{\dot{x}}}{s^2} + \alpha_T \frac{v\hat{\dot{y}}}{s^2} \qquad (23)$$

$$\hat{y} = \hat{y} + \alpha_L \frac{u\hat{\dot{y}}}{s^2} - \alpha_T \frac{v\hat{\dot{x}}}{s^2} \quad .$$

where

$$u = D_x \hat{\dot{x}} + D_y \hat{\dot{y}} \qquad (24)$$

$$v = D_x \hat{\dot{y}} - D_y \hat{\dot{x}} \quad .$$

A completely identical argument now produces the velocity smoothing equations,

$$\hat{\dot{x}} = \hat{\dot{x}} + \beta_L \frac{u\hat{\dot{x}}}{s^2} + \beta_T \frac{v\hat{\dot{y}}}{s^2} \qquad (25)$$

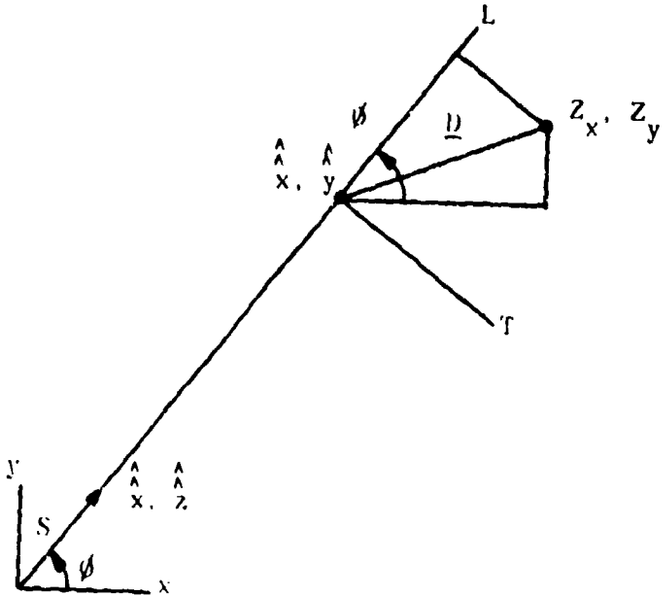

Figure 3-5. Track-Oriented Coordinate System

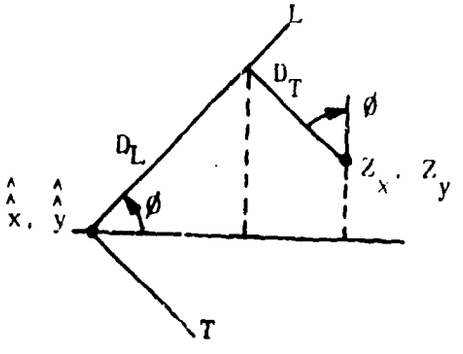

Figure 3-6. Track-Oriented Deviation Geometry

3.2.2.4 (continued) (25)

$$\hat{\dot{y}} = \hat{\dot{y}} + \beta_L \frac{\hat{u}\hat{y}}{s^2} - \beta_T \frac{\hat{v}\hat{x}}{s^2} \quad .$$

while the prediction equations are the same as for nonoriented S & P. Thus, in effect, we have performed our smoothing in a rotated system, but have preserved the use of the ordinary x, y coordinates for its implementation.

The effect of a data error distribution which is skew to the track direction may be introduced approximately by computing the variance of these errors along the L and T directions separately. Then cross-correlation is ignored (the error ellipse is reformed oriented in the track direction). If the polar coordinates of the predicted position are ρ, θ we can write

$$c_L^2 = c_\theta^2 \sin^2(\varphi-\theta) + c_\rho^2 \cos^2(\varphi-\theta) \qquad (26)$$

$$c_T^2 = c_\theta^2 \cos^2(\varphi-\theta) + c_\rho^2 \sin^2(\varphi-\theta) \quad .$$

Here c_θ^2 is the covariance in position (linear units) in the tangential direction and varies with ρ. c_ρ^2 is the range variance, a constant. c_L^2, c_T^2, may be used now to assist in the selection of suitable α, β, either by using covariance recursions (the more exact method), or by ad hoc methods.

3.2.2.5 Acceleration Smoothing

The S & P equations (17), (18), (19), representing a general α, β tracker, and their extension in the previous section to track oriented operations are optimum for a particular dynamics model in which aircraft accelerations are uncorrelated from scan to scan. We have chosen a particular model in which such random accelerations, once selected for a particular scan, are held constant for a scan interval. Slightly different assumptions, i.e., that the accelerations are serially uncorrelated impulses occuring just at each scan time, lead to the same α, β S & P equations, but a slightly different covariance recursion which defines optimal α, β. In any case, to justify the use of acceleration smoothing and an α, β, γ tracker, aircraft accelerations must have sufficient magnitude and be held consistently over a sufficiently large number of scans, so that their effects are detectable in the measured aircraft trajectory.

3.2.2.5 (continued)

This detection must occur in a timely fashion before the acceleration switches to another level, or else it is of no value in track S & P. Therefore, determining that an aircraft did maneuver with an estimated acceleration by examining past data history is inherently an easier task (estimation accuracy is higher) than detecting the maneuver in progress before it is complete. In the latter instance we must be particularly careful not to mistake a momentary velocity estimate fluctuation for a turn in progress.

In order to illustrate the fallacy of one uncritical view of tracker design, refer to figure 3-7. This figure shows the dynamic trajectory of a point in one dimension, x, as a function of time, t, up to the current time t_o. The path is a random walk which can be generated as the accumulated winnings of a long series of fair coin tosses. Assuming that the path can be observed with essentially zero error, what is the optimal track S & P procedure?

Obviously, the best smoothed position is x_o, the reported position at t_o. We know, further, that the future direction that x will take in such a gambling game is equally balanced between a tendency to rise or fall, regardless of previous behavior. Thus, the optimal prediction to a point in the future is also x_o. It avails us nothing to attempt to determine a velocity of the motion at x_o, much less to determine accelerations. Although, for example, a section of curve history preceding t_o could be fitted by polynomials, the accuracy of fit increasing with the order of the polynomial, these polynomials could not be extrapolated into the future to provide prediction (or smoothing) estimates superior to just x_o. In this case the order of the polynomial is analogous to the choice of state vector $(x, \dot{x}, \ddot{x}, \ldots)$ complexity, and an improved fit to old data is no proof of predictive power.

By adding measurement noise to the trajectory of Figure 3-7 and sampling it, we would obtain a type of model for which an α tracker (no velocity smoothing) would be optimal.

In order to determine whether consistent aircraft accelerations can be detected, consider a real aircraft trajectory: two straight portions connected by a 90^o turn traversed by 3 deg./sec. at a speed of 200 knots. The turn lasts 7.5 scans and the lateral acceleration, a, during this time changes from zero to .0465 nm/scan^2. The lateral deviation, d, from a straight path due to acceleration during one scan is about .023 nm. The standard deviation of the beacon data error, c, is about .1 nm.

$$d = \frac{1}{2}a = .023 \text{ nm.} \quad c = .1 \text{ nm.} \quad \frac{d}{c} = .23 . \tag{27}$$

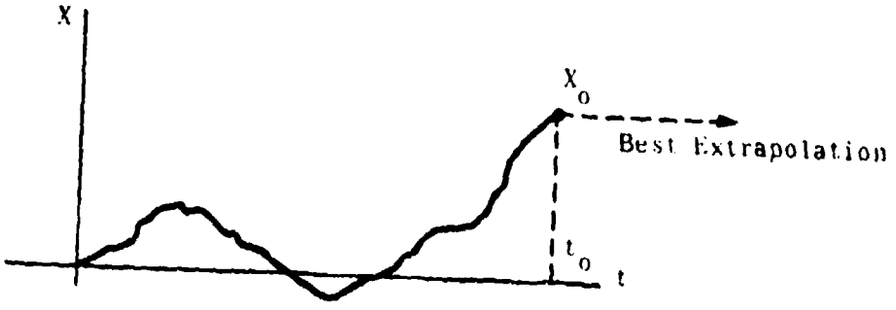

Figure 3-7. Random Walk-Tracking Example

3.2.2.5 (continued)

It can be demonstrated that if one desires to detect this acceleration signal in the data noise, the method which produces the best signal to noise ratio is the use of a matched filter. That is, a series of weights is derived, having the same progression as the signal to be detected; in our present case, this is a parabola. Then the series of weights is convolved with the noisy input signal. The resulting weighed sum is an estimate of acceleration with best signal to noise ratio.

Table 3-2 shows matched filters for acceleration estimation based on 3, 4, 5, 7 and 11 consecutive scans of data. The last column of this table exhibits the ratio of the acceleration estimate to the standard deviation of the noise in the estimate when the value of d/c in (27) is applied. In order for the acceleration to be evident with some reliability, $S/\sqrt{N}$ should be 2 or greater. We see immediately that 7 or more scans of data showing the consistent acceleration are required. But, at 7 scans into the 90^{o} turn, the turn is over, so that any track S & P which attempts to retain and use the acceleration estimate at that late point will not perform optimally.

For turns at 200 dt., the displacement, d, scales linearly with the turn rate, so that $1\frac{1}{2}^{o}$/sec turn yields $S/\sqrt{N}$ values one half as great. We see that about 10 scans of data are required for acceleration estimation. For a 90^{o} turn lasting 15 scans, this is likewise rather late in the turn for S & P purposes. In general, we conclude that acceleration estimation is not promising under current circumstances, and that a significant reduction of data error, c, or increase in scan rate (yielding a larger number of samples of the maneuver) would be necessary to change this conclusion.

These results are supported by computer studies in which a general α, β, γ tracker is assumed, and the smoothing constants are adjusted automatically by a hill-climbing routine to optimize the performance of the tracker over a population of straight and maneuvering tracks. Both track-oriented and non track-oriented systems were investigated. In all cases of practical interest, the program found optimal γ values of zero. Therefore, there appears to be no payoff under current circumstances in going beyond the α, β tracker.

If this conclusion is accepted, then some interesting corollaries follow from it. First of all, trackers which attempt to fit parabolic or higher order polynomials to past data cannot work effectively. The fitting of such curves is equivalent to making estimates of acceleration and higher order derivatives of motion, which is futile. The data quality only justifies the fitting of straight lines, i.e., position and velocity estimation.

TABLE 3-2. MATCHED FILTERS FOR ACCELERATION ESTIMATION

Number of Samples	Weights	N Noise Variance	S Signal Out	$\frac{S}{\sqrt{N}}$	Example $\frac{S}{\sqrt{N}}$
3	(1 -2 1)	$6c^2$	2d	$.817\frac{d}{c}$	.19
4	(1 -1 -1 1)	$4c^2$	4d	$2.00\frac{d}{c}$	.46
5	(2 -1 -2 -1 2)	$14c^2$	14d	$3.74\frac{d}{c}$	.86
7	(5 0 -3 -4 -3 0 5)	$84c^2$	84d	$9.17\frac{d}{c}$	2.1
11	(15 6 -1 -6 -9 -10 -9 -6 -1 6 15)	$858c^2$	858d	$29.3\frac{d}{c}$	6.7

3.2.2.5 (continued)

In fact, any other method of tracking which inspects past data patterns for evidence of the occurrence and direction of a turn maneuver and biases, or otherwise modifies the track S & P in the turn direction, will not enhance the tracking accuracy. (Our simulation studies also suggest this conclusion.)

The difficulty of detecting a consistent acceleration also suggests that it may be similarly difficult to assess from the data the magnitude (variance) of random accelerations. Since optimal determination of α, β depends on this paremeter, it would be convenient to be able to deduce from the data of the given track, adjusting α, β adaptively in response. This adjustment, in effect, controls the time constant, or memory of the tracking filter. Unfortunately, it can be shown (see section 3.2.3.7.) that maneuver estimation is somewhat limited. The most that can be achieved is to discriminate three levels of maneuvers.

3.2.2.6 Other Coordinate Systems

The above discussion and our study work support the use of the α, β tracker in an x, y system with track-oriented smoothing and p, θ error distribution features. There does not appear to be any positive advantage to reformulating these relations in another system, such as polar coordinates.

Note that since tracking operations are individually oriented for each track and the corresponding tracking error ellipse is variously oriented with respect to p, θ data errors, there is really no "natural" coordinate system. The main motive for choosing a p, θ description of track motion would be to avoid coordinate conversions in correlation processing. This processing in our colocated system is most conveniently done in p, θ. This does not seem sufficient incentive to abandon x, y tracking, especially since common x, y coordinates will almost certainly be the most convenient form for the multisensor, non-colocated system.

3.2.3 Selection of Smoothing Constants

3.2.3.1 Methods of Approach

The exact selection of α, β values which minimize S & P errors according to the random accelerations model is made by performing covariance recursions (19) once per scan per track and applying the results in relations (18). This is

3.2.3.1 (continued)

the approach taken in some existing trackers.* If we think in terms of track-oriented smoothing, then two sets, (α_L, β_L), (α_T, β_T), are required, controlled by their own independent covariance recursions. If time is measured in units of one scan (i.e., $\Delta t = 1$), the α, β and covariance relations (18), (19) are conveniently determined by a single parameter λ,

$$\lambda = \frac{a^2}{c^2} . \tag{28}$$

This parameter describes, equivalently, either the degree of random maneuverability of the track vs. the data error, or the mix of straight vs. maneuvering tracks in the population. The recursions select optimal α, β values for these conditions, depending on the sequence of hits and misses received.

The equivalence between design for a population mix of randomly maneuvering targets or of deterministic maneuvers can be justified by a nontrivial application of linear system theory. Some useful correspondences are paired off in table 3-3. For random inputs to our system, we measure mean square tracking error; for deterministic inputs, we measure the sum of the squares of the resulting tracking deviations. Of course, we must compare errors of a similar sort, such as the one step predictions vs. true positions which form the basis of the current discussion.

TABLE 3-3. CORRESPONDENCE BETWEEN RANDOM AND DETERMINISTIC MODELS.

	Random	Deterministic
Error measure	Mean square error.	Sum of error squares.
Noise	Random, uncorrelated.	Single deviation.
Turn (1)	Uncorrelated accelerations held constant through scan.	Sharp turn, pivot midway between scans.
Turn (2)	Uncorrelated accelerations. Impulsive at beginning of scan.	Sharp turn, pivot at scan.

*The Weighted Minimum Variance Tracker of the AN/SPS-48B Tracking Study, UNIVAC. Here a^2 is assumed to be zero, and a special device is used when data is missed to increase the covariance values.

3.2.3.1 (continued)

The response of the tracking filter under these measures is numerically the same for corresponding random and deterministic inputs. Thus the mean square tracking error for a unit standard deviation of random noise (the error that would be obtained on a straight track with data errors after initial transients die down) is the same as the sum of error squares obtained when such a track is perturbed at one point by a unit displacement. This latter effect is perhaps typical of clutter interference, so that in designing a filter to optimally operate with position data noise we are simultaneously optimizing behavior in clutter.

Similarly, random acceleration held constant throughout a scan can be shown to be equivalent to a deterministic sharp turn in which the pivot point occurs at midscan. Also, the model of random impulsive accelerations leads to results equivalent to a deterministic sharp turn pivoting precisely at a scan time.

In view of the added complexity of track-oriented operations, we should like to forego the exact method of α, β selection and, instead, base these selections on the more heuristic method of "firmness" control presently used in RBTL. In order to motivate this, we show that such control can be adjusted to provide α, β selections which are in substantial agreement with those of the exact method. Hence, the current firmness control can be retained. It requires only adjustment in order to function optimally.

3.2.3.2 Steady State Analysis

The simplest way to develop our discussion is through analysis of the steady-state. That is, the track has been acquired a long time in the past so that initial transients have died out, the maneuver parameter λ is held fixed, and no data are missed. Then, by iterating the covariance recursions (19), we find that σ_{xx}, $\sigma_{x\dot{x}}$, $\sigma_{\dot{x}\dot{x}}$ converge to fixed values and, through (18), so do α, β. These steady-state optimal α, β values depend on the single parameter λ. As λ varies from 0 to ∞, the α, β pairs may be plotted as a trajectory in the α, β plane. This trajectory is our "standard" α, β curve. It has the form:

Standard α, β curve:

$$\alpha = \sqrt{2\beta} - \frac{1}{2}\beta \ . \tag{29}$$

Had we used an impulse acceleration model with its slightly different covariance recursion, we would have obtained a simple explicit relation between optimal steady-state α, β, viz.,

Alternate standard:

$$\beta^2 = \frac{\alpha^2}{2-\alpha} . \tag{30}$$

3.2.3.2 (continued)

In addition to such optimal α, β values, we can explore the use of other α, β in steady-state S & P, that is, perform a sensitivity study. A linear systems analysis of the S & P equations (17) with fixed but arbitrary α, β reveals that there are stability limits on the selection of α, β. Stable track S & P can be obtained by picking α, β within the triangle shown in figure 3-8.

In the same figure, we have shown contours along which the variance of prediction errors produced by a unit random error is constant (or equivalently, the effect of a single unit position perturbation, as was discussed above). Obviously, small α, β are best from the point of view of noise error smoothing.

On the other hand, an analysis of maneuvers shows an opposite tendency. Figure 3-9 illustrates contours of constant sums of squares of prediction deviation due to a turn maneuver with pivot at a scan point (or alternatively, of deviation variance due to impulse accelerations). The contours corresponding to these for our standard (constant through each scan) acceleration model are simply equilateral hyperbolas in the α, β plane.

In figure 3-10, we show the lower left unit square portion of the triangle. Both the family of equilateral hyperbolas and the family of constant noise variance component contours are drawn. Their points of mutual tangency define our standard α, β curve, since such a point is reached by keeping the maneuver error component fixed while minimizing the effect of noise or vice-versa. The maneuver error contours of figure 3-9 are almost hyperbolic in the lower left corner also, so that the alternate α, β curve is close to our standard one, departing most at the upper end where the alternate α, β is exactly 1, 1 (see figure 3-11). Although the standard curve departs from the unit square at the upper end, reaching the values $\alpha = 1$, $\beta = 2$, for $\lambda = \infty$, these values are of little practical interest. A reasonable range of λ values, which are marked on the curve, restrict consideration to the area of the unit square.

One use for the double family of contours and their attached variance factors in figure 3-10 is to gauge the sensitivity of the prediction errors to departures from optimal α, β. We see that there is a rather wide strip running on either side of the optimal curve where a choice of α, β would result in only negligible degradation.

This point is further explored in figure 3-11, where we have analyzed the envelope of the samples of prediction error in making a sharp turn. Besides the standard and the alternate α, β curves which are included for reference, the diagram shows lines of constant damping ratio for the maneuver transient. A damping ratio, $\zeta = 1.0$, represents a critically dumped system. There is no oscillation or hunting of the S & P after the turn with these α, β pairs.

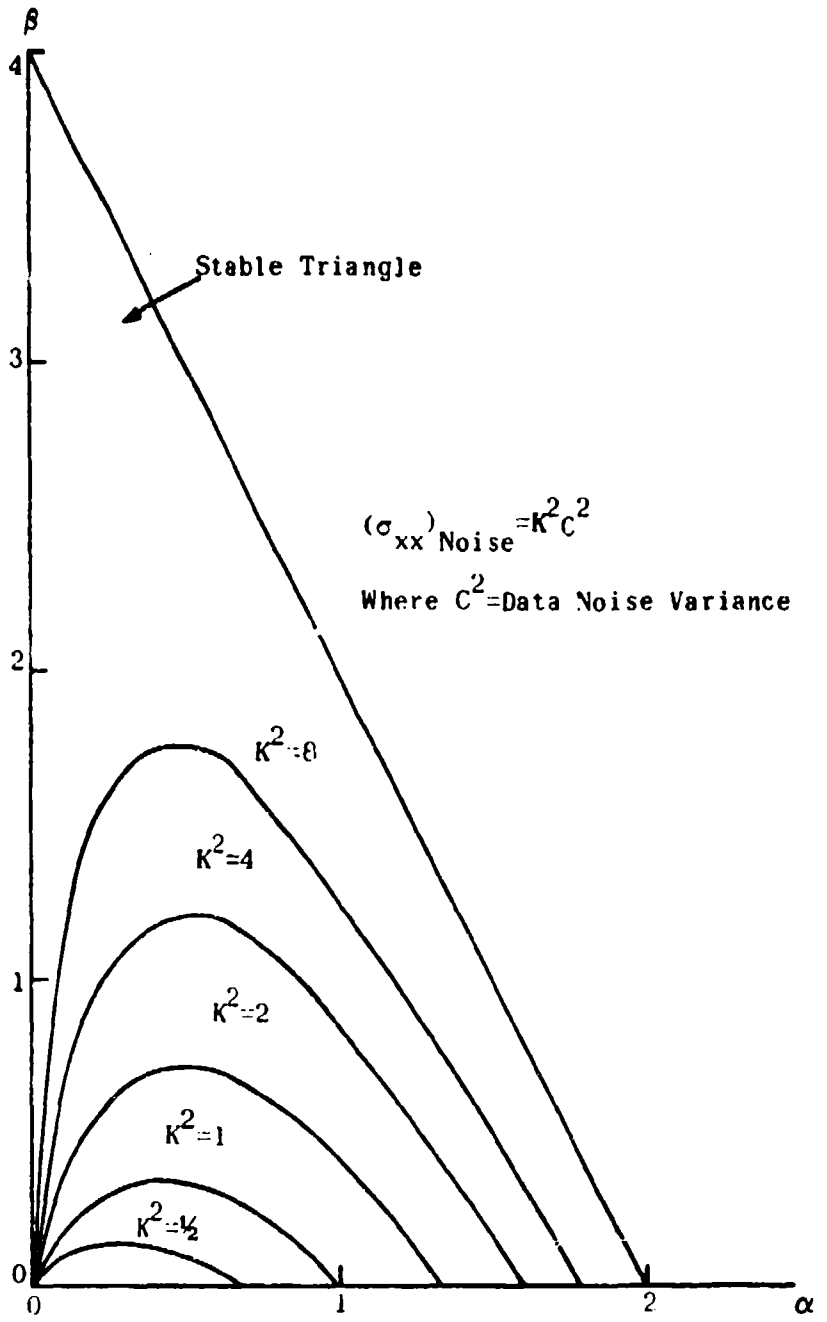

Figure 3-8. Variance Factor of Position Prediction Errors Due to Data Noise

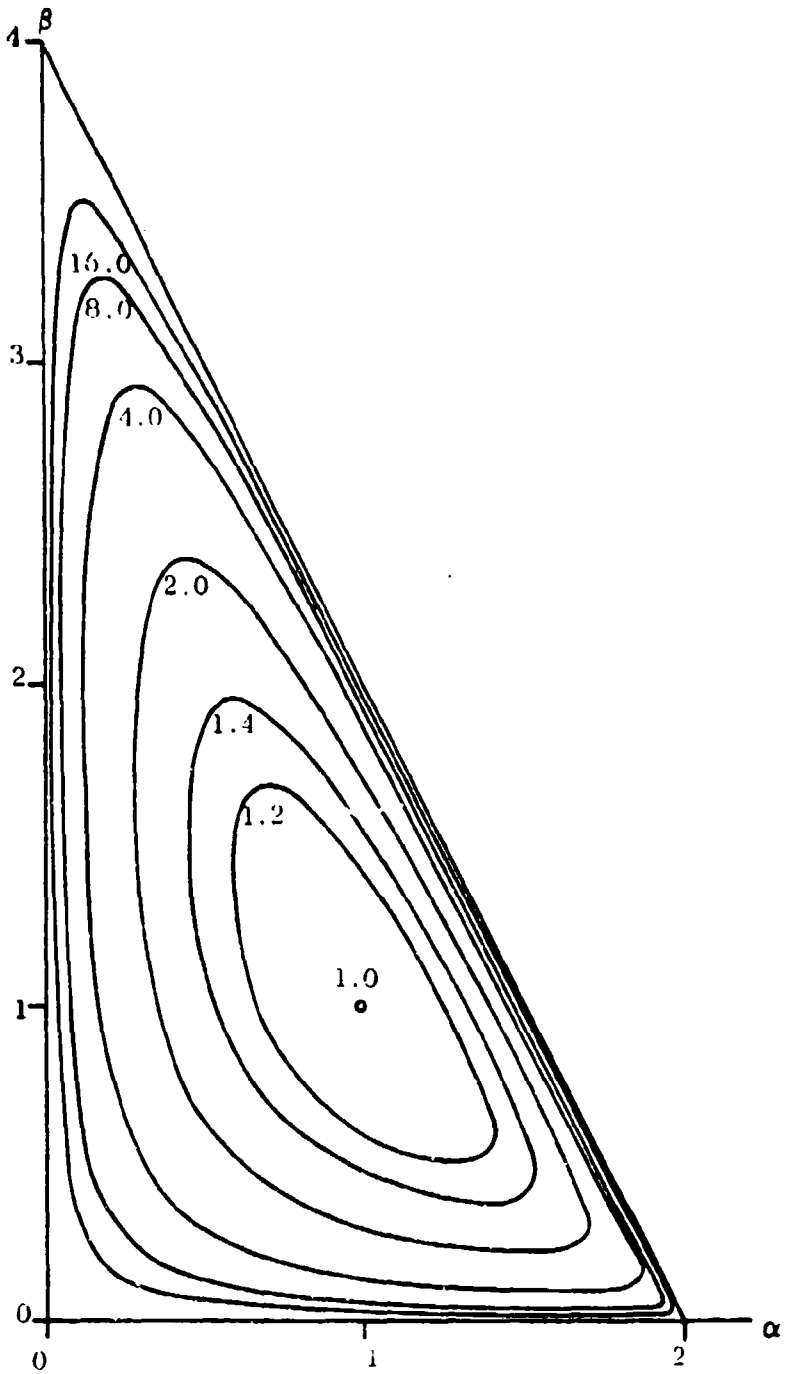

Figure 3-9. Sums of Squares of One Component of Prediction Error on Right Angle Turn

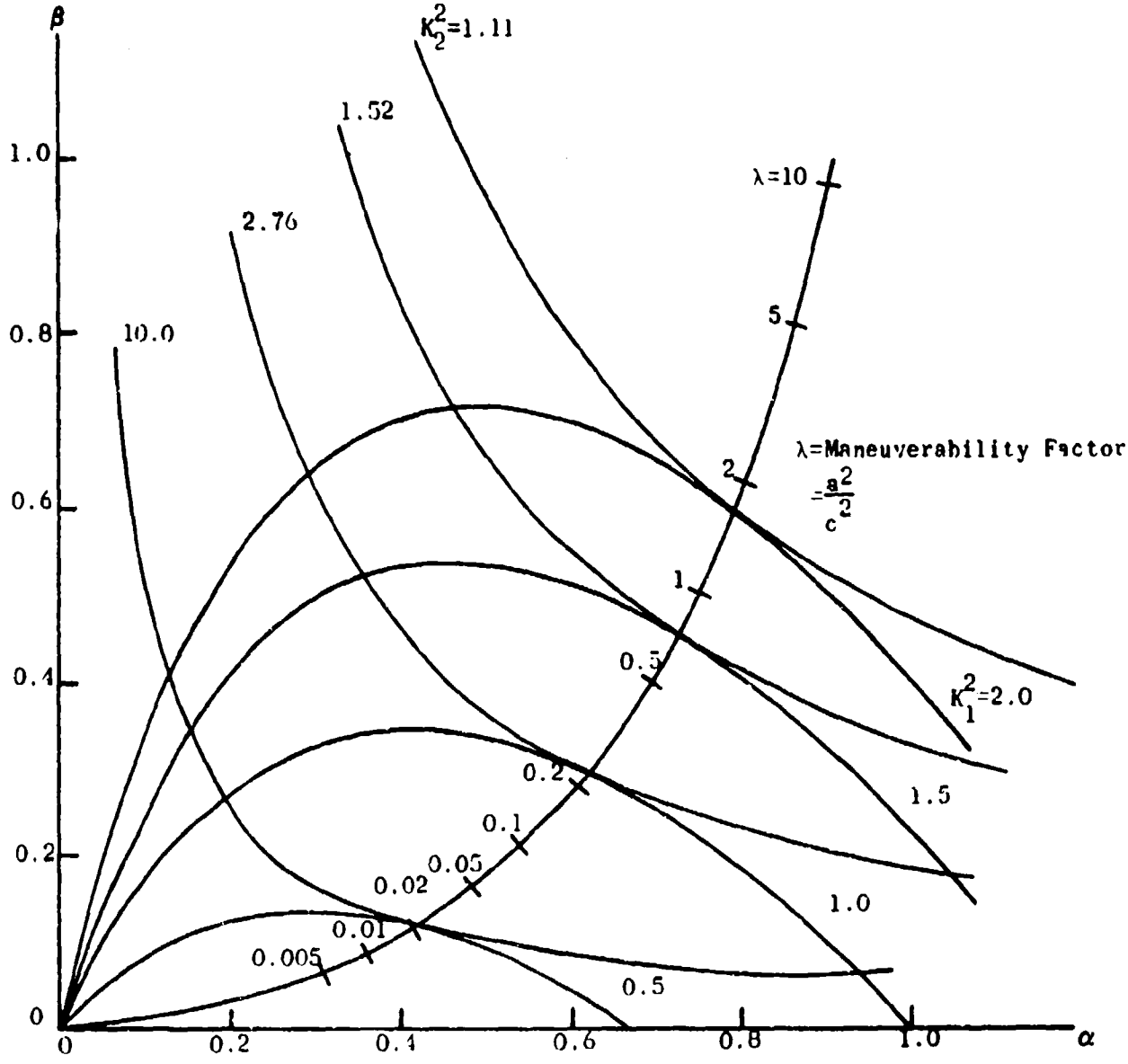

K_1^2 • C^2=Prediction Variance (Component) Due to Observation Errors

λK_2^2 • C^2=Prediction Variance (Component) Due to Random Maneuvers

Figure 3-10. Variance Factor Contours and Optimal α, β Curve

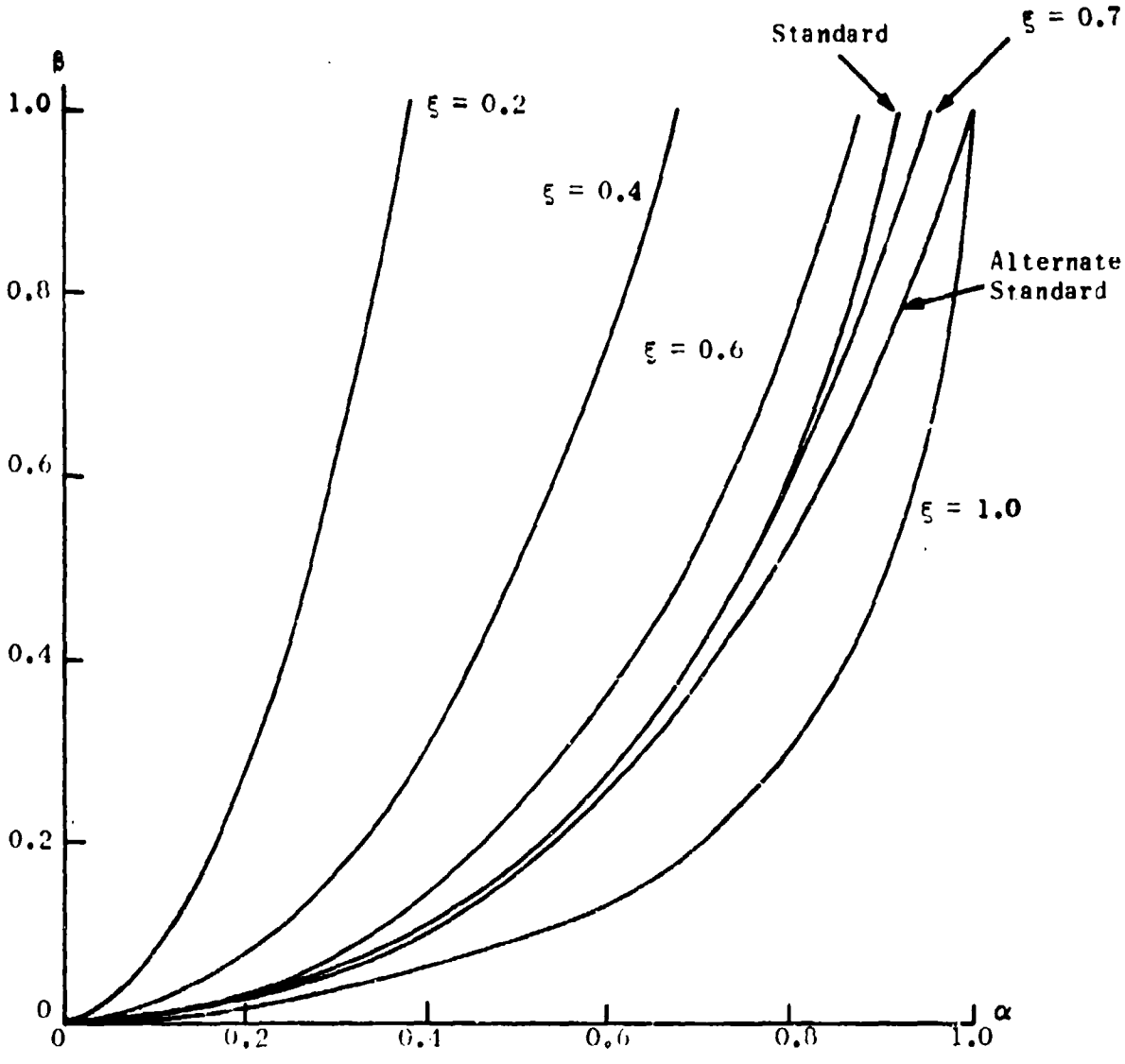

Figure 3-11. Optimal α, β Curves and Damping Contours

3.2.3.2 (continued)

When $\xi = 0.2$, the turn transient is quite underdamped, and, although the S & P estimates recover from the transient more quickly, they overshoot that recovery and oscillate several times before settling. Designers are accustomed to adjust such transient response to about $\xi = 0.7$, which provides a good compromise between quick recovery and degree of ringing. We note with satisfaction that our optimal standard α, β curve coincides closely with optimum damping.

In figure 3-12, we have plotted the current set of RBTL α, β values for comparison. Each successively lower point corresponds to a unit increase in the track firmness. The points match the standard curve quite nicely, except that they prefer the alternate curve end at $\alpha = 1$, $\beta = 1$. Since this end of the curve is sensitive to slight changes of the random acceleration model and since, as we shall see later, $\alpha = 1$, $\beta = 1$ is a prominent selection of optimal α, β in the start up (nonsteady-state) mode, we concur that the current α, β sequence represents an adequate and effectively optimal set.

3.2.3.3 Start-Up Mode

Having explored the steady state solutions of (18), (19), we now investigate the optimum α, β sequence which is appropriate for a track which has just been acquired. Initially we assume that any a priori information on the position and velocity of the aircraft is much cruder than that which can be obtained ultimately from the tracker. Mathematically, we set $\sigma_{xx} = A$, $\sigma_{\dot{x}\dot{x}} = A$, $\sigma_{x\dot{x}} = 0$ ($A > 0$, very large) to start the covariance recursions.

Substituting these initial ($n = 0$) values in (18), we find optimal $\alpha(0) = 1$, $\beta(0) = 0$, the expected result. That is, the initial data pickup is accepted, per se, as the initial position estimate, while velocity is not smoothed. Next, one use of the recursions shows that for the second ($n = 1$) return we need $\alpha(1) = 1$, $\beta(1) = 1$, again the expected result. The next iteration ($n = 2$) produces the values $\alpha(2) = (10 + \lambda)/(12 + \lambda)$, $\beta(2) = 3(4 + \lambda)/2(12 + \lambda)$. This process may be continued indefinitely. The sequence of optimal $\alpha(n)$, $\beta(n)$, which is produced for any λ parameter, converges finally to the steady state optimal α, β for that λ value.

Figure 3-13 shows such an α, β start up sequence for $\lambda = .1$ plotted in the α, β plane. The sequence (starting with $n = 1$) is plotted with large dots. It essentially converges to the steady state value by $n = 6$ and lies on the standard steady state curve as shown in the diagram. When this experiment is repeated for other λ values in the realistic range 0 to 5, somewhat different α, β trajectories are found. However, they all lie included within the boundaries of the standard curve on top and a similar lower envelope curve on the bottom as shown in the figure. Successive points fall somewhere on the series of heavy traces indicated between these boundaries. As the points descend, they follow the lower limit of these traces until they reach the β level appropriate for the assumed λ. Then the points converge into the steady state curve.

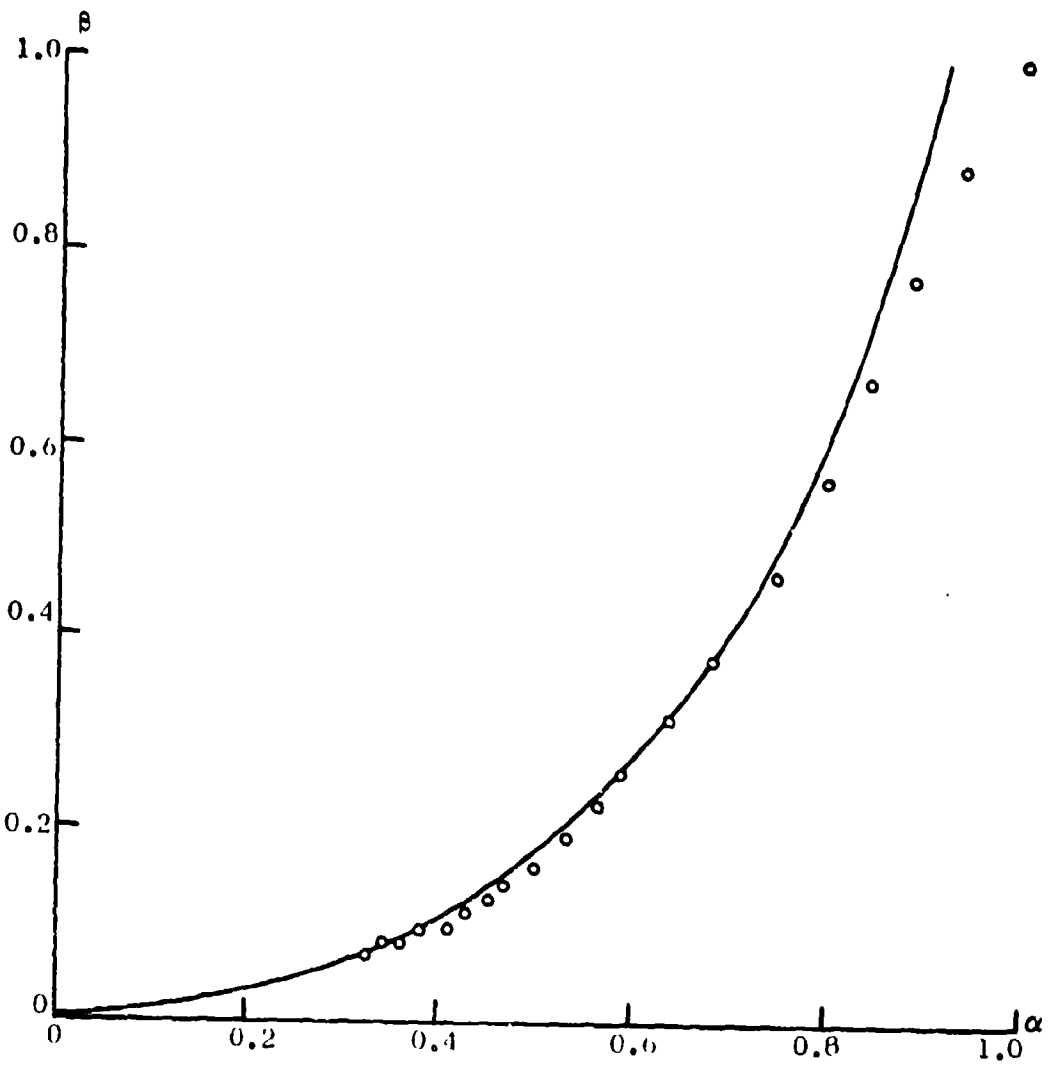

Figure 3-12. α, β Values Used in RBTL System (compared with standard curve)

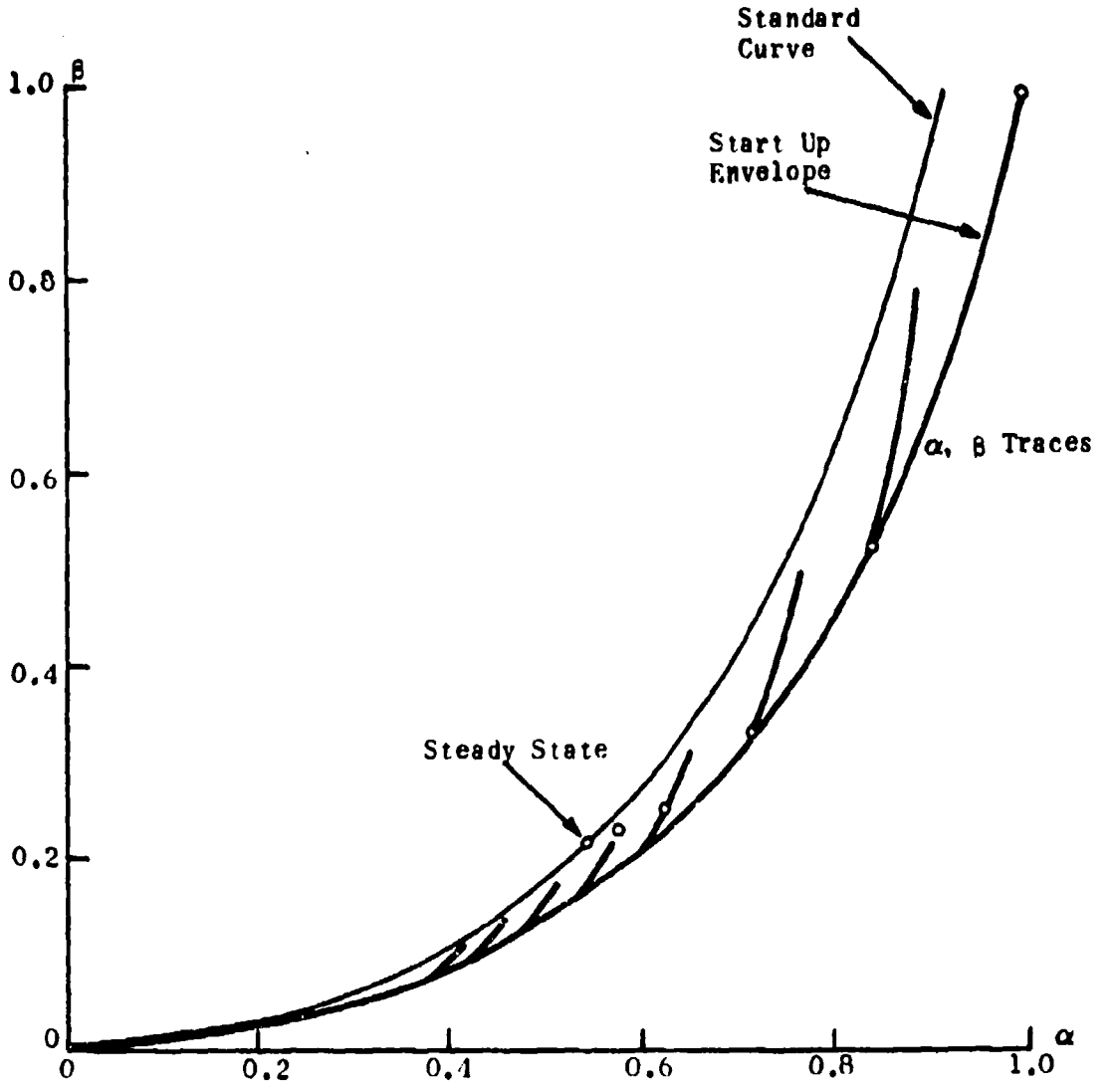

Figure 3-13. Optimal α, β Start-up Sequence

3.2.3.3 (continued)

Since the total constellation of optimal α, β values lies near the standard curve, this result shows that suitable α, β from the steady state curve may also be used for approximately optimal start up. Further, since the sequence values cluster along the heavy traces, we can define approximately a universal set of such steady state α, β opposite these traces which do not depend on λ. Then, in order to start up a track having a presumed λ, we follow the standard sequence as it descends until it reaches the level appropriate for that λ (the steady state α, β for that λ). The sequence then continues in a steady state mode with constant α, β.

By comparing the sequence of traces in figure 3-13 with the RBTL set of α, β values in figure 3-12, we see that a firmness increment of +3 for each successive return produces an appropriate selection of α, β from the RBTL set for start up.

3.2.3.4 Missed Returns

A similar study can be made of the progression of optimal α, β when returns are missed. For this purpose we assume that the S & P is initially in a steady state with no misses. Then a succession of data is missed. Finally the data resumes with no misses. This computation is performed using (18), (19) with $h(n) = 0$ during the miss sequence and $h(n) = 1$ otherwise. After each miss the values of α, β are determined for the next scan even though they may not actually be employed if data is again missed. In this way, we keep calculating an optimal α, β for use with the first return after a sequence of misses. On the subsequent scan after that the smoothing is said to be in a recovery mode.

In order to compare these results easily with the current RBTL smoothing, we must remember that the RBTL smoothing equation for velocity differs slightly from (17). In RBTL the velocity constant β is divided by the time since the last data was received prior to the return being smoothed. (Here we have taken $\Delta t = 1$, so that the assumed velocity units are nm/scan.) Thus, if m scans are missed in RBTL, β would be divided by m. In order that RBTL should use the β we desire according to (17), (18), we must premultiply our calculated optimal β values by m during the miss phase of operation. On recovery we revert to the normal situation.

Again the sequence of optimal α, β so computed depends on λ. In figures 3-14, 3-15, 3-16, we show the results for $\lambda = .2, .05, .01$ respectively, with a series of up to four misses. In each case, the α, β values start on the steady state standard curve and, with each miss, progress upward along, but not exactly on, the curve. Recovery is nearly completed in one scan back to the vicinity of the steady state α, β. Recovery values after four or fewer values lie along the heavy traces.

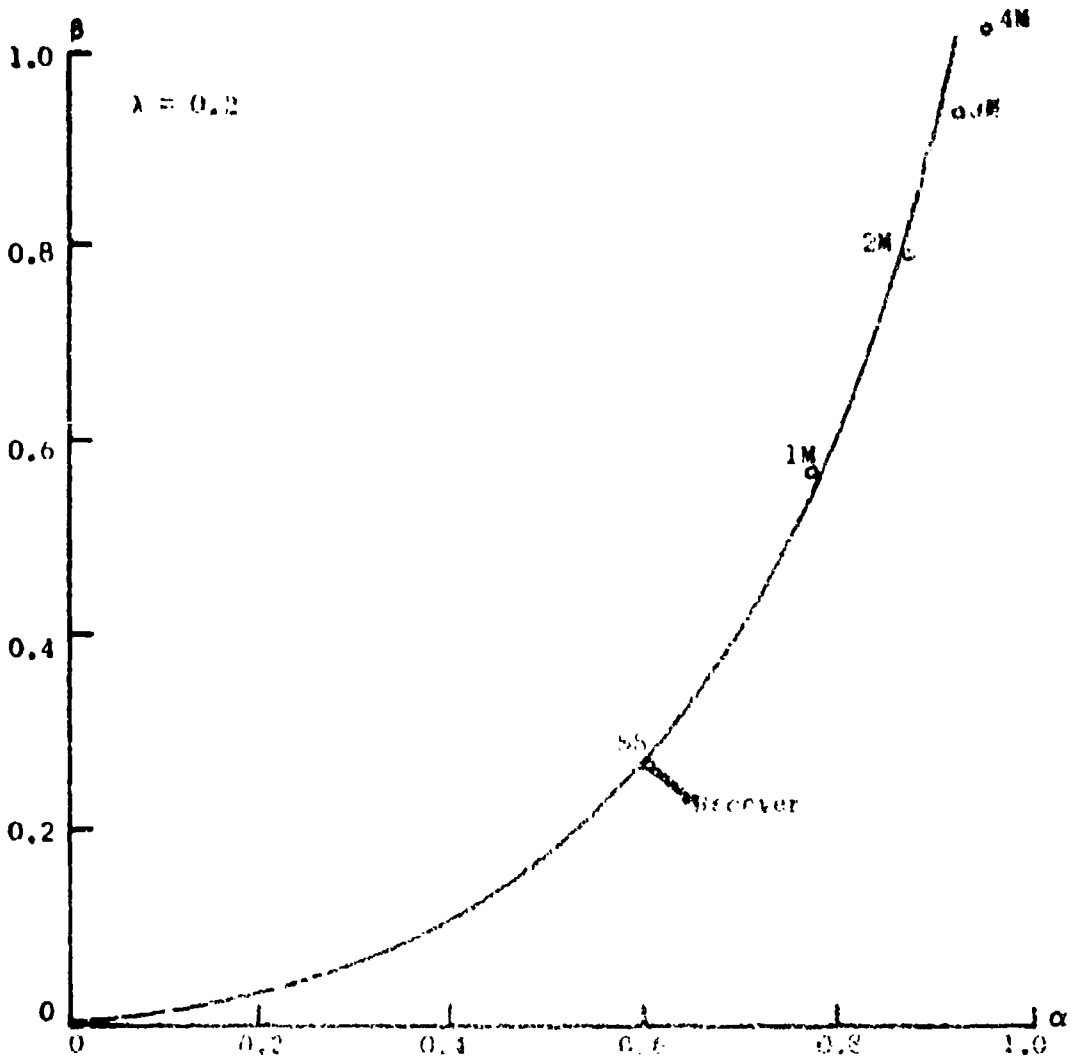

Figure 3-23 Optimal α, β for Missing Data Sequence

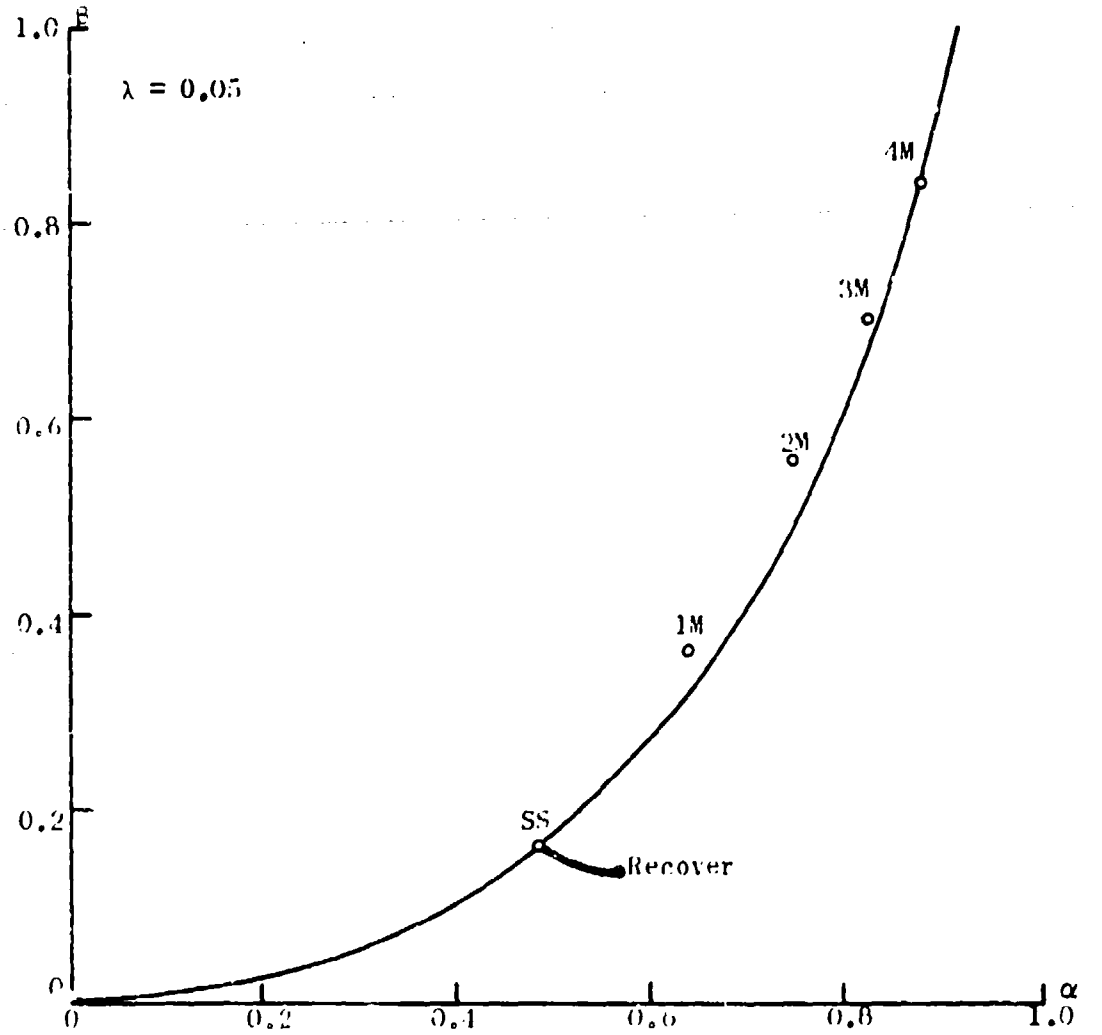

Figure 3-15. Optimal α, β for Missing Data Sequence

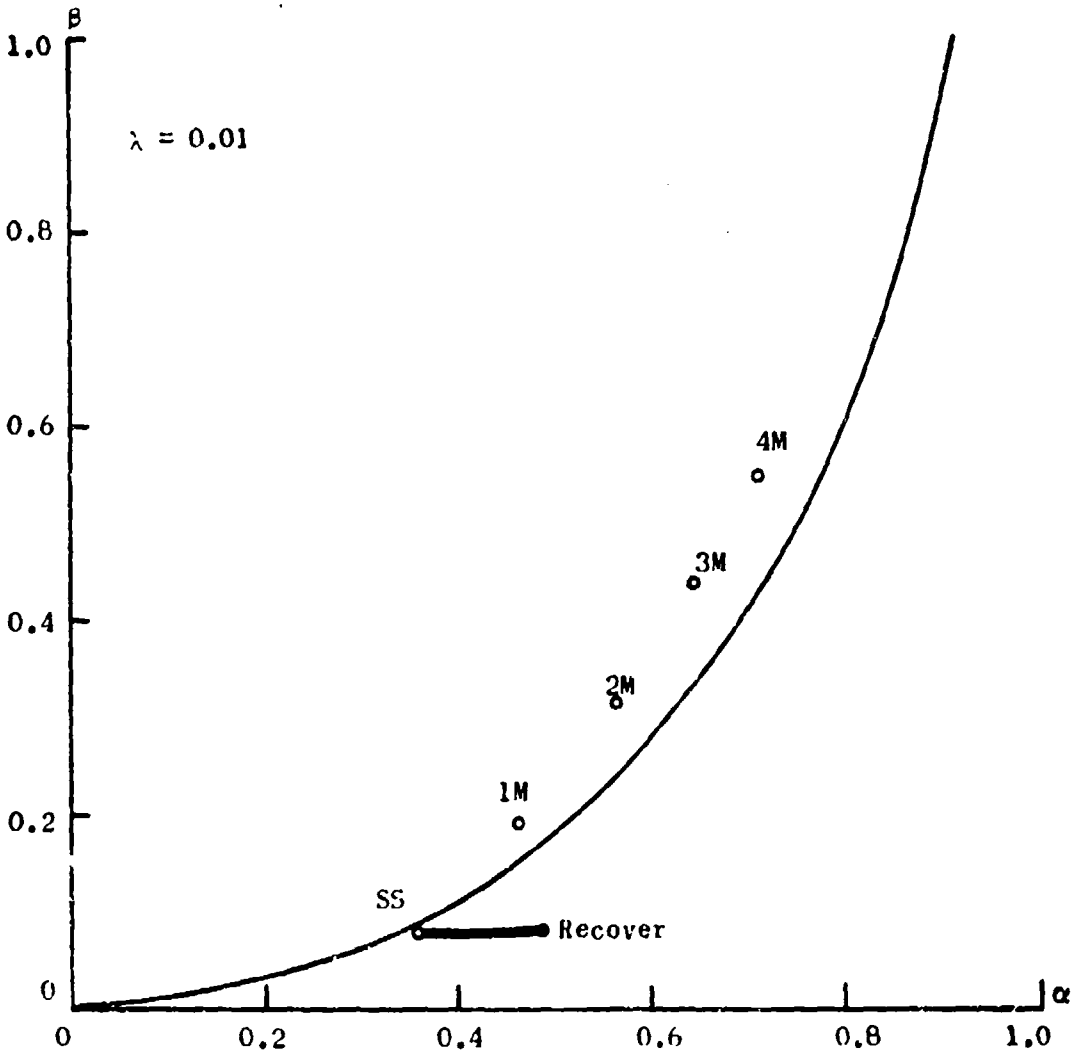

Figure 3-16. Optimal α, β for Missing Data Sequence

3.2.3.4 (continued)

These results again show that near optimal α, β can be selected from the standard curve, provided that the β smoothing is modified as in RBTL to divide the selected β by the number of scans since the last data (the number of misses plus one). The precise way in which the values are spaced up the curve, when data are missed, depends on λ. But, by taking $\lambda = .05$ as representative, we find that the spacings correspond to successive firmness changes of about -4, -3, -2, -1. On the other hand, recovery drops the α, β back at once to essentially the steady state level, and the firmness recovers likewise.

3.2.3.5 Data Combination and Variations

The above analysis applies to data of any of the three types: beacon only, radar only, or combined beacon and radar. For reference purposes, however, let us assume that the standard design is for beacon only data. In selecting a value of $\lambda = \frac{a^2}{c^2}$ for this case, we have designed for a particular population mix. The value of λ determines the maximum acceptable firmness according to the discussion in previous sections and limits the decrease of α, β values as firmness builds up.

Now, suppose instead that we are tracking with radar only. Assuming that the track population mix is still the same, the appropriate λ value scales inversely as c^2, the data error. Radar is somewhat more accurate than beacon but is more subject to extraneous (clutter) data. Hence, we should use an effective c^2 which increases in high clutter areas. Thus λ_r for radar is, in general, different from λ_b and more variable.

For either the beacon only or the radar only cases, the only effect of this λ selection is to provide a firmness limit. This limit itself may be taken as the primary parameter and made to depend on local clutter conditions, on the geography of the region, on flight plan information, and on the data error variance computed for each component of motion being tracked. Thus, we would increase the firmness limit of a radar track in the vicinity of clutter (as shown by the system clutter map). We would increase the limit in geographical regions where straight tracks predominate and decrease it where maneuvering tracks are most frequent. We would increase the firmness limit when, according to the flight plan, the track should be straight and decrease it during a time interval containing each planned maneuver. Maximum firmness would increase as the position measurement error variance decreases.

The picture that one obtains, therefore, is of a constantly varying firmness limit for each track which, if decreasing, may drag the current track firmness along with it.

3.2.3.5 (continued)

In view of the great uncertainty in assigning λ in the first place, exact analysis of the magnitudes of the above effects does not seem warranted. We can get a reasonable idea of the required changes in firmness limit first by relating firmness to λ through comparison of figures 3-10 and 3-12, and then by estimating the relative changes in a^2 and c^2 which form λ. A λ variation factor of 2 is equivalent to a firmness limit change of about 2. Thus, each of the above effects can be related to a simple (small) integer additive correction to the firmness limit. An appropriate table of correction values versus effect levels should be verified through simulation studies in varying data environments.

When a track has combined beacon and radar data without misses, the analysis is similar to the above, although the basic λ_{comb} (omitting variations) for which the system is designed is larger than either λ_b or λ_r. The S & P program now uses combined returns as in (11). Equation (12) shows that c^2_{comb} is smaller than either c^2_b or c^2_r. A typical relation is that $c^2_{comb} \approx c^2_b/3$, so that $\lambda_{comb} = 3\lambda_b$. Therefore, the firmness limit for beacon only tracking should be +3 or +4 units higher than for combined beacon and radar tracking.

When either beacon or radar (but not both) returns are missed in combined tracked data, it is in effect a partial miss. We have not inspected the detailed behavior of α, β via the exact recursions for this case (c^2 would vary from scan to scan). We suggest in this case that appropriate α, β can be found on the standard curve at a point whose firmness differs from the current track firmness by the same increment that the firmness limits differ for that type of data.

For instance, if a combined track loses a radar return, enter the α, β curve at the current firmness +3 or +4. A similar increase (not necessarily equal) would be applied to a radar return without beacon for its α, β lookup. On the other hand, the current firmness, as remembered in the track file, would follow the usual progressions based on hit or total miss. For that purpose one return would be equivalent to a combined report.

In practice, it would be quite difficult (or perhaps trivial) to distinguish a beacon only from a radar-plus-beacon track, since absence of radar may be only a temporary problem. Thus, we propose to establish tracks as beacon (discrete, nondiscrete, mode C classes) or radar tracks. A beacon track may or may not have radar data. Therefore, the above firmness control should actually be slaved to only these two types of tracks. This can be accomplished by inverting the operations described for the beacon-plus-radar case when radar is lost. That is, a beacon track with or without radar keeps firmness on the same basis as the beacon only track. The firmness limit is adjusted accordingly. When radar data also is received, the α, β table is entered at a lower level of firmness. When radar only data is processed, the table is entered at a firmness corresponding to the sum of two correction terms, one for adding the radar return and the other for subtracting the beacon. The control is the same as that previously described, only the reference is shifted to the beacon only alternative.

3.2.3.6 Track-Oriented α, β Control

In order to select suitable α, β for the longitudinal and transverse directions in track oriented S & P, one can simply adopt the approach of the previous section. There, the controlling ratio, $\lambda = a^2/c^2$, was different in different situations because c^2 varied. Here, the principal cause of variation is a different a^2 describing acceleration magnitudes separately along and across the track. As before, the present effect of λ is incorporated into the algorithm by way of the maximum firmness.

Since the maximum firmness is different in the two directions, we shall now need a separate running calculation of firmness in longitudinal and transverse directions for each track. Each such measure has its different limit. The limit on the longitudinal firmness is higher than on the transverse firmness (a difference of +10 to +15 is appropriate).

The previous controls on the limits based on data quality, etc., expressed in terms of limit shifts, may now be additionally applied. In particular, data error effects (ρ, θ elongation) may be applied separately by calculating (26), their variance resolution on the track oriented axes, and then entering a table of firmness limit shifts vs. c^2.

In order to provide somewhat smaller α, β values for longitudinal S & P, it may be necessary to extend the RBTL list of α, β to higher firmness levels.

3.2.3.7 Deviation Controlled Smoothing

It is interesting to note that the shifts in maximum firmness levels which have been proposed as a function of the local data conditions, component maneuverabilities, etc., (as sensed or provided by external information) alter, in effect, the S & P filter time constants. Or, in other words, the span of past data which is effectively used to produce current S & P estimates is made to vary in a way appropriate for the conditions. In this section, we consider using the data itself for this purpose.

We have already shown that varying the order of the filter to permit acceleration smoothing (equivalent to parabolic curve fitting) is not feasible for most track population assumptions under current conditions. Now let us consider the possibility of estimating the maneuver variance parameter, a^2, from the data.

We begin with an aircraft being tracked optimally in the steady state, firmly established, at low maneuverability ($\lambda = .02$). The error variance factors for $\alpha = .41$ and $\beta = .11$, optimal, may be read from the contours of figure 3-10.

3.2.3.7 (continued)

The maneuver variance factor is $K_2 = 11.2$; the measurement error variance factor is $K_1 = .47$. Together they imply that, if α, β remain fixed but $\lambda = a^2/c^2$ varies, the total one-scan position prediction error variance, e^2, in one component is given by,

$$e^2 = (K_1 + K_2\lambda)c^2 \qquad (31)$$
$$= (.47 + 11.2\lambda)c^2.$$

The difference between the predicted and measured component positions (called the deviation) is the sum of two uncorrelated errors, the above prediction error and the data error. Adding variances, we find that the deviation variance, D^2, is

$$D^2 = (1.47 + 11.2\lambda)c^2 \quad . \qquad (32)$$

In the optimal steady state condition, when $\lambda = .02$, this variance is $D^2 = 1.69c^2$.

Now suppose that the maneuverability of the aircraft increases, i.e., λ increases, but that the filter α, β are retained as before. The only evidence of such an increase in the data are the data deviations mentioned above. In order that such an increase be reliably evident from one sample, we would require λ to be large enough to produce a D^2 in (32) which is at least 4 times $1.69c^2$. The λ which does this is $\lambda = .47$. This process may be repeated starting with optimal tracking at $\lambda = .47$ to obtain the next level of $\lambda = 5.2$. These two jumps just about exhaust the distinguishable levels of maneuverability and correspond to firmness changes of -6.

It is interesting to note that this process will not work in the reverse order. If a track is established and optimally tracked in accordance with its maneuverability, and if the maneuverability then decreases, the decrease cannot be detected from one sample deviation. The measurement noise and nonoptimal (fast reaction) tracking in the new situation conspire to keep the deviations almost as large as before.

Therefore, deviation control on a one sample basis is strictly a mechanism for detecting maneuver increase. About three levels can be detected. Detection should be accompanied by a decrease in firmness. However, when no such detections are made, the firmness should be allowed to rise again in a normal start up progression until the limit is reached. Thus, the tracker always seeks to optimize for the least maneuverability for which it was designed, but it can be jumped temporarily to a more active state.

3.2.3.7 (continued)

Detection of the critical deviation can be based on comparison of this deviation with the search bin dimensions. In the next section, we show that an optimal search bin radius, R, is determined by the approximate relation $R^2 = 14D^2$, so that a deviation level threshold of $4D^2$ would imply that detection should occur at about $\sqrt{4/14}R$ or one-half of the bin radius.

The statistical problem of analyzing the use of more than one sample for deviation control is difficult because the sample deviations are correlated. Further, development of such methods and a more careful assessment of the basic idea are best based on simulation studies (see Appendix B). There is some evidence that use of two successive samples might be advantageous (each passing the critical deviation level).*

3.2.4 Search Bin Control

3.2.4.1 Mean Track Life

The object of search bin selection is to provide an area of search for data about a predicted position which, insofar as possible, will include the actual aircraft report but exclude extraneous data, such as clutter, reports from other aircraft, etc. Thus, we would like to make the search areas of minimum size, but are constrained to make them large enough to encompass the reports of the tracked aircraft. To be precise, we are interested in the position deviation vector $\underline{D}$ (see figure 3-5), used in the correlation process, as well as in track S & P.

$$\underline{D} = \begin{bmatrix} D_x \\ D_y \end{bmatrix} = \begin{bmatrix} z_x - \hat{\hat{x}} \\ z_y - \hat{\hat{y}} \end{bmatrix} \qquad (33)$$

Bins are generally centered on the predicted position, $\hat{\hat{x}}$, $\hat{\hat{y}}$.

$\underline{D}$ will fluctuate scan by scan as the data are received and S & P is performed. These fluctuations are produced both by data errors and by aircraft maneuvers. $\underline{D}$ is started within the search bin, and tracking continues until $\underline{D}$ becomes large enough to fall outside the bin. Then tracking falters because the data are no longer associated with the track and therefore cannot be used in S & P. We adopt the simple view here for purposes of analysis that the track is lost the first time $\underline{D}$ falls out of the bin. Thus, we do not consider the

*C40/50 Radar Inputs & Tracking Optimization - C50 Final Test report, Mitre Corporation.

3.2.4.1 (continued)

usefulness of any backup procedures (trial tracks, secondary bin data) for rescuing the track. Also, we neglect the perturbations in real world tracking caused by non-unity blip-scan. We assume that the aircraft maneuvers at random (random accelerations model).

For the tracking model which we have been studying, the mean value of $\underline{D}$ is zero, and the variance of a component of D (the x component), which we call σ^2, is given for the nth scan by

$$\sigma^2(n) = \sigma_{xx}(n) + c^2. \tag{34}$$

This result simply means that $\underline{D}$ consists of the sum of two uncorrelated errors, a prediction error affecting $\hat{x}$ and a measurement error affecting z. In principle, σ_{xx} is determined by the recursions (19). In particular, a steady state value of σ_{xx} leads through (34) to a steady state σ^2.

Now consider a population of cases in which we begin with the track well centered ($\underline{D} \approx 0$) and then observe the fluctuation of $\underline{D}$ until the track is lost. In each case we measure the track life in scans. We are interested in the mean track life as an indicator of the adequacy of the search bin size.

Exact mathematical solution of such a problem is difficult, but there exists a more tractable analogous problem whose solution can guide us. Consider the following analogy illustrated in figure 3-17. The particle of the figure has small mass and is attached to the center of the circle of radius R with a spring providing a linear restoring force. The particle motion is heavily damped by viscous friction in such a manner that, if the particle is released from an extended position, it returns to the center along a radial path, the distance diminishing exponentially with time constant, τ. Now assume that the particle begins at the center at time t = 0, and is subject to random external driving forces whose x, y components are independent, gaussian, white noise processes of zero mean. The particle will execute a continuous random walk about the center whose amplitude tends to increase until stopped by the restoring force. Let σ^2 be the steady-state variance of the amplitude thus achieved. The parameters τ and σ^2 completely describe the statistics of the motion of such a particle. At some time, T, the particle crosses the circle boundary for the first time. The average value $\overline{T}$ obtained by repeating this experiment is called the mean first passage time.

Now interpret the center as the predicted position of a track, while the particle represents the reported position. The circle corresponds to a correlation bin centered on the predicted position. The motion of the particle is a representation of the variation of the deviation vector as a function of time. τ is analogous to the time constant of the track filter, while σ^2 is the steady-state variance of each component $\underline{D}$. $\overline{T}$ is the mean time for the reports to first depart from the bin, i.e., the mean track life.

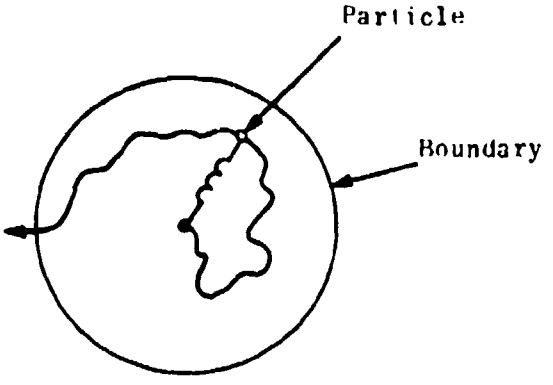

Figure 3-17. Analogy of Tracking Fluctuations by Particle Motion

3.2.4.1 (continued)

Of course the analogy is not complete, since we are approximating discrete jumps of the track difference vector by continuous motion. Further, the particle system is dynamically simpler than the usual tracking filters, since the latter involve not only position dynamics but velocity dynamics as well. The order of the difference (differential) equations is different. However, the replacement of discrete models by continuous ones has proved effective when applied to first passage times in the theory of sequential testing. Also, the tracking filter, as we have seen, is well damped for reasonable designs and exhibits an approximately exponential mode of decay. Thus, the approximations should be adequate for rough design guidance.

The solution of the particle first passage time problem is given by the formula,

$$\overline{T} = \tau f(\frac{R}{\sigma}) \ , \tag{35}$$

where the function f is graphed in figure 3-18. This plot shows a commanding feature. f varies rapidly over a range of 10 to 200 as R/σ varies from 3 to 4. The filter time constant τ can be deduced by observing the settling time of turn transients (see Appendix C). τ varies typically from 1 to 4 scans. Therefore, $\overline{T}$ is controlled principally by the selection of R/σ, which is rather critical. In order to insure a mean track life of 100 scans, we assign the design relation $R/\sigma = 3.75$, or, for adequate track life set:

$$R^2 = 14\sigma^2. \tag{36}$$

As an illustration of one use of this relation, let us estimate the data quality which will permit good tracking. (The following analysis neglects some of the dynamic adjustment or adaptive features of the tracker but provides a simple, rough, and useful result.) Suppose that the system has been following an aircraft in the steady-state, where, as usual, random maneuvers and data errors produce tracking error. The blip-scan is 1. The search radius R has been selected to produce good track life in these circumstances.

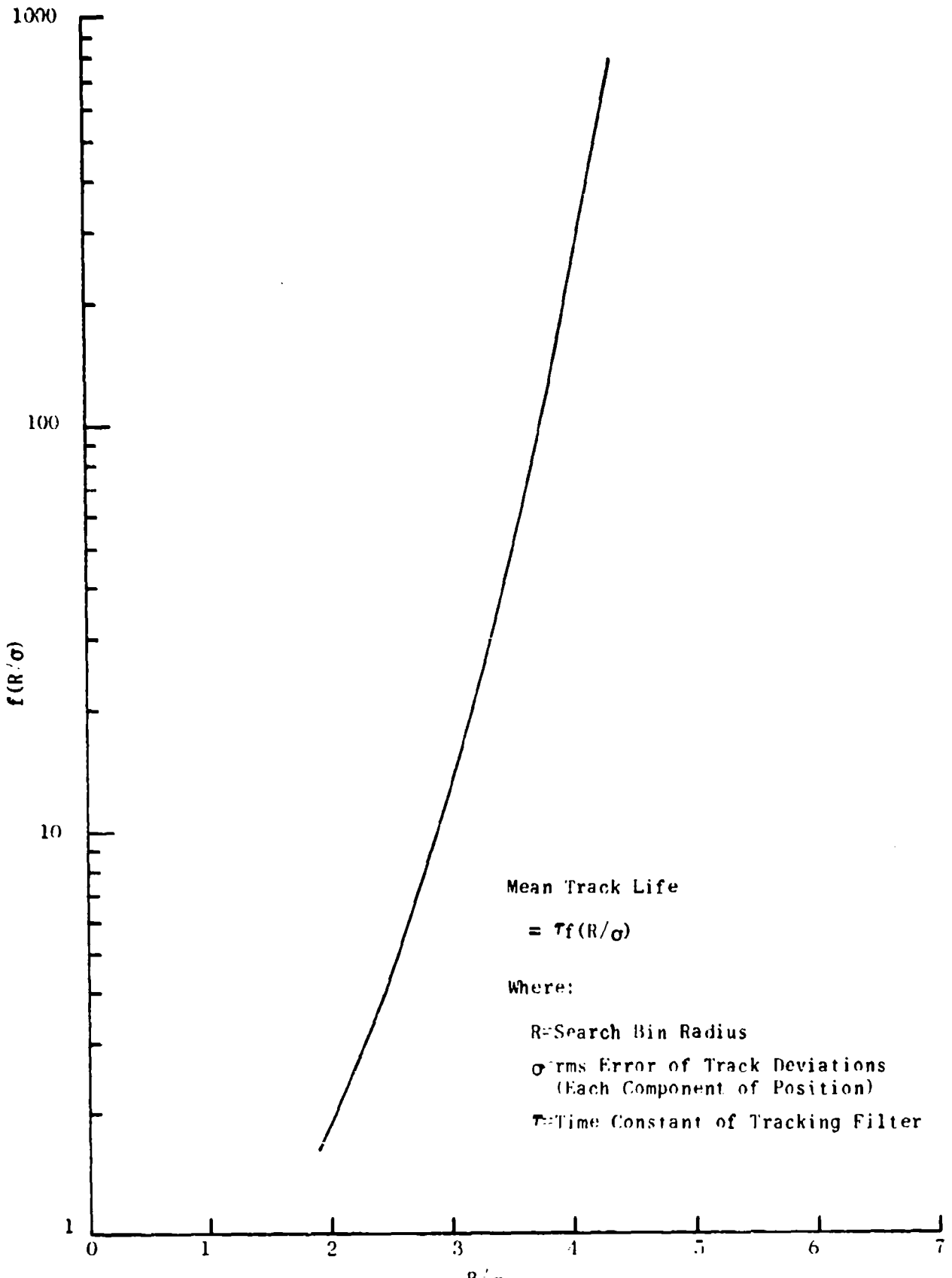

Figure 3-18. Mean Track Life Vs. Search Bin Size

3.2.4.1 (continued)

Now assume that the blip-scan reduces to a value $b < 1$, and the track runs into clutter with area density, A. Assume that the radius R remains fixed. The data error variance, c^2, is assumed small. How will clutter affect the tracking?

A major (perhaps the controlling) effect of clutter occurs when true track is lost and clutter is associated with the track instead. Because of an assumed nearest fit correlation logic, clutter rarely interferes when a true report is present. The rate at which clutter is associated for S & P is, therefore, $(1-b)\,A\pi R^2$ (for small A). The mean square deviation vector in such circumstances turns out to be $\frac{1}{2}R^2$, so that the mean square value of the clutter perturbations is $\frac{\pi}{2}(1-b)AR^4$. In order that these perturbations not be serious in reducing track life, they must at least be smaller than the mean square data noise perturbation $2c^2$ (two dimensions together). Thus we have a condition: $\frac{\pi}{2}(1-b)AR^4 < 2c^2$.

Using (36) and the approximate condition for steady state tracking, $\sigma^2 = 2c^2$. we find the condition

$$A(1-b)c^2 < .006 \text{ approximately.} \qquad (37)$$

For example, if we take c = .1 nm., A = .06 per degree mile, ($A \approx .18$ per nm^2 at 20 nm range) we find that $\beta = .8$ is adequate but $\beta = .5$ is not.

3.2.4.2 Bin Size Control

Now we consider the problem of controlling the size of correlation bins. We treat one component direction at a time, but recognize implicitly through (36) the existence of a second dimension. (A mean track life problem in two dimensions is not equal to a combination of two problems in one dimension.) The results apply to control of primary search bins, as in RBTL. Secondary bin sizes are made a constant multiple of the corresponding primary dimensions, just as in past designs.

Following the method used before for smoothing parameter selections, in this section we compare exact computation of bin sizes via the covariance recursion (18), relation (34) and criterion (36), with the more heuristic but computation saving procedure of firmness control. Again it appears that the firmness procedure can be adjusted to approximately match exact solutions.

We start by assuming that the track is in a start up mode (see Section 3.2.3.3). The recursions (18) produce a sequence of $\sigma_{xx}(n)$ prediction error variances for each successive scan, n, after the initial data report. The values become finite at n-2 and diminish gradually to a steady-state level which depends on the maneuverability parameter, λ.

3.2.4.2 (continued)

Corresponding behavior is seen for the deviation variance σ^2, according to the simple relation (34). Figure 3-19 shows a family of plots of this variance in normalized form $(\sigma^2(n)/c^2$ vs. scans after first data, n). We see that for various reasonable maneuverability assumptions (say $\lambda = .01$ to $\lambda = .1$), σ^2 has a steady-state level of about $2c^2$. Further, the general character of the curves is such that, as n increases, all curves descend in about the same manner until a steady-state level corresponding to λ is approached, where each curve breaks away from the family and remains at its own level.

In order to provide good track life, we would like to maintain relation (36). Therefore, figure 3-19 is also a plot of $R^2/14c^2$, and appropriate search bin sizes may be read from it. Therefore, the general behavior of R^2, as determined from these curves, is in conformance with the pattern of firmness control which we have previously suggested for α, β selection. Here we suggest that the ratio R/c be controlled by firmness. As data are received, firmness increases, and R/c decreases, until the (adaptively variable!) maximum firmness limit is achieved.

This concept is checked for a particular instance (beacon only, c = .1 nm) in table 3-4. Comparing the values in this table with current RBTL range bin values at corresponding stages of track life, we find that the RBTL values are somewhat excessive at initial stages. The sets of values cross at about n = 6, 7, and thereafter, as RBTL firmness continues to increase, the RBTL values become excessively small. The consequence of this has been verified in our computer experiments, where the RBTL tracker tends uniformly to lose tracks from the primary area in a maneuver due to bin constriction. (Of course, the secondary search mode of operation saves many of these potentially lost tracks.)

TABLE 3-4. SEARCH BIN SIZE VERSUS TRACK HISTORY

Scans After First Data	R (Suggested Search Interval)
2	5500 ft.
3	4100
4	3600
5	3300
6	3150
7	3000
8	2900
9	2800
10	2750

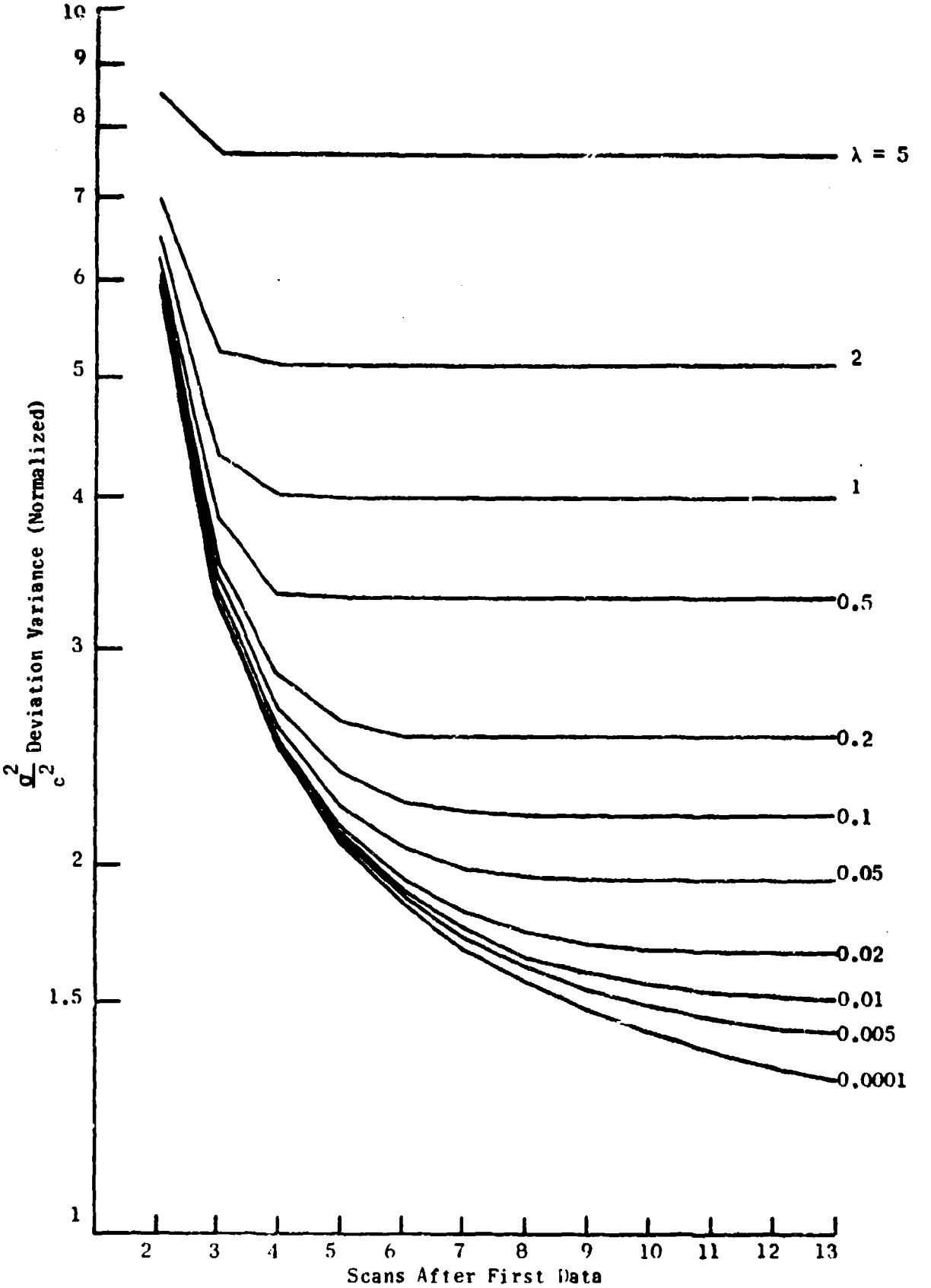

Figure 3-19. Deviation Variance Behavior in Start-up Sequence

3.2.4.2 (continued)

Note the important fact that we propose to control the ratio R/c with firmness, not R directly. By using the c values appropriate for the data type being used, the area of operation, or the direction component, we can produce a search bin size which is matched to the various data conditions. We shall call the table of R/c vs. firmness our "standard" table.

As before, for the α, β analysis, we can exercize the covariance recursions (19) for a track beginning in the steady-state, missing consecutive data (4 misses), and recovering. Again, the normalized deviation variance, $\sigma^2(n)/c^2$, is plotted for the successive scans, one curve in figure 3-20 being obtained for each value of λ. If the rate at which these curves rise with missing data is gauged and compared with the start up curve ($\lambda = .0001$) in figure 3-19, we see that firmness changes of about -4, -3, -2, -1 produce an appropriate increase in search size through firmness control as successive reports are missed. This corresponds to a similar result obtained for α, β control, and reinforces the conclusion that a common firmness measure can control both α, β and search bin size selection.

The above analysis is applicable to data from either a radar only or beacon (with or without radar). In each case, R/c is controlled and R is computed for the appropriate data standard deviation, c, based on the track type and local conditions.

The above parallelism of the firmness control procedure for α, β and R/c selection is not fortuitous. It is rigidly established by relations (18), (34), and (36). In fact, with them, optimal α can be expressed in terms of optimal R/c:

$$\alpha = 1 - \frac{c^2}{\sigma^2} = 1 - 14\,\frac{c^2}{R^2} \,. \qquad (38)$$

Therefore, a method for α selection (and β through the standard curve) is equally a method for R/c selection. Firmness control of either parameter can be based on the identical set of levels and variations. For example, in deviation control of smoothing, we discuss appropriate firmness level jumps for α, β selection. Relation (38) shows how to apply the same selection process to the operation of deviation controlled search bins; e.g., if α is increased as a result of a large deviation, R/c is increased in subsequent scans according to (38).

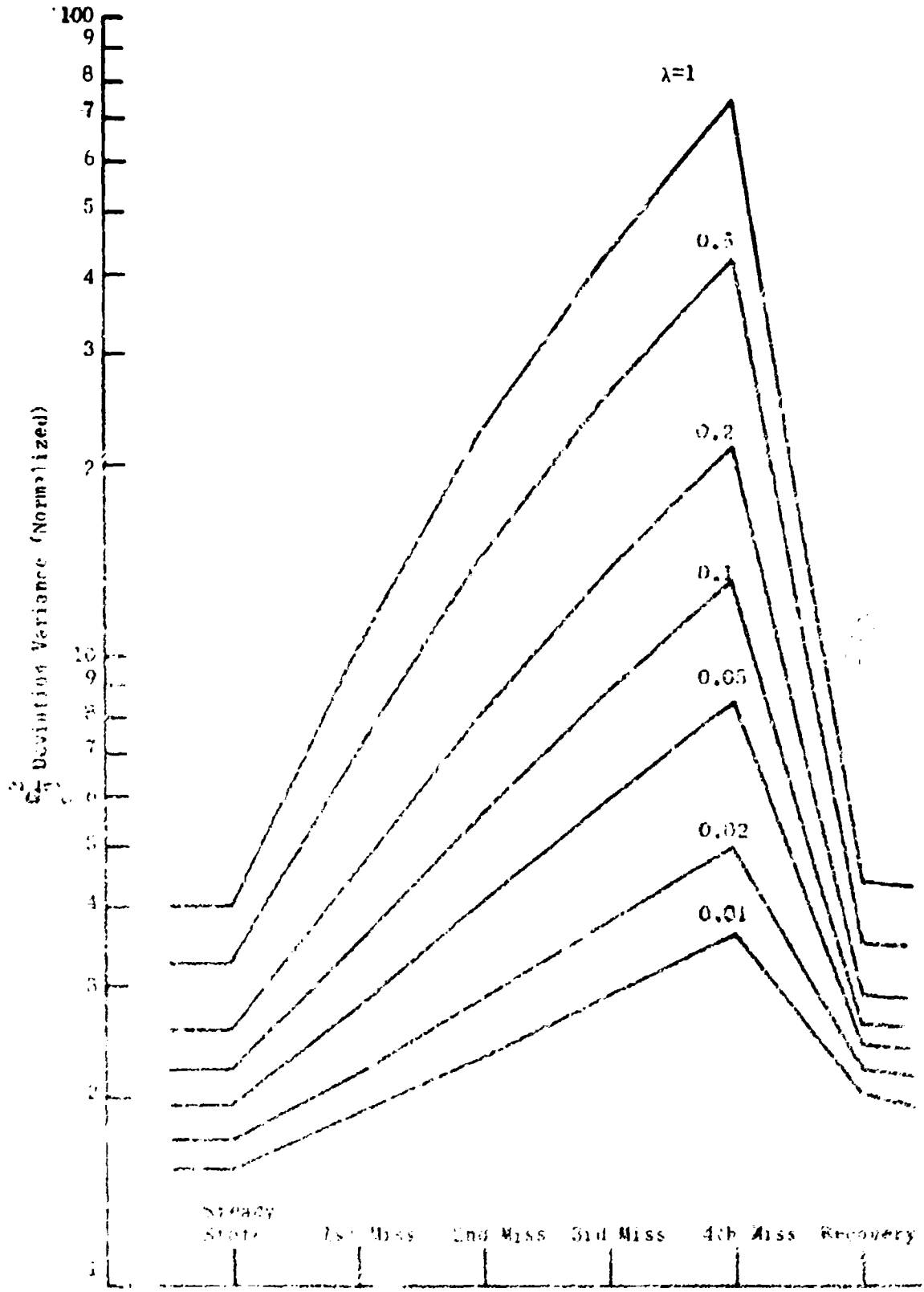

[illegible], Deviation Variance Behavior in Missing Data Sequence

3.2.4.2 (continued)

The above process of bin size control results in a selection of a radar bin for a radar track and a beacon bin for a beacon track. The correlation routine (section 3.1), however, constructs an additional radar bin, in the latter case, for the correlation sequence. Since, in the augmented configuration, the radar and beacon data error variances are similar functions of range, and since the radar yields backup data rather than intimately determining track life, the dimensions of the radar bin may be determined more freely. In particular, they may be made a simple fraction of the beacon dimensions, may be deliberately undersized to exclude more clutter, and may have this fraction varied according to local clutter (clutter map) conditions.

One final point needs to be mentioned. The recursions (19) yield infinite variances and, thus, infinite search bins for the first report after the initial report. This result is solely due to the fact that no speed constraint was placed in the dynamic assumption or initial conditions of the model. Therefore, the first search bin requires a special consideration based on the maximum speed of the aircraft population to be tracked. Very simply, we should set

$$R = V_{max}\Delta t + 2.5c \qquad (39)$$

in order to be sure to find that second report.

3.2.4.3 Bin Shape Control

We discuss bin shape control in terms of the most general example: track-oriented S & P with unequal ρ, θ radar or beacon errors. Track-oriented operations are carried out with two independent firmness measures corresponding to along-and across-track directions. Each measure controls its own direction's α, β selections and R/c selections. In addition to longitudinal and transverse differences in the maneuver parameter, λ, the maximum firmness values allowed in each direction can be made to depend on the locally determined components of the data error. These oriented components are provided by projecting the ρ, θ error ellipse via equations (26) onto the track oriented axes.

The result of these operations is to define two values of bin size: $\pm R_L$, longitudinal bin, and $\pm R_T$, transverse bin. In effect, we now have another ellipse oriented orthogonally to the track direction. If, as before, we ignore the skew aspect of this shape with respect to the local ρ, θ axes, we can project it onto these axes. The projection relations are analogous to (26) and use the same $\sin^2(\varphi-\theta)$ value.

$$R_\rho^2 = R_L^2\cos^2(\varphi-\theta) + R_T^2\sin^2(\varphi-\theta) \qquad (40)$$

$$R_\theta^2 = R_L^2\sin^2(\varphi-\theta) + R_T^2\cos^2(\varphi-\theta).$$

3.2.4.3 (continued)

Then R_ρ and R_θ would be used in the usual ρ, θ correlation checks.

This method preserves as much of the information of the various error shapes as appears justified. At present, it appears worthwhile to preserve the feature of the simple ρ, θ correlation checks. At some later point it may be worthwhile to explore performance tradeoffs of (40) vs. retention of the oriented R_L, R_T ellipse or box.

3.3 TRACK INITIATION AND TERMINATION

3.3.1 Introduction

Target initiation and termination (I & T) are those decision processes by which tracks are identified, started, or dropped in the computer. Here we shall consider only the use of automatic logic applied to this task. This is an area where human operators tend, with experience, to become quite adept by employing an innate power of feature recognition in a visual display. But as always, when the load of such work increases there is need for mechanization. Then there arises a need to derive appropriate algorithms and to gauge the performance levels to be expected from them.

The problem of I & T has been considered in the context of an overall tracking surveillance problem from the point of view of maximum likelihood estimation and decision techniques.* These results which originally were based on a model in which the scan intervals, Δt, were of random duration, have been revised to fit the current constant scan rate. The main structural conclusions have not been altered by this. They provide a framework for the following discussions.

A major conclusion is that optimal design of track correlation, smoothing and prediction, and initiation and termination should and can be an integrated whole. There is no conflict among the various tasks. For example, optimal tracking S & P uses the data provided by optimal correlation, and vice-versa (through feedback of the track predictions). Optimal I & T is based on the same basic scoring procedure that is used in optimal correlation, while optimal correlation provides the proper data for optimal I & T.

---

*Robert W. Sittler, "An Optimal Data Association Problem in Surveillance Theory", IEEE Transactions on Military Electronics, Vol. MIL-8 n 2, pp. 125-139, April 1964.

3.3.1 (continued)

Therefore, we can at once say that the correlation technique proposed in Section 3.1 and the S & P techniques proposed in Section 3.2 are immediately applicable to tracks of all categories, established, tentative, or dropping.

One special feature deserves comment: initiation processing is commenced as usual from the unused report file. However, as with the usual subsequent correlation of Section 3.1, a combined report file is not used. Instead, the beacon file is searched first. When an unused beacon return is found, that position is used to search for a supporting unused radar return. If found, the scoring is adjusted accordingly, and the combined report is delivered for (trivial) track S & P. The required search bin is just big enough to contain the sum of the beacon and radar data errors. Hence it is this point in processing, when combination occurs, which is the same as that of the present RBTL design. Subsequent combinations, of course, are made with larger bins and routinely delivered by correlation to S & P.

Beacon or beacon and radar reports are removed as they are picked up in this first pass. Then a pass of the radar file is made for radar only initiation. During these passes it will be desirable to produce a mask of initial reports on an area basis, so that only a limited density of first report pickups can occur. Also, the clutter report map can be utilized to suppress first pickup in high clutter areas. In view of the subsequent discussion, this appears necessary to limit false initiations on radar only data in bad data situations.

I & T procedure can be further discussed on several levels. On one level, the maximum liklihood theoretical approach is useful in order to motivate the structure of algorithms. On the other hand, I & T performance estimates can be made (short of a full simulation approach) only by specializing the conceptual model to eliminate scoring nuances. On this second level, a successfully correlated report is given a fixed score; lack of a report is given another. Some performance estimates and tradeoffs, as well as optimal scores and thresholds, follow from this level of analysis.

However, the performance calculations at this level are based on approximate formulas used in the theory of sequential testing. These tend to be quite inaccurate in the current setting. Therefore, in order to reach a tractable and generally useful conclusion, we are on the third level of analysis, reduced to a detailed consideration of a specific restricted I & T decision logic which is not optimal but which yields to analysis. This is the set of rules where n consecutive reports are required for initiation and m consecutive misses are required for a termination. These can be implemented immediately within the current RBTL framework. Use of the sequential type of tests with the variable scores will require more extensive analysis/simulation work.

3.3.2 Maximum Likelihood Decision Scoring

In this section, we further pursue the maximum likelihood approach and define the data score on which it is based. We use the results of the analysis of a simplified problem in which tracking is not track-oriented, data is of one type (say radar only), and the data errors are isotropic. Conclusions based on this score can then be extended, in principle, to the more complex scoring of more elaborate models. This score is identifiable with the cumulative sum of individual scores used in track correlation processing throughout the life of the track.

Theory shows that each track has an attached total score consisting of the following score components:

$$L_o = \ln \frac{A_o b}{A_N(1-a(1-b))}, \qquad \text{the value of the initial report.} \tag{41}$$

$$L_i = \ln \frac{a^{n+1} b(1-b)^m}{2\pi\sigma^2 A_N} - \frac{1}{2\sigma^2}(D_x^2 + D_y^2) \qquad \text{the value for each scan where a report is present.}$$

$$L^* = [a^{m'+1}(1-b)^{m'} + (1-a)] \qquad \text{the value of the misses since the last report, if the current report is missed.}$$

Here the various quantities signify:

A_o = area density of the tracks entering the system.

A_N = area density of clutter.

b = track blip-scan.

a = track life factor (fraction of original population surviving after one scan).

m = number of successive misses between the last report and the present report.

m' = number of successive misses since the last report if the present scan has no report.

D_x, D_y = components of the deviation vector, the difference between predicted and reported position.

σ = standard deviation of either deviation component.

3.3.2 (continued)

Thus the total track score has the form

$$L = L_0 + \sum_{L=1}^{k} L_i + \begin{cases} 0 & \text{if report is present this scan,} \\ L^* & \text{if no report is present this scan.} \end{cases} \qquad (42)$$

Against this track score we have the competing total theoretical score value of L=0 when all reports in the track history are interpreted as clutter.

Consideration of the form of the second term of (41) motivates the choice of scoring function for our proposed method of correlation. The same features can be retained for I & T. In fact, we can utilize the same scores as computed and supplied by the correlation algorithm. In particular, these scores incorporate such effects as hit count in their composition which, thus, can be retained for I & T.

Note the important fact that this scoring system operates independently from the firmness system used to control α, β and bin selection. Thus, for the I & T decisions we are introducing a new methematical object which can reflect more of the nuances present in the data for the purposes of identification.

3.3.2.1 Initiation

As shown by previous analysis*, the use of the total score (42) for I & T revolves around the setting of certain thresholds or critical decision levels. The value of the score for the initial return is given by L_0. When the accumulated score passes the level L=0, initiation is accomplished (a track is not more probable than a spurious clutter trail). Typically for a radar system, we find that $L_0 < 0$, so that initiation on one report alone is not possible, and supporting reports are required. However, for beacon, especially discrete beacon with handoff information, the ratio of A_0/A_N (probability of finding the aircraft report vs. the probability of finding a spurious beacon report) would be quite high. Hence, under some circumstances, $L_0 < 0$ and the first report initiates a track. In any case, by substituting assumed values into the expression for L_0, the decision level difference $(0-L_0)$ is found, which is the score that the sum $\sum L_i$ must exceed for initiation.

* Ibid, pp. 125-139.

3.3.2.1 (continued)

In addition to the decision that a track is present, we also identify its category: radar only, or beacon (or combined) for tracking purposes, as well as discrete vs. nondiscrete, Mode C vs. non Mode C for correlation. For this we propose a simple hierarchical decision logic. A track is first assumed to be a radar only track until informed otherwise either by the receipt of external information or of beacon data. Beacon data will be correlated with this track if available, which irrevocably changes its status to beacon. The decisions within the beacon categories are controlled as in RBTL.

Reports used for initiation purposes are obtained as in RBTL, from a file of unused reports, after correlation of established tracks for that sector of operation has been completed.

As we have noted above, the α, β and bin selection processes are essentially the same as explained in the previous sections of 3.2. One exception occurs for the second track return, where we use a special bin size selection (39) based on maximum velocity and $\alpha = 1$, $\beta = 1$.

Proper bin size selection is based on a model of aircraft motion. Thus, on every scan, the bin delimits the region of search in accordance with the assumed dynamic acceleration model. However, the track S & P is neutral when it comes to restricting the velocity estimates. It will equally track an object of zero motion or of very rapid motion if they have acceptable accelerations. Thus, an added dimension of discrimination is provided by speed checks.

Three situations are shown in figure 3-21. In each case, the estimated speed is plotted (in continuous form for pictorial purposes - actually the values are sampled) as a function of the time since receipt and S & P of the second report. The true aircraft track has a speed estimate, crude at first, but eventually settling into a smaller steady-state fluctuation with average value about equal to the true speed. Physical minimum and maximum true speed limits are indicated. The Poisson clutter track speed estimate begins with a finite value. From there it fluctuates with the amplitude of variation growing without limit. Eventually, both the minimum and maximum speed limits are reached and recrossed repeatedly. On the other hand, the fixed clutter track speed estimate shows a steady fluctuation near or below minimum speed.

In order to provide speed or velocity filtering of equal applicability to all these cases, we would then define a table of upper and lower speed limits as a function of scans since the first return. These limits would be such that 1) the upper limit is equal to the maximum design speed plus 3 to 4 times the standard deviation of aircraft speed fluctuations (see table 3-5), and 2) the lower limit is equal to the minimum speed minus the same 3 to 4 standard deviations (or zero, whichever is larger). Finally, in order to handle the general case of nonunity blip-scan, this scan dependence would be altered to a similar dependence on firmness.

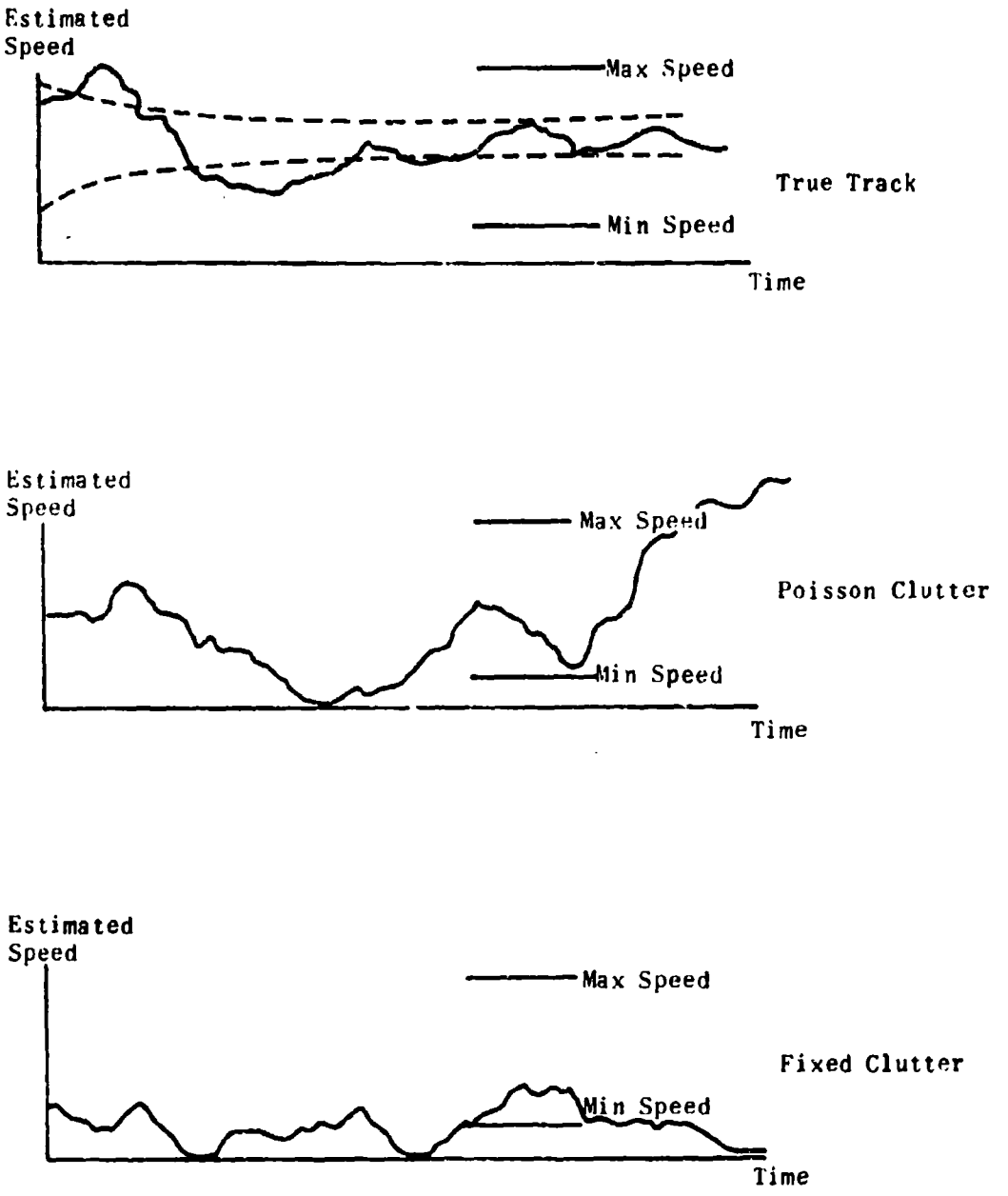

Figure 3-21. Estimated Speed Behavior in Three Situations

TABLE 3-5. STANDARD DEVIATIONS OF SPEED FLUCTUATIONS (for $\lambda = 0.01$)

Scans since 1st report	(Std. Dev./c) in nm/scan
2	2.00
3	1.06
4	0.67
5	0.50
6	0.41
7	0.36
8	0.34
9	0.33
steady-state	0.32

(Note c = std. dev. of either component of measurement error, assumed equal.)

3.3.2.1 (continued)

Thus, to reiterate, a suggested initiation procedure sets an initial score L_0 by (41) and accumulates the running score increments L_i, computed with the help of the already available data correlation scores. Speed checks are applied at every scan via the speed criterion table listed vs. firmness. If the score passes up through zero, the track status changes to established (normal). If it passes down through the original L_0, the track is dropped. (The maximum likelihood analysis shows this in Appendix C.) The α, β and bin size selection are the same as described for track S & P.

3.3.2.2 Termination

In order to logically investigate the track termination decision, we can use the model scoring system (41). The analysis is simplified if we use the assumption that the life of the objects being tracked is very long (compared with any reasonable sequence of data misses, say). This assumption is the same as setting a = 1 in (41).

When this is done we find that (41) specializes to:

$$L_0 = \ln \frac{A_0}{A_N} \tag{43}$$

$$L_i = \ln \frac{b}{2\pi\sigma^2 A_N} - \frac{1}{2\sigma^2} (D_x^2 + D_y^2) + m \ln(1-b)$$

$$L^* = m' \ln(1-b).$$

Analysis of these scores shows that track termination may occur in one of two ways. Either the cumulative score (42) using (43) can descend back down to the zero level, the original initiation threshold (then the track is dissolved because it is more likely, in its entirety, pure noise), or the increment provided by the first term of L_i, the only positive contribution, is less than the starting score, L_0. This latter case is the more likely, since the entire weight of past data does not have to be discarded. It signifies that although the track is not dissolved, any report that arises is more valuable as an initial pickup for a new track than a continuation of the old one.

3.3.2.2 (continued)

The condition for termination is

$$\ln \frac{b}{2\pi\sigma^2 A_N} < \ln \frac{A_o}{A_N} \qquad (44)$$

or $2\pi\sigma^2 A_o > b$

or $\pi R^2 A_o > 7b$ (using (36)).

In other words, termination occurs when the average number of new tracking objects to be found in the expanding search bin is 7b. This optimal probability criterion is, from a practical standpoint, somewhat extreme. But it points up the main anticipated conclusion that termination occurs when the expanding bins encounter an appreciable probability of finding reports from a brand new object. Actually A_o is a somewhat subjective parameter; for discrete beacon, it would be quite small, for non-discrete beacon, somewhat larger, and for radar only, larger still. So we can do little better than assigning a maximum allowable search radius on the basis of general knowledge of the aircraft activity.

Before the theoretical limit of (44) is reached, one probably finds more practical constraints, such as search time in correlation, poor tracking accuracy even when correlated, etc. We conclude that there are few theoretical or practical guidelines for the termination of tracks on this level of analysis. The method of dropping after m missing reports is further analyzed in Section 3.3.4, and more practical results are achieved.

3.3.3 Performance Estimates and System Balance

In order to assess the performance of the above initiation procedures, simulation work is required. In order to predict the outcome, however, we have available a method which will serve to provide some guidance in design. This second level of analysis is based on a (nontrivial) application and extension of Wald's sequential testing theory.

3.3.4 Analysis of Simplified Initiation and Termination Procedures

In order to make further progress in initiation and termination (I & T) analysis in this section, we postulate a simple decision logic. Although we know from our previous considerations that the logic is somewhat short of being optimal, it has the virtue of leading to a finite number of decision states which are linked in a structure that is quantitatively and exactly analyzable. The results of this analysis provide some new insights into the design problem and suggest specific I & T system parameter values for a variety of data conditions.

Thus, we consider here I & T logics in which n consecutive reports are required for initiation, while m consecutive missed reports are required to drop a track. Figure 3-23 shows the relevant state diagrams for this logic. System states are represented by nodes in the figure, while transitions among them are shown as directional branches with attached transition probabilities.

A true aircraft enters the system in the state labeled Start. If a report is obtained on the first scan (blip scan = b), the status changes to First Report and initiation begins. Consecutive reports then cause the sequence of initiating states to be traversed, until after n reports the Initiate (Maintain) state is reached. If at any point a miss occurs, the initiating track is dropped to the state Fail Initiation, from where it continues to attempt to reenter the initiation sequence with another First Report.

Once the Initiate (Maintain) state is reached, additional reports maintain the track in this state. However, when misses occur, the track enters the dropping sequence. m consecutive misses are required for a drop; any intervening report returns the track to the Initiate (Maintain) state. Although actually a dropped track here would again attempt initiation, we will not be required to explicitly consider this in the analysis.

The operation of the logic on clutter is essentially the same (probability of one or more clutter returns in the search bin = p). However, the emphasis is different. Here any uncorrelated report becomes a First Report. Succeeding supporting clutter reports or misses then cause the state to change as before, except that drops at any stage are equivalent for the purpose of our analysis.

The state diagrams and transition probabilities of this model logic are based on the assumption of Poisson clutter and serially uncorrelated report sequences for a true aircraft. Thus, runs of consecutive misses are considered no more likely than those obtained from independent scan-to-scan trials with probability b. (A similar analysis can be made for serially correlated data models.)

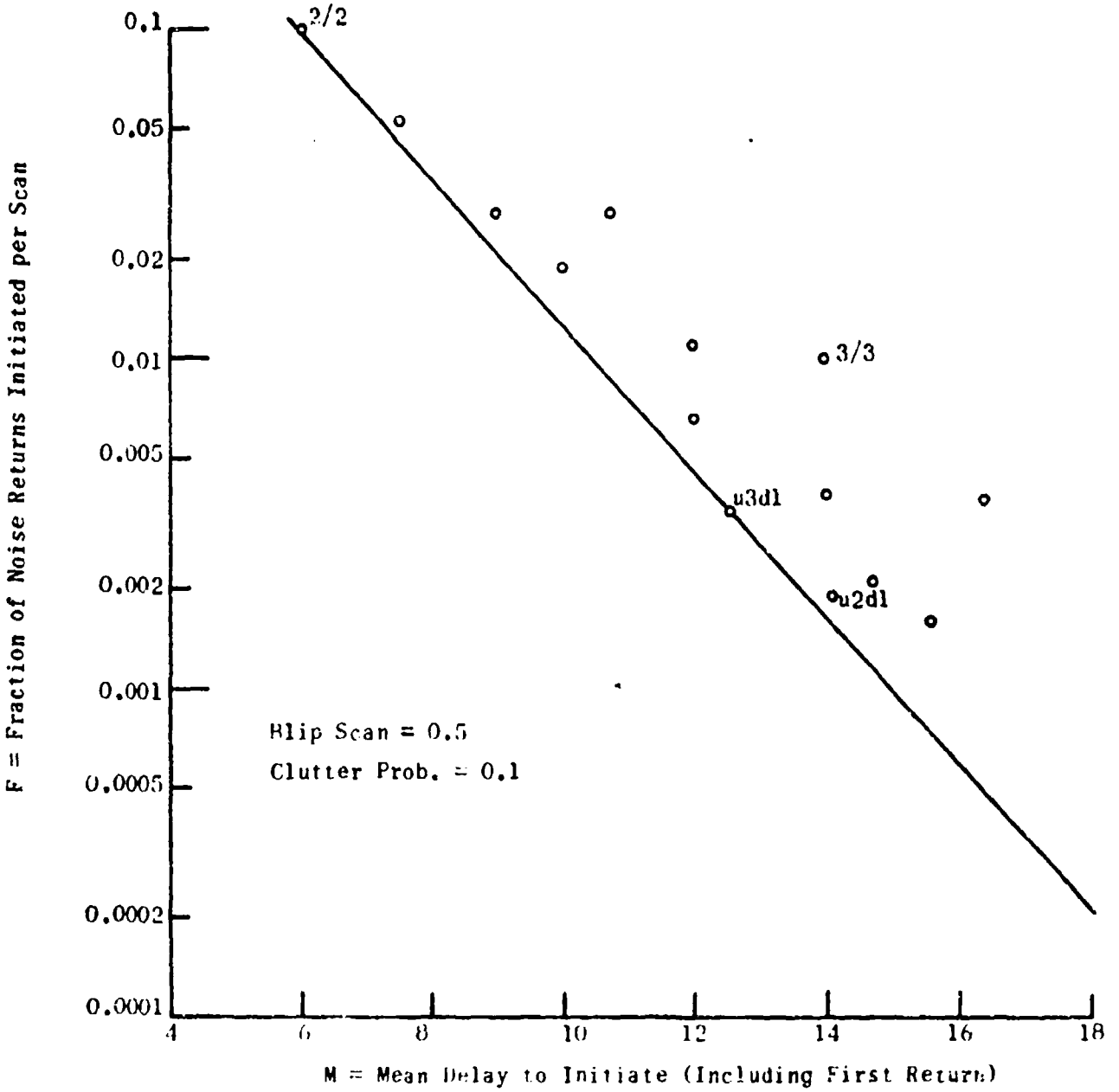

Figure 3-22. Optimal Trade-off Curve for Track Initiation

3.3.3 (continued)

The general result is:

$$M = \frac{\ln\left[1 + \frac{b-pK}{FK}\right]}{b \ln \frac{b}{p} + (1-b)\ln \frac{1-b}{1-p}} \qquad (45)$$

where

$$K = \frac{p^2}{b^2} \left(\frac{1-p}{1-b}\right)^{\frac{3}{b} - 3}$$

Here

M = mean delay

F = false initiation fraction

b = blip-scan (true target)

p = probability of clutter in the search bin

$\ln \frac{b}{p}$ = score increment for each report

$\ln \frac{1-b}{1-p}$ = score increment for no report

$\ln K$ = upper threshold

$\ln K'$ = lower threshold (See (46).).

One furthur aspect of performance needs to be mentioned. If there are N clutter reports per scan, then there are approximately N initial reports each scan (most are new, uncorrelated reports). On the succeeding scan we would like to remove as many of these as possible from consideration, lest the track memory required build from N to 2N slots. This prevents a rapid overload of machine capacity when N is rather large. (Say N = 200, or 0.06 reports per degree mile times 3300 degree miles.) Thus, we must impose a two report restriction. Only initial tracks whose initial report obtains immediate confirmation will be retained. This restriction has already been included in the derivation of (45) and figure 3-22.

For the case of 200 clutter reports per scan, we find from the figure that a total false initiation rate of one false track per scan requires a decision delay of about 12 scans. An increased delay to 16 scans produces a rate of

3.3.3 (continued)

0.1 false track per scan. Thus, the data conditions assumed here require rather extensive decision delays. Of course, automatic acquisition of beacon targets would be quicker (discrete beacon-very quick) because the probability, p, of spurious reports would be much lower. In the radar only case, where decision is so prolonged, even the two hit restriction is not completely effective in keeping track store requirements down. The mean number tracks in the process of initiation at any one time N^* is given by

$$N^* = N \left[1 + \frac{F \ln \frac{p}{b} K' + (p - F) \ln \frac{p}{b} K}{p \ln \frac{b}{p} + (1-p) \ln \frac{1-b}{1-p}} \right] \qquad (46)$$

where

$$K' = \frac{b}{F} - \left(\frac{p}{F} - 1\right) K.$$

For cases where F is very small, application of (46) to our example problem ($b = 0.5$, $p = 0.1$, $N = 200$) yields $N^* = 370$.

Thus, the desirability of establishing tracks by autoinitiation depends critically on data conditions (and the judicious use of a clutter map) determined from false rates NF and track load N^*. There is a complete range of feasibility from good to bad. For the radar only case in bad clutter with no map discrimination, autoinitiation is not attractive. For beacon or combined beacon and radar, use of a low value of p in (45), (46) indicates feasibility. (These relationships are quantified further in section 3.3.4.)

Unfortunately, derivation of (45) and (46) is based on an approximation which requires that the number of score increments needed to reach either threshold be moderately large. Thus, it is a continuous approximation to a discrete problem. The formulas for M and especially N tend to be inaccurate for the cases of interest here where only a few hits or missed reports are needed for an initiation and termination decision.

Fortunately, in such cases, the simpler decision logic of the next section is not so far off optimum. (cf. 2/2 and 3/3 points in figure 3-22). The optimum character of sequential tests is strongest just when the number of steps to decision is large. When the number of such steps is small, we can obtain useful results by restricting analysis to a set of simpler logics.

3.3.4 Analysis of Simplified Initiation and Termination Procedures

In order to make further progress in initiation and termination (I & T) analysis in this section, we postulate a simple decision logic. Although we know from our previous considerations that the logic is somewhat short of being optimal, it has the virtue of leading to a finite number of decision states which are linked in a structure that is quantitatively and exactly analyzable. The results of this analysis provide some new insights into the design problem and suggest specific I & T system parameter values for a variety of data conditions.

Thus, we consider here I & T logics in which n consecutive reports are required for initiation, while m consecutive missed reports are required to drop a track. Figure 3-23 shows the relevant state diagrams for this logic. System states are represented by nodes in the figure, while transitions among them are shown as directional branches with attached transition probabilities.

A true aircraft enters the system in the state labeled Start. If a report is obtained on the first scan (blip scan = b), the status changes to First Report and initiation begins. Consecutive reports then cause the sequence of initiating states to be traversed, until after n reports the Initiate (Maintain) state is reached. If at any point a miss occurs, the initiating track is dropped to the state Fail Initiation, from where it continues to attempt to reenter the initiation sequence with another First Report.

Once the Initiate (Maintain) state is reached, additional reports maintain the track in this state. However, when misses occur, the track enters the dropping sequence. m consecutive misses are required for a drop; any intervening report returns the track to the Initiate (Maintain) state. Although actually a dropped track here would again attempt initiation, we will not be required to explicitly consider this in the analysis.

The operation of the logic on clutter is essentially the same (probability of one or more clutter returns in the search bin = p). However, the emphasis is different. Here any uncorrelated report becomes a First Report. Succeeding supporting clutter reports or misses then cause the state to change as before, except that drops at any stage are equivalent for the purpose of our analysis.

The state diagrams and transition probabilities of this model logic are based on the assumption of Poisson clutter and serially uncorrelated report sequences for a true aircraft. Thus, runs of consecutive misses are considered no more likely than those obtained from independent scan-to-scan trials with probability b. (A similar analysis can be made for serially correlated data models.)

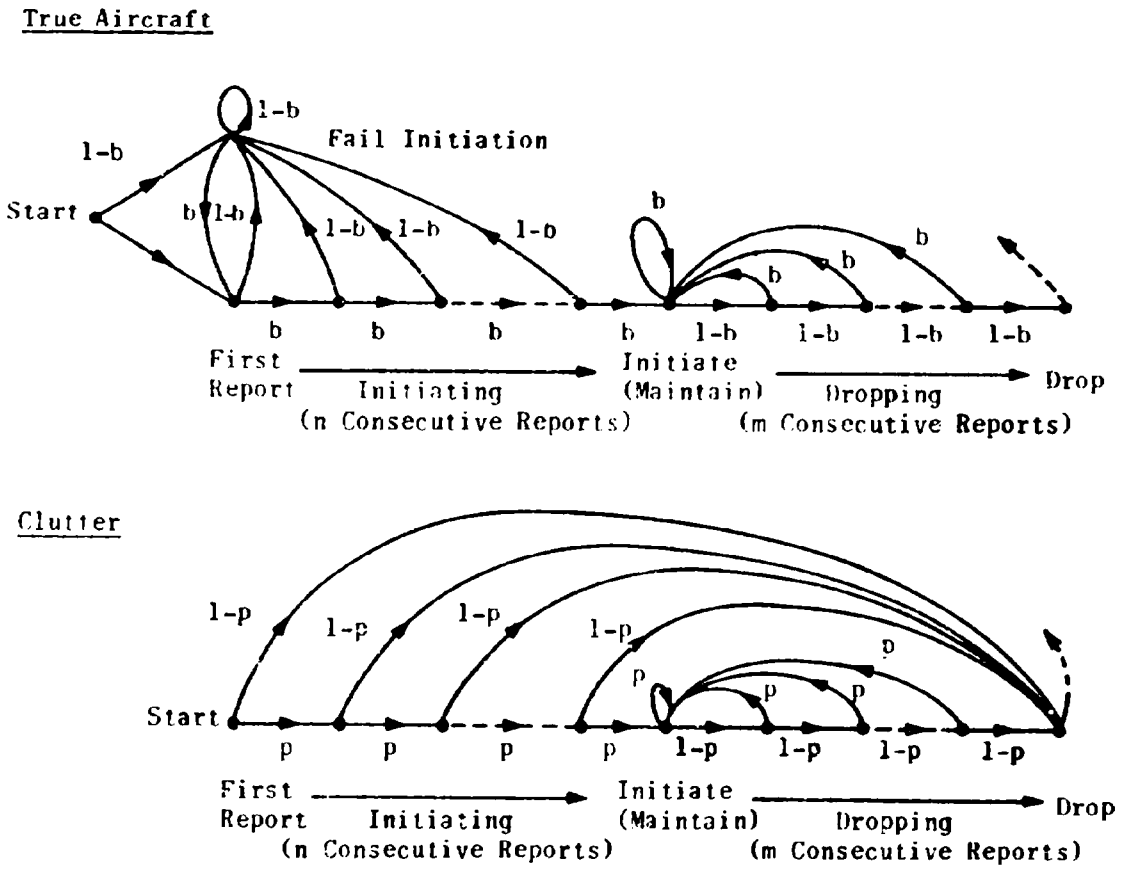

Figure 3-23. State Diagrams for Initiation and Termination Logic Analysis

3.3.4 (continued)

Three aspects of performance of this I & T logic will be considered. It can easily be proven that the mean delay to initiate on a true aircraft is given exactly by the formula

$$M = \frac{1}{1-b} \left(\frac{1}{b^2} - 1\right). \tag{47}$$

A similar analysis shows that the mean time that a true aircraft track lasts before being inadvertently dropped because of bad data (starting from Initiate (Maintain)) is

$$T = \frac{1}{b} \left(\frac{1}{(1-b)^m} - 1\right). \tag{48}$$

In order that I & T performance be adequate, we must insist on the constraints

$$M \leq M_c \,, \qquad T \geq T_c \,. \tag{49}$$

For numerical study, we have chosen $M_c = 6$ scans as the central case and explored also $M_c = 4$ and $M_c = 9$. We have also selected $T_c = 200$ scans in most cases, so that the resulting track life T is about the same as the track life F in section 3.2.4.1. (Otherwise the track would be inadvertently dropped on the overage by I & T decisions before the aircraft even escapes from the search bin.)

The current logic is favorable from the point of view of minimizing the number of clutter tracks carried in the initiating states. The number of such initiating tracks is approximately equal to the total number of clutter reports obtained in each scan. Hence, we concentrate on the final false alarm problem and evaluate the total average number of false tracks which are at any one time in the Initiate (Maintain) or Dropping states. This number is given exactly by

$$L = \left(\frac{A_i}{A_s}\right) L_F \tag{50}$$

where

$$L_F = p^{n-2} \left[\frac{1}{(1-p)^m - 1}\right] \ln\left(\frac{1}{1-p}\right)$$

and

A_i/A_s = ratio of the total area where autoinitiation is carried out to search bin area.

3.3.4 (continued)

Here we assume that the search bin area is constant and that the ratio A_I/A_S is on the order of 1000.

In order that I & T performance be adequate in clutter, we impose a constraint,

$$L_F \leq L_{FC} \tag{51}$$

In the numerical study we have chosen $L_{FC} = 0.01$, which corresponds to an average of 10 false tracks in the system as established tracks at any one time. Excursions on this value are made to $L_{FC} = 0.05$ and $L_{FC} = 0.002$.

Machine computation now may be used to exercise (47), (48) and (50) under the performance constraints (49), (51). In this computation, we seek data conditions b, p and corresponding I & T parameters (n, m) which meet the constraints. The numerical tabulations which result are given in appendix C, section C.4 for a variety of constraint values. (In the appendix KI ≡ n and KT ≡ m.)

The meaning of the results is exhibited in figure 3-24. This figure is drawn for the central case (table C-25 with $M_c = 6$, $T_c = 200$, $L_{FC} = 0.01$) which is appropriate for large area autoinitiation. In the figure, each point of the plane represents a given data quality. Sufficiently good data permits design constraints to be met by a suitable selection of (n, m). The region of adequate data quality occurs on the upper left of the figure and is separated from the inadmissible region by a step-like boundary.

Each corner of the boundary is labeled with an acceptable (n, m) parameter combination; this signifies that, with these I & T parameters, constraints can be met under data conditions as good as or better than at that point. For instance, the acceptable data region for n = 3, m = 4 is shown on the diagram. The total acceptable data region is composed of such overlapping rectangles, one for each of the (n, m) combinations shown. It is possible that other (n, m) values meet the constraints. But if their rectangles lie within the acceptable region, they are dominated by one of the (n, m) selections already shown and are not calculated or plotted.

Design of an I & T logic now reduces to selection of one of the corner (n, m) of this diagram. This selection depends on the data conditions that must be covered. No one selection does uniformly well for all conditions. For example, n = 3, m = 4 will be appropriate if $b \leq 0.72$ and $p \leq 0.12$. For higher clutter operations we might switch to (4, 3) which would, however, require higher blip-scan. To operate at lower blip-scans, we might select

3.3.4 (continued)

(2, 5) if clutter were less. These parameter switches might be controlled through the agency of the system clutter map.

In the RBTL system, maximum clutter conditions correspond to about the range p = 0.1 to 0.2. We see that autoinitiation on an area basis would be possible for such conditions if blip-scan were suitable high ($b \leq 0.85$). Use of the clutter map to switch parameters is seen to be very useful in such circumstances, for then in regions of low clutter the I & T logic can be used for considerably lower b. We note that successful operation at $b < 0.5$ is impossible unless clutter is near zero, and operation at $p < 0.3$ is impossible unless blip scan is essentially unity. These are the practical data condition limits for operation under the assumed constraints.

The table C-25 through C-35 show I & T analysis results for a variety of constraint conditions. In each case, a figure such as 3-24 can be constructed and interpreted. We note that although we have been discussing the problem in terms of radar clutter, the quantity p can also be interpreted for beacon (combined) report applications as the probability of finding one or more spurious beacon (combined) reports in the search bin. Thus, these results are of wide applicability if appropriate interpretations are made.

Figure 3-25 and table C-34 report results for a somewhat different application. Here $M_C = 6$ but $T_C = 50$ and $L_{FC} = 0.05$. These constraints are more appropriate for "intruder" tracker where autoinitiation is done only in local areas immediately adjacent to established tracks. Here the requirements on track life are not so severe and the L_F factor can be higher because the area A_i over which initiation is performed is correspondingly reduced. Thus L in (50), the false track load, would remain about the same as before.

The figure shows that the area of acceptable data conditions is now enlarged over the previous example. For instance, the region for (3, 3) has the same b limit as (3, 4) before, but operation in a higher clutter environment is now possible.

One difficulty with intruder tracking should be mentioned. The inevitable initiation decision delay implies that the initiating process must be started at a rather long range for the sake of reliability. For example, two aircraft whose combined approach speed is 300 kt (0.5 nm/scan) would have to begin intruder initiation on the untracked member of the pair at a range of about 2 x 10 scans or 10 nm. Thus, if one begins intruder tracking at this range for very many controlled (and tracked) aircraft, the whole airspace is nearly covered by such operation. One might then just as well institute autoinitiation in an entire control area.

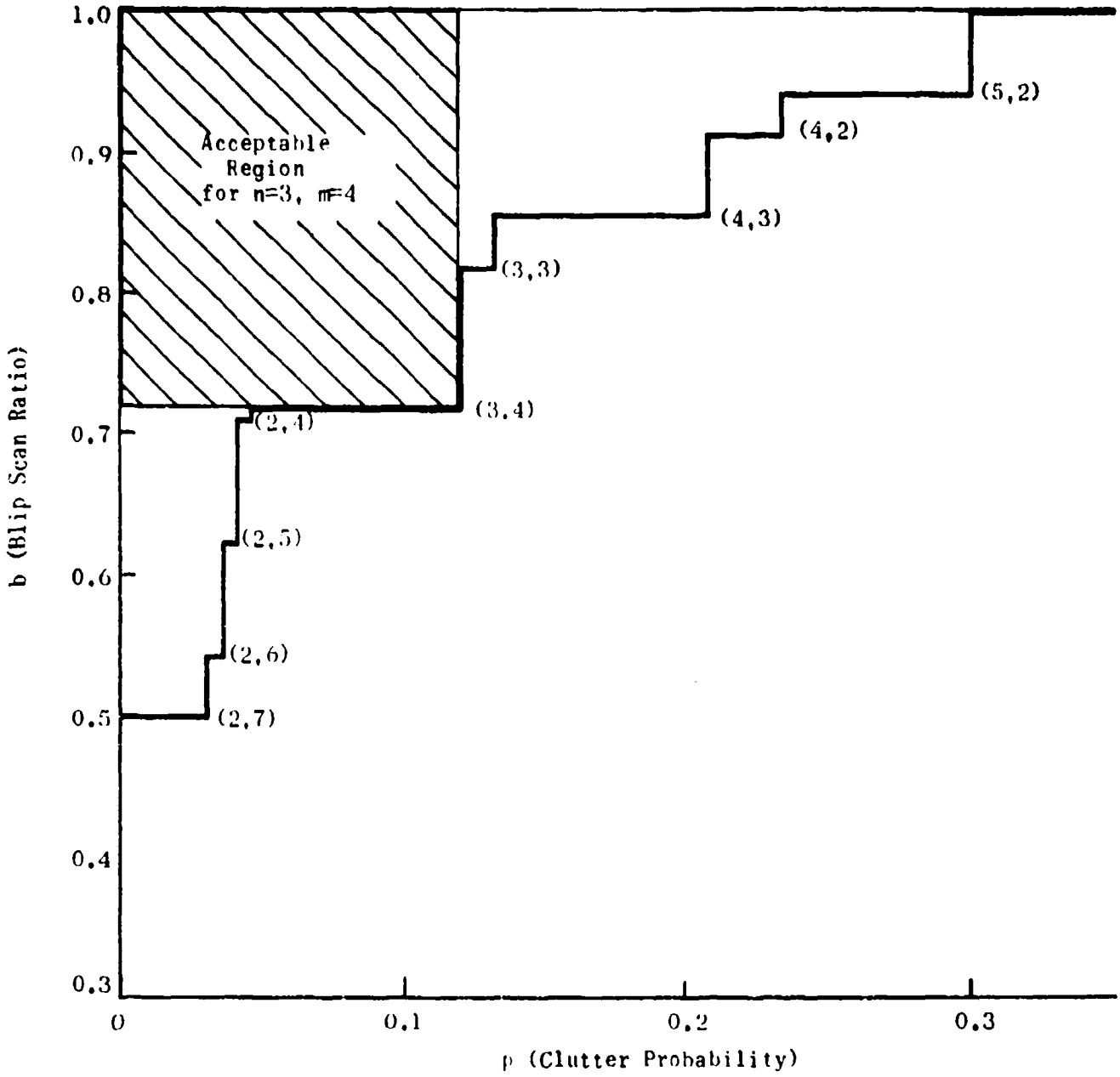

Figure 3-24. Data Characteristics and Initiation/Termination Rules Meeting Performance Constraints (Area Initiation - Table C-25)

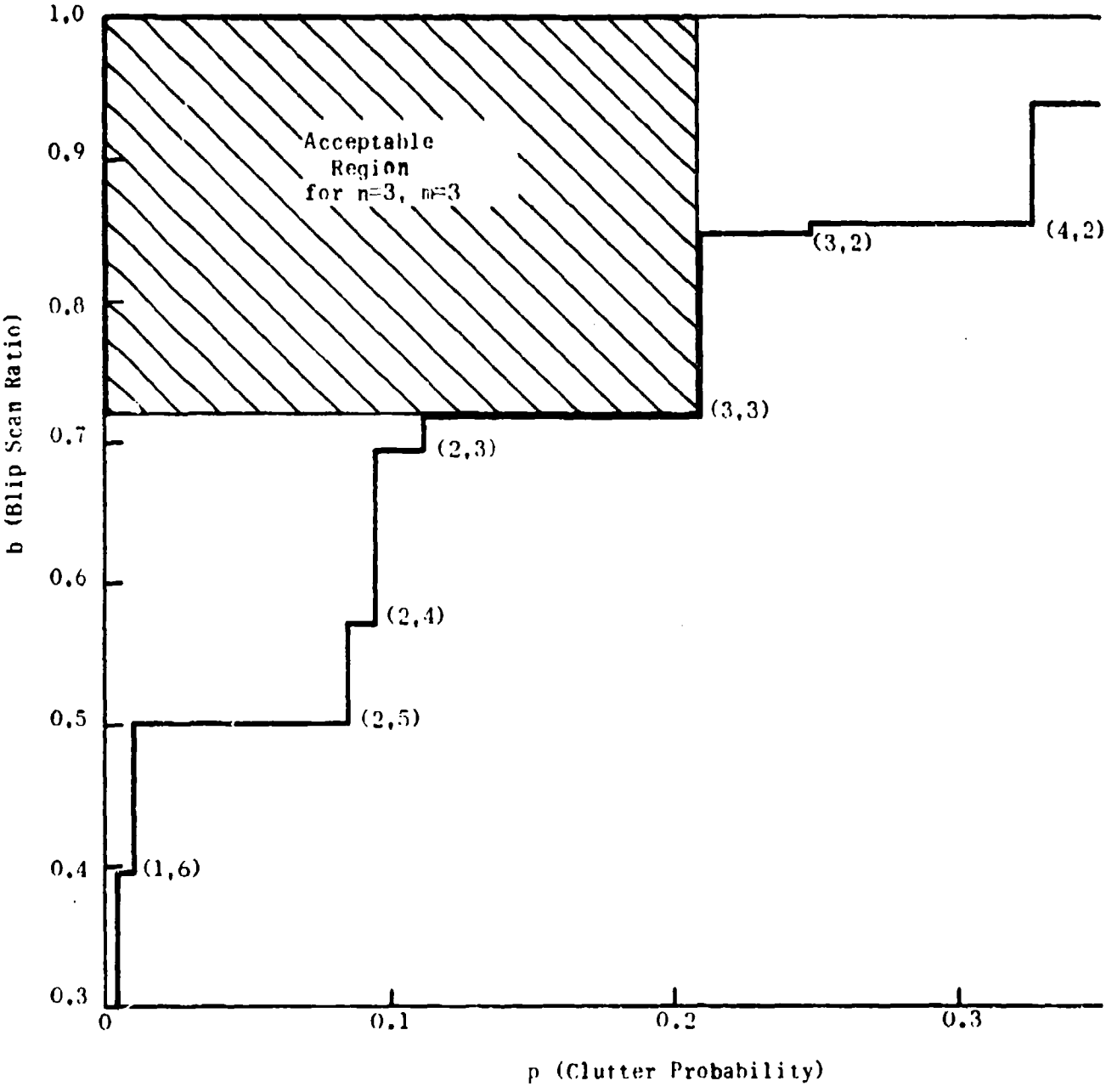

Figure 3-25. Data Characteristics and Initiation/Termination Rules Meeting Performance Constraints (Intruder initiation - table C-34)

3.3.4 (continued)

On the other hand, when controlled aircraft are sparse, intruder initiation becomes especially attractive owing to the reduced sensitivity to poor data conditions.

With the correlation algorithm proposed in the report (a version of nearest fit smoothing), considerable discrimination power is gained for the assignment of target reports when two tracked aircraft cross. In order that intruder initiation or initiation on all aircraft provide improved no swap performance, such an algorithm is required. Thus, the current effort to improve RBTL correlation should provide the basis for instituting autoinitiation under adequate data quality conditions.

Implementation of autoinitiation appears feasible with the proviso that, in order to handle the first report load (on the order of 100-200), a special compact file and routine be constructed to process initiating tracks through the receipt of a second supporting report. Thereafter, normal tracking procedures can be followed without undue loads. Control of I & T thresholds (m, n) through the clutter map appears desirable and perhaps mandatory in the case of large area autoinitiation.

3.4 TARGET DETECTION ENHANCEMENT

3.4.1 Introduction

The purpose of this task was to review the radar and beacon target detection function in the Basic RBTL system as it relates to the tracking and radar/beacon integration functions. The first section of the technical discussion addresses the problem of whether it is desirable and possible to make use of aircraft track file history data to enhance radar and beacon target detection. The second section addresses the problem of whether the presence of a beacon report can and should be used to enhance the detection of a radar report from the same aircraft. The final section provides conclusions and recommendations.

3.4.2 Technical Discussion

3.4.2.1 Tracking Feedback

The process whereby track file history data is made available for the enhancement of target detection will be referred to as tracking feedback. The use of

3.4.2.1 (continued)

tracking feedback to enhance detection has intuitive appeal. Anyone who has attempted to visually follow targets on a radar display will testify that the probability of visually detecting a target "blip" on a given scan is higher when that blip appears as a new report in a sequence or trail of reports from a target which the observer has been following for several scans. Faint blips can appear at random around the surveillance area and not be visually detected as targets at all, but if one of these appears where the observer expects to see a target report (because of visual history accumulated over several scans), the same blip will be detected and become a part of the observer's "track history file". The problem of this section is to determine whether this intuitively appealing concept has application in an automated target detection and tracking system.

3.4.2.1.1 Need for Enhancement. The first question which must be answered is whether there is ever a need to enhance radar or beacon target detection in an automated system. If, for instance, there were always a high probability of detecting radar and beacon targets, it would be a waste of time and effort to employ a tracking feedback function to enhance detection further. With regard to radar target detection within an automated system, reference 1 indicates that the probability of detection (P_d) for radar targets detected by the Radar Video Data Processor (RVDP) varies from near 0% to near 100% as target signal strength increases from 2 db to 6 db. These results were obtained while the system was operating at a probability of false alarm (P_{fa}) of about 10^{-6}, which is considered a normal operating P_{fa}. Appendix B of reference 5 indicates that similar results hold for simulated radar targets. Data in this document indicate that the P_d varies from near 20% to near 100% as target signal strength increases from 3 db to 6 db. The system was again assumed to be operating at a P_{fa} of 10^{-6}. Thus, it appears that for weak radar targets (in general signal strength less than 6 db), there is room for improvement on P_d.

The need for beacon target detection enhancement is less obvious since the cooperative nature of the beacon system ensures that under normal conditions the power of the beacon target returns is high enough to guarantee detection. Recent data collected at the Knoxville ARTS II site indicates, however, that there exist situations wherein the number of beacon replies received from a aircraft is significantly reduced. This results in a decrease in beacon target detection probability. This situation usually occurs when the beacon transponder antenna aboard the aircraft is shielded from the beacon interrogator antenna due to aircraft attitude. Thus there is room for improvement in beacon detection probability.

3.4.2.1.2 Method of Enhancement. Now, given that there is room for improvement of both radar and beacon detection, the question arises as to whether or not there exists a method to bring about an improvement. In both the radar and beacon detection logic the m out of n detector is applied to target hits at the same range over several azimuth sweeps to distinguish real targets from false alarms. In radar detection the m is often called the lead edge threshold (T_L) and the n is called the window size. The m is chosen in the case of radar detection to hold the probability of false alarm (P_{fa}) at some normal operating value (e.g. 10^{-6}). In the case of beacon detection, the m is chosen to discriminate against fruit (asynchronous replies) and beacon reflections. A natural approach to the problem of target detection enhancement is simply to lower the value of m in areas where a target is anticipated. What must be determined is the extent to which the lowering of m enhances P_d and whether the side effects of lowering m can be tolerated. In the case of radar detection, the lowering of m will bring about a corresponding rise in P_{fa}. In the case of beacon detection, the lowering of m will increase the probability that fruit or a reflection is declared as a target.

Several graphs are discussed below which show the effect of lowering the m threshold in the radar detection process. Figure 3-26 is a graph of P_d versus P_{fa} for various target strengths in the RVDP detection system (reference 1). In this graph the system is operating at a 5% noise level. The n is equal to 13 and m values of 7 and 5 are plotted. Note that when the system is operating with m = 7, the P_{fa} is 10^{-6} and the P_d for 2 db, 4 db, and 6 db targets is 5%, 14% and 93%, respectively. When m is decreased to 5, P_{fa} rises to 3×10^{-4} and P_d increases to 25%, 73% and 98%, for 2 db, 4 db, and 6 db targets. respectively. This is an increase of 20%, 59%, and 5% for the 2 db, 4 db, and 6 db targets.

Figure 3-27 is a similar graph of data from the same system operating at a 7% noise level. Note that the increase in P_d is 18%, 33%, and 13%, for 2 db, 4 db, and 6 db targets, respectively, when m is lowered from 7 to 5. At the same time P_{fa} rises from 10^{-5} to 1.4×10^{-3}.

Figure 3-28 shows similar results for the same system operating on 9% noise. In this case m is lowered from 9 to 7 with an increase in P_{fa} from 2×10^{-7} to 5×10^{-5}. This brings about an increase in P_d for 2 db, 4 db, and 6 db targets of 14%, 40%, and 15%, respectively.

Figures 3-29 through 3-31 show the results of simulating the detection functions in an automated terminal radar detection system for noise levels of 5%, 7.5%, and 10%. In this system n = 17. Note that when m is lowered by a value of 2, P_d is increased and there is an accompanying increase in P_{fa}.

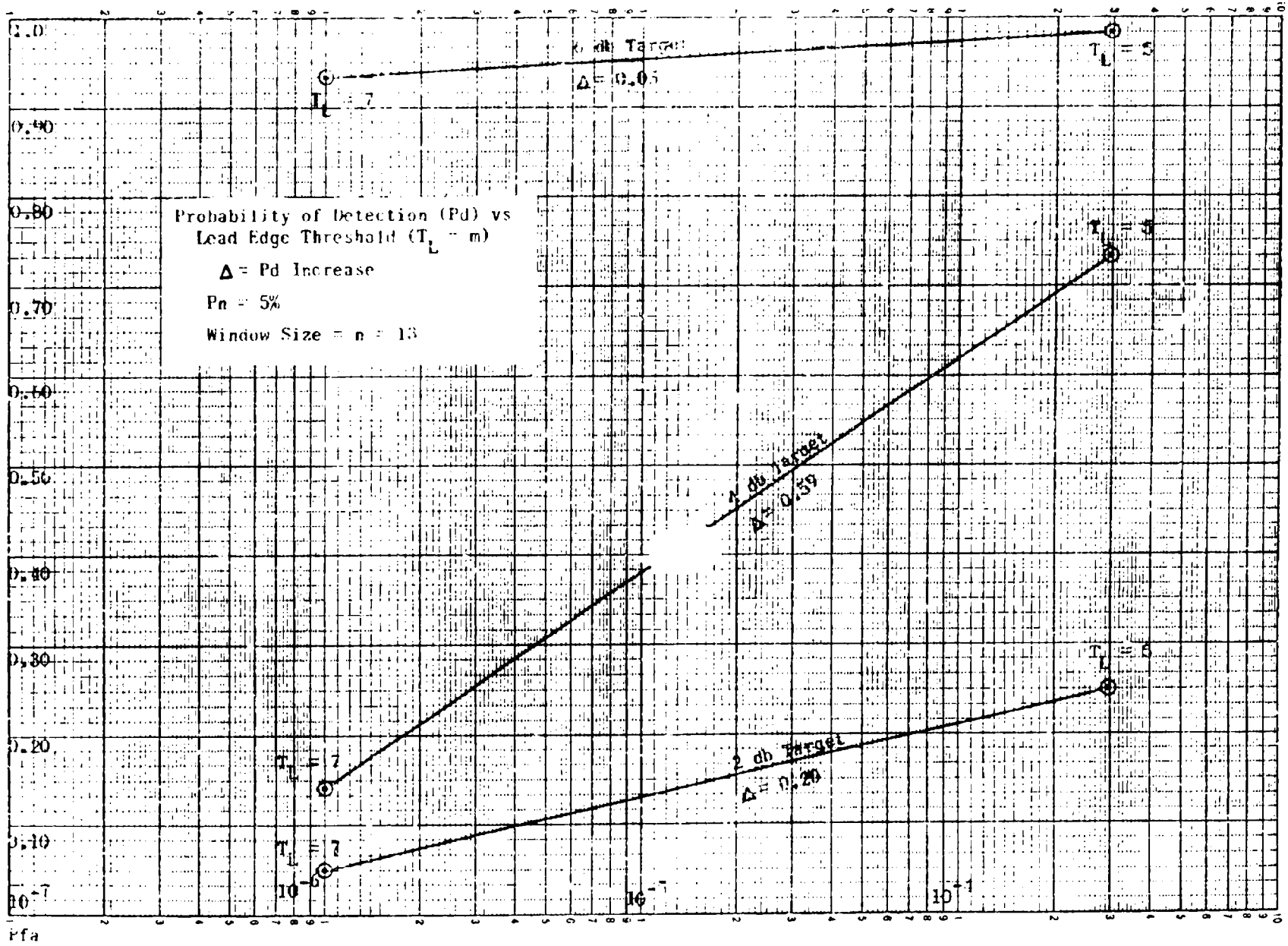

Figure 3-26. Radar Target Detection Enhancement (RVDP, 5% Noise)

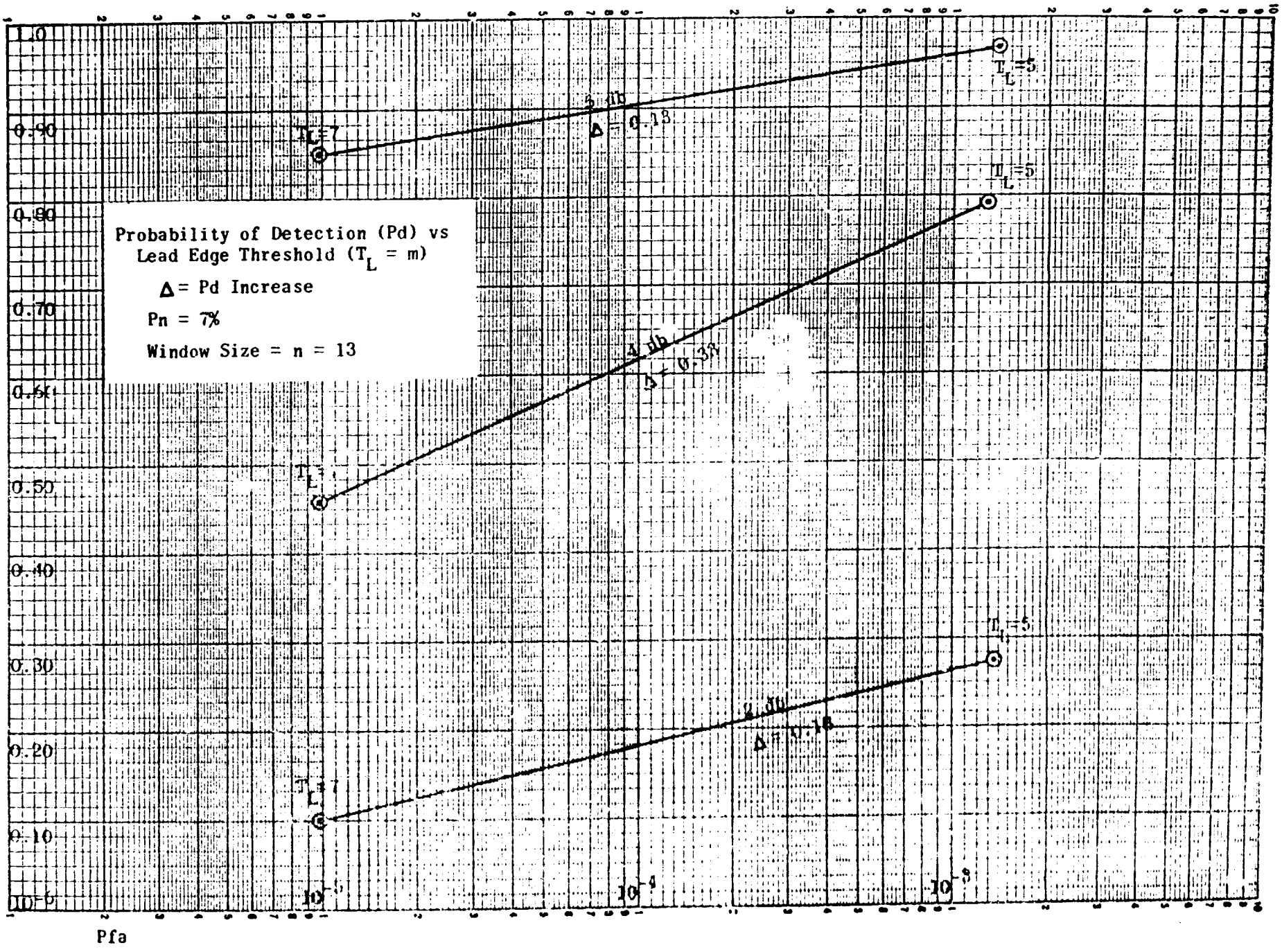

Figure 3-27. Radar Target Detection Enhancement (RVDP, 7% Noise)

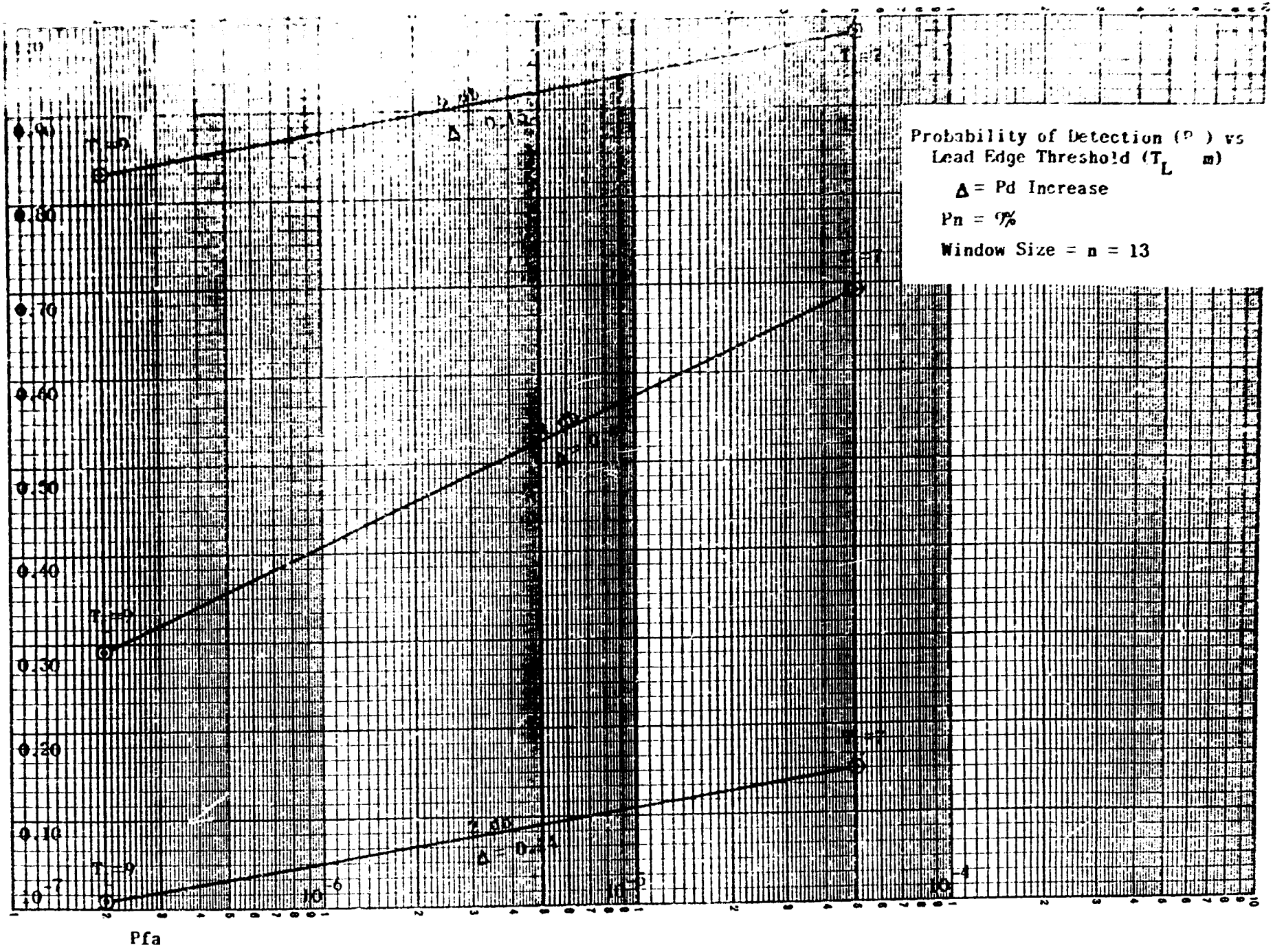

Figure 3-28. Radar Target Detection Enhancement (RVDP, 9% Noise)

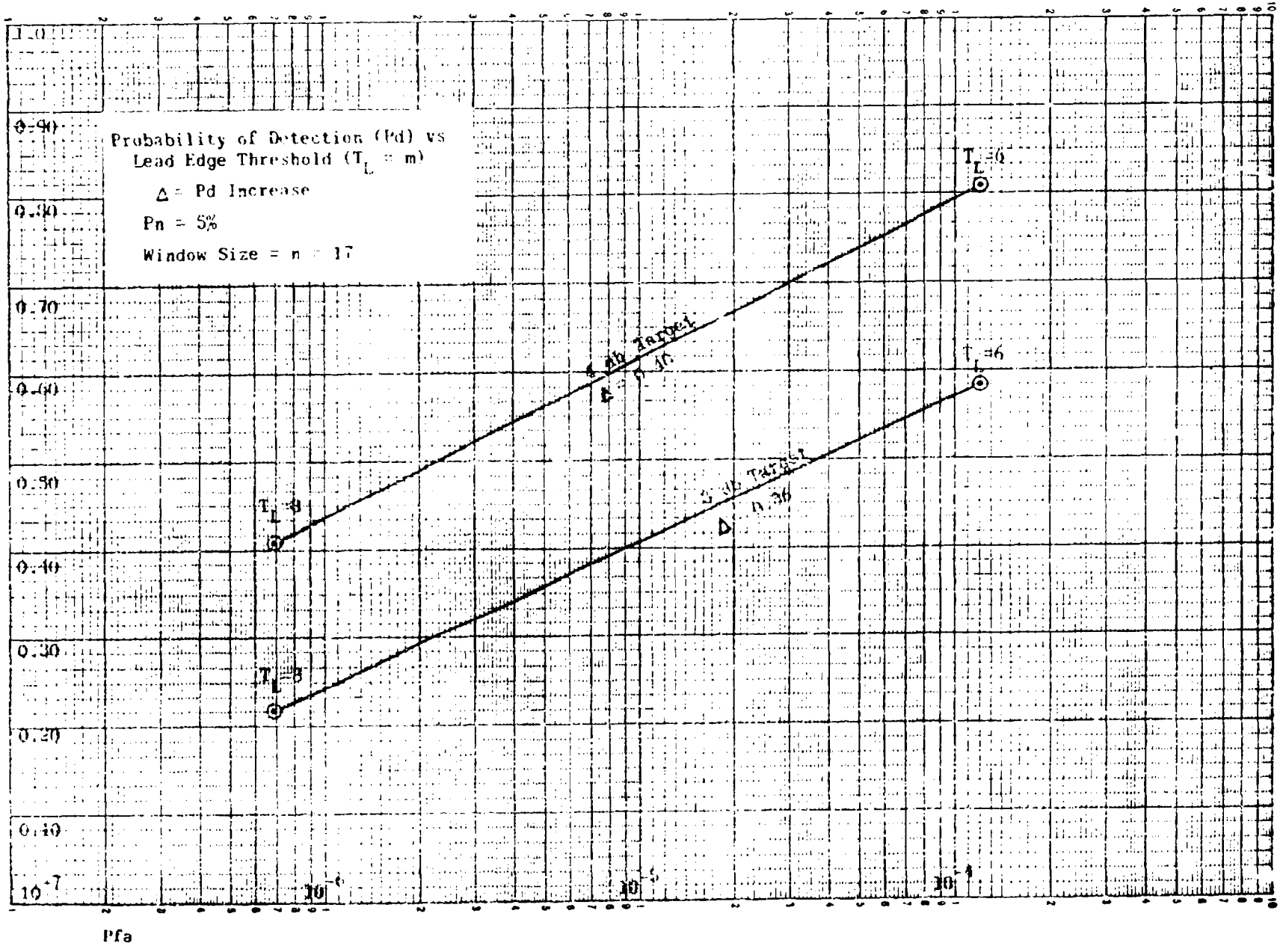

Figure 3-29. Radar Target Detection Enhancement (Terminal Simulation, 5% Noise)

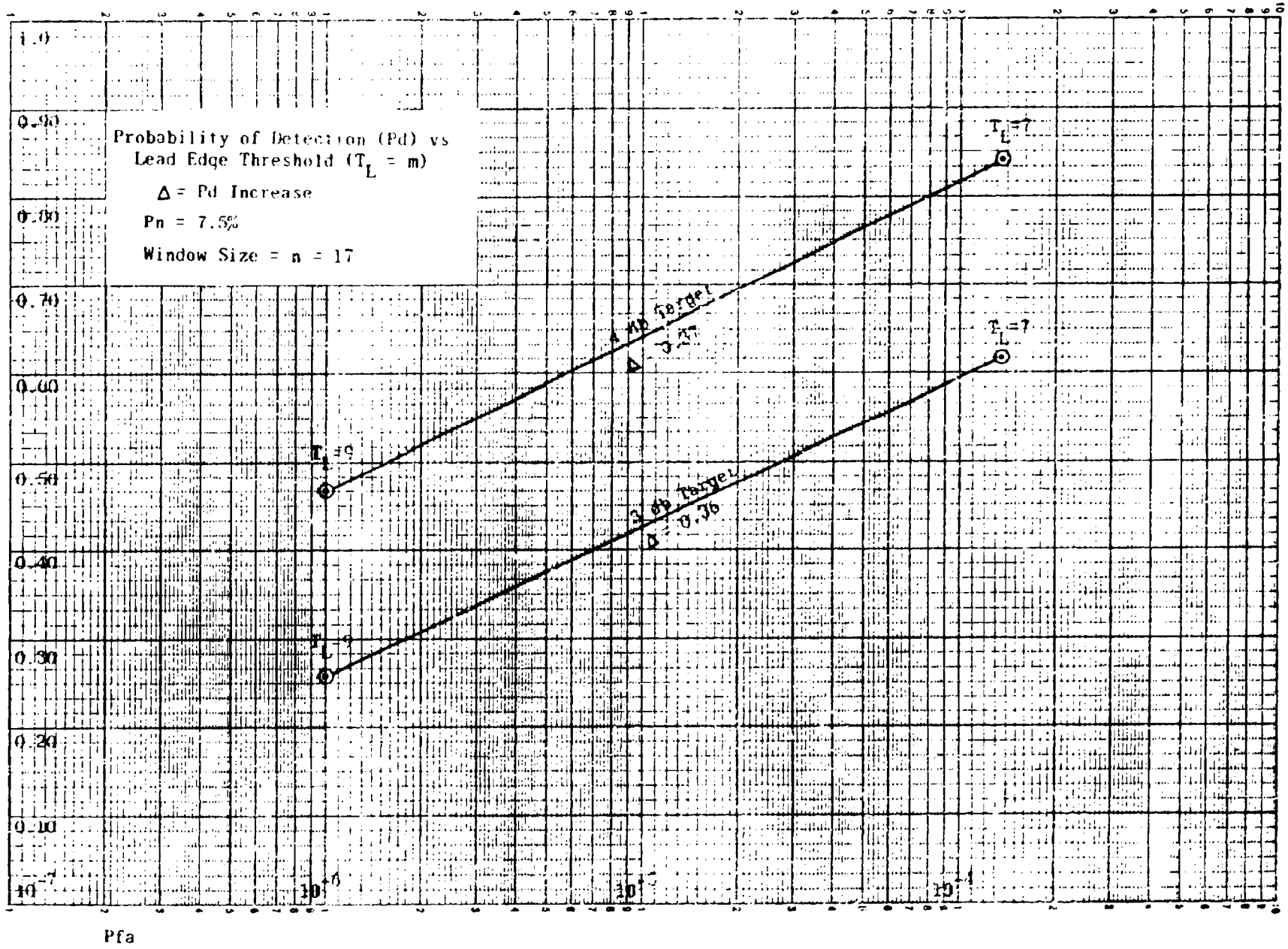

Figure 3-30. Radar Target Detection Enhancement (Terminal Simulation 7.5% Noise)

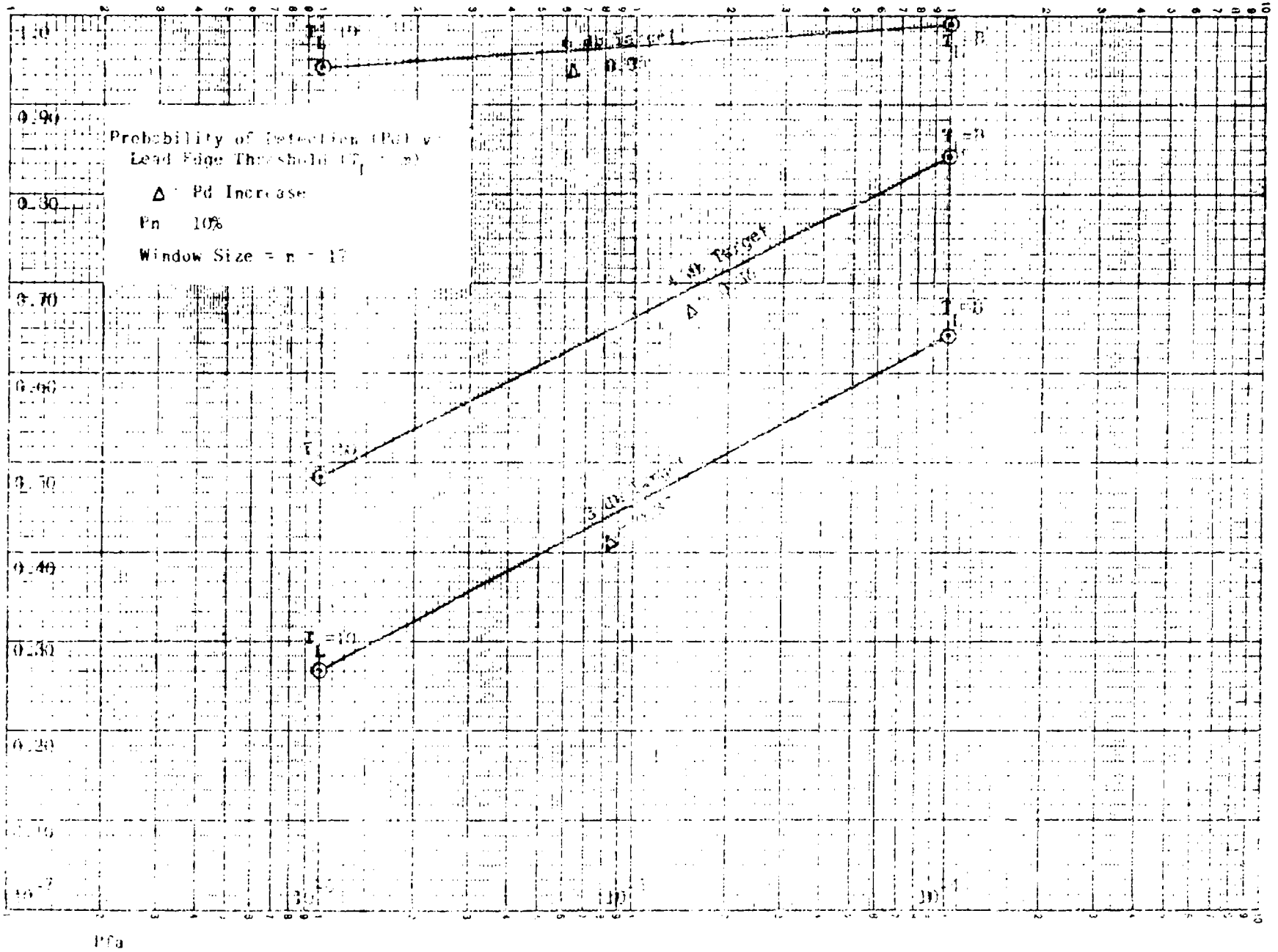

Figure 3-31. Radar Target Detection Enhancement (Terminal Simulation, 10% Noise).

3.4.2.1.2 (continued)

Figure 3-32 is a graph of the mean increase in P_d for various target strengths. It is a consolidation of the data contained in figures 3-26 through 3-31. Data from the RVDP analysis (reference 1) is shown as a solid line, whereas data from the simulation of the terminal system is shown as a dotted line. Note that the mean increase in P_d starts at about 20% for a 2 db target, peaks at about 40% for the 4 db target, and drops off to about 10% for the 6 db target.

From the foregoing graphs it can be seen that an increase in the P_d for radar detection can be attained for targets with signal strength less than 6 db by lowering the m value in the m out of n detector, but that there is a corresponding increase in P_{fa}. It can be seen that the curve for P_d improvement drops off rapidly near 2 db and 6 db with a peak near 4 db.

Unfortunately, a reference citing empirical or simulation data on the effect of lowering the m value in the beacon target detection logic is not available. It is apparent from the Knoxville data, however, that beacon reports from real aircraft are being discriminated against because of their low hit count. Although it is impossible to determine the increase in P_d which could be brought about by lowering the m threshold, there is reason to believe that this technique will bring about some improvement. The degree to which the P_d is enhanced and the effect on false alarm declaration can be determined only by testing the beacon detection system in a live environment.

3.4.2.1.3 Minimizing Cost of Enhancement. It has been shown that the P_d in radar target detection can be increased for weak targets by lowering the m threshold in the m out of n detector. It has also been seen that this has the undesirable side effect of raising P_{fa}. The question to be addressed now is whether this increase in P_{fa} should be tolerated to obtain an increase in P_d. First of all, it is apparent that there is very little to be gained by lowering the m threshold to detect targets with signal strength greater than about 6 db since the probability of detection is already near 100% when the system is operating at a normal P_{fa}. For targets of signal strengths less than 6 db, however, especially targets near 4 db, a significant increase in P_d can be attained by lowering m. A tradeoff must be made between increasing P_d and minimizing P_{fa}. The graphs discussed earlier show that decreasing m by two counts causes an increase in P_{fa} of about two orders of magnitude. Thus, if a system were operating in the 10^{-6} P_{fa} area, a modification of two counts in m would change the P_{fa} to near 10^{-4}. Since in the terminal automated radar detection system there are 2.3 million 1/8 nm range cells throughout the surveillance area, an average of about 2.3 false alarms per scan can be expected when the system is operating at a P_{fa} of 10^{-6}. Increasing the P_{fa} to 10^{-4} would give an expected number of false alarms per scan of about 230. Clearly, such a large count of false alarms per scan would be an undesirable

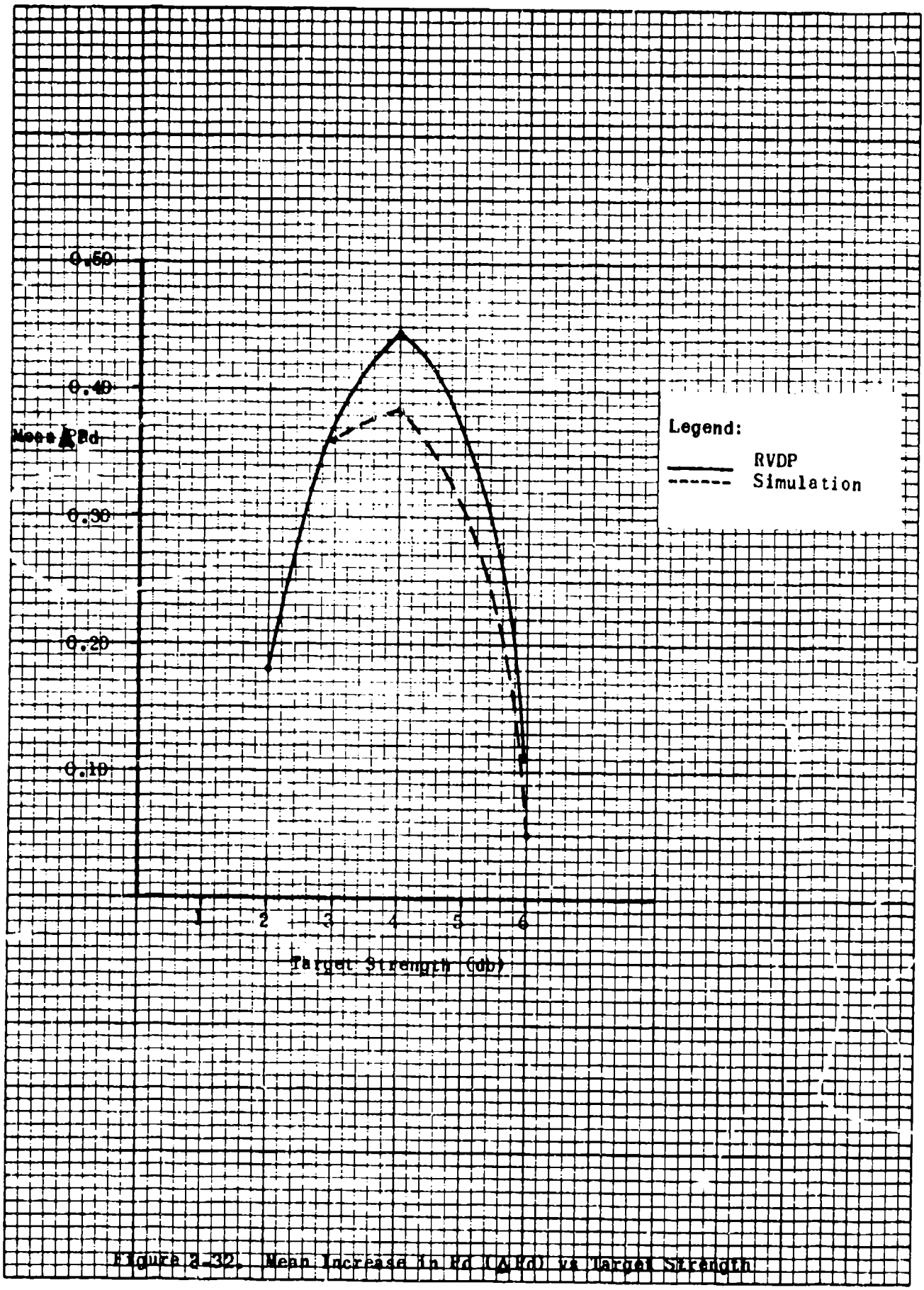

Figure 2-32. Mean Increase in Pd (ΔPd) vs Target Strength

3.4.2.1.3 (continued)

situation. Fortunately, however, included in the track file history data is a predicted position for the target being tracked. It is therefore possible to determine a small region about the predicted position of the track wherein the m threshold can be lowered in expectation of a radar target report.

This eliminates the problem of the high quantity of false alarms which would be caused by lowering the m threshold throughout the surveillance area. The expected number of false alarms becomes a function of the size of the region wherein m is lowered. This region will be called the sensitized region.

The determination of the size of the sensitized region must take two factors into consideration. The region must be large enough to insure that the radar report is contained within it and small enough to minimize the probability of a false target appearing within the region due to the use of the lower m threshold. A reasonable approach to this problem is to assume that both the track's predicted position (X_p, Y_p) and the new radar report position (X_r, Y_r) are independently distributed with bivariate normal distributions about the true target position. It is then possible to define a two sigma region about the predicted position (X_p, Y_p) such that the probability that (X_r, Y_r) is in this region is about 95%. Such a region would virtually insure that the new report is within the sensitized region. The number of range cells contained in the sensitized region will vary depending upon the position and standard deviation of the predicted position. It is desireable to put some maximum on the number of range cells which a sensitized region may contain. This would guarantee that the mean number of false alarms in any region is held to some maximum.

The following argument can be used to determine the maximum size of the region. Since the predicted position for a track in general has a smaller standard deviation than the raw reports being correlated to it, the standard deviation of the raw reports will be in general an upper bound for the standard deviation of the predicted position. The maximum region size will be constructed by assuming that the standard deviation in the predicted position equals the standard deviation in the raw report position. Thus, for example, if the standard deviation in the raw reports is 0.1 nm in range and 3 Azimuth Change Pulses (ACP) in azimuth, the two sigma region about the predicted position would be .57 nm in range and 17 ACP in azimuth. This is about 100 1/8 nm range cells. This value would then be used as an upper limit on the size of the sensitized region. If the P_{fa} in a region consisting of 100 range cells is raised to 10^{-4}, the expected number of false alarms is 0.01.

3.4.2.1.3 (continued)

To see that the limiting of the size of the sensitized regions has the desired effect of keeping the mean number of false alarms at a low level, consider the following example. Assume a worst case situation in which 200 aircraft are being actively tracked and that 50 of these tracks satisfy the conditions for sensitized region generation; moreover, assume that the 50 sensitized regions are at their maximum size (100 range cells) and are non-overlapping. Thus, in 5000 range cells, P_{fa} is 10^{-4}, giving an expected number of false alarms of 0.5. In the remaining 2.295 million cells the P_{fa} is 10^{-6}, giving an expected number of false alarms of about 3. Thus, the expected number of false alarms for the total surveillance area would 3.5. This is an increase of only 0.5 in the expected number of false alarms over the case wherein no sensitization takes place at all.

As in the case of radar targets, it must be determined under what conditions the m threshold in the beacon detection logic should be lowered. It was shown above that there is little to be gained by lowering the threshold for radar targets with signal strengths greater than 6 db since P_d is already near 100%. By the same token it can be argued that there is little to be gained by lowering the m threshold for beacon detection to detect any beacon target under normal conditions. This is true because the signal to noise power of the beacon returns is generally high enough to insure detection. Only when an abnormal situation exists is there something to be gained in detectability by lowering m. Specifically, in the case of beacon fade it may be useful to lower m. It is possible to use the geographic location of the beacon antenna as a basis for designating certain areas wherein an aircraft turn is likely to shield its transponder antenna, causing a loss of some or all of the beacon replies. For example, the fading of beacon replies has been noted at JFK airport in certain areas wherein the departure pattern calls for a tight turn. Areas such as this could be mapped out and the m threshold in the beacon detection logic could be lowered in a two sigma region about the predicted position of the track if this predicted position happens to fall into a designated fade area. As in the case of radar, the two sigma region would be generated based on the distribution of both the target report and the track predicted position. Alternatively, the direction and rate of an aircraft's turn relative to the beacon antenna could be used as a criteria for setting up a sensitized region around the predicted track position. Where the technique of generating two turning trial tracks (bifurcation) is employed to detect turns, a sensitized region would be centered about each of the predicted turning trial track positions.

3.4.2.1.3 (continued)

An alternate method for determining when to lower the m in the m out of n beacon detector is to test all beacon reports in the two sigma region about the track's predicted position using the normal m threshold. Only when no target reports are declared using the normal threshold would a lower enhancing threshold be applied. This technique would have the advantage of insuring that the lower threshold is applied only when the higher threshold would not have declared the target.

3.4.2.1.4 Enhancement Criteria. It has been determined that only radar reports with signal strengths less than 6 db should be considered for enhancement. The use of radar report signal strength as one of the criteria for enhancement presumes that there is some method of predicting the strength of a radar prior to its entrance into the detection system. A logical way to approach this problem is to collect radar report history on the strength of the previous reports from the aircraft being tracked to get an estimate of what the signal strength of the new report will be. In order to use this approach, it must be determined first whether the signal strength of the previous reports can be ascertained, and second, whether this knowledge is of any use in predicting the signal strength of the new report.

In order to answer the first question, the Basic RBTL software radar detection algorithm was programmed to operate on Monte Carlo simulated radar targets, with signal strengths of 3 db, 6 db, 9 db, and 12 db. For each signal strength, targets were generated over 10% noise until 100 were detected. The Basic RBTL software detector employs a Sequential 4/8 predetector with a sliding window final detector (Reference 6). It also employs an expanding window technique to collect hit data for target center azimuth declaration. The simulation was designed so that the number of hits (hit count) in the final expanded window (i.e., the total number of target hits) could be averaged over the 100 detections. Figure 3-33 is a graph of the mean hit count versus the report signal strengths. The solid line indicates data for a final detection threshold (T_L) of 10 out of 19. In the software detection algorithm this corresponds to a P_{fa} of about 10^{-6}. The dotted line indicates data for a T_L of 8. This corresponds to a P_{fa} of approximately 10^{-4}. Note that the mean hit count for a 3 db target detected with $T_L = 10$ is within two counts of the mean hit count for a T_L of 8, and that the mean hit count does not differ for P_{fa}'s of 10^{-4} and 10^{-6} on target strengths of 6 db, 9 db, and 12 db. Note also that there is a correspondence between mean hit count and signal strength. It does appear to be possible to use hit count as a measure of signal strength. It must be emphasized, however, that since the standard deviation of these hit counts, denoted by the brackets, is about 3 counts, it is not possible to make fine distinctions between targets of nearly equal signal strengths. For instance, it is not possible to distinguish between a 3 db and a 4 db target on the basis of hit count. It is possible, however, to make a general distinction between weak and strong targets.

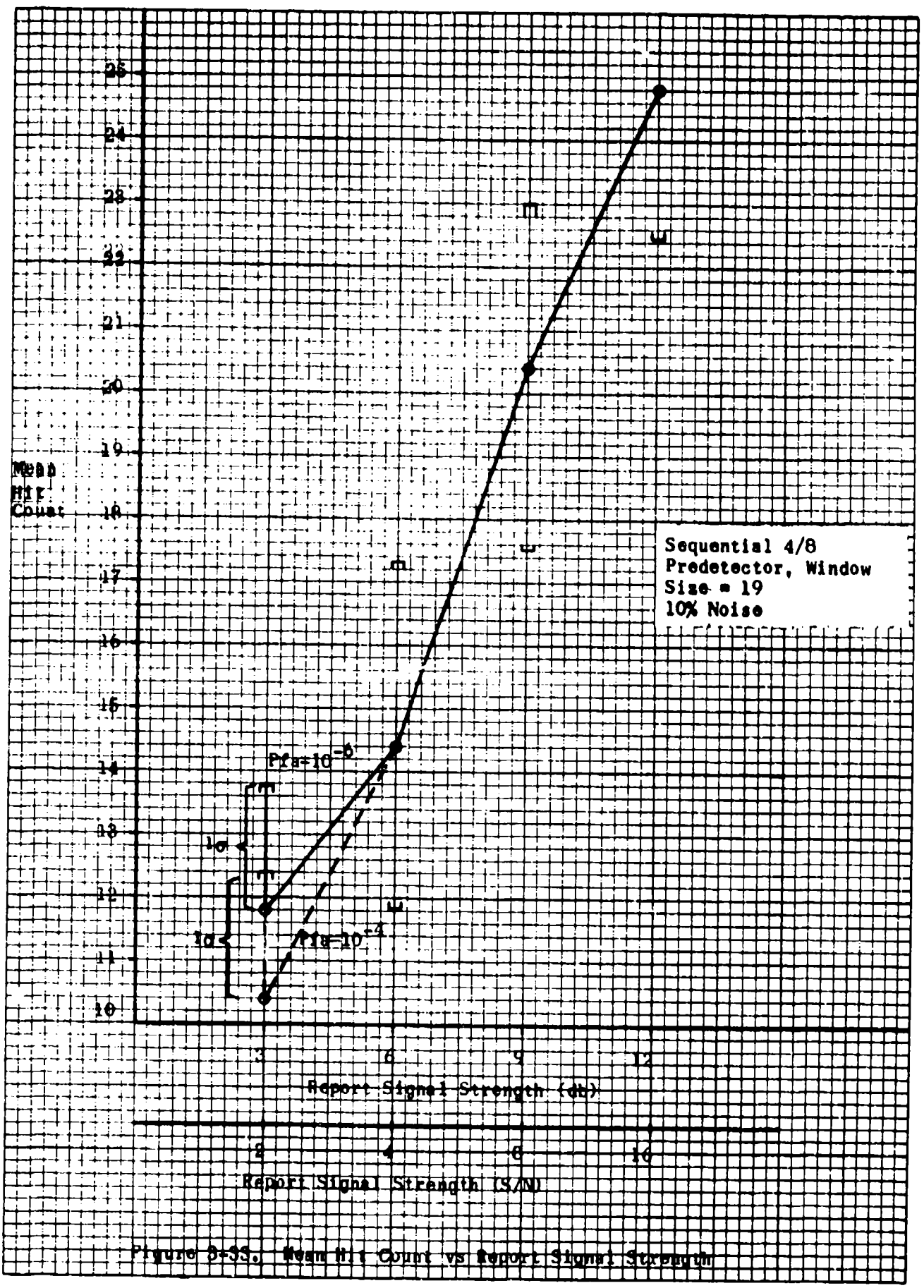

Figure 3-35. Mean Hit Count vs Report Signal Strength

3.4.2.1.4 (continued)

Having determined that is possible to make a distinction between weak and strong targets on the basis of hit count, we now turn to the second question cited above: can this information be used to predict when and where a weak report from a tracked target will enter the detection system? In order to solve this problem, some information as to the distribution of radar target report strengths from scan to scan must be ascertained. By using radar target strength history data, one would actually be taking a statistical sample from the scan-to-scan distribution of the target reports strengths. In reference 2, Skolnid gives a description of the Swerling Type 1 Model for the distribution of radar target cross section on a scan-to-scan basis. Since, under the assumptions discussed below, radar cross section can be related to signal strength by a linear function, this model is a reasonable place to begin the discussion of radar target strength estimation. First some background on the Swerling Type 1 Target Model will be given.

The Swerling Type 1 Model applies to radar targets consisting of many independent fluctuating scatterers of approximately equal echoing areas. This description applies to a typical aircraft target. The model assumes that radar pulse echoes received from a target on any one scan are constant in amplitude throughout the entire scan (no pulse-to-pulse variation) but independent from scan to scan. Under these conditions and assumptions, the Swerling Type 1 Model posits a negative exponential distribution for the radar cross section from scan to scan.

The probability density function for the negative exponential distribution is given by the following equation:

$$P(A) = (1/A_{AV}) \exp(-A/A_{AV}),\ A \geq 0 \qquad (52)$$

where:

A = radar cross section.

A_{AV} = average cross section over all target fluctuations.

(Note that the mean and standard deviation of this distribution is A_{AV}.)

3.4.2.1.4 (continued)

Since the signal strength and not the radar cross section is of interest in this dicussion, the former must be related to the latter. Chapter 2 of Reference 4 gives the basic radar equation in the following form:

$$P_r/P_t = (G_t G_r L^2 F_t^2 F_r^2/(4\pi)^3)(A/R^4) \quad (53)$$

where

P_r = received signal power.
P_t = transmitted signal power.
G_t = transmitting antenna power gain.
G_r = receiving antenna power gain.
A = radar target cross section.
L = wave length.
F_t = pattern - propagation factor for transmitting antenna-to-target path.
F_r = pattern - propagation factor for target-to-antenna path.
R = radar to target distance.

Putting equation 53 in the form below

$$P_r = (P_t G_t G_r L^2 F_t^2 F_r^2/(4\pi)^3)(A/R^4) \quad (54)$$

it can be seen that the quantities in the parentheses are a function of the radar system and are constant for our purposes. Setting the variables within the parentheses equal to c, we get the following equation:

$$P_r = cA/R^4 \quad (55)$$

It is now necessary to introduce the target signal-to-noise ratio into the equation. To do this we note that

$$(S/N) = P_r/P_n \quad (56)$$

where

(S/N) = signal-to-noise ratio
P_n = power of noise in receiving system
(Note: $P_n = kT_sB_n$, where k=Boltman's constant,
T_s = system noise temperature, and
B_n = noise bandwidth)

3.4.2.1.4 (continued)

Thus

$$P_r = (S/N)P_n = (S/N)kT_sB_n \quad (57)$$

Since k, T_s and B_n are constant for our purposes, we let their product equal d and get

$$P_r = (S/N)_d \text{ or } (S/N)=P_r/d \quad (58)$$

Combining equation 55 with 58 we get

$$(S/N) = (c/d)A/R^4 \quad (59)$$

It would now be convenient to assume that R is also constant over some time interval. In order to determine whether this assumption can be made, we will look at how much R is likely to change over the time interval determined by the number of radar reports (samples) which are used for an estimate of target strength. Assuming that an aircraft is flying radially (worst case) at V knots, that N reports are used for the target strength estimate, and that the scan time is 4 seconds, the range change (RC) over the sampling period is given by the following equation:

$$RC = (V \times N)/900\text{nm} \quad (60)$$

Thus, for example, if 10 reports were used for the sample, and if the aircraft were traveling at a speed of 150 knots, the range change would be 1-2/3nm. In order for the constant range assumption to be reasonable, the number of samples must be kept low so that RC is small. This fact will have an effect later when the appropriate sample size will be determined.

Under the assumption of constant range, equation 59 becomes

$$(S/N) = qA \quad (61)$$

where $q = c/dR^4$.

3.4.2.1.4 (continued)

Since (S/N) is equal to a constant times A, and since A has a negative exponential distribution, (S/N) will also have a negative exponential distribution. Figure 3-34 is an illustration of the negative exponential distribution. Note that 94% of the distribution is contained in the one sigma interval about the mean and that the mean is equal to the standard deviation.

As was stated earlier, the estimates of signal strength on individual scans will be based on the target hit count. Since the distribution of (S/N) is negative exponential, probability statements can be made about the statistics used to estimate its mean. The relationship between (S/N) and the signal strength in db's is given by the following equation:

$$(S/N)_{db} = 10\log_{10}(S/N) \tag{62}$$

where

$(S/N)_{db}$ is the signal-to-noise power in db's.

The lower scale on the graph shown in figure 3-33 indicates the value for (S/N) which correspond to $(S/N)_{db}$, the signal strength measured in db's.

The signal strength prediction for the next scan will be based upon the following statistic:

$$\bar{X} = (1/N) \sum_{i=1}^{N} X_i \tag{63}$$

where the Xi's are the signal strength (S/N) samples over N scans. (If a radar report is not available on a given scan, $X_i=0$).

$\bar{X}$ is distributed with an approximate normal distribution having a mean equal to the mean target signal strength and a standard deviation of $\sigma/\sqrt{N}$, where σ is the standard deviation of the target signal strength. It can be seen that as N increases, $\bar{X}$ becomes a better estimate of signal strength because its standard deviation is decreased. Unfortunately, N cannot be increased too high for our purposes without invalidating the constant range assumption.

At this time, an appropriate value for N, the sample size, will be determined. table 3-6 shows the 95% confidence intervals for X under various mean signal strengths and sample sizes. The size of N must be chosen large enough to discriminate between weak and strong targets but small enough to keep the range change small so that the constant range assumption will be valid. Note that a sample size of 4 would not discriminate between targets below 6 db and targets above 6 db, since the 95% confidence intervals overlap extensively. Using a sample size of 16 tightens the confidence intervals enough to allow discrimination, but this choice makes RC equal to 16V/900nm. Thus, if the radial velocity were only 100 knots, the range would be nearly 2nm. The change becomes excessive for higher radial velocities. The choice of 9 as a compromise sample size minimizes confidence interval overlap. The associated range change is given by 9V/900 nm. This is a 1 nm change for a 100 knot radial target and a 3 nm change for a 300 knot radial target.

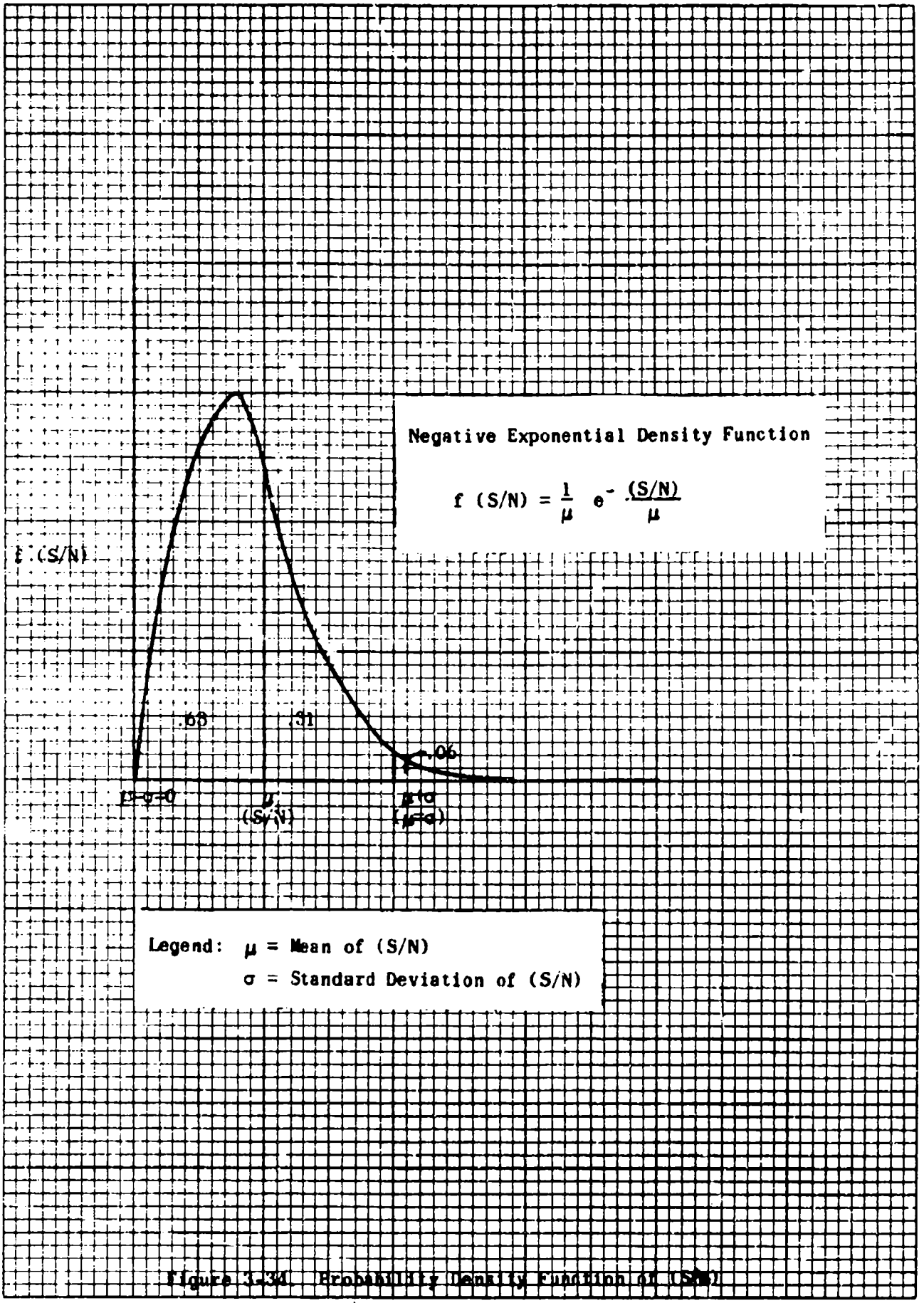

Figure 3-34. Probability Density Function of (S/N)

TABLE 3-6. NINTY-FIVE PERCENT CONFIDENCE INTERVALS FOR $\bar{X}$

(S/N) db	$\bar{X}$	Sample Size N				
		4	9	16	25	36
3	2	(0, 4)	(.7, 3.3)	(1, 3)	(1.2, 2.8)	(1.3, 2.7)
6	4	(0, 8)	(1.3, 6.7)	(2, 6)	(2.4, 5.6)	(2.7, 5.3)
9	8	(0, 16)	(2.7, 13.3)	(4, 12)	(4.8, 11.2)	(5.3, 10.7)
12	16	(0, 32)	(5.3, 26.7)	(8, 24)	(9.6, 22.4)	(11.7, 21.3)

3.4.2.1.4 (continued)

It has been determined that a sensitized region should only be generated to detect weak targets and that a reasonable method for determining when weak targets are in the system does exist. It will now be determined which tracks should be used to generate sensitized regions. Tracks can be classified by their quality or firmness. Usually a track's firmness is based on the success with which it correlates to new reports. Tracks which are in the process of starting up (initial tracks) have low firmness because only a small amount of history data has been accumulated. Tracks which have been in the system for a long time and have been successfully correlated (normal tracks) have high firmness. Initial track data should not be used to generate sensitized regions for two reasons: 1) An insufficient number of radar reports has been correlated to allow an accurate estimate of predicted signal strength; and 2) the predicted position has a high degree of uncertainty due to lack of history. Only normal tracks should be considered for sensitized region generation because these drawbacks are then lessened.

3.4.2.1.5 Tracking Feedback Summary. In summary, the following theoretical conclusions have been reached with respect to tracking feedback:

1) It is possible to improve radar target detection on weak targets (below the 6 db range) by reducing the m in the m out of n detector.

2) The increase in P_{fa} which occurs when m is lowered can be tolerated if restricted to sensitized areas wherein a weak target is expected.

3) There is reason to expect some improvement in beacon detection by lowering the m in the m out of n beacon detector when beacon fade is anticipated.

4) It is possible to obtain a reasonable estimate of signal strength on the basis of target hit count.

5) Only firm tracks should be used to generate sensitized regions.

3.4.2.2 Beacon-In-Process Enhancement

The purpose of this section is to determine whether the presence of a beacon report can and should be used to enhance the detection of its corresponding radar report. The use of beacon presence to enhance radar detection will be referred to as beacon-in-process enhancement. It was shown in the discussion of tracking feedback that there is considerable room for improvement in the detectability of weak radar reports. It was also shown that a method for

3.4.2.2 (continued)

improving probability of detection (P_d) is to lower the m in the m out of n detector, accepting the accompanying increase in probability of false alarm (P_{fa}) in order to increase P_d. It is possible to use the same technique of lowering m to improve P_d on weak radar targets in the area of an already declared beacon target. The use of this technique naturally assumes that radar target detection is designed to follow beacon target detection so that the existence of the beacon target is known prior to the time that the radar target detector operates. As in the case of tracking feedback, the determination of whether beacon-in-process enhancement is feasible reduces to a trade-off decision between the advantage of increased P_d and the disadvantage of increased P_{fa}.

3.4.2.2.1 Advantage Of Beacon-In-Process Enhancement. First of all, recall from the tracking feedback discussion in the previous section that only on weak radar targets can a significant increase in P_d be realized by lowering the detection threshold. Thus the discussion of the advantage of beacon-in-process will only apply to these targets. The advantage of beacon-in-process enhancement is simply that if the detectability of weak radar reports is increased, the number of radar reports available for correlation to beacon reports and/or track files is increased.

There are several advantages in having available not only an aircraft's beacon report, but also its corresponding radar report. First of all, the accuracy of the radar report is better than that of the beacon report. Reference 7 indicates that the standard deviation in azimuth is 0.33° (3.8 ACP) for beacon as opposed to 0.25° (2.9 ACP) for radar. By properly combining a beacon report with its corresponding radar report (using radar positional data with beacon identity and altitude information), an increase in positional reporting accuracy can be attained and tracking accuracy thereby enhanced. If beacon and radar reports are not combined but are instead correlated to the track files separately, there will still be an improvement in tracking accuracy because of the availability of the more accurate radar report.

Another advantage of having both a radar and a beacon report available from the same aircraft is that their combined presence can be used to differentiate between true beacon reports and false alarms due to reflections or fruit. When a beacon report is reinforced by its corresponding radar report, there is a high probability that it has been generated by a real aircraft. When it is not reinforced, its validitiy is suspect. The reinforcement of beacon by radar can be used as a criterion for automatic track acquisition, normal track correlation, or selective display of untracked beacon symbology.

3.4.2.2.2 Disadvantage of Beacon-In-Process Enhancement. The disadvantage of beacon-in-process feedback is that the P_{fa} is increased in the area wherein the detection threshold is lowered to obtain the higher radar P_d. This

3.4.2.2.2 (continued)

problem can be critical, especially if the sensitized region is large and happens to fall in a clutter area wherein the P_{fa} is not well controlled. Moreover, the technique of lowering the detection threshold only when a weak radar target is about to enter the system cannot be used to minimize the risk of false alarms, as it is so used in tracking feedback. This is true because the decision on enhancing the detection probability of the radar report based on beacon presence must take place prior to track correlation. Thus, no history is available to be used to estimate radar report strength at the time the decision as to whether or not to lower the detection threshold is made.

3.4.2.2.3 Advantage Versus Disadvantage of Beacon-In-Process Enhancement. The question to be answered now is whether the advantage of beacon-in-process enhancement, i.e., increased P_d on weak radar targets, outweighs the disadvantage, i.e., higher P_{fa}, in the sensitized region. It must be kept in mind that the number of weak radar reports whose detectability is enhanced by beacon-in-process feedback will be small. Moreover, since a beacon report is assumed to be available prior to enhancement, the loss of weak radar reports would not have as serious an effect on tracking reliability as the loss of a weak radar report when a beacon report is not available. Large increases in P_{fa} would certainly be too high a price to pay for increased detectability on a relatively small number of radar targets.

In order to make beacon-in-process feedback feasible, the increase in P_{fa} must be made small enough to balance the relatively small gain achieved by lowering the detection threshold. This can be done by minimizing the size of the sensitized region around the beacon report and still have a high probability of capturing the corresponding radar report within it. Assuming that the radar and beacon report from the same aircraft are range and azimuth distributed independently and normally about the true aircraft position, a 2 sigma region can be constructed about the beacon report position. This is done by first noting that the standard deviation in range for beacon and radar reports is about 0.1 nm. Under the normal assumption, the 2 sigma interval about the beacon report range would then be 0.57 nm. Since the standard deviations in azimuth for the beacon and radar are 0.33^0 (3.8 ACP) and 0.25^0 (2.9 ACP), respectively, the 2 sigma interval about the beacon report range is 1.66^0 (19 ACP). This implies that the sensitized region would be 0.57 nm in range and 19 ACP in azimuth. This would correspond to approximately 100 1/8 nm range cells. Thus, for example, if the P_{fa} is increased from 10^{-6} to 10^{-4} in order to enhance radar target detection, the expected number of false alarms in the sensitized region would go up from 0.0001 to 0.01, which is still a tolerable number.

3.4.2.2.4 Beacon-In-Process Enhancement Summary. By way of summary, the following conclusions have been reached regarding beacon-in-process enhancement:

1) Beacon-In-Process Enhancement can be used to enhance detection on weak radar targets.

2) The relative increase in number of targets declared through the use of Beacon-In-Process Enhancement is small.

3) The use of Beacon-In-Process Enhancement can be made feasible by minimizing the size of the sensitized region.

3.4.3 References

1) Final Report, "Test and Evaluation of the Radar Video Data Processor," Report No. NS-67-1, June 1967.

2) Skolnik, Merrill I., Introduction to Radar Systems, New York: McGraw Hill Book Company, Inc., 1962.

3) Swerling, P., "Probability of Detection for Fluctuating Targets," IRE Transactions, Volume IT 6 pp 269-308, April, 1960.

4) Radar Handbook, Merrill I. Skolnik, Editor In Chief, New York: McGraw Hill Book Company, Inc., 1970.

5) Final Report, "Investigation of Video Processing Concepts for ARTS-III Basic Radar Beacon Tracking Level Systems," Contract Number DOT-FA70WA-2289, Project Number 19180, October, 1970.

6) Final Report, "Expansion of the ARTS-III System to the Basic Radar Beacon Tracking Level Systems," Contract Number DOT-FA70WA-2289, Project Number 19180, March, 1971.

7) Steichen, P. E., "Definition of System and Environment Conditions for the Improved Basic Tracking Study," May, 1971.

3.5 DEDS/ARTCC INTERFACE

3.5.1 Introduction

The Data Entry and Display Subsystem (DEDS) provides the primary controller-system interface. Through the use of keyboard messages, quick look switches, and field inhibit switches, the controller can manually control the amount of alphanumeric data (i.e., target report symbology, aircraft information, and system information) to be presented on a display and aid the tracker by initiating, modifying, and deleting aircraft information and flight plan data. He can also manually initiate, accept, and recall the handoff of aircraft information.

Similarly, the Air Route Traffic Control Center (ARTCC) - ARTS III interface provides the tracker with aircraft information contained in flight plan data. In addition, if the ARTCC system has tracking capability, manual handoffs of track data blocks are made between the ARTCC and ARTS III.

Although the ARTS III system is intended to provide a man/machine interface which minimizes the controller workload required in supplying information to the computer, a need for enhancement in this area exists. Specifically, it is not only desirable but imperative that, in supplying information to the computer, a minimum amount of time (ideally no time) be required by the controller that would divert his attention from the display presentation. This allows the controller to devote full time to his primary function, i.e., monitoring and controlling the air traffic flow. In performing this function, it is essential that the controller be given a display presentation that contains a minimal amount of congestion due to display formats.

This section discusses methods of better computer utilization of the data received from and transmitted via the DEDS/ARTCC interface to meet the following objectives.

1) Increase tracking performance.

2) Reduce controller workload necessary to initiate and maintain correct alphanumeric association with radar/beacon targets.

3) Reduce display congestion.

3.5.2 Technical Discussions

3.5.2.1 Track Handoffs

The ARTS III program only provides, through a keyboard entry, a manual capability for the handoff of track data blocks both within the ARTS III

3.5.2.1 (continued)

system (intrafacility) and between ARTS III and the ARTCC (interfacility). With the addition of prestored data (site variable), the automatic handoff of track data blocks could be performed. This prestored data, specifically position, beacon code, and controller identification, together with the flight plan information received from the ARTCC, would enable the program to automatically initiate the handoff of a track data block to the appropriate controller when that track penetrates the designated area. For tracks designated as arrivals, intrafacility automatic handoffs would be initiated between the sequence controllers and the final approach controllers. For departures and overflights, interfacility handoffs would be initiated from the departure controller to the ARTCC. However, interfacility handoffs would only be made to an ARTCC with tracking capability.

Track handoffs from the ARTCC to ARTS III contain aircraft information that could be used to increase tracking performance. After an arrival flight plan message is received from the ARTCC, a handoff is initiated from the ARTCC. Between the time the handoff is received and the time it is accepted by the ARTS III controller, track update messages are received from the ARTCC. Contained in each update message are the current velocity components, as determined by the ARTCC tracker. These components are currently used only to compute the track's speed in tens of knots, which is used for display purposes in the track's data block. An additional use of the velocity components would be to aid the ARTS III tracking in the initial stages of tracking after accepting the handoff. By using this velocity as part of the track's history data, the probability of computing an erroneous initial velocity would be reduced.

3.5.2.2 Prime Keyboard Functions

To aid the tracking program in maintaining correct association between track data blocks and radar/beacon targets and to implement the transfer of data blocks to the appropriate controlling positions, the controller must enter at the keypack a specific keyboard function together with the appropriate alphanumeric data. Since these keyboard entries increase the controller's workload and divert this attention from the display, it is desirable to reduce or eliminate the required keypack entries. The majority of entries made by a controller in this capacity fall under the following keyboard functions:

1) Track Start.

2) Track Reposition.

3) Track Handoff.

3.5.2.2 (continued)

Since these keyboard functions would be the most used, it is advantageous to the controller that the operational program consider these functions as prime. The prime function capability would allow the controller to make maximum use of the slewball, which does not divert his attention from the display, and minimize the data entries from the keypack.

3.5.2.2.1 Track Start: For those tracks that are not actively tracked, the aircraft identity or discrete beacon code or tabular line identification, together with the slewball entry by the controlling position, would initiate active tracking on the aircraft.

3.5.2.2.2 Track Reposition: For those tracks that are actively tracked but have lost correct association with their radar/beacon target, the aircraft identification together with the slewball entry, would position the track data block onto the correct target. The loss of correct association would primarily apply to those tracks that are radar only or that have a non-discrete beacon code.

3.5.2.2.3 Track Handoff: For those tracks that are actively tracked but not in handoff status, a slewball entry would initiate the handoff of the track to the appropriate controller, based on the entering controller. This entry could be used in lieu of the automatic handoff capability discussed in Section 3.5.2.1, or in addition to automatic handoff, where this prime function could be used prior to the automatic handoff criteria being met.

For tracks that are actively tracked and in handoff status, a slewball entry at the receiving controller position would result in the acceptance of the handoff.

3.5.2.3 Data Block Congestion

Currently, through the use of the display Quick Look switches, data block Field Inhibit switches, range and off-centering controls, and keyboard function keys, a controller is able to select/inhibit the amount of tracked and untracked alphanumeric data that is displayed. Obviously, individual human factors govern the amount and types of data that each controller can monitor. However, the program should make use of all available information to aid the controller in making his decision in the selection of data. This is particularly true when dealing with the concept of all digital displays, i.e., no broad band video. Although this concept is beyond the scope of this study,

3.5.2.3 (continued)

certain basic considerations for the display of both tracked and untracked formats necessary in an all digital system should be mentioned at this point. Probably the most important consideration from a controller's standpoint is the ability to determine the relative strength of a radar return from a digitized symbol on a display. Without this ability, his confidence in the system, and therefore his acceptance of it, would certainly be questionable. Additional considerations are methods of presenting velocity vector, and some history data, e.g., a number of previous scans positions. Both of these can be quite costly in terms of both computer processing time and memory, and once again, additional alphanumerics and vectors may simply add to the problem of display congestion. A possible solution to the problem of representing target strength would be to present the targets with varying display intensities, e.g., one-quarter to full intensity, based on the quality of the target.

Although the use of current select/inhibit options allows the control of the amount of data to be presented, they do not necessarily allow for the desired amount. For example, if the only data blocks being presented to a controller through filter selections are those being controlled by him, together with a number of tracked data blocks being quick looked and a few untracked data blocks, both of which are in his control sector and which must be monitored by him, congestion may still be a problem. Further options to be considered at this point are condensed track data blocks, individual selection of data blocks, improved automatic offset schemes, and placement of data blocks on a callup basis.

Currently, track data blocks consist of two lines of up to seven characters per line and are divided into four fields. The first line, field one, is a seven character field that contains the aircraft identification (ACID). The second line contains fields two, three, and four. Field two is a three character field which contains the aircraft's altitude (if present) in hundreds of feet upon successful correlation, or the letters CST if the track is coasting. Field three is a one character field containing controller identification for a track in handoff. Field four is a three character field containing the track's speed in tens of knots (two digits) or special emergency symbology. A typical format would appear as follows:

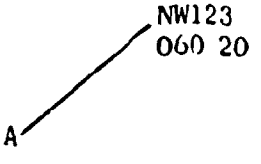

or

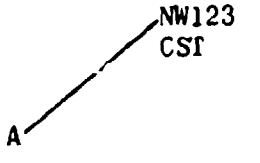

A savings in total display area could be realized by condensing non-hand-off data blocks as follows:

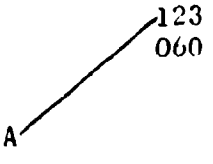

or

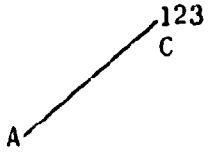

3.5.2.3 (continued)

Here, the flight number only is displayed in field one; field two contains the altitude or coast indication (C); and fields three and four have been inhibited with the field inhibit switches. For radar only or non-mode C aircraft, the altitude field would also be blank. When desired, a quick check on the velocity could be made by momentarily setting the field four inhibit to the off position. Since a common active track buffer is currently employed for outputting track data blocks, this method of condensing data blocks would result in increased storage needed for buffering because of the option of displaying the complete or the condensed ACID.

The option of individual selection of data blocks could be provided through the addition of a keyboard message. By selection a particular function and using the slewball for identification, a controller could select only those data blocks he wishes to see. Two methods for implementing this option could be considered. First, through the use of the field inhibit switches, all data blocks could be inhibited except those selected with the keyboard messages. Those selected data blocks would be forced (as are handoffs) and would overide the field inhibits. A second method would be to display only the selected data blocks. These data blocks would not be forced, and the field inhibit switches could be used to further suppress portions of these data blocks. Both of these methods require additional computer processing time and memory. However, the main drawback to this option is that it requires additional input from the controller, thus adding to his decision making tasks.

A similar option to that of individual selection of data blocks would be one in which data blocks are displayed on a call-up basis. Here again, a keyboard entry would be required to inform the program which data blocks are to be called up and which are to be placed in call-up status. This added requirement of more input data from the controller, together with the added burden of having to visually associate an aircraft with a target, or vice versa, would probably overide any benefits derived from the feature.

An attempt to solve the problem of overlapping track data formats is currently being made through the implementation of an automatic offset program. The obvious advantage to this approach is that all decision making is placed on the computer. Given a number of constants (e.g., alphanumeric size, leader length, etc.) together with the current display range and off centering information, the program creates a map by setting bits in a matrix to correspond to the area occupied by each data block controlled at a particular display. When overlaps are detected, different offset directions are tried to find one that results in no overlap. However, to obtain the desired results, each display must be adjusted precisely to the alphanumeric size, leader length, etc., corresponding to the values used by the program. In addition, the matrix map only approximately represents the actual area occupied by a data block. These problems, together with the inability of the software to

3.5.2.3 (continued)

detect many of the necessary hardware settings, result in the opinion of many controllers using the system that automatic offset is unusable. Alternate software algorithms, e.g., increasing the size of the matric map and/or computing display coordinates to represent the four corners of the data block, together with a capability of software detection of the many hardware settings would result in a usuable automatic offset system. However, the cost of an optimum system in both computer processing time and memory and in additional hardware features would be rather substantial, but improvement of the current automatic offset program should be considered.

3.5.3 DEDS/ARTCC Interface Summary

To meet the objectives of this section a number of possibilities have been discussed. Those that increase the controller's workload by either requiring additional input from the controller or by diverting his attention from the primary function of monitoring the display would not be considered enhancements and therefore would not be recommended. However, if the additional input required is only related to a "start-up" function, e.g., providing leader measurements to be used by the automatic offset program, which in the long run contributes to meeting an overall objective, it would not necessarily be considered as adding to the workload.

With the primary objective of having the machine work for the man, the following items are presented for consideration in the augmented tracking design:

1) Automatic track handoffs.

2) Prime keyboard functions.

3) Use of ARTCC data, specifically velocity components, to aid tracking.

4) Improved automatic data block offset.

5) Use of display intensity to show quality of a target.

SECTION 4
CONCLUSIONS AND RECOMMENDATIONS

In the course of this study we have a examined a wide variety of data utilization methods with the objective of defining those techniques which would contribute to an improved tracking system. This analysis is intended to supply the necessary components around which such a tracking system may be structured; it is not intended to totally describe an augmented tracking system, since this will be accomplished in a design effort to follow this study. Within this section is provided a summary of those techniques which have been investigated and which are recommended for further consideration during the design effort.

Within this study we have analyzed the data association problem and performed an exhaustive survey of correlation techniques applicable to the augmented ARTS-III system. We have chosen the maximum likelihood criterion as the basis for the correlation process. The selected algorithm uses a generalized nearest fit method for the processing of beacon and radar reports. By making fuller use of the available data, this method will result in improved track reliability, particularly in the presence of radar clutter. The generalized nearest fit method also has the capability to take into account available indication of data quality, such as validation and hit count.

The proposed correlation algorithm is initially intended as a replacement for the primary correlation routine in the RBTL system. Since it is able to evaluate and exchange pairs of locally best and second-best report-to-track assignments, the proposed algorithm is expected to perform much better in ambiguous situations than the "first-come-first-served" scheme employed by the RBTL primary correlation routine. Significant improvement is expected in track life and resistance to track swapping in crossing or parallel track situations.

Our studies of track smoothing and prediction have concentrated on improving performance of primary bin tracking and extending its range of adaptability to various data conditions. A variety of analytic tools and computational studies has been utilized to establish the following points.

1) Comparative study of a Kalman tracker with the RBTL tracker has shown that the basic form of the latter can be retained.

2) The firmness concept is retained and extended allowing α, β and search bin selections which are appropriate for:

Section 4 (continued)

a) Track initiation

b) Arbitrary sequences of missed reports.

c) Various data combinations (radar only, beacon only, combined).

d) Varying data error at various localities.

3) A major overall supervisory and adaptive control on the firmness operation is exerted by variable assignment of maximum firmness.

4) Range-angle coordinate system tracking has been rejected.

5) Acceleration smoothing in any form (e.g., polynomial fitting) has been found useless under current conditions and has been rejected.

6) Track oriented coordinate tracking (retaining x, y basic variables) has been found desirable. Implementation includes definition of two separate maximum firmness limits.

7) Bin size tables have been founded on track life analysis. Primary bin tracking is thereby improved.

8) Bin shapes have been arranged to account for various orientations of track error and data error ellipses.

9) The tracker is adaptive to more general environmental conditions. Flight plan and airway layout information can be used to control the filter. Clutter maps and hit counts can also be utilized.

10) Analysis can estimate clutter/blip-scan conditions which will permit effective tracking.

11) Deviation controlled smoothing and bin selection have been found to be possible to a limited extent. Further tests are required in this area.

12) Techniques such as coast correction, turn sensing and data pattern history analysis have been found to be of no value under current data conditions.

13) Multistage smoothing is not used for track smoothing and prediction (it is used for correlation). Instead, combined radar beacon reports are used for this purpose when available.

In addition to the above conclusions, some general principles have been established for smoothing and prediction. These include the basic equivalence of the optimal design of a tracker for accuracy of estimates, track life, and resistance to track swaps. Short and long range prediction, and accuracy of

position and velocity estimates can all be optimized together. Design of the tracker for special conditions such as holding patterns can be reduced to a definition of a track population; the α, β tracker permits only one parameter for this, λ, which forms the basis of all our design.

On the basis of our tracking studies, we believe that although the full Kalman recursions provide a very neat computational framework for the inclusion of various effects of mixed data sequences, different data errors, and so forth, the RBTL α, β tracker is actually more flexible in approach and represents a lesser technical risk. The simplicity and presence of only a few adjustable parameters in the Kalman recursions is purchased at the expense of sensitivity to the correctness of assumed data models. The firmness controlled α, β tracker, on the other hand, can be matched to approximate the Kalman tracker, or it can be adjusted to meet the exigencies of new data characteristics and aircraft populations without destroying its structure.

Track initiation and termination has been studied on several levels. Theoretical studies indicate that optimal initiation and termination logic should be a sequential test procedure. Initiation is based on two score thresholds: an upper one for the acceptance decision and a lower one for rejection. Scoring increments are based on the data fit (nearness of data to predicted track positions) and on the hit/miss report sequence. A suitable data fit score component which also contains information on hit count is available from the correlation routine.

The decision process is continued after initiation occurs in order to monitor the tracking. If the successive score increments, computed on the same basis as before, are positive, tracking is good and no action is taken. When the score increments are negative, the track enters the dropping mode, and the termination decision is made when the accumulated score drops a predetermined distance below the previous high.

These initiation/termination decision processes operate independently of the firmness score. Tracking during initiation, for example, proceeds under exactly the same α, β and bin size selection processes as normal tracking.

Exact values, however, for the various decision thresholds are difficult to assign on the basis of this theory and are best adjusted empirically via simulation. Some guidance has been provided for initiation logic design. Approximate formulas giving optimal upper and lower thresholds and score increment sizes for various data conditions have been provided.

In order to circumvent the approximate character of these evaluations, we have also made a more specific study of (n, m) initiation/termination logics (n consecutive reports to initiate, m consecutive misses to drop). For various assumed performance constraints (low mean delay to initiate, long track life, and low false track load) we have determined the best (n, m) logics to use and

the range of data conditions over which they may be successfully applied.

The following conclusions have been reached:

1) The mechanisms for controlling track smoothing and search bin selection which were developed for normal tracking are equally applicable to automatic initiation.

2) Area autoinitiation of all aircraft appears feasible, provided that the data quality can be controlled. For example, for a blip scan ratio greater than 0.72 and a clutter probability of less than 0.12 in the search bin, a (3, 4) logic meets reasonable performance constraints.

3) An alternative to strict data quality control is to modify the (n, m) or sequential logic in accordance with conditions as shown by the clutter map.

4) Intruder initiation is more feasible than area initiation. Data conditions and corresponding (n, m) decision rules have been mapped out for this type of operation. Together with the new correlation routine, this should substantially improve swap performance.

5) Track load problems can best be ameliorated by providing a separate, condensed first report track file. Most of the additional computer memory load imposed by autoinitiation results from first reports.

6) Speed checks appear to be effective as a screen to eliminate either stationary or Poisson clutter. They can be implemented in the form of upper and lower speed limit tables as a function of firmness. Tracks which violate these limits are terminated.

The discussion of tracking feedback has shown that it is possible to increase the probability of detection on weak radar targets by lowering the radar detection threshold. It was also shown that it is theoretically possible to use track file history data accumulated over several scans to predict when and where a weak report is about to enter the detection system. This information can be used to insure that the detection threshold is only lowered to enhance the detection of weak targets. Finally, it was shown that the increase in P_{fa} which accompanies the lowering of the detection threshold can be kept below a tolerable level by contructing a two sigma sensitized region around the track predicted position and employing an upper bound on the number of range cells included within this region.

It is recommended that a tracking feedback function for the augmented tracking level system be evaluated. This function should be implemented by generating sensitized regions about the predicted position of firm tracks when

weak radar targets are expected to enter the detection system. The prediction that a weak radar target will enter the system should be based on radar report track history accumulated over several scans.

It has been shown in the beacon-in-process enhancement discussion that lowering the detection threshold in a region around a beacon report in order to enhance the detection of its corresponding radar report increases the detectability of weak radar targets. The fact that no history data is available to estimate target signal strength requires that beacon-in-process enhancement be applied whether weak or strong targets are entering the detection system. Beacon-in-process enhancement can be made feasible by taking advantage of the error characteristics of radar and beacon reports to generate small sensitized regions.

It is recommended that a beacon-in-process enhancement function be incorporated and evaluated in the augmented tracking level system. This function should be implemented by generating a two sigma sensitized region about the beacon reports. Within that region, the radar detection threshold should be lowered in order to increase P_d on weak radar targets.

In the area of interface between the tracking function and the controller (via the DEDS), a number of items have been introduced which are intended to ease the controller work load. It is recommended that the data entry sequence be made less detailed through the use of prime keyboard functions, to perform the basic operations of track start, track reposition, and track handoff. The visual presentation of track data on the display can be made more comprehensive through condensed data blocks, improved automatic data block offset, and the use of display intensity to depict target quality. Finally, the continuous task of track handoffs, both interfacility and intrafacility, could be improved through the use of automatic handoff sequences.

This report contains algorithms, procedures, methods and suggestions (positive and negative) for upgrading the augmented ARTS-III system in the areas of data correlation, track smoothing and prediction, automatic initiation and termination, target detection, and DEDS/ARTCC interface. The work was limited to analysis aided by computer calculations and experiments and computer simulation of tracking conditions. Although we have confidence in the results obtained, a considerable amount of work is still required to apply them to the real world.

In order to assign particular parameter values, more extensive simulation and live testing will be required in many cases. Only in this way can a sufficient range of real data conditions be explored.

Many areas of the present study might also be further developed through additional work. For example, the quantitative advantage of deviation controlled smoothing and search bin selection is a somewhat subtle problem which was not

fully explored. Different initiation/termination criteria other than the single (n, m) type might be analyzed in numerical detail. Detailed handling of various data situations by the correlation routine and the selection of scoring parameters could be researched more fully. In each of these cases, as well as others, further quantitative development is possible which could reduce the extent of future simulation study required to make a definite design.

APPENDIX A

SYSTEM AND ENVIRONMENT CONDITIONS

A.1 SYSTEM CONFIGURATION

The system configuration to be taken as the baseline for the Augmented Tracking Study is the Basic RBTL system. The Basic RBTL system is designed as a single beacon/single radar configuration. It is comprised of four major subsystems as delineated below:

1) Data Processing Subsystem (DPS).

2) Beacon Data Acquisition Subsystem (BDAS).

3) Radar Video Digitzer (RVD-3).

4) Data Entry and Display Subsystem (DEDS).

Figure A-1 shows the functional relationship of the subsystem and identifies the principal paths of signal flow. A further description of the subsystem can be found in the document entitled "Expansion of the ARTS-III System to the Basic Radar Beacon Tracking Level System" (Reference 1).

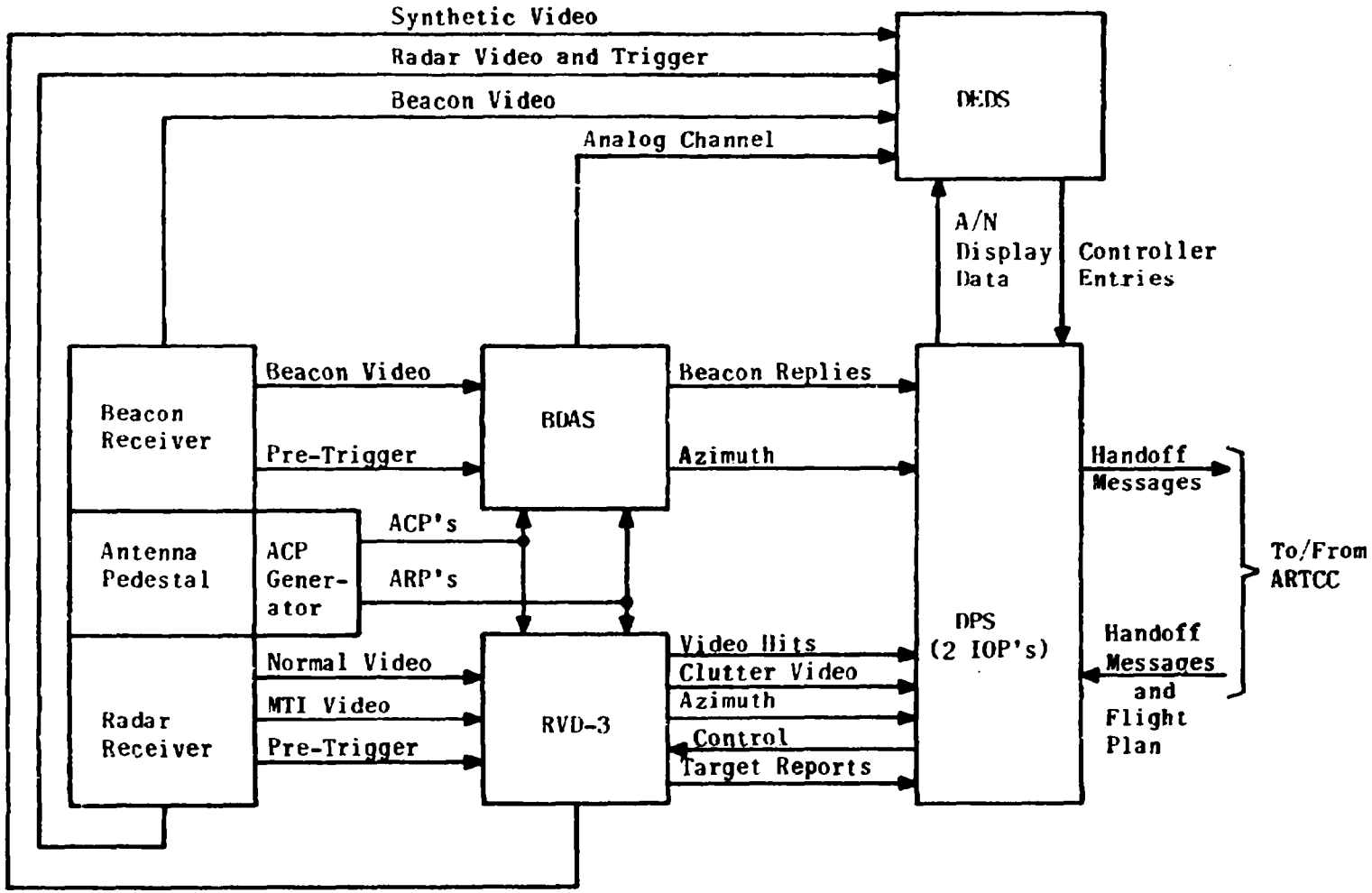

Figure A-1. Simplified Block Diagram of Basic Radar/Beacon Tracking Level System

A.2 RADAR PROCESSING SUBSYSTEM PERFORMANCE

Range:	Coverage	0 - 60 nm
	Accuracy (standard deviation)	0.05 nm
	Bias (adjustable to near zero) (Range error is approximately normally distributed).	
	Resolution	½ nm
Azimuth:	Accuracy (standard deviation)	¼° (2.9 ACP)
	Bias (adjustable to within 1 ACP) (Azimuth error is approximately normally distributed)	
	Resolution	3.5° (40 ACP)
Target Detection (probability)		¼ - 1 (typical range)
	Splits	1.5 - 2.5%
Clutter Density		0.06 reports/degree - nm heavy weather
		0.001 reports/degree - nm clear

(The number of clutter reports in a range-azimuth region can be modeled as a Poisson random variable.)

A.3 BEACON PROCESSING SUBSYSTEM PERFORMANCE

Range:	Coverage	0 - 55 nm
	Accuracy (standard deviation)	0.05 nm
	Bias (adjustable to near zero) (Range error is approximately normally distributed)	
	Resolution	0.8 nm
Azimuth:	Accuracy (standard deviation) (Azimuth error is approximately normally distributed)	$1/3^{0}$ (3.8 ACP)
	Bias (adjustable to 1 ACP)	
	Resolution	7.5^{0} (85 ACP)
Target Detection (probability)		0.75 - 1.00 (typical range)
	Splits (% of targets)	1%
	Reflections	not available
	Fades	7 - 10/turn
Radar/Beacon Reporting Statistics (typical)		
	Both radar and beacon reports	89%
	Beacon reports only	4%
	Radar reports only	6%
	Misses for both radar and beacon	1%
Radar/Beacon Range Difference (due to transponder delays)		0 - 1/8 nm

A.4 RADAR CHARACTERISTICS

	ASR-4	ARSR
Frequency Range	2700-2900 MHz	
Pulse Repetition Frequency	1140, 1170, 1200/sec	
	Staggered PRF (optional)	
Pulse Width	.833 u sec	
First Blind Speed (no stagger)		
PRF 1200	120-130 knots	
1170	117-126 knots	
1140	114-122 knots	
Beamwidth		1.25^{o}
Horizontal	1.5^{o}	
Side lobes	13 db down	
Back radiation	30 db down	
Elevation Pattern: cosecant^2 (see figure A-2 for ASR-7 specification)	18,500 ft @ 45 nm	
Scan Rate	15 rpm (13 rmp for ASR-7)	6 rpm
Maximum Configuration of radars for multi-sensor	3 ASR 1 ARSR (100 nm)	

A.5 BEACON CHARACTERISTICS

PRF (1/3 of radar)	400 max
Beamwidth	3^{o}
Beacon Mode Ratio (3/A, C) or (3/A, 3/A, C)	 1:1 2:1
Rotation	Slaved to radar

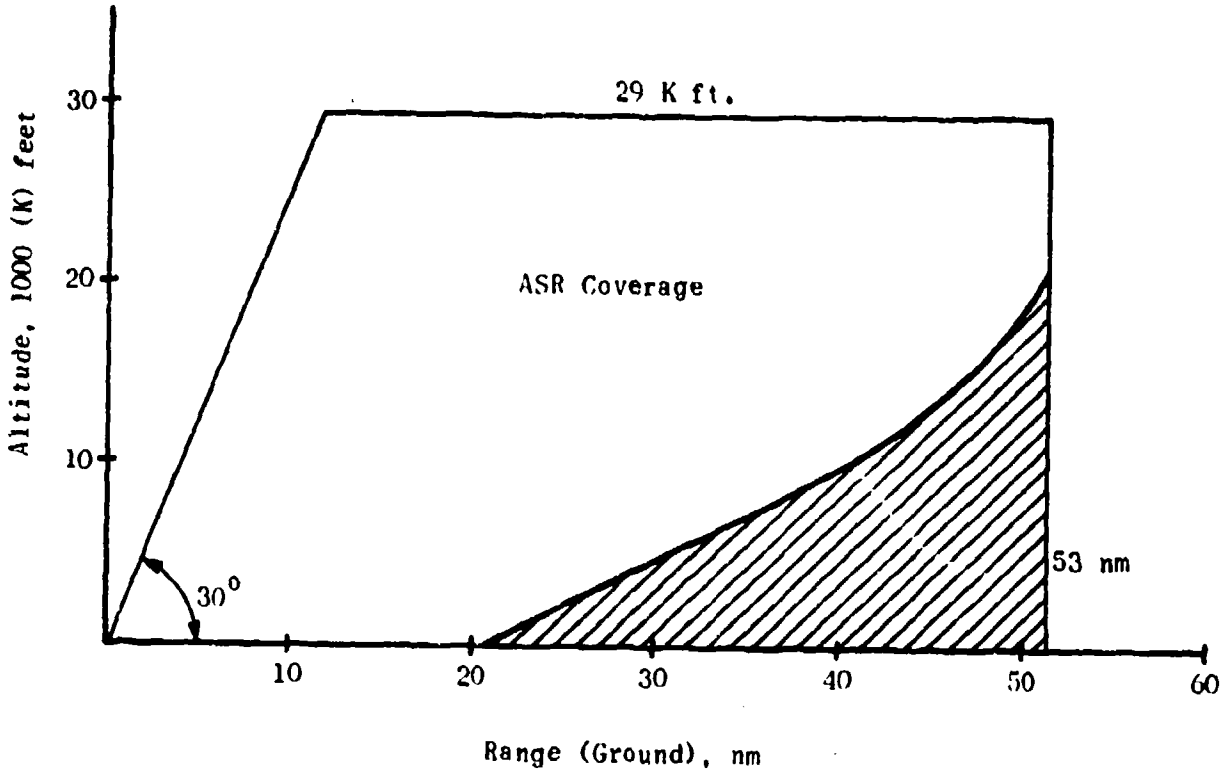

Figure A-2. ASR Elevation Coverage *

* Taken from ASR Specification FAA-R-864c (Feb 9, 1968)

A.6 TRACK ENVIRONMENT

Maximum radar targets/scan	ASR 500 ARSR 1000
Maximum beacon targets/scan	ASR 350 ARSR 700
Maximum beacon targets/45^0	ASR 70
Ratio of controlled to noncontrolled aircraft	2:3
Active associated tracks	200
Average active track life	40 min
Track controlled time (ave)	10 min
Track creation rate (ave, max)	3 - 7 per min
File of flight plans	500
Interfacility flight data transfers	1800/hr
No. of controller consoles	3 - 20
Beacon equipped targets	25% (mode C)

A.7 REFERENCES

1) "Expansion of the ARTS III System to the Basic Radar Beacon Tracking Level System," FAA Contract L/C DOT FA70WA-2289, March, 1971.

2) "ARTS III System Design Data," Volume I, FAA Contract DOT FA69WA-2071, 1 November 1969.

3) "Test and Evaluation of the Radar Video Data Processor," Report No. NS-67-1, Project No. 231-001-01X, June, 1967.

4) "Experimentation with the Terminal-Configured Radar Video Data Process," Report No. FAA-RD-70-33, July, 1970.

5) "NAS En Route Stage A, Radar Video Data Processor Modifications," Report No. FAA-NS-70-1, August, 1970.

6) "Airport Surveillance Radar System ASR-4 Theory of Operation," Manual No. FR-518-1.

7) "ASR Specification," FAA-R-864c, Feb. 9. 1968.

8) Work Statement for ARTS III Enhancement Program," Contract DOT FA70WA-2289.

APPENDIX B

THE TRACKING SIMULATOR

B.1 PURPOSE

At the beginning of the augmented tracking study, a decision was made to develop a computer-based tool to carry out preliminary evaluations of selected tracking algorithms. This effort was indeed worthwhile, since the process of building and using the tool provided valuable insight into the fundamental causes of many types of tracking difficulties. With this tool and our readily available computer, it became routine to (1) conceive of algorithms and expected results, (2) program the essentials of the algorithms and perform experiments, and then (3) judge the value of the algorithms. Through many repetitions of this process, we obtained a good understanding of the tracking process and gradually became prepared to formulate algorithms which combined the desired features of prior work.

B.2 COMPONENTS OF THE TRACKING SIMULATOR

The tracking simulator was designed to represent the essential features of the tracking environment and, initially, the RBTL algorithm as a point of departure. Throughout the design and construction of the simulator, steps were taken to keep the program simple while, at the same time, representing the environmental features which were considered critically important. Thus, for example, we programmed aircraft maneuvers and spurious radar returns, but we chose to use a convention for the placement of the sensor so that reports could be generated directly in the coordinate system of the tracker without additional conversion. The tracking simulator was made up of the following components, each of which we will now discuss:

1) Trajectory generator.

2) Report generator.

3) Tracking bookkeeping features.

4) Correlation and smoothing algorithms.

5) Performance statistics generator.

B.2.1 Trajectory Generator

This program was written to compute the coordinates of the true position of a simulated aircraft at the time of each radar scan. Since we were primarily interested in isolating tracking performance, this trajectory generator was built to represent only a small segment of a typical flight trajectory - a segment composed of only one or two parameterized turns. Thus, the essential

B.2.1 (continued)

numeric inputs to the trajectory generator were limited to the following small set of parameters:

1) Aircraft speed (knots).

2) Entry heading (degrees true).

3) Heading at coordinate origin (degrees true).

4) Exit heading (degrees true).

5) Turn rate (degrees per second).

In addition to the foregoing information, the program made use of certain conventions to simplify the computation of position. First, by convention, each trajectory was defined in cartesian coordinates and was constrained to pass through the coordinate system origin at the time of the 21st scan on the heading specified by the user. Since the user had the freedom to specify three headings, he could cause the trajectory generator to produce trajectories in the form of:

1) A straight line at any heading.
(All three headings numerically equal.)

2) A right turn.
(Exit heading to the right of heading at origin and heading at origin to the right of entry heading.)

3) A left turn.
(The converse of (2).)

4) An S turn.
(Heading at origin to the right or left of both the other two.)

Since each turn was constrained by program convention to be less than 180 degrees, no other data was required to allow the user to unambiguously specify a trajectory.

Typically, trajectory segments of about 40 scans duration were used in our study. In most cases, this allowed sufficient time for a steady state to be reached prior to the turn, as well as after the turn.

B.2.2 Report Generator

The report generator of the tracking simulator is actually made up of three separate program sections which simulate the essential report level outputs from beacon and radar data acquisition systems. Each of these three sections may prepare position reports and put them into a memory table refered to as the report store.

The first section prepares beacon reports. It simulates the beacon blip/scan process at the reporting level by comparing the output of a pseudo-random number generator with a beacon blip/scan ratio supplied by the user. Next, it simulates the beacon "fade" process which is a consequence of antenna shielding. For fade simulation, we chose to simply allow the user to specify those scans (by identification number) on which no beacon transponder return would be received due to shielding. When a simulated beacon report is to be generated, the program computes and adds a separate normal deviate to each component of the true aircraft position and stores the resulting pair of coordinates in the report store as a beacon report.

The second section, similar to the first, simulates primary radar blip/scan and measurement noise and then stores radar reports in the report store. It should be noted that the standard measurement errors for beacon and radar are each specified separately in range and azimuth. Each of these four quantities is specified by the user in nautical miles and, as a simplification, is held constant throughout the simulation. We feel this simplified representation to be sufficient for our analysis because we have concentrated on flight segments of relatively short duration, and other allowances for varying azimuthal errors can be made.

The third section of the report generator is a program which simulates radar clutter. Radar clutter reports are taken to be Poisson distributed at a mean clutter density specified by the user. As clutter reports are generated, they are placed into the report store where they appear to the correlation and tracking logic to be identical in form with valid radar reports. However, for summary statistical purposes, they are identified as clutter reports (see Subsection B.2.5).

The mechanism by which clutter reports are generated is not entirely straightforward and, thus, deserves comment here. It consists of three steps: clutter area definition, area subdivision, and clutter generation.

In step 1, an area for clutter generation is defined as a rectangle containing all currently predicted track positions. In this process, the track store is searched for maximum and minimum values of X and Y coordinates of predicted track positions. Of course, if only one track is being simulated, this rectangle reduces to a point at the predicted position of that track.

B.2.2 (continued)

In step 2, a large buffer strip is added all around the rectangle to assure that a large enough area around the track can be covered by clutter. The width of this buffer strip is a system parameter, held at 1.0 nm throughout our study. It should be noted that the only reason for this clutter area definition is to limit computational load caused by clutter generation and processing, and to do so without biasing the results of the study.

In step 3, after the clutter area is defined, it is logically subdivided into a set of strips as shown in figure B-1. Each strip has a width of one radar range grain ($\frac{1}{16}$ nm) and crosses the clutter area at a constant range from the sensor. These strips then represent the ranges at which clutter reports may occur.

Now the clutter sampling process can be reduced to a one-dimensional problem if one simply envisions all the strips placed in line, end-to-end. The user-specified average clutter density, C, (clutter reports per unit area) is converted to an average interclutter distance (d) along that line by multiplying by the strip width ($\frac{1}{16}$ nm) according to:

$$d = 1 \; / \; (C \times \frac{1}{16}).$$

Sampling can now be carried out by making use of the fact that intersample intervals in the Poisson distribution are exponentially distributed. We obtain a sample, s, from the exponential distribution of mean, d, using a pseudo-random number generator. The sample length, s, is placed on the strip line and the clutter report coordinates are obtained by division and differencing. This sampling process then continues until the line is exhausted.

However, one additonal check is made to ascertain that clutter reports are not generated closer together than the resolution of the RDAS allows. If the sampled clutter separation distance, s, is less than the azimuthal resolution (converted to distance), the sample is simply rejected and a new sample obtained. Thus, this clutter generation procedure provides, we believe, an appropriate level of realism in generating Poisson clutter while accounting for both the range granularity of the sensor and the system's azimuthal resolution.

B.2.3 Tracking Bookkeeping Features

The bookeeping features provided in the tracking simulator are centered about two important data tables which are logically very similar to those found in the Basic RBTL program. As in the RBTL, we refer to these tables as the central track store and the report store.

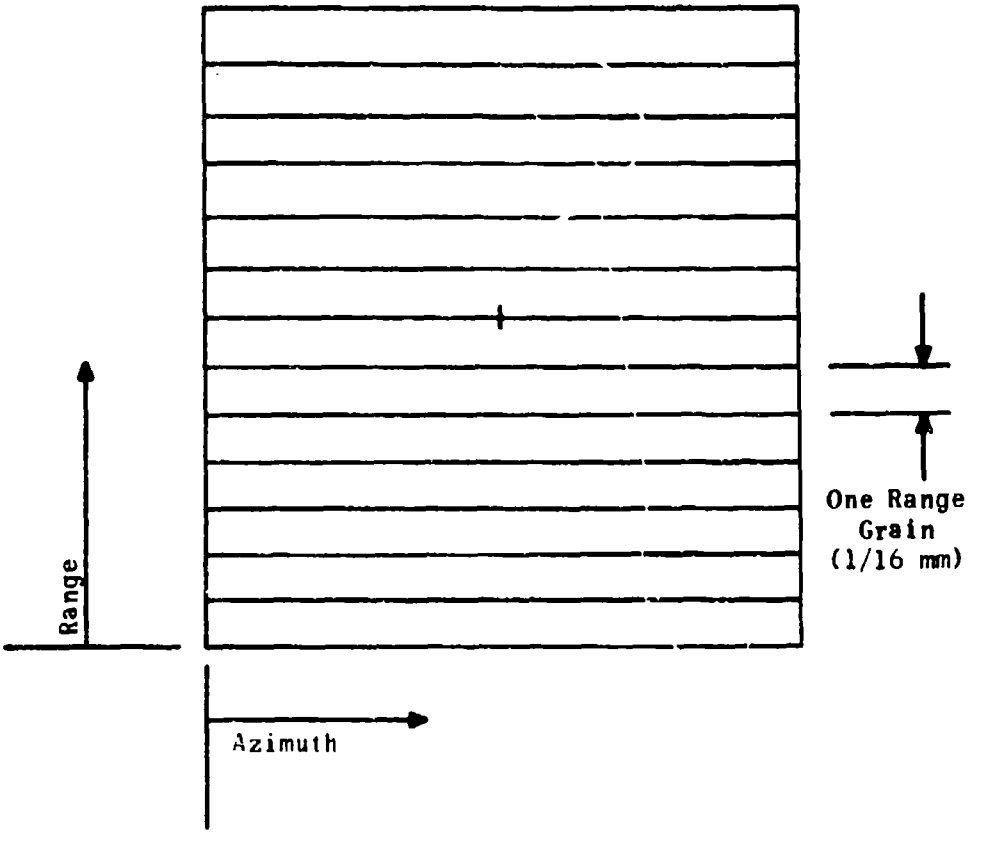

Figure B-1. Subdivision of the Clutter Area

B.2.3 (continued)

The central track store contains all the essential information needed to carry out tracking. Its elements are as follows:

1) Track class (initial, normal, parent, etc.).

2) Track X coordinate (smoothed).

3) Track Y coordinate (smoothed).

4) Predicted X coordinate.

5) Predicted Y coordinate.

6) Rate of change of X coordinate (smoothed).

7) Rate of change of Y coordinate (smoothed).

8) Track firmness number.

9) Track status (coast count).

The report store contains only the following three elements:

1) Reported range (Y coordinate).

2) Reported azimuth (X coordinate).

3) Report type (beacon, radar, or clutter).

As mentioned earlier, the distinction between radar and clutter reports is used only in the preparation of summary statistics and is not made available to the tracking programs.

The basis of operation of the tracking simulator is the program loop shown in figure B-2. This loop is exercised once for each sensor scan to be simulated. In our study we restricted the loop to 41 iterations for each trajectory.

In addition to this loop, a control logic was provided to allow specified numbers of replications of each trajectory to be flown and sets of different trajectories to be handled in sequence. Thus, it was possible for us to define a numerical experiment as a set of different trajectories, each of which was to be flown a uniquely specified number of times. A program which served to accumulate and display performance statistics was also included as part of the experiment control loop.

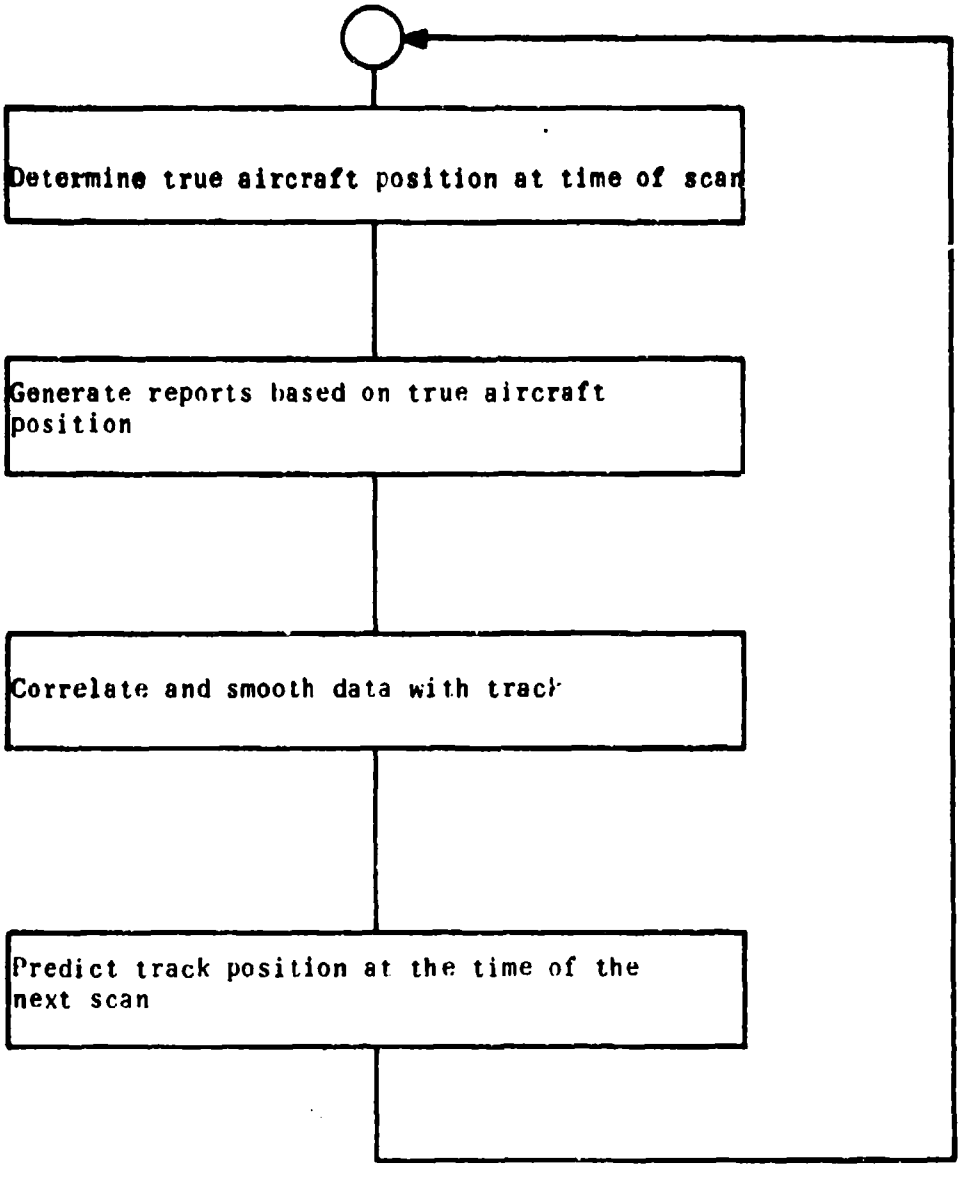

Figure B-2. The Basic Tracking Simulator

B.2.3 (continued)

Throughout our experimentation, we found it to be helpful to display in graphical form certain data from the trajectory generator, the report generator, and the correlation and smoothing programs. As work continued and our interests shifted, a flexible graphical display capability gradually developed. That capability is controlled through data switches on the computer and is, consequently, highly responsive to user's wishes. The following list of data switch functions illustrates the final state of the grapnical and tabular display features of the tracking simulator programs.

1) Pause.

2) Print content of report store at each scan.

3) Print true, radar, and beacon report positions at each scan.

4) Print content of central track store at each scan.

5) Plot true trajectory positions.

6) Plot radar observations (less clutter).

7) Plot beacon observations.

8) Plot, at enlarged scale, all observations.

9) Plot search bins, either scale.

10) Print debugging messages.

11) Plot predictions, either scale.

Examples of some of these graphical display features are included here as Figures B-3 through B-8, which show the following:

B-3) True trajectory positions.

B-4) Radar observations and true trajectory positions.

B-5) Beacon observations and true trajectory positions.

B-6) Search bins and true positions.

B-7) All observations and search bin at enlarged scale (for one scan).

B-8) Predicted and true positions.

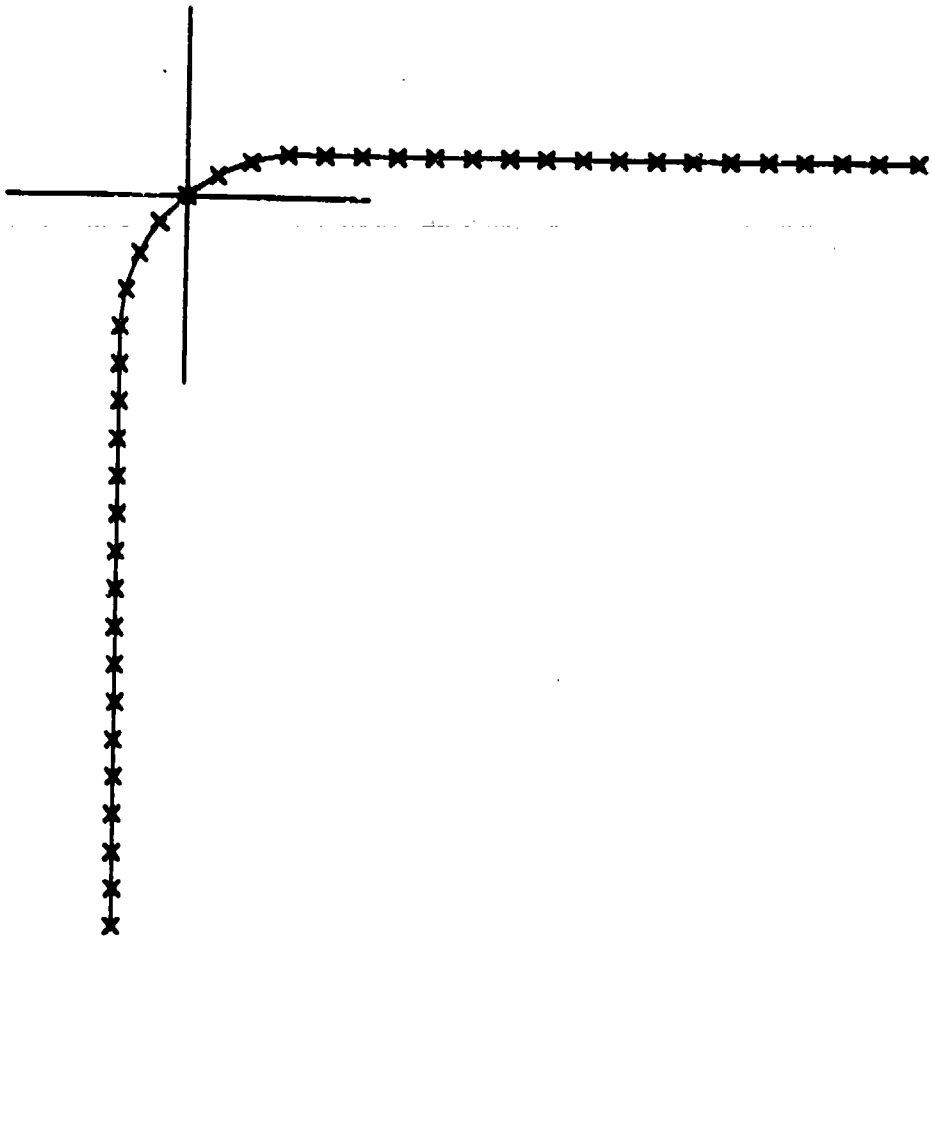

Figure B-3. True Trajectory Positions

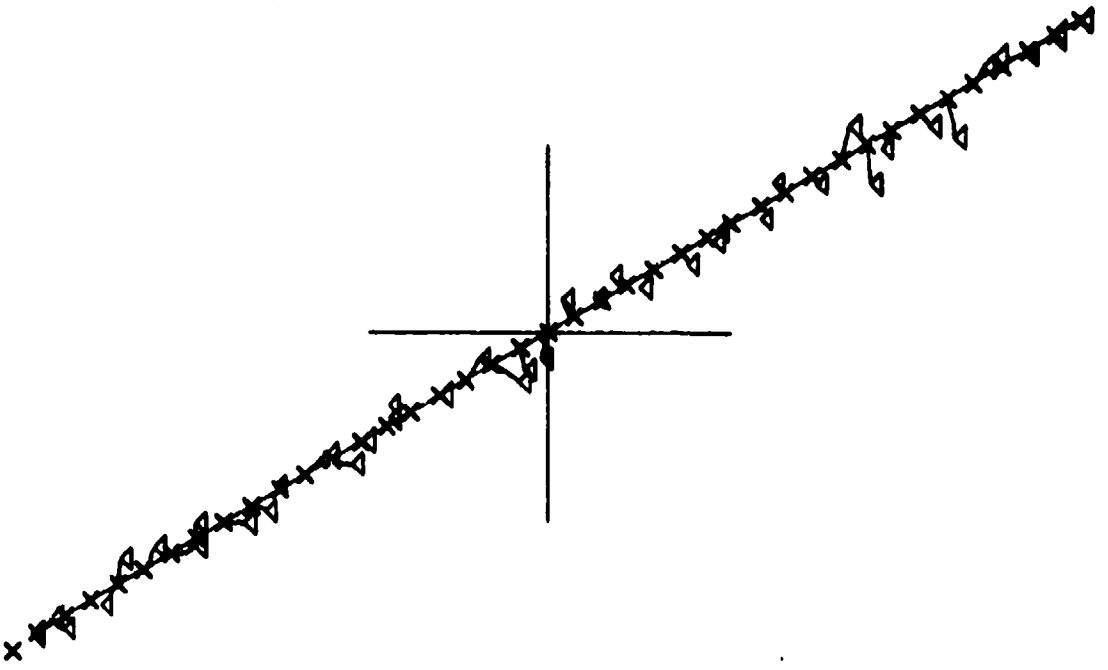

Figure B-4. Radar Observations and True Trajectory Positions

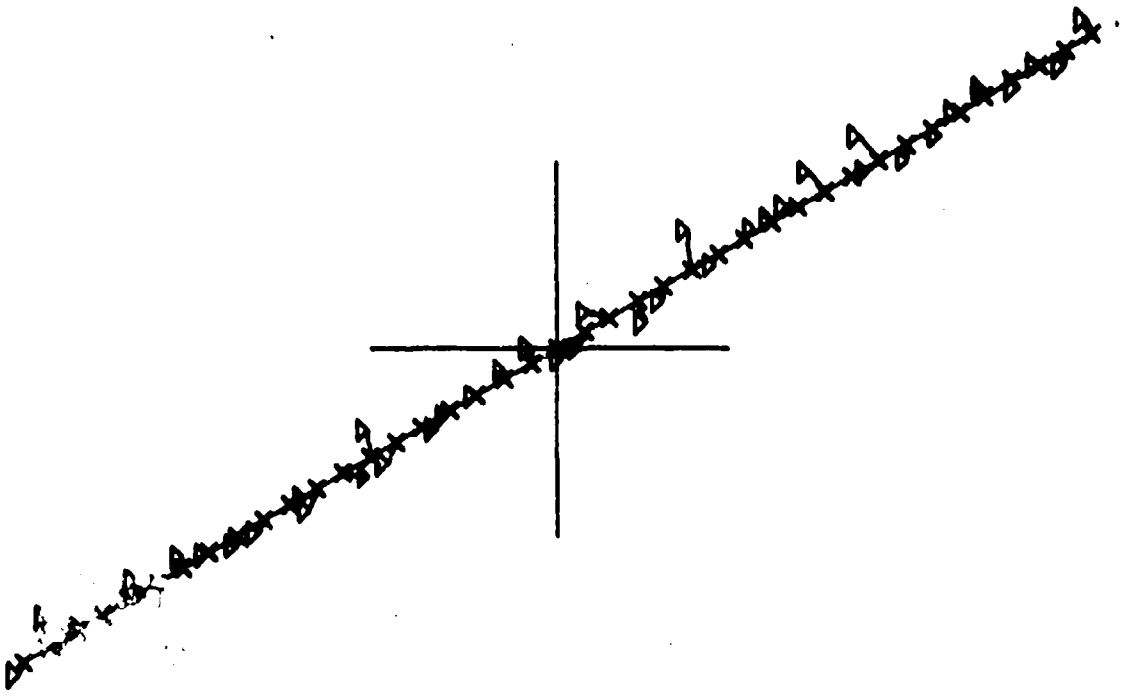

Figure B-5. Beacon Observations and True Trajectory Positions

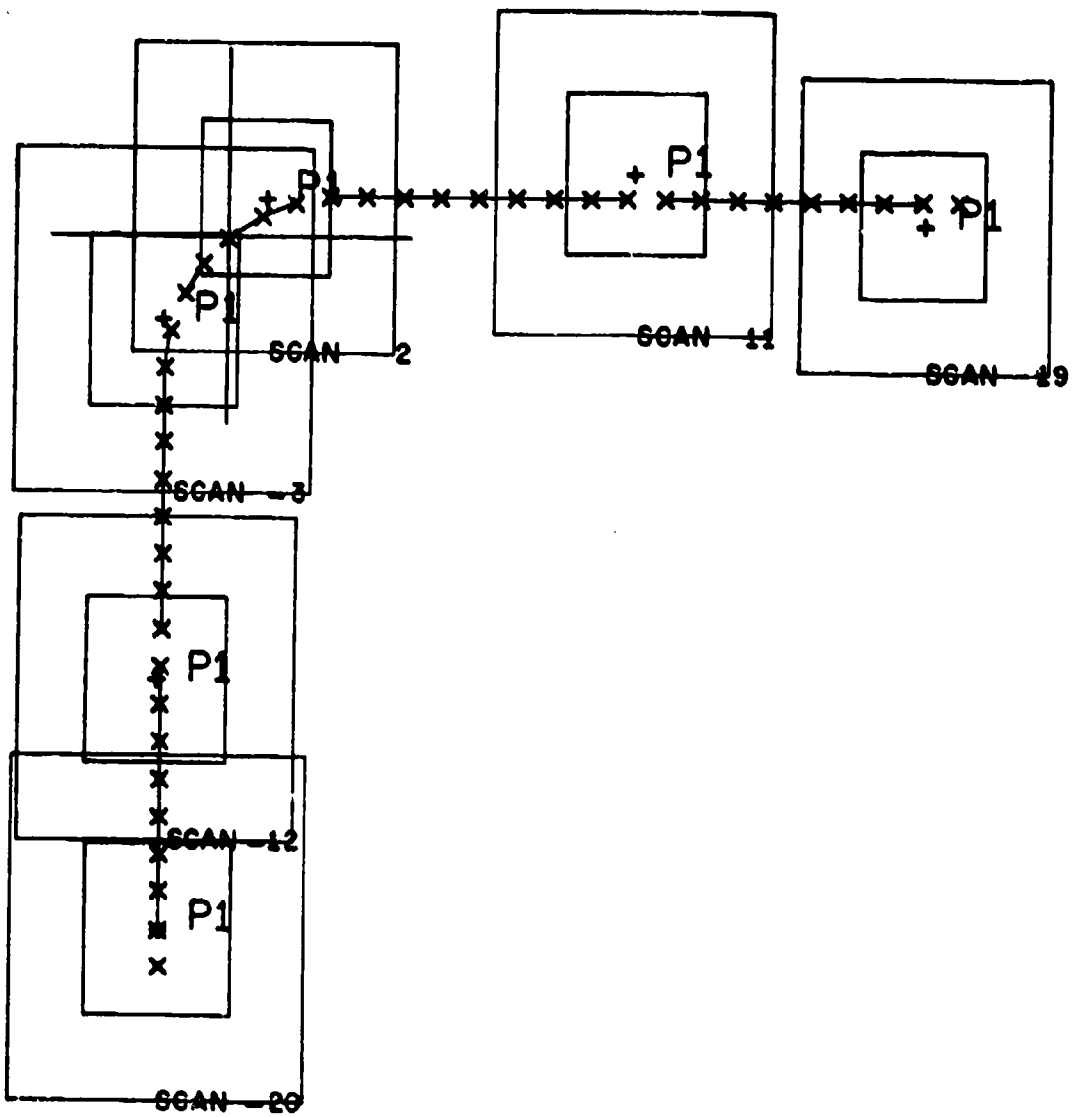

Figure B-6. Search Bins and True Positions

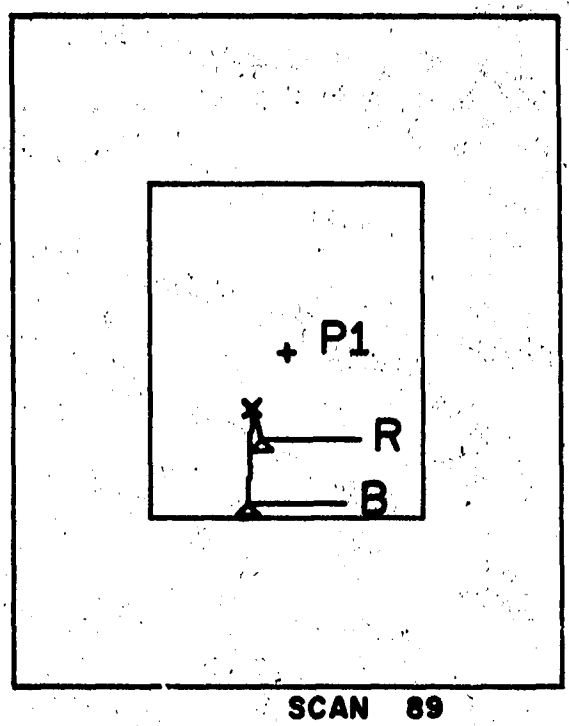

Figure B-7. All Observations and Search Bin at Enlarged Scale (for one scan).

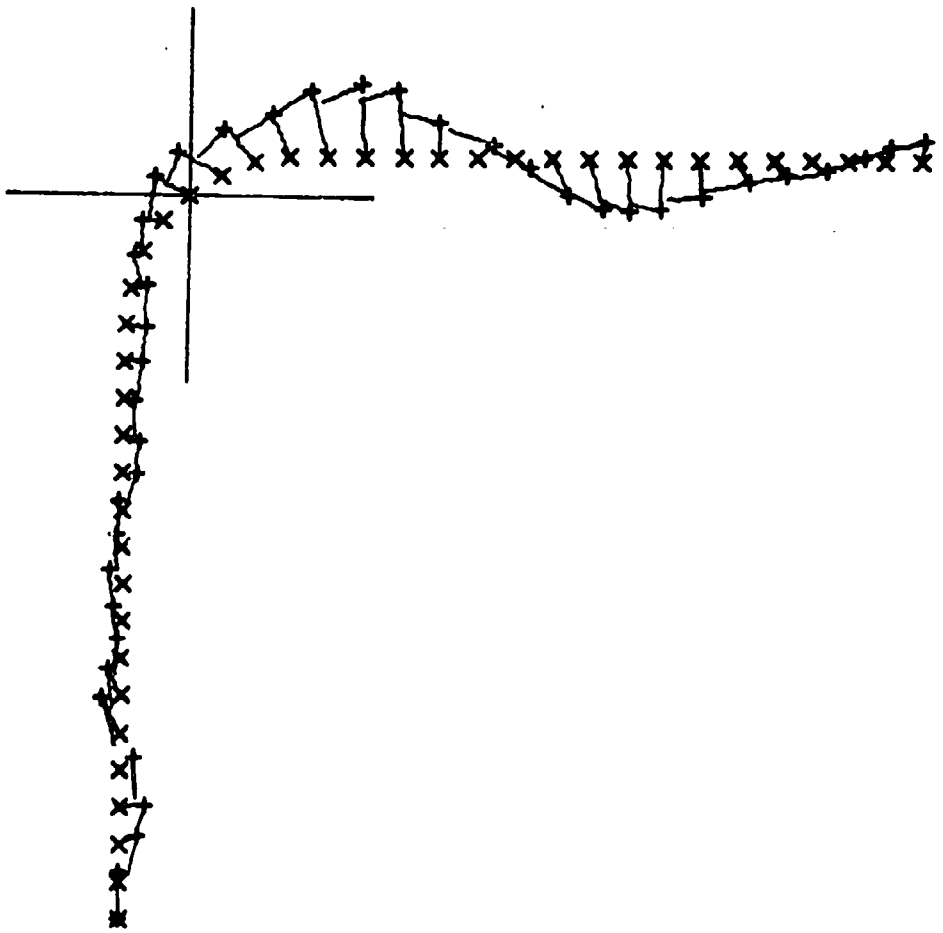

Figure B-8. Predicted and True Positions

B.2.3 (continued)

In figure B-3, the sequence of true trajectory positions is simply indicated by an "x" at each true position at scan time and a line connecting successive true position points.

In figures B-4 and B-5, observations are plotted in addition to the true trajectory points. The deviations found in radar and beacon data are, in general, very large in relation to the aircraft movements from one trajectory point to the next. Consequently, it is often impossible to tell in a simple plot of trajectory positions and data exactly which data were derived from which trajectory point. In order to eliminate this kind of ambiguity to the human viewer, we have seen fit to have the program plot lines which connect the plotted observations with the true trajectory positions from which they were derived. These lines, then, are plots of the data derivations themselves and, of course, represent quantities not available to any tracking program.

Figure B-6 shows the progression of primary and secondary search bins. These bins are centered on predicted positions and, consequently, this figure shows the unsteadiness in predicted positions as well as the bin size (firmness) response of the tracker.

Figure B-7 shows at an enlarged scale (2.5" = 1.0 nm) the entire set of data pertinent for a single scan. The symbology used in this type of enlarged scale plot is basically the same as that used in the other plots.

The type of plot shown in figure B-8 is used to represent in a fairly concise fashion the overall operation of the tracking system. Added by the plot format is a line leading from the last smoothed track position (+). Thus, this line shows the smoothed velocity used in prediction. Again, to lessen the possibility of misleading ambiguity in this plot, the predicted position (+) is connected with the associated true position (X) by a line which represents the momentary error in the predicted position.

B.2.4 Correlation and Smoothing Algorithms

The correlation and smoothing subroutine was the part of the Tracking Simulator which was changed most often in our investigation of various ideas. Once the correct functioning of the experiment control loop was established, program changes to accommodate the investigation of different tracking algorithms were almost entirely restricted to the correlation and smoothing subroutines.

Approximately ten distinct correlation and smoothing program decks were prepared throughout the study, each with parameters whose values were adjusted to alter the operational details of the algorithms. A more detailed discussion of these various correlation and smoothing programs and the associated experimental results is presented in section B.3 of this appendix.

B.2.5 Performance Statistics

A set of performance measures was defined to allow numerical comparisons of the performance of the various tracking algorithms. A separate subroutine was then prepared to accumulate these measures throughout the course of each experiment and print them at appropriate points during, as well as at the end of, the experiment. These performance statistics, along with the various graphical displays provided by the tracking simulator, proved invaluable in disclosing both quantitative and qualitative features of algorithm performance. The statistics accumulated and displayed at the end of each set of iterations of each trajectory are the following:

1) Track life (number of scans).

2) Track life (percent).

3) Average tracking errors.
   - X coordinate
   - Y coordinate
   - RMS distance.

4) Overall average search bin area (square mile).

5) Average search bin size versus scan number (a histogram).

6) Number of clutter reports used by the tracker.

7) A histogram showing the number of track drops versus scan number for a set of iterations of a simgle trajectory.

At the end of an entire experiment composed of a set of iterations on each of a set of trajectories, the overall track life (number of scans and percent) is printed and an overall track drop vs. scan number histogram i prepared.

B.3 USE OF THE TRACKING SIMULATOR

As we began using the tracking simulator in this study, it became apparent that one could not reasonably devise, test, and, in any sense optimize the design of a tracking algorithm without first hypothesizing some population of track characteristics. This observation remains as valid today as it was at the outset. Indeed, it seems to be one of our most important observations that it is possible to make tracking system design improvements only to the extent that distinct trajectory and data characteristics can be identified and processed accordingly. For example, whereas a straight trajectory segment is tracked best when highly smoothed, a turning track segment must be smoothed much less and, indeed, the recognition of the transition from straight to

B.3 (continued)

turning track (or the converse) is the central problem in tracking system design. As another example, we have seen that there is considerable advantage in applying different tracking algorithms to the radar only, the nondiscrete beacon (and radar) target, and the discrete beacon (and radar) target. The general composite system faces two distinct problems: errors in report association and normal sensor measurement errors. Track accuracy can be improved only to the extent that both these problems can be solved. It is with regard to the problem of correct report association that the various classes of trajectories are most highly differentiated and require separate processing.

We chose an approach making use of a set of distinct trajectories which could be flown separately by the trajectory simulator, but could also be combined later at the performance measure level if desired. That set of trajectories consisted of:

1) A straight (diagonal) segment (150 kts).

2) A 60^{0} turn (180 kts, 3^{0}/sec.).

3) A 90^{0} turn (180 kts, 3^{0}/sec.).

4) An "S" curve consisting of two 50^{0} turns (190 kts, 3^{0}/sec.).

By observing the computed performance statistics on each on these trajectories, it was possible to understand the sometimes subtle differences among the performance characteristics of the various algorithms which were tested.

A total of more than 120 separate numerical experiments were performed with the tracking simulator. While most of these experiments were only exploratory and intended to determine appropriate combinations of various parameters for each algorithm, nevertheless, a wide range of algorithms was tested. These algorithms included the following:

1) RBTL (primary bin tracking).

2) Deviation controlled firmness.

3) Deviation controlled smoothing.

4) Coast correction logic.

5) Radar-Beacon report averaging.

6) Multi-stage smoothing.

B.3 (continued)

The remainder of this appendix presents brief discussions of the experimental findings associated with each of these six classes of algorithms.

B.3.1 RBTL (Primary Bin Tracking)

The simulation of RBTL primary bin tracking logic served two purposes: first, to provide a numerical basis for comparison with other simulated results, and, second, to provide an intuitive understanding of the point-of-departure RBTL system. It was soon discovered that the RBTL primary bin system was virtually unable to track turning aircraft. Simulated turns of more than about 30 degrees 3^{o}/sec. led invariably to a drop from the primary bin and a recourse to the secondary bin/turning track operation. We believe that in a well designed system, most of the track maintenance should be performed by the primary correlation and smoothing. This should include straight trajectories as well as the majority of well behaved turns. The secondary system provides a recovery from a primary drop and should be used as infrequently as possible. For these reasons, we chose to concentrate attention on making improvements in primary bin tracking alone. Thus, we recommended that the RBTL turning track logic be retained to reacquire the hopefully smaller number of tracks which would still be dropped from primary bin tracking by the improved algorithms.

B.3.2 Deviation Controlled Firmness

As a result of observing plots of simulated trajectories, predictions, and primary search bins, we noted that the RBTL system made no significant attempt to expand the primary search bin in turns and, consequently, increased prediction errors were encountered. It became apparent that the firmness/bin size relationship used by the RBTL logic made the RBTL firmness changing mechanism virtually nonresponsive to turns, particularly when high firmness tracks began turning. This motivated an investigation of the performance of several algorithms which attempted in different ways to change the track firmness value in response to observed deviations between predicted and reported positions.

The firmness logic of the RBTL primary system (figure B-9) is, in a limited sense, deviation controlled, since

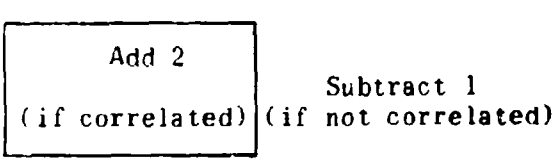

Figure B-9. Firmness Adjustment in the RBTL Logic

B.3.2 (continued)

very large deviations (reports beyond primary bin correlation limits) lead to reductions of firmness. Our experiments included modifications of this logic, attempting to make firmness more responsive to observations. Firmness increments such as those shown in Figure B-10 were tested, and it was found that under certain circumstances, significant improvements in primary bin track life could be achieved. In the system illustrated in Figure B-10, for example, if a report is found in the center 1/3 of the primary bin, firmness is increased by 2, in the intermediate 1/3, by 1, and if the report is beyond the intermediate 1/3, firmness is decreased by 1. These experiments motivated much of the analytical work in this area reported in section 3.2.

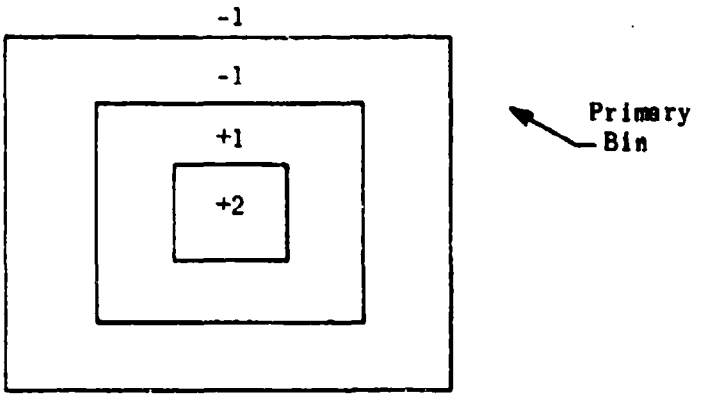

Figure B-10. A Form of Deviation Controlled Firmness Setting

B.3.3 Deviation Controlled Smoothing

The simulation results indicated that the RBTL system is not sufficiently responsive to data and frequently loses tracks on turns. An ideal solution to this problem would adjust the responsiveness of the smoothing filter to match the characteristics of the trajectory. Unfortunately, these characteristics can only be roughly inferred from the noisy data, and the desired filter adjustment cannot always be achieved. The RBTL system uses track firmness to influence the choice of the smoothing constants and thereby adjusts the tracking filter responsiveness. Since RBTL firmness is a long term measure of correlation behavior, the filter characteristics are not easily disturbed by data noise and are quite stable. For the same reason, however, the filter response to a change in trajectory direction is very slow, resulting in an inability of the primary tracking system to follow turns. A faster filter response would most certainly improve tracking on turns, but it would also adversely affect performance on straight track segments.

B.3.3 (continued)

A number of experiments were carried out to explore several techniques to directly control the smoothing constants via the deviation of the data reports from the predicted position on the last several scans. We first made use of the instantaneous deviation on the last scan to select smoothing constants. Secondly, we tested a deviation control system which used the last n deviations in selecting smoothing constants. As indicated earlier, the motivation for deviation control was to make the system more responsive to the data when large deviations were observed.

As expected, the use of larger smoothing constants yielded better tracking on turns, but at the same time it made tracking our straight flight segments less reliable. The deviation control notion was an attempt to combine the best of the small smoothing constants for straight segments and the large smoothing constants for turning on maneuvering segments. This is not qualitatively different from the action of the RBTL logic, since turning tracks, when in use, employ generally larger smoothing constants. However, the method we were testing was, in effect, a gradual transition between "normal" and "turning" track processing in the place of the step transition of RBTL. In general, our results were encouraging. The best overall results were obtained from a relationship between observed deviation and smoothing constants shown in figure B-11. The small smoothing constants used for small deviations did, as expected, yield good tracking on straight segments, and the larger constants associated with larger deviations made the system perform much better on turns than the RBTL primary bin tracker. However, even the most satisfactory method did not eliminate track drops, and it became obvious that further increases in responsiveness to data could only degrade performance. Basing the selection of smoothing constants on a combination of deviations observed on the last two scans instead of just one also resulted in a degradation of tracking performance.

B.3.4 Coast Correction Logic

It was observed that simulated low blip/scan data during straight flight segments had little effect on track accuracy and virtually none on track life. However, on turns, such absence of data almost always led to a tracking drop. Therefore, a test was made of a system which, in the absence of data, would use the data pattern observed on the preceding two scans to estimate a turn rate and predict a new position (a curvilinear coast).

The coast correction logic seemed to provide significant improvement in turn tracking but, even with very high blip/scan ratios, it led to unsteadiness and occasional tracking drops on straight tracks. It later became clear that the use of only the two preceding data points makes turn rate estimates much too noisy to be of value. Whereas the use of more than three or four preceding data points might offer hope of reducing the incidence of false coast corrections, it would also introduce unacceptable delays into the turn detection process. Consequently, the investigation of the coast correction logic was dropped. These results were supported by the conclusions of Section 3.2 regarding the feasibility of estimating acceleration.

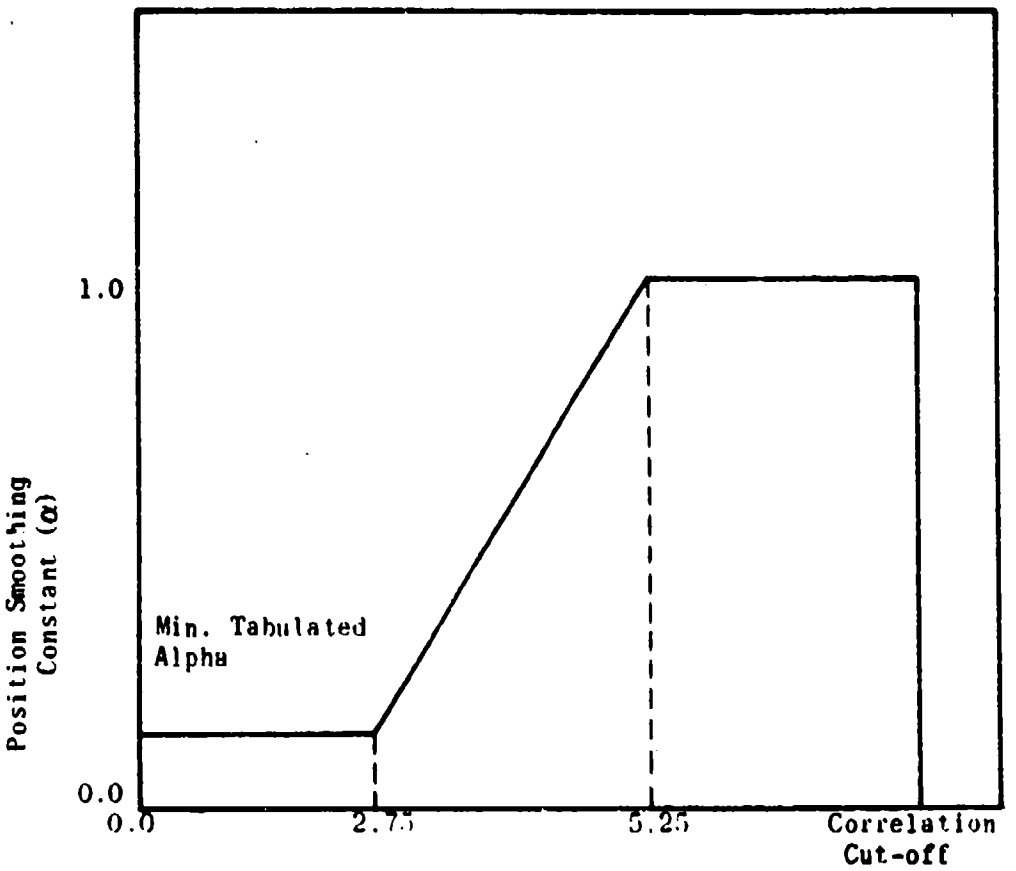

Figure B-11. The Preferred Relationship Between Smoothing Constants and Observed Deviations

B.3.5 Radar-Beacon Report Averaging and Multi-Stage Smoothing

The study also included experimental investigations of general methods for combining radar and beacon reports in correlation and smoothing in the presence of radar clutter. In the first of these tests, the RBTL algorithm was modified to use both radar and beacon reports when one of each was found in the track's primary bin. The reports were combined by weighted averaging and then smoothed as a single report. Only a small improvement over the RBTL operation was obtained.

Next, a sequential smoothing technique was investigated. In this method, smoothing was done first using correlated beacon data. Then, a second smoothing operation was carried out on the radar data. Because of this separation of beacon and radar processing, it was possible to add other tests between the two smoothing operations. The first of these centered a radar bin around the beacon data, and a small reduction in performance was noted. Second, a radar bin centered about the beacon-smoothed track position was tested, and a significant improvement in performance was noted. This algorithm makes use of radar data, even when more than one radar report is within the correlation bin, by using a single radar report which is nearest to the beacon-smoothed track position and disregarding any others. Testing of this "multi-stage" smoothing algorithm was continued in a heavy clutter environment, and it was concluded that it offered promise of significantly improved track accuracy and a surprising degree of insensitivity to clutter.

APPENDIX C

COMPUTER STUDIES OF SMOOTHING, INITIATION, AND TERMINATION

C.1 INTRODUCTION

This appendix contains a summary of some numerical conclusions studies which support the conclusions and results reported in preceding sections. Three different studies are included and the appendix is divided into corresponding parts.

In the first of these, the Kalman relations (18), (19) are exercised to provide optimal solutions for the basic α, β tracker model postulated in sections 3.2.2.1 through 3.2.2.3. These solutions are then used as standards of comparison and as source data for much of the subsequent development.

The second part of the appendix reports on some experiments with track-oriented and/or acceleration smoothing and prediction. These experiments were conducted with aircraft maneuvers which were somewhat more realistic than those assumed for the basic dynamics model of section 3.2.2.1. An empirical hill climbing method was used to optimize the design (select smoothing constants).

The third section of the appendix summarizes calculations which determine suitable initiation/termination rules meeting design requirements. In each case, the range of data conditions (blip-scan ratio and clutter probability) which may be tolerated has been computed.

C.2 EXACT α, β TRACKER ANALYSIS

Many of the numbers and figures used in our work (as well as the arguments and conclusions) are based on exact calculations of the Kalman model of the optimal α, β tracker proposed in section 3.2.2. This model is constructed upon the assumption that aircraft accelerations (held constant through each scan) are selected independently at random in each scan from a distribution with zero mean and known variance. Kalman covariance recursions for this model are given in (19); the optimal α, β are computed from relations (18).

In order to provide results with the maximum utility, the covariance recursions are treated in a normalized form. Thus, in the following results:

1) Time is in units of one scan, (i.e., $\Delta = 1$).

2) Prediction error covariance elements (σ_{xx}, $\sigma_{x\dot{x}}$, $\sigma_{\dot{x}\dot{x}}$) are normalized with respect to the data position error variance, c^2. (i.e., the values reported should be multiplied by c^2 to convert to nautical mile units for any specific application).

3) The maneuver parameter is $\lambda = a^2/c^2$, which is the same definition used throughout this report.

C.2 (continued)

The results of a series of computer calculations which exercize the recursions (19) and relations (18) are summarized in Tables C-1 through C-15. Each table is devoted to a particular value of the maneuverability parameter, λ. The λ sequence is given in descending order; extreme (and unrealistic) values, $\lambda = 100$ and $\lambda = .0001$, are included as points of reference. The practical range of λ is mostly confined to the values $\lambda = 10$ through $\lambda = .005$.

Each table is computed in accord with the same scenario of hits and missed data and exhibits three typical standard situations: a start up sequence with no misses, the steady state with no misses, and a succession of four misses followed by recovery (beginning from the steady state). These situations are natural stages of one continuous computational run starting with the assumption of no a priori track data.

The first column of the table indicates the stage, n, a particular scan of the tracking process. $n = 2$ refers to the second scan after receipt of the first data. This is the earliest scan at which the prediction covariances are finite. On the preceding scans, optimal α, β are trivially (all for all λ),

$$\text{For} \quad n = 0 \quad \alpha = 1 \quad \beta = 0 \qquad \text{(C-1)}$$

$$n = 1 \quad \alpha = 1 \quad \beta = 1$$

These uniform initial results do not explicitly appear in the tables. Results for succeeding start up scans, $n = 3$, etc., are reported until either the convergence to the steady state is nearly complete or the sequence must be terminated because of lack of space.

The steady state results are next given under SS. Thereafter, the results for scans after successive misses, 1M, 2M, 3M, 4M, are tabulated, and most of the immediate recovery process back to the steady state follows (unlabeled).

Each row of the table, referring to a particular scan, gives the one scan prediction error covariances for the estimated position and velocity at that scan (before receipt of data), as well as the optimal α, β for smoothing data on that scan. One additional column, β_{eq}, is provided, which multiplies β values in the miss sequence by the scan interval since the last data. β_{eq} is the velocity constant directly comparable to the RBTL parameter in the miss situation.

Many smoothing and prediction problems may be solved using the results in these tables. Examples follow.

C.2 (continued)

Example 1.

What steady state β is appropriate to use with $\alpha = .5$?

Scan the tables for an SS entry near $\alpha = .5$. We find that $\lambda = .05$ yields the closest set, $\alpha = .486$, $\beta = .160$. By interpolating the tables we estimate that for $\alpha = .5$, we would have $\beta \approx .175$. Let us adopt $\lambda = .05$ as a typical condition in the succeeding examples.

Example 2.

For $\lambda = .05$ and a data error standard deviation $c = 0.1$ nm, what is the one step position prediction error standard deviation in the steady state?

Using Table C-9, we find σ_{xx} (normalized) = .946. Thus, the position prediction standard deviation is $(.1)\sqrt{.946} = .0972$ nm.

Example 3.

What are the fluctuations in the velocity estimate vector for a 200 kt. aircraft under the condition of Example 2?

Again using Table C-9, we find $\sigma_{\dot{x}\dot{x}} = .1766$, so that each velocity component estimate (predicted or smoothed) has a standard deviation of $(.1)\sqrt{.1766} = .042$ nm./scan. Since the 200 kt. aircraft proceeds at .222 nm/scan (4 second scan), velocity fluctuations are ± 18.9% of the speed for ± one standard deviation. The corresponding velocity vector angle fluctuations are approximately $\pm \tan^{-1} .189 = \pm 10.7^{0}$.

Example 4.

What is the smoothed position error standard deviation under Example 2 conditions?

It can easily be shown that the normalized smoothed position variance is numerically identical with the optimal α under each circumstance. Since here $\alpha = .486$, we find the smoothed position error standard deviation to be $(.1)\sqrt{.486} = .0697$ nm.

Example 5.

What is the position prediction error for an 11 scan prediction under the conditions of Example 2?

C.2 (continued)

One step prediction results are listed in the table. We can extend them for 10 more scans by using the formula

$$\sigma^2 = \sigma_{xx} + m\dot{\sigma}_{xx} + m^2\ddot{\sigma}_{xx},$$

with m = 10. We find $\sigma^2 = 180.7$, almost wholly determined by $\ddot{\sigma}_{xx}$. Thus, the extended prediction standard deviation is (.1) $\sqrt{180.7} = 1.34$ nm. We note that this result is sensitive to the assumed aircraft motion model. The value found here is correct for random accelerations, but would be exceeded if accelerations were more persistent.

C.3 STUDY OF VARIOUS TRACKING OPTIONS

C.3.1 Methods and Models

In these sections we describe a series of computer experiments carried out to explore various alternatives to the use of the isotropic (constant) α, β tracker. The variations were as follows:

a) Isotropic α, β (reference case; α, β the same in x and y).

b) Track oriented α, β.

c) Track oriented α, β with γ (acceleration) smoothing in a direction transverse to the track.

d) Isotropic α, β, γ (acceleration smoothing).

e) Track oriented α, β, γ.

The ordinary isotropic α, β tracker is optimal for steady state tracking with the random acceleration dynamics model of section 3.2.2.1 or, equivalently, for a maneuver population of abrupt turns and velocity changes. Therefore, exploration of the above options is predicted on the hope that since actual aircraft motion is somewhat more restrained, track oriented and/or acceleration smoothing may offer some additional improvement in track smoothing and prediction (S & P) performance.

In order to explore this possibility, 90^0 turn maneuvers executed at standard rates of about 3^0/sec, and $1\frac{1}{2}^0$/sec were used in the present study (actually 7 scans and 15 scans, respectively, to complete the turns). Since these manuevers and the above tracking options procluded a simple mathematical treatment of the turn transients, the S & P behavior was explicitly evaluated by tracking each case by computer.

TABLE C-1

λ = 100

n	σ_{xx}	$\sigma_{xx}^{\cdot}$	$\sigma_{xx}^{\cdot\cdot}$	α	β	β_{eq}
2	55.00	76.00	127.0	.982	1.393	
3	47.12	69.75	118.3	.979	1.449	
4	46.14	68.71	117.2	.979	1.458	
5	46.00	68.56	117.1	.989	1.459	
ss	45.97	68.54	117.0	.989	1.459	
1m	325.1	235.6	217.0	.997	.722	1.444
2m	1038.	502.7	314.0	.999	.484	1.442
3m	2385.	869.7	417.0	1.000	.364	1.456
4m	4567.	1336.	517.0	1.000	.293	1.455
	152.4	176.1	225.8	.993	1.148	
	51.92	74.78	123.6	.981	1.413	
	46.77	69.37	117.9	.979	1.452	

TABLE C-2

$\lambda = 10$

n	σ_{xx}	$\dot{\sigma}_{xx}$	$\ddot{\sigma}_{xx}$	α	β	β_{eq}
2	10.00	10.50	14.50	.909	.955	
3	9.795	10.43	14.47	.907	.966	
4	9.736	10.36	14.39	.907	.965	
ss	9.731	10.35	14.39	.907	.965	
1m	47.34	29.75	24.39	.979	.615	1.231
2m	113.7	59.14	34.39	.993	.439	1.316
3m	288.9	98.54	44.39	.997	.340	1.360
4m	532.9	147.9	54.39	.998	.277	1.355
	17.45	18.68	23.40	.946	1.012	
	9.965	10.50	14.49	.909	.958	
	9.751	10.38	14.42	.907	.966	

TABLE C-3

$\lambda = 5$

n	σ_{xx}	σ'_{xx}	σ''_{xx}	α	β	β_{eq}
2	7.500	6.750	8.250	.882	.794	
3	6.610	6.183	7.889	.869	.813	
4	6.608	6.177	7.864	.869	.812	
5	6.591	6.161	7.849	.868	.812	
ss	6.590	6.160	7.849	.868	.812	
1m	28.01	16.50	12.84	.966	.569	1.138
2m	75.12	31.85	17.84	.987	.418	1.255
3m	157.9	52.20	22.84	.994	.328	1.313
4m	286.4	75.55	27.84	.997	.270	1.349
	9.710	9.694	11.92	.907	.905	
	7.116	6.555	8.150	.887	.808	
	6.598	6.163	7.856	.868	.811	

TABLE C-4

$\lambda = 2$

n	σ_{xx}	σ'_{xx}	σ''_{xx}	α	β	β_{eq}
2	6.000	4.500	4.500	.857	.643	
3	4.250	3.250	3.607	.810	.619	
4	4.142	3.214	3.595	.806	.625	
5	4.141	3.211	3.586	.806	.625	
ss	4.133	3.204	3.580	.805	.624	
1m	14.62	7.784	5.580	.936	.498	.966
2m	36.27	14.36	7.580	.973	.385	1.156
3m	73.07	22.94	9.580	.987	.310	1.238
4m	129.0	33.52	11.58	.992	.258	1.288
	4.945	4.195	4.937	.832	.707	
	4.720	3.682	3.977	.825	.644	
	4.218	3.249	3.606	.808	.623	

TABLE C-5

$\lambda = 1$

n	σ_{xx}	$\sigma_{xx}^{\cdot}$	$\sigma_{xx}^{\cdot\cdot}$	α	β	β_{eq}
2	5.500	3.750	3.250	.846	.577	
3	3.336	2.163	2.086	.769	.499	
4	3.024	2.006	2.007	.752	.498	
5	3.005	2.005	2.007	.750	.501	
6	3.004	2.003	2.002	.750	.500	
ss	3.000	2.000	2.000	.750	.500	
1m	9.250	4.500	3.000	.902	.439	.878
2m	21.50	8.000	4.000	.956	.356	1.067
3m	41.75	12.50	5.000	.977	.292	1.169
4m	72.00	18.00	6.000	.986	.247	1.233
	3.291	2.308	2.561	.767	.538	
	3.412	2.357	2.320	.773	.534	
	3.152	2.094	2.060	.759	.504	

TABLE C-6

$\lambda = .5$

n	σ_{xx}	$\sigma_{\dot{x}\dot{x}}$	$\sigma_{\ddot{x}\ddot{x}}$	α	β	β_{eq}
2	5.250	3.375	2.625	.840	.540	
3	2.847	1.592	1.302	.740	.414	
4	2.336	1.307	1.143	.700	.392	
5	2.240	1.272	1.131	.691	.393	
6	2.233	1.273	1.131	.691	.394	
ss	2.229	1.270	1.127	.690	.393	
1m	6.023	2.648	1.627	.858	.377	.754
2m	13.07	4.525	2.127	.929	.322	.965
3m	24.37	6.902	2.627	.961	.272	1.088
4m	40.93	9.779	3.127	.976	.233	1.166
	2.413	1.329	1.346	.707	.389	
	2.439	1.467	1.328	.709	.427	
	2.369	1.378	1.201	.705	.407	
	2.284	1.297	1.141	.696	.395	

TABLE C-7

$\lambda = .2$

n	σ_{xx}	$\sigma_{xx}^{\cdot}$	$\sigma_{xx}^{\cdot\cdot}$	α	β	β_{eq}
2	5.100	3.150	2.250	.836	.516	
3	2.542	1.239	.8233	.718	.350	
4	1.857	.8394	.5894	.650	.294	
5	1.630	.7366	.5428	.620	.280	
6	1.566	.7165	.5365	.610	.279	
ss	1.552	.7145	.5346	.608	.280	
1m	3.566	1.349	.7346	.781	.295	.591
2m	7.049	2.183	.9346	.876	.271	.814
3m	12.40	3.218	1.134	.925	.240	.960
4m	20.02	4.452	1.334	.952	.212	1.059
	1.817	.7032	.5913	.645	.250	
	1.610	.7654	.6158	.617	.293	
	1.544	.7846	.5913	.622	.297	
	1.623	.7552	.5585	.619	.288	
	1.585	.7290	.5411	.613	.282	

TABLE C-8

$\lambda = .1$

n	σ_{xx}	$\sigma_{\dot{x}\dot{x}}$	$\sigma_{\dot{x}\dot{x}}$	α	β	β_{eq}
2	5.050	3.075	2.125	.835	.508	
3	2.438	1.120	.6620	.709	.326	
4	1.682	.6728	.3970	.627	.251	
5	1.382	.5290	.3282	.580	.222	
6	1.260	.4828	.3107	.558	.214	
7	1.217	.4712	.3076	.549	.213	
ss	1.203	.4694	.3064	.546	.213	
1m	2.473	.8258	.4064	.712	.238	.475
2m	4.557	1.282	.5064	.820	.231	.692
3m	7.652	1.838	.6064	.884	.212	.849
4m	11.96	2.495	.7064	.923	.192	.962
	1.558	.4686	.3261	.609	.183	
	1.240	.4734	.3403	.554	.211	
	1.241	.5015	.3402	.554	.224	
	1.254	.5018	.3280	.557	.223	
	1.242	.4889	.3163	.554	.218	

TABLE C-9

$\lambda = .05$

n	σ_{xx}	$\sigma_{\dot{x}\dot{x}}$	$\sigma_{\ddot{x}\ddot{x}}$	α	β	β_{eq}
2	5.025	3.037	2.062	.831	.504	
3	2.385	1.060	.5811	.705	.313	
4	1.592	.5872	.2991	.614	.227	
5	1.245	.4176	.2160	.555	.186	
6	1.077	.3493	.1884	.519	.168	
7	.997	.3228	.1796	.499	.162	
8	.963	.3141	.1774	.490	.160	
ss	.946	.3119	.1766	.486	.160	
1m	1.758	.5135	.2266	.638	.186	.372
2m	3.024	.7651	.2766	.752	.190	.570
3m	4.844	1.066	.3265	.829	.183	.730
4m	7.316	1.418	.3766	.880	.171	.853
	1.368	.3302	.1847	.578	.139	
	1.007	.3031	.1886	.502	.151	
	.9592	.3188	.1928	.490	.163	
	.9686	.3287	.1910	.492	.167	
	.9746	.3280	.1861	.494	.166	

TABLE C-10

$\lambda = .02$

n	σ_{xx}	σ'_{xx}	σ''_{xx}	α	β	β_{eq}
2	5.010	3.015	2.025	.834	.502	
3	2.354	1.024	.4324	.702	.305	
4	1.537	.5351	.2397	.606	.211	
5	1.159	.3478	.1469	.537	.161	
6	.9550	.2619	.1109	.488	.134	
7	.8373	.2198	.09581	.456	.120	
8	.7695	.1991	.08951	.435	.113	
9	.7320	.1896	.08709	.423	.109	
ss	.6993	.1843	.08587	.412	.108	
1m	1.158	.2802	.1058	.537	.130	.259
2m	1.830	.3961	.1258	.647	.140	.420
3m	2.753	.5319	.1458	.734	.142	.566
4m	3.968	.6878	.1658	.799	.138	.694
	1.151	.2190	.09064	.535	.102	
	.8121	.1801	.08832	.448	.099	
	.7224	.1793	.09041	.419	.104	
	.7048	.1860	.09163	.413	.109	
	.7080	.1904	.09133	.415	.112	

TABLE C-11

$\lambda = .01$

n	σ_{xx}	$\sigma_{\dot{x}\dot{x}}$	$\sigma_{\ddot{x}\ddot{x}}$	α	β	β_{eq}
2	5.005	3.007	2.012	.833	.501	
3	2.343	1.012	.5162	.701	.303	
4	1.518	.5175	.2199	.603	.205	
5	1.130	.3240	.1235	.531	.152	
6	.9115	.2313	.08425	.477	.121	
7	.7777	.1822	.06624	.437	.103	
8	.6926	.1551	.05755	.409	.0916	
9	.6383	.1399	.05334	.390	.0854	
10	.6043	.1318	.05138	.377	.0821	
11	.5840	.1277	.05055	.369	.0806	
ss	.5624	.1249	.05000	.360	.0799	
1m	.8649	.1799	.05999	.464	.0965	.193
2m	1.287	.2449	.06999	.563	.1071	.321
3m	1.849	.3199	.07999	.649	.1122	.449
4m	2.572	.4049	.07999	.720	.1133	.567
	.9934	.1624	.05408	.498	.0814	
	.7046	.1273	.05084	.413	.0747	
	.6066	.1210	.05133	.378	.0753	
	.5729	.1225	.05221	.364	.0779	
	.5652	.1255	.05266	.361	.0802	

TABLE C-12

$\lambda = .005$

n	σ_{xx}	σ'_{xx}	σ''_{xx}	α	β	β_{eq}
2	5.002	3.003	2.006	.833	.500	
3	2.338	1.006	.5081	.700	.301	
4	1.509	.5088	.2099	.601	.203	
5	1.115	.3120	.1118	.527	.148	
6	.8892	.2158	.07075	.471	.114	
7	.7465	.1628	.05110	.427	.0932	
8	.6510	.1316	.04092	.394	.0797	
9	.5854	.1126	.03542	.369	.0710	
10	.5400	.1009	.03242	.351	.0655	
11	.5088	.09387	.03080	.337	.0622	
ss	.4557	.08531	.02920	.313	.0586	
1m	.6568	.1170	.03420	.396	.0706	.141
2m	.9263	.1537	.03920	.480	.0798	.239
3m	1.274	.1954	.04420	.560	.0859	.343
4m	1.710	.2421	.04920	.631	.0893	.446
	.8385	.1194	.03257	.456	.0649	
	.6120	.09226	.02953	.380	.0572	
	.5199	.08427	.02986	.342	.0554	
	.4790	.08281	.03023	.324	.0559	
	.4623	.08371	.03043	.316	.0572	

TABLE C-13

$\lambda = .002$

n	σ_{xx}	$\sigma_{\dot{x}x}$	$\sigma_{\dot{x}\dot{x}}$	α	β	β_{eq}
2	5.001	3.001	2.002	.833	.500	
3	2.335	1.002	.5032	.700	.301	
4	1.503	.5035	.2039	.601	.201	
5	1.106	.3048	.1047	.525	.145	
6	.8757	.2063	.06260	.467	.110	
7	.7273	.1509	.04190	.421	.0873	
8	.6250	.1170	.03071	.385	.0720	
9	.5515	.09533	.02428	.355	.0614	
10	.4972	.08087	.02042	.332	.0540	
11	.4567	.07106	.01805	.314	.0487	
12	.4261	.06437	.01658	.299	.0451	
13	.4032	.05982	.01568	.297	.0426	
ss	.3482	.05192	.01441	.258	.0385	
1m	.4669	.06733	.01641	.318	.0459	.0918
2m	.6185	.08475	.01841	.382	.0523	.157
3m	.8070	.1041	.02041	.447	.0576	.230
4m	1.036	.1255	.02241	.509	.0616	.308
	.6474	.07733	.01666	.393	.0469	
	.5004	.06098	.01503	.333	.0406	
	.4278	.05420	.01455	.300	.0379	
	.3885	.05146	.01450	.280	.0370	
	.3670	.05065	.01459	.268	.0370	

TABLE C-14

$\lambda = .001$

n	σ_{xx}	σ'_{xx}	σ''_{xx}	α	β	β_{eq}
2	5.000	3.000	2.001	.833	.500	
3	2.334	1.001	.5016	.700	.300	
4	1.501	.5017	.2019	.600	.201	
5	1.103	.3024	.1023	.524	.144	
6	.8712	.2031	.05987	.466	.109	
7	.7208	.1468	.03881	.419	.0853	
8	.6161	.1121	.02727	.381	.0693	
9	.5397	.08938	.02049	.351	.0580	
10	.4822	.07385	.01630	.325	.0498	
11	.4378	.06295	.01362	.305	.0437	
12	.4032	.05515	.01186	.287	.0393	
13	.3759	.04950	.01070	.273	.0359	
ss	.2857	.03585	.008466	.222	.0278	
1m	.3661	.04482	.009468	.268	.0328	.0676
2m	.4655	.05479	.01046	.318	.0373	.1119
3m	.5858	.06576	.01146	.369	.0414	.1656
4m	.7290	.07773	.01246	.422	.0449	.2245
	.5207	.05442	.009974	.342	.0357	
	.4223	.04431	.009025	.297	.0311	
	.3671	.03936	.008645	.269	.0287	
	.3338	.03676	.008515	.250	.0275	
	.3131	.03556	.008501	.238	.0276	

TABLE C-13

$\lambda = .0001$

n	σ_{xx}	$\sigma_{\dot{x}x}$	$\sigma_{\dot{x}\dot{x}}$	α	β	β_{eq}
2	5.000	3.000	2.000	.833	.500	
3	2.333	1.000	.5001	.700	.300	
4	1.500	.5001	.2001	.600	.200	
5	1.100	.3002	.1002	.524	.143	
6	.8671	.2003	.05741	.464	.107	
7	.7149	1432	.03602	.417	.0837	
8	.6080	.1076	.02415	.378	.0667	
9	.5289	.08394	.01705	.346	.0549	
10	.4682	.06739	.01254	.319	.0459	
11	.4201	.05540	.009549	.296	.0390	
12	.3812	.04644	.007488	.276	.0336	
13	.3492	.03960	.006026	.259	.0293	
ss	.1529	.01073	.001468	.132	.0093	
1m	.1748	.01224	.001565	.149	.0104	.0208
2m	.2009	.01386	.001665	.167	.0115	.0345
3m	.2303	.01557	.001765	.187	.0126	.0504
4m	.2632	.01739	.001865	.208	.0137	.0685
	.2375	.01544	.001725	.192	.0124	
	.2184	.01406	.001632	.179	.0115	
	.2038	.01306	.001570	.169	.0108	
	.1925	.01232	.001528	.161	.0103	

C.3.1 (continued)

Tracking was performed using the α, β, γ smoothing and prediction equations (20) adapted to track oriented operations, as in section 3.2.2.4, which preserves the computations in an x, y framework. Position and velocity smoothing equations then are identical with (23), (25). In addition, however, we also have acceleration smoothing equations

$$\ddot{\hat{x}} = \ddot{\hat{x}} + \gamma_L \frac{\hat{u}\dot{\hat{x}}}{s^2} + \gamma + \frac{\hat{v}\dot{\hat{y}}}{s^2} \qquad \text{(C-2)}$$

$$\ddot{\hat{y}} = \ddot{\hat{y}} + \gamma_L \frac{\hat{u}\dot{\hat{y}}}{s^2} - \gamma + \frac{\hat{v}\dot{\hat{x}}}{s^2} \quad .$$

By variously setting some of the α, β, γ parameters to zero or equal to each other, one can obtain each of the above tracker options. Note that e.) is the general case, and, when $\alpha_L = \alpha_T$, $\beta_L = \beta_T$, $\gamma_L = \gamma_T$, the track-oriented operations yield results identical with simple x, y tracking (isotropic S & P may be described by vectors independent of any coordinate description).

In order to analyze the performance of each tracker option for any selected α, β, γ values, we define a population track mix consisting of

1) straight aircraft paths with added position noise and

2) 90^0 turn maneuvers with no added noise.

For population 1), the mean square value of the one scan position prediction errors per unit data error variance is calculated. This variance factor is determined separately for the longitudinal and transverse track directions, in terms of the respective α, β, γ constants, by means of an analytically derived formula.

$$\text{Noise variance (SSNL or SSNT)} = \frac{2\beta(\alpha\beta + 2\alpha^2 + 2\beta) - \gamma\alpha(4 - 2\alpha - \beta)}{(4 - 2\alpha - \beta)(2\alpha\beta - \gamma(2 - \alpha))} \qquad \text{(C-3)}$$

Before applying this formula, stability conditions for the tracker are checked,

$$0 \leq \gamma \leq \frac{2\alpha\beta}{2-\alpha} \leq 4\alpha \qquad \text{(C-4)}$$

$$0 \leq \beta \leq 4 - 2\alpha$$

C.3.1 (continued)

and if they fail, a very large noise variance is assigned. The two resulting variances, SSNL (longitudinal) and SSNT (transverse), are added to produce a two dimensional mean square error SSN due to data error effects. This addition is weighed by an arbitrary factor TF (TF = 1, usually).

$$SSN = SSNL + TF*SSNT \tag{C-5}$$

Population 2) of 90^0 turns without data errors, on the other hand, is tracked by computer simulation of the tracking process. Only S & P is performed. Data correlation is assumed to be perfect and the blip-scan ratio is unity, so that only one turn is tracked and the need for Monte Carlo techniques is avoided. During this turn the sums of squares of the one scan position prediction error components are separately accumulated along (SSML) and across the track (SSMT) and added to provide a two dimensional sum of squares. (The unit of distance used here is the distance moved by the aircraft in one scan time.) Again, the weighting factor TF is used to provide generality.

$$SSM = SSML + TF*SSMT \tag{C-6}$$

SSM is a measure of the severity of turn transient produced by the tracker.

Finally, SSN and SSM are weighted together with a maneuverability or population mix parameter, γ, to provide an overall mixed performance value.

$$VALUE = SNN + \gamma*SSM \tag{C-7}$$

γ controls the relative weight given to data noise smoothing vs. faithful maneuver following in evaluating a specific set of α_L, β_L, γ_L, α_T, β_T, γ_T. It thus plays the same role here as previously in the random maneuver α, β model.

We note that since the S & P equations are strictly linear for isotropic S & P and are approximately linear (for small noise perturbations) for track-oriented S & P, we can think of the two populations 1), 2) as combined into one. The two measures, SSM and SSN, and the sum, VALUE, would be thus obtained by analysis of a noisy, turning track. Let $e_N(n)$ be the series of prediction errors obtained from data noise alone (of variance c^2), while $e_M(n)$ is the series of errors due to the maneuver. By superposition, the total error then is

$$e(n) = e_N(n) + e_M(n). \tag{C-8}$$

C.3.1 (continued)

The mean square of e(n) over the noise ensemble is

$$\overline{e^2(n)} = \overline{e_N^2(n)} + \overline{2e_N(n)}\, e_M(n) + e_M^2(n) \qquad \text{(C-9)}$$

$$= \overline{e_N^2(n)} + e_M^2(n) \quad .$$

The average of $\overline{e^2(n)}$ over N scans (enough for the turn transient to die out) is

$$\frac{1}{N}\sum_{n=1}^{N} \overline{e^2(n)} = \overline{e_N^2(n)} + \frac{1}{N}\sum_{n=1}^{N} e_M^2(n) \qquad \text{(C-10)}$$

In a final step we normalize (C-10) with respect to the data error variance, σ^2.

$$\frac{1}{N\sigma^2}\sum_{n=1}^{N} \overline{e^2(n)} = \frac{\overline{e_N^2(n)}}{\sigma^2} + \frac{1}{N\sigma^2}\sum_{n=1}^{N} e_M^2(n), \qquad \text{(C-11)}$$

(C-7) and (C-11) have similar forms, and we can identify their respective terms. Thus, analysis of the combined noise/maneuver model is equivalent to separate analyses of idealized populations 1) and 2), followed by a subsequent weighting.

The track-oriented operations are only approximately linear. This means that in our analysis, we neglect the random perturbations of the oriented axes that would be induced by a superimposed data noise. If large enough, such effects can be expected to dilute the effectiveness of the oriented operations. Therefore, our results on such oriented S & P will tend to be slightly over optimistic and must be cleared by more extensive Monte Carlo runs. Our method here was specifically designed to avoid lengthy Monte Carlo experimentation.

Now, the object of the above analysis and mix of populations 1) and 2) is to vary α, β, γ constants under one of the contraint options a), b), c), d), e)

C.3.1 (continued)

in order to minimize the error measure (C-7). This optimization is repeated for various values of the maneuverability parameter, λ, and produces optimal α, β, γ trajectories analogous to the standard α, β curve which was derived analytically for the simpler model (cf. section 3.2.3.2.).

The method of optimization used in this study is a direct-search hill-climbing (descending) technique.* In it, the α, β, γ constants are perturbed one at a time in an attempt to improve the solution. This variation is followed by larger adjustments when a change proves fruitful in an attempt to accelerate the improvement. When no further progress is achieved with a given increment step size, the step is halved and the process continues. The process ceases when the step has reached some minimum size with no further improvement. The most general option, e), requires independent adjustment of six smoothing parameters.

C.3.2 Results

Numerical results of the various experiments are summarized in tables C-16 through C-24. These tables list the various α, β values and the various noise and maneuver contributions to the system performance measure. Table C-16 provides a reference, based on the isotropic α, β tracker, with which to judge the effectiveness of the other tracker options. Figure C-1 shows a plot of the optimal α, β curve for this case. The standard curve, derived from the random acceleration model, is also shown for comparison.

We see from Figure C-1 that empirical adjustment of α, β to optimize for the population of 3^0/sec, 90^0 turns lead to larger β values for a given α than the standard model. In fact, we find that the more the actual aircraft motion consists of long, constantly held accelerations, the greater the departure. In particular, a similar curve for a $1\frac{1}{2}^0$/sec, 90^0 turn would show an ever steeper increase of β as a function of α.

By analysis, it can be shown that the error coefficient for constant accelerations with the α, β tracker is just $1/\beta$. That is, if the transverse acceleration (say) is maintained for a long period of time, at a $nm/scan^2$, then the transverse prediction error eventually builds up to a/β nm. The departure of the α, β curve in figure C-1 from the standard is thus seen as a rebalancing of α β in the direction of increased β values, in order to adapt the tracker to turn maneuvers in which accelerations are sustained. (Previous results, figure 3-18, then show that the resulting tracker is considerably

*R. Hooke and T. A. Jeeves, 'Direct Search' Solution of Numerical and Statistical Problems, J. Assn. Comp. Mach 8, 212 (1961).

underdamped.) In the light of this result, further simulation work might be fruitful in exploring trackers based on α, β relationships other than the standard curve.

Now consider the corresponding isotropic α, β, γ tracker option, table C-18. We see that except for $\lambda = 100$ (an unrealistically high value of maneuverability which corresponds to a population of nearly all 90^0 turns and very few straight noisy tracks), the γ value is optimally adjusted to near zero. This means that the acceleration smoothing has been disabled by the optimization and that it does not improve performance.

Table C-17 shows the results obtained for track-oriented smoothing with 3^0/sec, 90^0 turns. Optimal curves for α_T, β_T and α_L, β_L are shown in figure C-2. Here it is evident that the single curve in figure C-1 has split into two separate parts, one for longitudinal parameters, the other for transverse. The longitudinal set indicates heavy smoothing; the transverse set indicates lighter smoothing for given values of λ.

In figure C-4, the noise variance component, SSN, is plotted vs. the maneuver error sum of squares, SSM, for both track-oriented α, β and isotropic α, β trackers. We see that for a given maneuver error, we can reduce the noise error or vice-versa by using the track-oriented option. Improvement appears substantial and nearly constant for all values of λ.

In figure C-5, a similar tradeoff plot is made using only the transverse components of the respective errors SSMT, SSNT. We see that the curves nearly coincide (the track-oriented performance is slightly worse). Thus, most of the improvement from the track-oriented smoothing is attributable to net reduction of longitudinal errors. Transverse errors are little affected.

Exploration of tracker option e), track-oriented α, β, γ smoothing, is reported in table C-19. We see again, even more positively than before, that except for extremely high λ, the acceleration constants are set to zero. The tracker thus reverts optimally to track-oriented α, β smoothing.

Results for option c), track-oriented α, β with γ smoothing only in the transverse direction, were so uniformly negative that they are not explicitly reported here. In every instance, γ was set to zero.

In order to check sensitivity of the above results to the maneuver assumption, a series of runs was also made with $1\frac{1}{2}^0$/sec, 90^0 turns. Table C-20 gives basic data for a track-oriented α, β operation. Corresponding optimal α, β curves are shown in figure C-3, indicating the even greater separation of optimal smoothing constants for the two track directions.

C.3.2 (continued)

Table C-21 shows results of the track-oriented α, β, γ option. Although γ smoothing survives to slightly lower γ values than previously, again the result is essentially negative. The acceleration smoothing is disabled for optimum tracking.

Tables C-22, C-23, C-24 show results of a similar series of experiments in which the transverse error measures were weighted by a factor of 4 over the longitudinal errors. Maneuvers are at 3^{o}/sec. We find no change in the quantitative merits of the track-oriented α, β option. The γ smoothing is again rapidly disabled, except for the highest λ values.

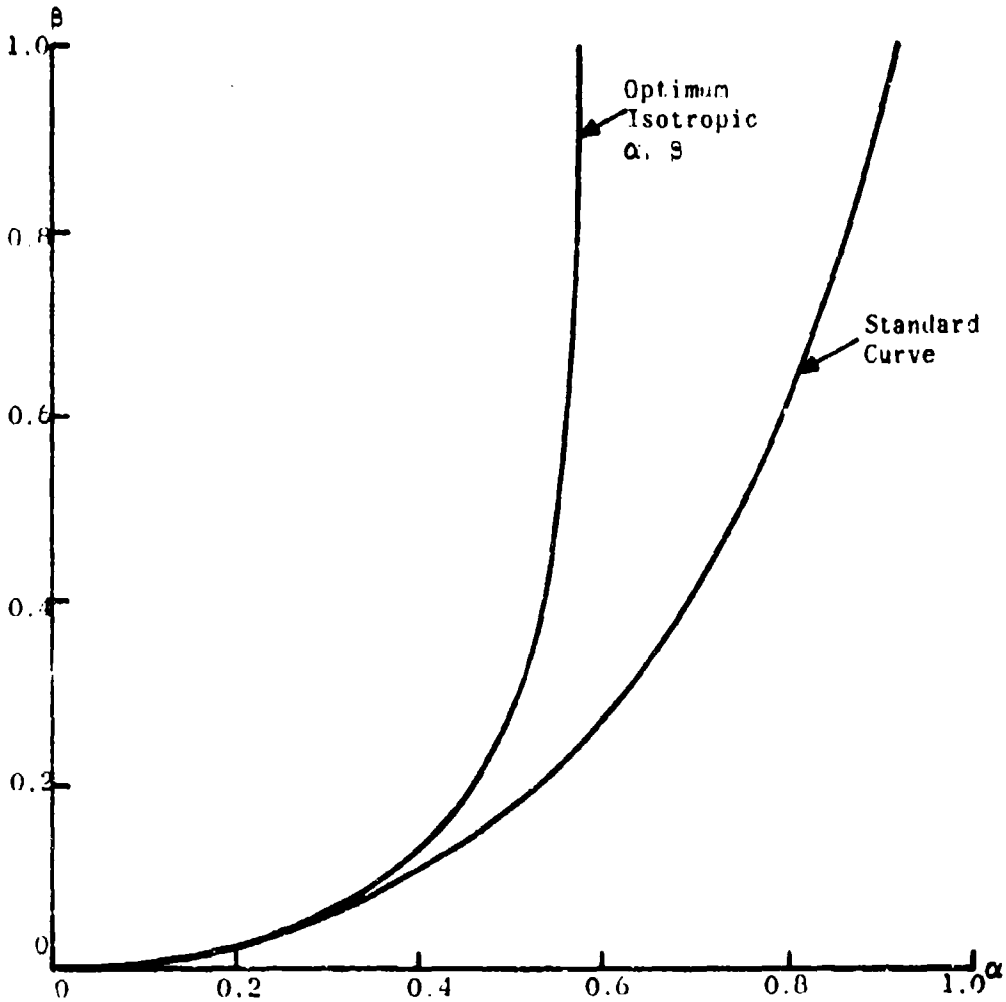

Figure C-1. Optimum Isotropic α, β for 3^0/Sec, 90^0 Turn

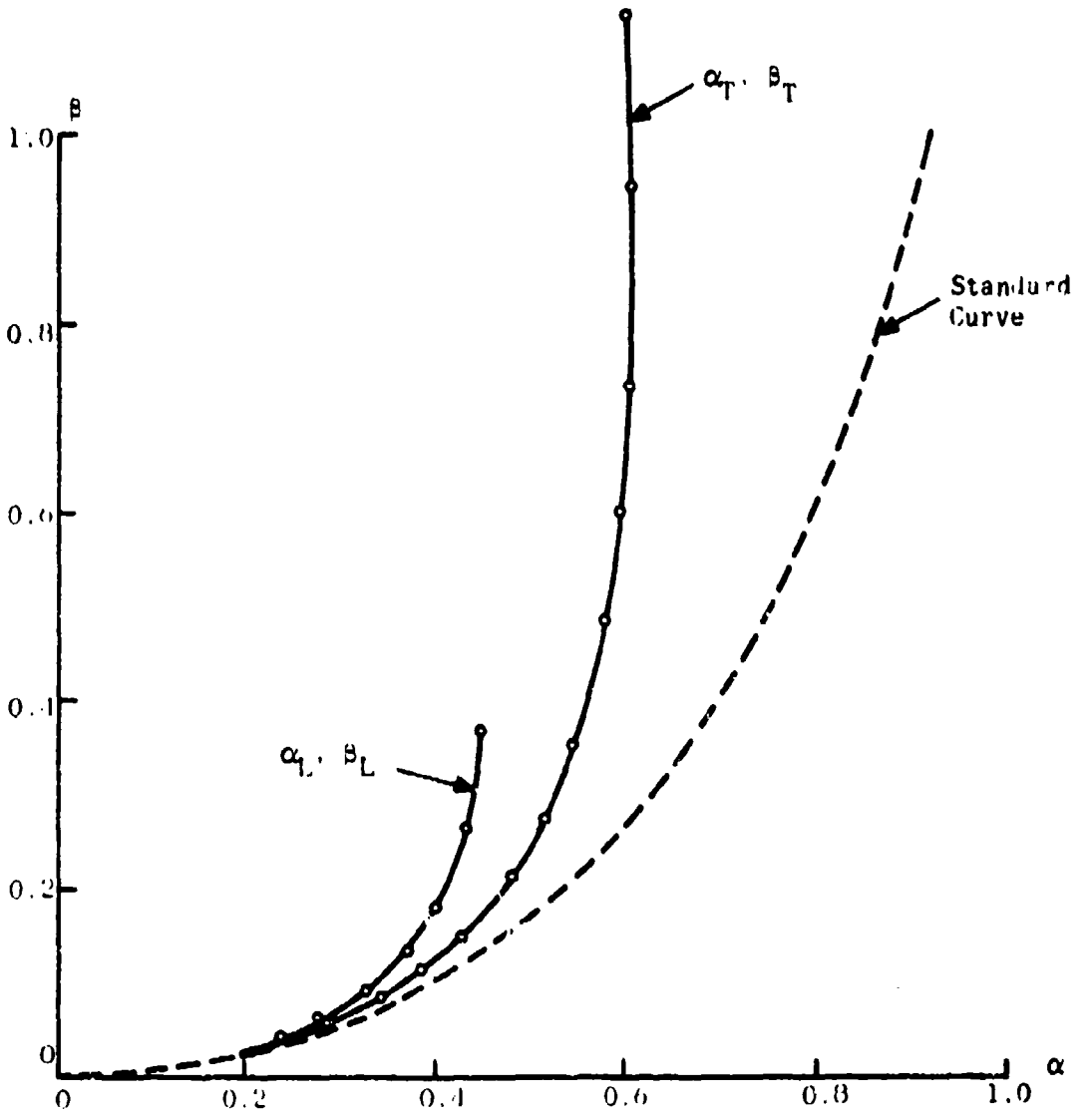

Figure C-2. Optimum Track Oriented α, β for 3°/Sec, 90° Turn

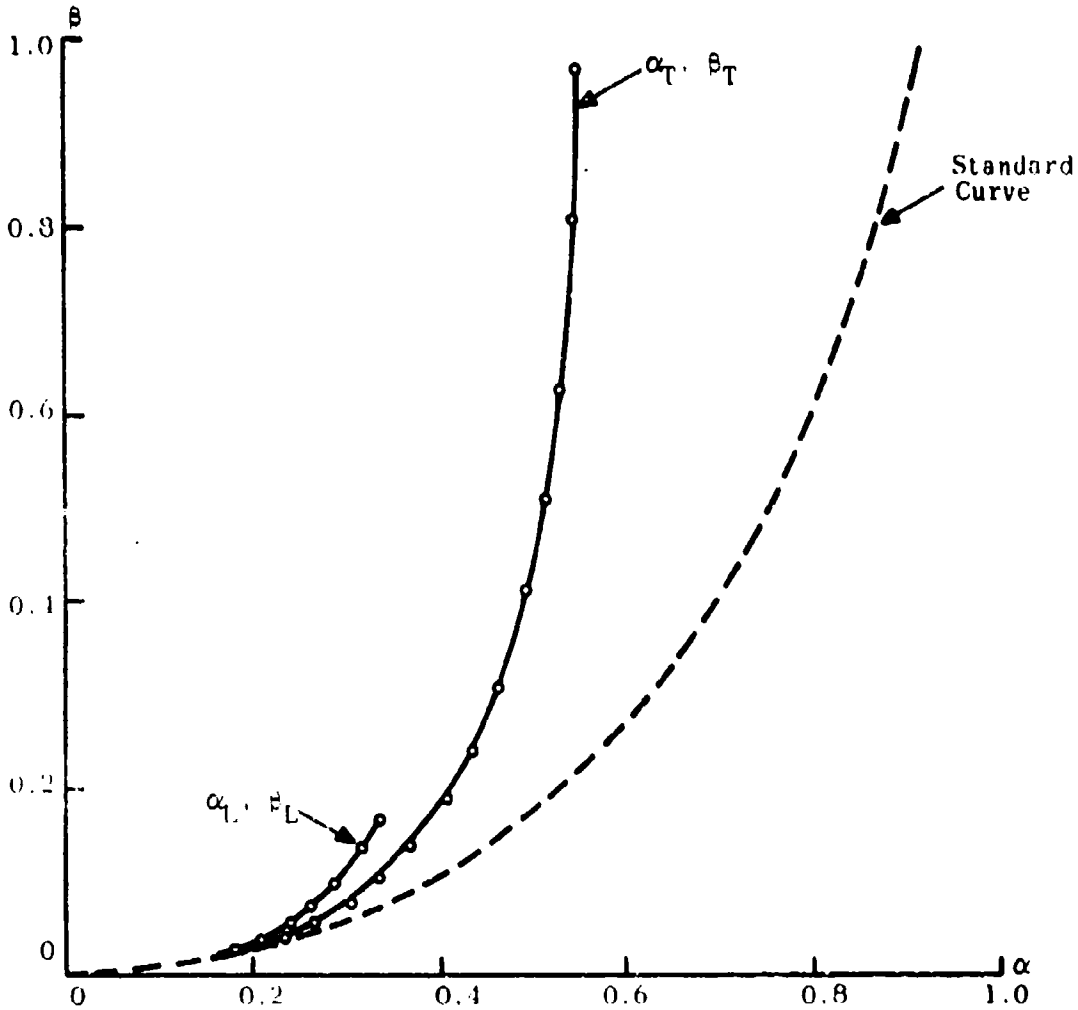

Figure C-3. Optimum Track Oriented α, β for 1½°/Sec, 90° Turn

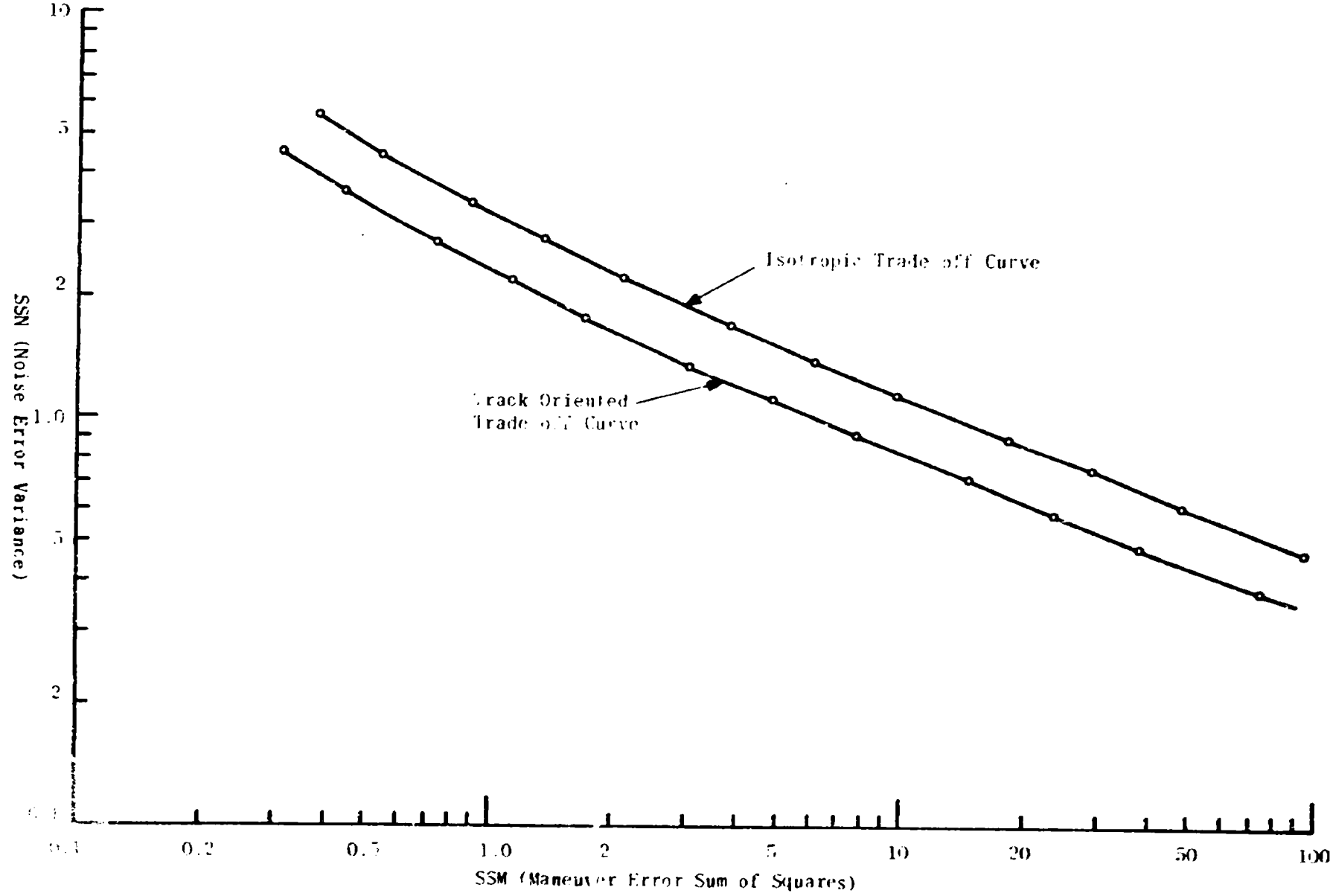

Noise vs. Maneuver Total Error Comparison For Isotropic and Track Oriented Smoothing

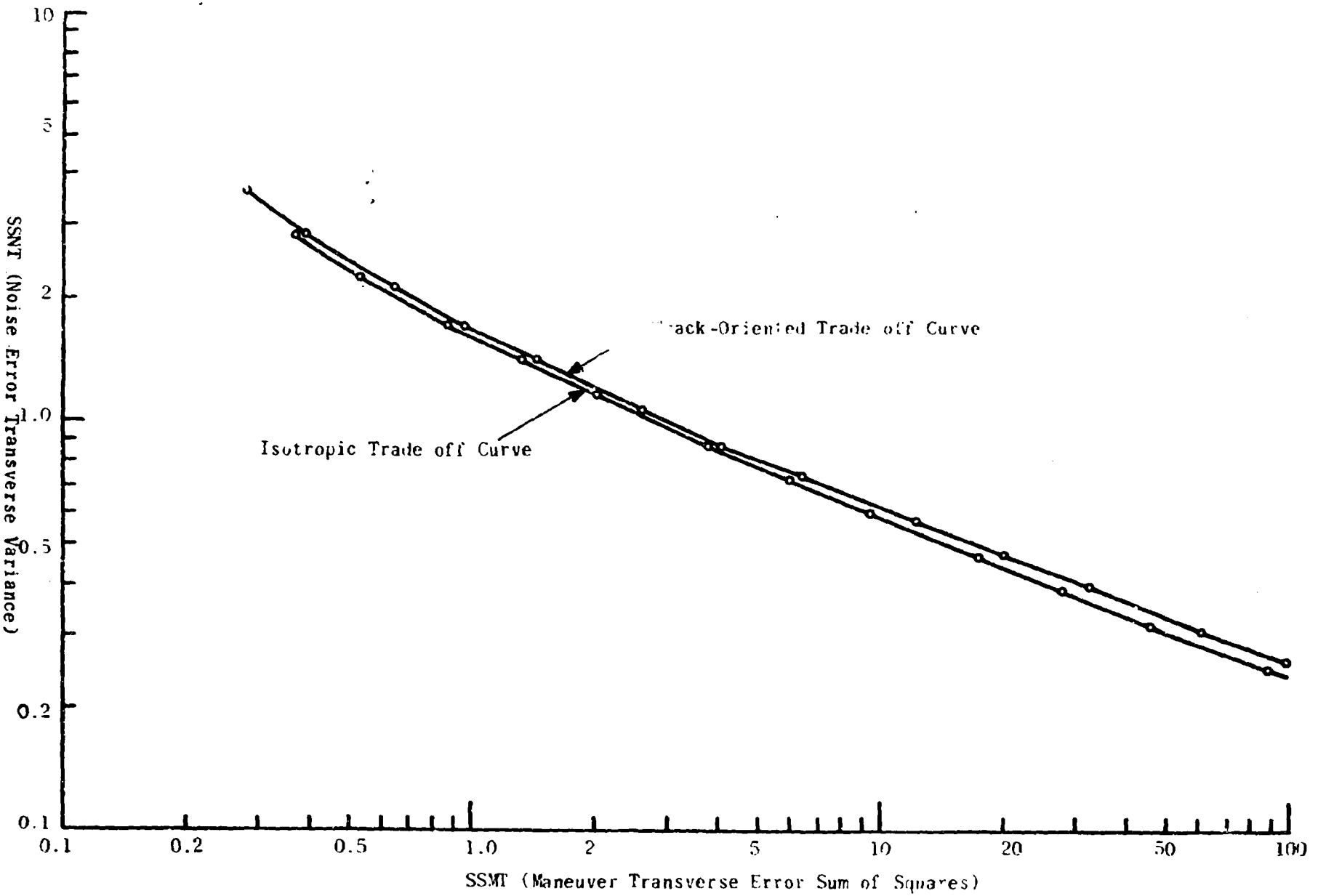

Figure C-5. Noise vs. Maneuver Transverse Error Comparison for Isotropic and Track Oriented Smoothing

TABLE C-16
ISOTROPIC α, β

NCIRC = 8 (3°/sec turn)
TF = 1

MIN. Step = 0.003

λ	α	β	SSNT (or) SSNL	SSML	SSMT	SSN	SSM
100	.547	1.603	6.568	.002	.136	13.13	.138
10	.578	.950	2.847	.00398	.376	5.695	.380
5	.572	.794	2.285	.0055	.535	4.570	.540
2	.562	.612	1.730	.0085	.885	3.461	.894
1	.550	.494	1.408	.0116	1.338	2.816	1.349
.5	.531	.391	1.147	.0158	2.074	2.295	2.090
.2	.500	.278	.878	.0261	3.802	1.756	3.828
.1	.466	.212	.720	.0498	6.060	1.459	6.109
.05	.428	.162	.596	.113	9.513	1.192	9.626
.02	.378	.109	.461	.393	17.82	.921	18.21
.01	.337	.0812	.382	.937	28.37	.763	29.31
.005	.297	.0594	.315	2.154	45.93	.629	48.08
.002	.250	.0375	.242	6.230	89.46	.484	95.69
.001	.216	.0281	.203	11.75	139.8	.407	151.6
.0001	.131	.00833	.107	106.8	783.2	.213	890.0

TABLE C-17
TRACK-ORIENTED α, β

NCIRC = 8 (3°/sec. turn)

TF = 1

MIN. Step = 0.0001

λ	α_L	α_T	β_L	β_T
100	.472	.530	.666	1.803
10	.449	.600	.342	1.128
5	.435	.608	.264	.945
2	.400	.603	.181	.736
1	.366	.592	.133	.600
.5	.327	.576	.097	.483
.2	.276	.546	.062	.355
.1	.239	.515	.044	.277
.05	.206	.480	.030	.214
.02	.165	.425	.018	.150
.01	.139	.383	.012	.114
.005	.116	.340	.008	.086
.002	.089	.287	.004	.059
.001	.074	.250	.003	.044
.0001	.021	.137	.0001	.017

TABLE C-17 (Cont'd.)
TRACK-ORIENTED α, β

NCIRC = 8 (3^{o}/sec. turn)

TF = 1

MIN. Step = 0.0001

λ	SSNL	SSML	SSNT	SSMT	SSN	SSM
100	1.854	.0088	8.51	.111	10.36	.120
10	1.000	.0306	3.641	.2795	4.641	.310
5	.820	.0486	2.866	.3971	3.686	.446
2	.625	.0922	2.129	.651	2.754	.743
1	.508	.1494	1.719	.969	2.227	1.118
.5	.414	.238	1.401	1.467	1.815	1.705
.2	.315	.431	1.076	2.629	1.391	3.064
.1	.256	.687	.885	4.161	1.141	4.848
.05	.207	1.100	.730	6.648	.938	7.749
.02	.156	2.098	.569	12.47	.725	14.57
.01	.1252	3.527	.472	20.10	.597	23.63
.005	.1004	5.979	.393	32.50	.493	38.48
.002	.0744	12.32	.309	61.26	.384	73.58
.001	.0584	21.35	.258	99.59	.317	121.4
.0001	.01383	134.2	.1458	526.6	.1596	660.9

TABLE C-18

ISOTROPIC α, β, γ

NCIRC = 8 (3^{o}/sec. turn)

TF = 1

MIN. Step = 0.003

λ	α	β	γ	SSNT (or) SSNL	SSML	SSMT	SSN	SSM
100	.869	1.128	.572	6.91	.0298	.084	13.51	.113
10	.581	.944	.006	2.85	.0070	.370	5.69	.377
5	.378	.787	.004	2.28	.0088	.530	4.56	.538
2	.566	.609	.002	1.73	.0150	.873	3.47	.888

(For $\lambda < 2$; $\gamma = 0$ and results are the same as in Table C-16)

TABLE C-19

TRACK-ORIENTED α, β, γ

NCIRC = 8 (3^{0}/sec. turn)

TF = 1

MIN. Step = 0.0001

λ	α_L	α_T	β_L	β_T	γ_L	γ_T
100	.556	.534	.574	1.794	.0909	.0104
10	.452	.692	.335	1.125	.0085	.0015
5	.437	.608	.262	.945	.0011	.0000
2	.402	.603	.180	.736	.0002	.0000

λ	SSNL	SSML	SSNT	SSMT	SSN	SSM
100	1.893	.0075	8.50	.109	10.4	.117
10	1.019	.0299	3.64	.278	4.66	.308
5	.820	.0485	2.87	.397	3.69	.446
2	.624	.0923	2.13	.651	2.75	.744

(For $\lambda < 2$: $\gamma_L = \gamma_T = 0$ and results are the same as in Table C-17.)

TABLE C-20

TRACK-ORIENTED α, β

NCIRC = 15 ($1\frac{1}{2}^{o}$/sec. turn)

TF = 1

MIN. Step = 0.0008

λ	α_L	α_T	β_L	β_T	SSNL	SSML	SSNT	SSMT	SSN	SSM
100	.431	.514	.362	1.615	1.047	.00396	6.58	.0688	7.63	.0728
10	.336	.548	.167	.964	.580	.0178	2.88	.191	3.46	.209
5	.312	.544	.131	.805	.492	.0286	2.30	.274	2.79	.303
2	.287	.529	.0929	.623	.394	.0551	1.741	.458	2.14	.513
1	.264	.514	.0703	.509	.332	.0926	1.427	.689	1.759	.782
.5	.241	.496	.0516	.410	.277	.159	1.176	1.059	1.453	1.218
.2	.207	.464	.0336	.303	.217	.319	.916	1.926	1.133	2.245
.1	.181	.435	.0242	.239	.181	.530	.764	3.07	.945	3.60
.05	.157	.406	.0172	.187	.153	.879	.641	4.92	.791	5.80
.02	.127	.367	.0109	.131	.117	1.67	.511	9.36	.628	11.03
.01	.107	.337	.0078	.103	.0974	2.65	.431	15.49	.529	18.15
.005	.0898	.307	.0055	.0789	.0804	4.29	.365	25.6	.445	29.9
.002	.0719	.265	.0034	.0539	.0626	7.91	.290	51.6	.353	59.5
.001	.0615	.232	.0018	.0406	.0471	15.65	.245	86.7	.291	102.3
.0001	.0195	.136	.0003	.0164	.0166	57.8	.143	460.3	.159	518.2

TABLE C-21

TRACK-ORIENTED α, β, γ

NCIRC = 15 ($1\frac{1}{2}^{o}$/sec. turn)

TF = 1

MIN. Step = 0.0008

λ	α_L	α_T	β_L	β_T	γ_L	γ_T
100	.944	.336	.488	1.007	.408	.411
10	.403	.552	.139	.957	.0174	.0021
5	.353	.549	.121	.799	.0080	.0014
2	.298	.531	.0925	.623	.0018	.0006

(For $\lambda < 2$: $\gamma_L = \gamma_T = 0$, and results are the same as in Table C-20.)

TABLE C-21 (Cont'd.)
TRACK-ORIENTED α, β, γ

NCIRC = 15 ($1\frac{1}{2}^{0}$/sec. turn)

TF = 1

MIN. Step = 0.0008

SSNL	SSML	SSNT	SSMT	SSN	SSM
3.160	.0125	5.10	.0371	8.26	.0496
.629	.0141	2.36	.187	3.49	.202
.526	0255	2.29	.271	2.82	.297
.408	.0544	1.741	.454	2.15	.508

(For $\lambda < 2$: $\gamma_L = \gamma_T = 0$. and results are the same as in Table C-20.)

TABLE C-22

ISOTROPIC α, β

NCIRC = 8 (3^{o}/sec. turn)

TF = 4

MIN. Step = 0.0008

λ	α	β	SSNT (or) SSNL	SSML	SSMT	SSN	SSM
100	.527	1.740	7.39	.0015	.1156	15.78	.1171
10	.576	1.068	3.33	.0033	.299	6.67	.303
5	.574	.893	2.65	.0044	.421	5.29	.425
2	.566	.701	1.988	.0068	.683	3.98	.689
1	.557	.571	1.613	.0095	1.014	3.23	1.024
.5	.543	.458	1.315	.0129	1.546	2.63	1.558
.2	.516	.333	1.007	.0197	2.78	2.01	2.80
.1	.487	.256	.924	.0311	4.41	1.648	4.44
.05	.454	.195	.676	.0644	7.04	1.352	7.10
.02	.405	.131	.520	.221	13.28	1.039	13.50
.01	.364	.0970	.428	.562	21.4	.855	22.0
.005	.324	.0704	.351	1.366	34.8	.703	36.2
.002	.273	.0462	.273	3.90	65.8	.546	69.7
.001	.237	.0337	.227	7.83	105.7	.453	113.6
.0001	.142	.0110	.1215	6.93	547.	.243	617.

TABLE C-23

TRACK-ORIENTED α, β

NCIRC = 8 (3^{o}/sec. turn)

TF = 4

MIN. Step = 0.0008

λ	α_L	α_T	β_L	β_T	SSNL	SSML	SSNT	SSMT	SSN	SSM
100	.335	.520	.689	1.304	2.04	.0092	8.47	.1101	10.51	.1196
10	.410	.585	.431	1.132	1.226	.0197	3.64	.275	4.86	.295
5	.416	.591	.342	.952	.999	.0306	2.87	.389	3.87	.420
2	.402	.583	.234	.745	.745	.0597	2.14	.636	2.88	.695
1	.373	.568	.1711	.611	.595	.1019	1.730	.944	2.33	1.041
.5	.339	.550	.1242	.495	.480	.1659	1.412	1.417	1.892	1.583
.2	.292	.520	.0805	.367	.365	.306	1.087	2.52	1.452	2.82
.1	.259	.492	.0571	.283	.297	.477	.895	3.97	1.191	4.45
.05	.229	.460	.0407	.222	.241	.716	.737	6.35	.981	7.07
.02	.192	.412	.0248	.155	.1858	1.302	.573	11.96	.759	13.26
.01	.163	.374	.0165	.116	.1504	2.17	.474	19.40	.625	21.6
.005	.145	.335	.0110	.0868	.1225	3.66	.393	31.6	.516	35.3
.002	.1195	.285	.0061	.0579	.0923	7.99	.307	60.8	.399	68.7
.001	.1031	.249	.0040	.0423	.0758	14.15	.254	99.9	.330	114.9
.0001	.0570	.152	.0006	.0149	.0349	99.3	.140	518.	.175	617.

TABLE C-24

TRACK-ORIENTED α, β, γ

NCIRC = 8 (3°/sec. turn)

TF = 4

MIN. Step = 0.0003

λ	α_L	α_T	β_L	β_T	γ_L	γ_T
100	.305	.919	1.003	1.142	.609	.641
10	.675	.745	.754	.370	.196	.213
5	.418	.596	.339	.944	.01374	.0056
2	.421	.586	.233	.740	.0067	.0024
1	.383	.570	.171	.609	.0020	.0009
.5	.342	.559	.1238	.495	.0005	.0001

(For $\lambda < .5$: $\gamma_L = \gamma_T = 0$ and results are the same as in table C-23.)

TABLE C-24 (Cont'd.)
TRACK-ORIENTED α, β, γ

NCIRC = 8 (3^0/sec. turn)

TF = 4

MIN. Step = 0.0008

SSNL	SSML	SSNT	SSMT	SSN	SSM
6.15	.0314	7.60	.0741	13.75	.1055
2.90	.0965	3.45	.224	6.35	.320
1.046	.0318	2.86	.386	3.91	.418
.774	.0605	2.13	.633	2.91	.693
.608	.1017	1.729	.938	2.34	1.039
.483	.1654	1.412	1.416	1.895	1.581

(For $\lambda < .5$: $\gamma_L = \gamma_T = 0$ and results are the same as in table C-23.)

C.4 INITIATION/TERMINATION DESIGN EVALUATIONS

Tables C-25 through C-35 show numerical results of a series of initiation/termination designs to meet specified performance constraints. In each table, the range of blip scan and clutter probability consistent with these constraints is mapped out, together with the decision rules which implement the corresponding designs. The step level of the computation is such that all designs are constructed whose critical p level differs by more than .001 from neighboring designs.

The use and interpretation of these tables is explained in section 3.3.4. The notation is as follows:

Performance constraints:

MC = mean time to initiate a true track (scans)

TC = mean track life at true track as limited by inadvertent drop (scans)

LFC = load factor for clutter tracks (see section 3.3.4)

Achieved performance:

M (corresponds to MC)

T (corresponds to TC)

LF (corresponds to LFC)

Initiation/Termination Parameters:

KI = number of consecutive reports to initiate (n)

KT = number of consecutive reports to terminate (m)

Corner Data Conditions:

B = blip scan ratio (true aircraft)

P = probability of one or more clutter reports in a search area

TABLE C-25

MC = 0.6000E 01 TC = 0.2000E 03 LFC = 0.1000E-01

KI	KT	B	P	M	T	LF
1	9	0.3839	0.0010	0.2604E 01	0.2012E 03	0.9046E-02
2	7	0.5009	0.0339	0.5980E 01	0.2570E 03	0.9477E-02
2	6	0.5429	0.0369	0.5233E 01	0.2003E 03	0.9569E-02
2	5	0.6199	0.0409	0.4214E 01	0.2019E 03	0.9747E-02
2	4	0.7109	0.0459	0.3384E 01	0.2001E 03	0.9760E-02
3	4	0.7199	0.1189	0.5997E 01	0.2245E 03	0.9949E-02
3	3	0.8179	0.1319	0.4544E 01	0.2014E 03	0.9886E-02
4	3	0.8559	0.2069	0.5990E 01	0.3898E 03	0.9989E-02
4	2	0.9269	0.2319	0.4852E 01	0.2011E 03	0.9878E-02
5	2	0.9429	0.2989	0.5983E 01	0.3249E 03	0.9826E-02
5	1	0.9959	0.3499	0.5061E 01	0.2474E 03	0.9943E-02

TABLE C-26

MC = 0.6000E 01 TC = 0.2000E 03 LFC = 0.5000E-01

KI	KT	B	P	M	T	LF
1	20	0.1669	0.0019	0.5988E 01	0.2254E 03	0.4088E-01
1	12	0.2879	0.0039	0.3472E 01	0.2010E 03	0.4936E-01
1	8	0.4279	0.0059	0.2336E 01	0.2015E 03	0.4946E-01
2	7	0.5009	0.0709	0.5980E 01	0.2570E 03	0.4967E-01
2	6	0.5429	0.0769	0.5233E 01	0.2003E 03	0.4945E-01
2	5	0.6199	0.0849	0.4214E 01	0.2019E 03	0.4966E-01
2	4	0.7109	0.0949	0.3384E 01	0.2001E 03	0.4898E-01
3	4	0.7199	0.1869	0.5997E 01	0.2245E 03	0.4989E-01
3	3	0.8179	0.2079	0.4514E 01	0.2014E 03	0.4912E-01
4	3	0.8559	0.2879	0.5990E 01	0.3898E 03	0.4987E-01
4	2	0.9269	0.3249	0.4852E 01	0.2011E 03	0.4953E-01
5	2	0.9429	0.3899	0.5983E 01	0.3249E 03	0.4946E-01
5	1	0.9959	0.4579	0.5061E 01	0.2474E 03	0.4970E-01

TABLE C-27

MC = 0.6000E 01 TC = 0.2000E 03 LFC = 0.2000E-02

KI	KT	B	P	M	T	LF
2	7	0.5009	0.0159	0.5980E 01	0.2570E 03	0.1927E-02
2	5	0.6199	0.0189	0.4214E 01	0.2019E 03	0.1930E-02
2	4	0.7109	0.0209	0.3384E 01	0.2001E 03	0.1880E-02
3	4	0.7199	0.0729	0.5997E 01	0.2245E 03	0.1959E-02
3	3	0.8179	0.0809	0.4544E 01	0.2014E 03	0.1973E-02
4	3	0.8559	0.1449	0.5990E 01	0.3898E 03	0.1975E-02
4	2	0.9269	0.1619	0.4852E 01	0.2011E 03	0.1966E-02
5	2	0.9429	0.2259	0.5983E 01	0.3249E 03	0.1978E-02
5	1	0.9959	0.2629	0.5061E 01	0.2474E 03	0.1980E-02

TABLE C-28

MC = 0.9000E 01 TC = 0.2000E 03 LFC = 0.1000E-01

KI	KT	B	P	M	T	LF
1	9	0.3839	0.0019	0.2604E 01	0.2012E 03	0.9046E-02
2	9	0.3939	0.0299	0.8950E 01	0.2277E 03	0.9606E-02
2	8	0.4279	0.0319	0.7795E 01	0.2015E 03	0.9664E-02
2	7	0.4799	0.0339	0.6423E 01	0.2005E 03	0.9476E-02
2	6	0.5429	0.0369	0.5233E 01	0.2003E 03	0.9569E-02
3	6	0.6029	0.1019	0.8969E 01	0.4218E 03	0.9951E-02
3	5	0.6499	0.1089	0.8410E 01	0.2019E 03	0.9821E-02
3	4	0.7109	0.1189	0.6157E 01	0.2001E 03	0.9949E-02
4	4	0.7399	0.1889	0.8980E 01	0.2942E 03	0.9813E-02
4	3	0.8179	0.2069	0.6778E 01	0.2014E 03	0.9988E-02
5	3	0.8319	0.2709	0.8979E 01	0.2521E 03	0.9944E-02
6	3	0.8959	0.3249	0.8969E 01	0.9901E 03	0.9870E-02
6	2	0.9269	0.3559	0.7889E 01	0.2011E 03	0.9971E-02
7	2	0.9409	0.4029	0.8995E 01	0.3038E 03	0.9897E-02
8	2	0.9749	0.4429	0.8982E 01	0.1634E 04	0.9829E-02
8	1	0.9959	0.4919	0.8147E 01	0.2474E 03	0.9847E-02

TABLE C-29

MC = 0.9000E 01 TC = 0.2000E 03 LFC = 0.5000E-01

KI	KT	B	P	M	T	LF
1	20	0.1609	0.0019	0.6211E 01	0.2017E 03	0.4088E-01
1	12	0.2879	0.0039	0.3472E 01	0.2010E 03	0.4936E-01
2	9	0.3939	0.0619	0.8980E 01	0.2277E 03	0.4985E-01
2	8	0.4279	0.0659	0.7795E 01	0.2015E 03	0.4961E-01
2	7	0.4799	0.0709	0.6423E 01	0.2005E 03	0.4967E-01
2	6	0.5429	0.0769	0.5233E 01	0.2003E 03	0.4945E-01
3	6	0.6029	0.1579	0.8969E 01	0.4218E 03	0.4907E-01
3	5	0.6199	0.1709	0.8410E 01	0.2019E 03	0.4982E-01
3	4	0.7109	0.1869	0.6167E 01	0.2001E 03	0.4989E-01
4	4	0.7399	0.2619	0.8980E 01	0.2942E 03	0.4943E-01
4	3	0.8179	0.2879	0.6778E 01	0.2014E 03	0.4986E-01
5	3	0.8319	0.3509	0.8979E 01	0.2521E 03	0.4967E-01
6	3	0.8959	0.4019	0.8969E 01	0.9901E 03	0.4934E-01
6	2	0.9269	0.4419	0.7889E 01	0.2011E 03	0.4922E-01
7	2	0.9409	0.4849	0.8995E 01	0.3038E 03	0.4931E-01
8	2	0.9749	0.5209	0.8982E 01	0.1634E 04	0.4941E-01
8	1	0.9959	0.5849	0.8147E 01	0.2474E 03	0.4965E-01

TABLE C-30

MC = 0.9000E 01 TC = 0.2000E 03 LFC = 0.2000E-02

KI	KT	B	P	M	T	LF
2	9	0.3939	0.0139	0.8980E 01	0.2277E 03	0.1907E-02
2	7	0.4799	0.0159	0.6423E 01	0.2005E 03	0.1927E-02
3	6	0.6029	0.0629	0.8969E 01	0.1213E 03	0.1957E-02
3	5	0.6199	0.0669	0.8410E 01	0.2019E 03	0.1925E-02
3	4	0.7109	0.0729	0.6167E 01	0.2001E 03	0.1959E-02
4	4	0.7399	0.1329	0.8980E 01	0.2912E 03	0.1913E-02
4	3	0.8179	0.1419	0.6778E 01	0.2011E 03	0.1975E-02
5	3	0.8319	0.2049	0.8979E 01	0.2521E 03	0.1956E-02
6	3	0.8959	0.2589	0.8969E 01	0.9901E 03	0.1965E-02
6	2	0.9269	0.2819	0.7889E 01	0.2011E 03	0.1963E-02
7	2	0.9409	0.3309	0.8995E 01	0.3038E 03	0.1970E-02
8	2	0.9749	0.3739	0.8982E 01	0.1634E 04	0.1988E-02
8	1	0.9959	0.4159	0.9117E 01	0.2474E 03	0.1984E-02

TABLE C-31

MC = 0.4000E 01 TC = 0.2000E 03 LFC = 0.1000E-01

KI	KT	S	P	M	T	LF
1	9	0.3839	0.0010	0.2604E 01	0.2012E 03	0.9046E-02
2	5	0.6409	0.0409	0.3994E 01	0.2600E 03	0.9747E-02
2	4	0.7109	0.0459	0.3384E 01	0.2001E 03	0.9760E-02
2	3	0.8179	0.0529	0.2737E 01	0.2014E 03	0.9663E-02
3	3	0.8689	0.1319	0.3999E 01	0.5103E 03	0.9886E-02
3	2	0.9269	0.1519	0.3498E 01	0.2011E 03	0.9788E-02
3	1	0.9959	0.1929	0.3024E 01	0.2474E 03	0.9896E-02

TABLE C-32

MC = 0.4000E 01 TC = 0.2000E 03 LFC = 0.5000E-01

KI	KT	B	P	M	T	LF
1	14	0.2509	0.0029	0.3984E 01	0.2238E 03	0.4301E-01
1	9	0.3839	0.0049	0.2604E 01	0.2012E 03	0.4625E-01
1	6	0.5429	0.0079	0.1841E 01	0.2003E 03	0.4956E-01
2	5	0.6409	0.0849	0.3994E 01	0.2600E 03	0.4967E-01
2	1	0.7109	0.0949	0.3381E 01	0.2001E 03	0.4898E-01
2	3	0.8179	0.1109	0.2717E 01	0.2014E 03	0.4979E-01
3	3	0.9689	0.2079	0.3999E 01	0.5103E 03	0.4912E-01
3	2	0.9269	0.2419	0.3493E 01	0.2011E 03	0.4964E-01
3	1	0.9959	0.3069	0.3024E 01	0.2471E 03	0.4986E-01

TABLE C-33

MC = 0.4000E 01 TC = 0.2000E 03 LFC = 0.2000E-02

KI	KT	B	P	M	T	LF
2	5	0.6409	0.0139	0.3994E 01	0.2600E 03	0.1931E-02
2	4	0.7109	0.0209	0.3384E 01	0.2001E 03	0.1880E-02
2	3	0.8179	0.0249	0.2717E 01	0.2014E 03	0.1997E-02
3	3	0.8689	0.0809	0.3999E 01	0.5103E 03	0.1973E-02
3	2	0.9269	0.0929	0.3498E 01	0.2011E 03	0.1956E-02
3	1	0.9959	0.1179	0.3024E 01	0.2474E 03	0.1982E-02

TABLE C-34

MC = 0.6000E 01 TC = 0.5000E 02 LFC = 0.5000E-01

KI	KT	B	P	M	T	LF
1	13	0.1669	0.0029	0.5988E 01	0.5841E 02	0.3988E-01
1	9	0.2519	0.0049	0.3968E 01	0.5016E 02	0.4525E-01
1	6	0.3979	0.0079	0.2512E 01	0.5027E 02	0.4956E-01
2	5	0.5009	0.0949	0.5980E 01	0.6251E 02	0.4967E-01
2	4	0.5719	0.0949	0.4804E 01	0.5034E 02	0.4898E-01
2	3	0.6969	0.1109	0.3493E 01	0.5013E 02	0.4979E-01
3	3	0.7199	0.2079	0.5997E 01	0.6186E 02	0.4912E-01
3	2	0.8189	0.2419	0.4199E 01	0.5946E 02	0.4964E-01
4	2	0.8559	0.3249	0.5990E 01	0.5511E 02	0.4959E-01
5	2	0.9129	0.3899	0.5983E 01	0.3249E 03	0.4946E-01
5	1	0.9809	0.4579	0.5298E 01	0.5251E 02	0.4970E-01

TABLE C-35

MC = 0.6000E 01 TC = 0.1000E 03 LFC = 0.5000E-01

K1	KT	B	P	M	T	LF
1	16	0.1669	0.0029	0.5988E 01	0.1054E 03	0.4931E-01
1	9	0.3229	0.0049	0.3096E 01	0.1003E 03	0.4625E-01
1	6	0.4769	0.0079	0.2096E 01	0.1003E 03	0.4956E-01
2	6	0.5009	0.0769	0.5989E 01	0.1272E 03	0.4946E-01
2	5	0.5539	0.0819	0.5063E 01	0.1094E 03	0.4966E-01
2	4	0.6499	0.0919	0.3905E 01	0.1009E 03	0.4898E-01
3	4	0.7199	0.1869	0.5997E 01	0.2245E 03	0.4989E-01
3	3	0.7659	0.2079	0.5235E 01	0.1095E 03	0.4912E-01
4	3	0.8559	0.2879	0.5990E 01	0.3898E 03	0.4987E-01
4	2	0.8949	0.3249	0.5319E 01	0.1001E 03	0.4959E-01
5	2	0.9429	0.3899	0.5983E 01	0.3249E 03	0.4946E-01
5	1	0.9909	0.4579	0.5138E 01	0.1106E 03	0.4970E-01

APPENDIX D

DETAILED PROBLEM SIMULATION

D.1 INTRODUCTION

This report presents a general summary of the work being performed in developing methods of detailed problem simulation as part of the Augmented Tracking development effort. The development of such a simulation tool stems from the need for a uniform and realistic means of evaluating and comparing tracking algorithms for use in an air traffic control environment, as well as providing a means for development of new and refined tracking schemes. In fulfilling this objective the following considerations have been made. First, a simulated terminal environment which describes the real environment in as much detail as is feasible is provided. Second, a variety of target tracks with independent characteristics and performing various maneuvers are available. Third, a flexible means of algorithm substitution is provided to allow rapid comparison of their relative performance. Fourth, a list of performance measures which rate the algorithm on a number of relevant topics is tabulated and printed in a fixed format to allow easy cross reference.

This simulation effort is generally referred to as the "tracking analyzer," which describes its use in qualifying tracking algorithms by measuring their performance with respect to known target activity. Four basic components make up the tracking analyzer, namely:

1) True track generator

2) Target report generator

3) Correlation and tracking algorithms

4) Statistical analyzer

The block diagram shown in figure D-1 points out these basic components along with the data flow between each. The following paragraphs describe the integral workings of the tracking analyzer in sections as suggested by figure D-1.

D.2 TRUE TRACK GENERATOR

The track generator computes the true target positions and velocities along a predetermined path. This path is defined by the user, who is provided with several track options which he may select according to the level of analysis being performed. These options provide a series of data sequences as described below.

The first track option provides a single target performing a predetermined series of maneuvers. With this single track, we can eliminate much report to track correlation logic and can concentrate on the operation of the track smoothing algorithm exclusively. In addition to providing a uniform means of comparing various tracking schemes, this allows for a type of "fine tuning" of a particular tracking algorithm.

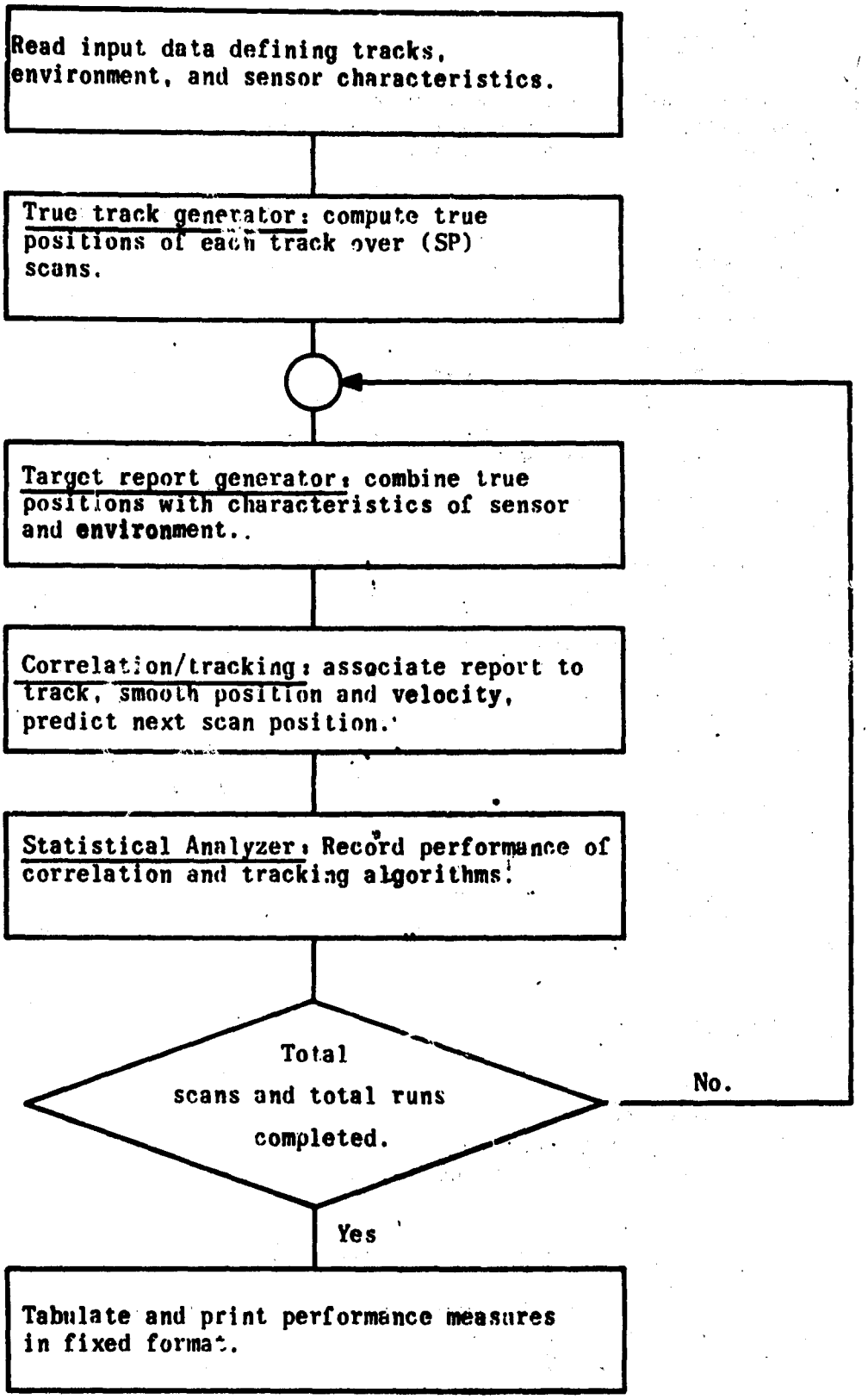

Figure D-1. Tracking Analyzer Block Diagram

D.2 (continued)

The track path currently defined is that shown in figure D-2, which is designated the standard track. This path is defined so as to exercise the tracker over a series of maneuvers which increase in severity by performing a series of turns to both the right and left with increasing accelerations (from 1/16 to 1/2 g, assuming a 250 knot target speed). This path was chosen so as to subject the tracker to a variety of important tests. First, a straight line portion is generated, during which measurements can be made to determine the tracker's ability to a) "lock on" to the target, and b) to smooth the report data along a straight line segment. Next, the target is made to perform a series of turns with increasing accelerations, each ending in straight line flight. This provides a measure both of its tracking ability in the various turns and also its ability to recognize the transition from straight line flight to a turn and back to straight line flight. Finally, the target is made to execute an "S" turn in which the tracker's ability to handle rather violent heading changes can be measured.

The path which has been described is only semi-permanent, in that it can be modified, if desired, by making slight modifications within the tracking analyzer. A number of inputs to the track generator are variable and, as such, must be supplied by the user. These inputs include:

1) Initial target range (radar miles from the sensor site)

2) Initial target azimuth (degrees with respect to sensor site)

3) Initial target heading (degrees)

4) Target speed (radar miles per hour)

The second track option is provided as the next logical sequence in evaluating tracking methods, by introducing the correlation decision. It is intended that those track smoothing algorithms which have been optimized to perform on the "standard track" be paired with various correlation algorithms and further evaluated at this level. Here two tracks are introduced which are made to intersect at a predetermined position at the same point in time. This imposes a correlation conflict which must be resolved correctly or a track swap will result.

These tracks are specified completely by the user within the following inputs.

1) Point of intersect (X, Y distances from the sensor site, radar miles)

2) Initial heading each target (degrees)

3) Heading of each target at point of intersect (degrees)

4) Final heading each target (degrees)

5) Speed of each target (radar miles per hour)

Note: Acceleration is related to target speed and sensor scan interval; acc = (s/1000 • T) • n
s = target speed (knots)
T = sensor scan interval (seconds)
n = acceleration constant: (1, 2, 4, 8, 3 for progressive turns).

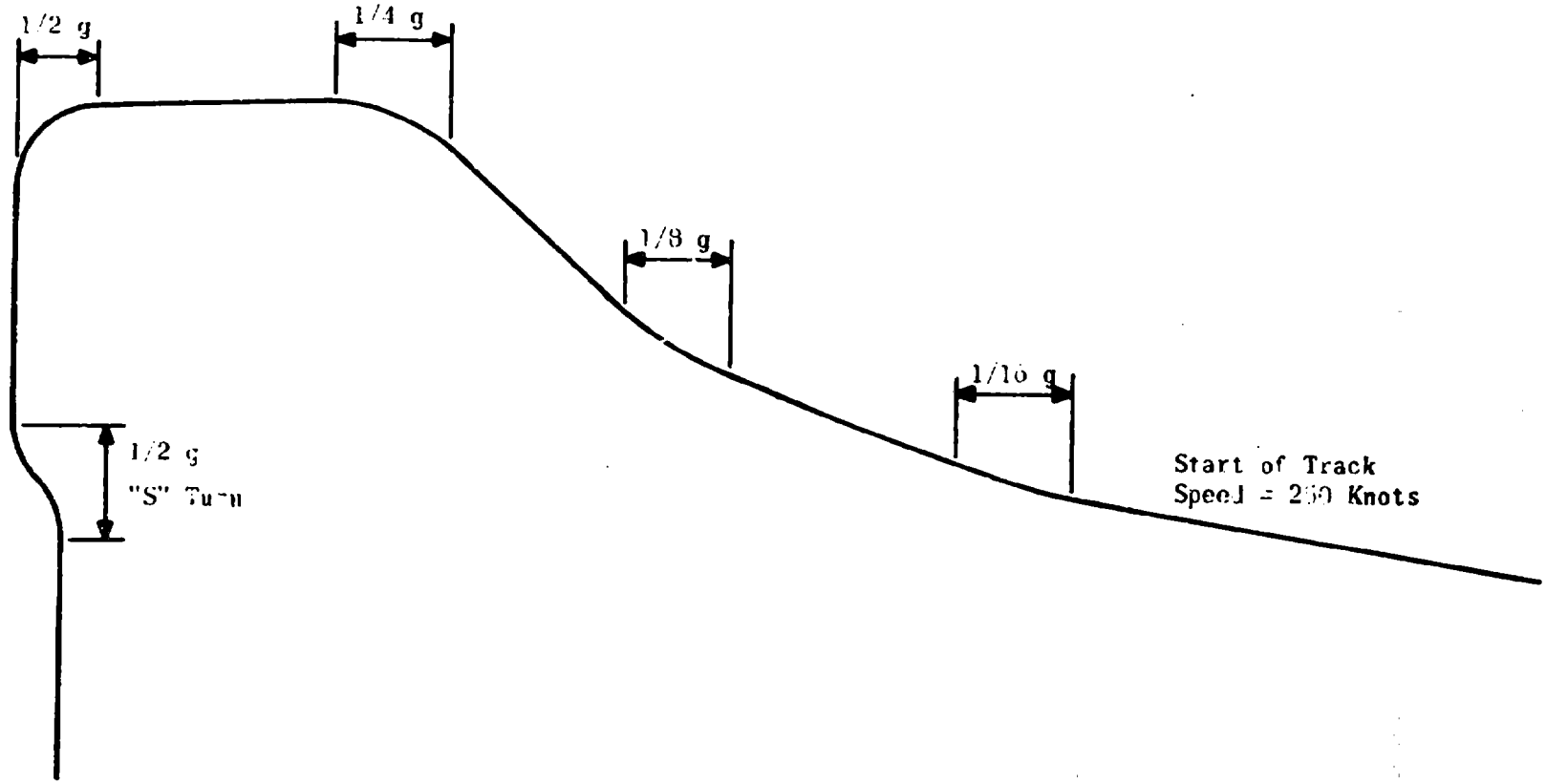

Figure D-2. Tracking Analyzer Standard Track Path

D.2 (continued)

6) Turn rate of each target (degrees per second)

7) Intersect heading increment and number of heading differences to be evaluated.

This series of inputs allows a wide variety of conflicting target paths to be defined. This includes any combination of straight line tracks and maneuvering tracks with a wide range of maneuverability. A factor which influences the correlation decision most drastically is the relative heading difference of the tracks at the time of intersect. Within this track option is provided executive logic, which will repeat the generation of target tracks over the number of runs specified, each time adjusting the relative heading by the selected increment. This provides a measurement of the correlation/tracking algorithm performance in terms of the tendency for track swap, track loss, etc., as a function of the relative heading at intersect.

The final track option which is provided allows for greater flexibility in defining target paths by providing a free format in which up to six tracks may be specified. Each track performs independent of the others and is completely defined by the user through the following inputs.

1) Initial target range (radar miles from the sensor site)

2) Initial target azimuth (degrees with respect to sensor site)

3) Initial target heading (degrees)

4) Target speed (radar miles per hour)

For each track defined by the above parameters, up to five maneuver segments may be specified by supplying a turn indication (right, left, or straight), an acceleration constant (up to 1 g), and the number of scans over which the maneuver is to continue.

For any of the track options which are described above, the following information is generated for each track on each sensor scan.

1) Ture target range at each observation

2) True target azimuth at each observation

3) True target x coordinate at each observation

4) True target y coordinate at each observation

5) True target x velocity at each observation

D.2 (continued)

6) True target y velocity at each observation

7) True time at each observation

D.3 TARGET REPORT GENERATOR

The Target Report Generator provides reported target positions for both radar and beacon sensor systems by combining the noise characteristics of the air traffic control sensor with the true positions provided by the track generator. In addition to the insertion of noise into each target report, the true terminal environment is further simulated by allowing a varying blip/scan ratio in the range from 1 to .5 for the radar and 1 to .75 for the beacon sensor to represent tracking conditions from ideal to extremely adverse.

The generation of each target report assumes a stationary independent Gaussian noise distribution in range and azimuth, and a constant blip/scan ratio. First, a random number in the range from 0 to 1 is generated against which the selected blip/scan ratio is compared. When the random number is greater than this ratio, a missed report is declared; otherwise a report is generated. For this report, two normally distributed pseudo-random numbers of zero mean and standard deviation corresponding to the range and azimuth distributions of the sensor, are generated and combined with the true position supplied by the track generator. This sequence is repeated for each sensor (radar and beacon) separately, and for each target track.

For beacon reports, a further consideration which is made is that of beacon fade, which is often experienced in turns due to shielding of the beacon transponder. Two methods of simulating beacon fade are provided: the first requires that those scans of the turn where fade is to occur be specified by the user; for those tracks which are free format and which are frequently changed, a second method is provided, in which the number of scans in which fade occurs is computed through a random number process. This allows a fade duration which is independent for each turn and which is distributed uniformly around the mid-point of the turn.

In addition to the generation of true target reports as described above, the real environment is further simulated by introducing radar clutter reports within a region whose size and placement is specified by the user. Also specified is the clutter density within this region. On each scan, the number of clutter reports which are to be generated are computed as a Poisson random variable and distributed within the specified region.

Variable inputs to the Target Report Generator which must be supplied by the user are:

1) Sensor scan interval (seconds)

2) Blip/scan ratio each sensor

D.3 (continued)

3) Standard deviation of range error each sensor

4) Standard deviation of azimuth error each sensor

5) Clutter region dimensions and clutter density.

These inputs are applied in the processes described above to provide the following target report information.

1) Reported target range at each observation

2) Reported target azimuth at each observation

3) Reported target x coordinate at each observation

4) Reported target y coordinate at each observation

5) Reported time at each observation

6) Report identification

This data is supplied for both radar and beacon sensors within separate output tables. The report identification designates the track for which the report was generated and identifies those reports which are clutter. All output data other than the report identification is made available for correlation and tracking. The identification is only available to the Statistical Analyzer, which compares the true report with the assignment made by correlation and the resultant smoothed position provided by tracking.

D.4 CORRELATION/TRACKING

The correlation/tracking section has the task of establishing and maintaining target tracks, using only the sequence of reported positions and times which have been provided by the Target Report Generator. This includes making correct report to track associations for valid reports, and recognizing and discarding false reports.

The majority of the processing within this segment will be devoted to the tracking methods being evaluated. The task of any algorithm will be to take the sequence of input positions and times, make a correlation decision between each track and the available reports, and based on this association, to compute smoothing estimates of target position and velocity. These smoothed values, along with the identification code of the target report assigned by correlation, are provided as output from the correlation tracking section.

The tracking algorithms which are evaluated within this section are described, along with the results of their operation, in the following Appendix E.

D.5 STATISTICAL ANALYZER

The final task of the tracking analyzer is that of compiling a list of performance measures which describe the qualities of the tracking algorithm and presenting these performance measures to the user. Of central importance to this tracking study is the development of measures of performance that reflect, in so far as possible, the qualities desired in an air traffic control tracking algorithm.

Two primary levels of performance measures are provided which are directed at describing separately the performance of correlation and track smoothing. This allows for substitution of various correlation algorithms which can be compared with the same track smoothing algorithm or vice versa. However, it must be realized that these are not entirely independent sequences, and that improper correlation decisions may adversely affect track smoothing while erroneous track smoothing in turn tends to complicate the correlation decision.

The correlation decision is monitored through a comparison of the true track identification with the identification code of the target report which has been assigned. If a correlation conflict could not be resolved, this identification will indicate that a coast condition has been declared. For each track, the following data is accumulated over the life of the track.

1) Number of coasts when a valid radar or beacon report is present

2) Number of times radar and beacon reports are both present but not merged

3) Number of times a radar clutter report is merged with the beacon report

4) Number of times a radar clutter report is assigned (no beacon report found)

5) Number of times a correct assignment is made

6) Track swap indication (continuous correlation with target reports of another track)

7) Track loss indication (tracking discontinued after unsuccessful correlation on (SP) consecutive scans)

These values are accumulated over a number of identical runs and a statistical average computed. The data is then tabulated and printed in the format shown below to provide a hard copy output. In addition to the above performance statistics, a summary of data conditions is also provided as shown. For multiple track options, additional conditions such as target speeds, relative headings at intersect, etc. are also provided.

D.5 (continued)

GLOSSARY

NLT = LOST TRACK
NCA = NUMBER OF CORRECT ASSIGNMENTS
NCT = NUMBER OF ASSIGNED CLUTTER
NST = NUMBER OF COASTS WHEN VALID REPORT PRESENT
NCL = NUMBER OF CLUTTER MERGED WITH BEACON
NRU = VALID RADAR REPORTS PRESENT BUT NOT USED
NSW = NUMBER OF TRACK SWAPS

CLUTTER DENSITY = .00 REPORTS PER DEGREE - N.M.
RADAR BLIP/SCAN RATIO = .90
BEACON BLIP/SCAN RATIO = .95

	NLT	NCA	NCT	NST	NCL	NRU	NSW
TRACK #1	.00	199.63	.00	.37	.00	7.87	.00

The second level of performance measures describes the tracking accuracy which is provided by the track smoothing algorithm, using track history data accumulated over previous scans, and the new target report assigned by correlation. Four basic performance measures are defined:

1) Position error

2) Velocity error

3) Position dispersion

4) Velocity dispersion

These items provide a measure of how much inherent position and velocity error the tracking algorithm has, as well as how much noise (disperion) in position and velocity it has. The performance measures are designed, using normalization procedures, to eliminate the affect of as many parameter variations as possible, including target range, azimuth, heading, speed, sensor scan interval, and level of sensor noise. This enables the tracking analyzer to be easily adapted to a new tracking environment. The remaining parameters of interest are then completely dependent upon the tracking algorithm only.

To provide a concise and uniform method of presentation, these performance measures are plotted for each track as shown in Figure D-3. Since all values are normalized, this plot can be used to show the relative performance of various tracking algorithms receiving identical input data, or the relative performance of a variety of data conditions within a particular tracking algorithm. The symbology used for this plot corresponds to the following:

P = Position error - the average error between the true and smoothed positions at each observation (scan), normalized by the distance that the target travels in one scan interval.

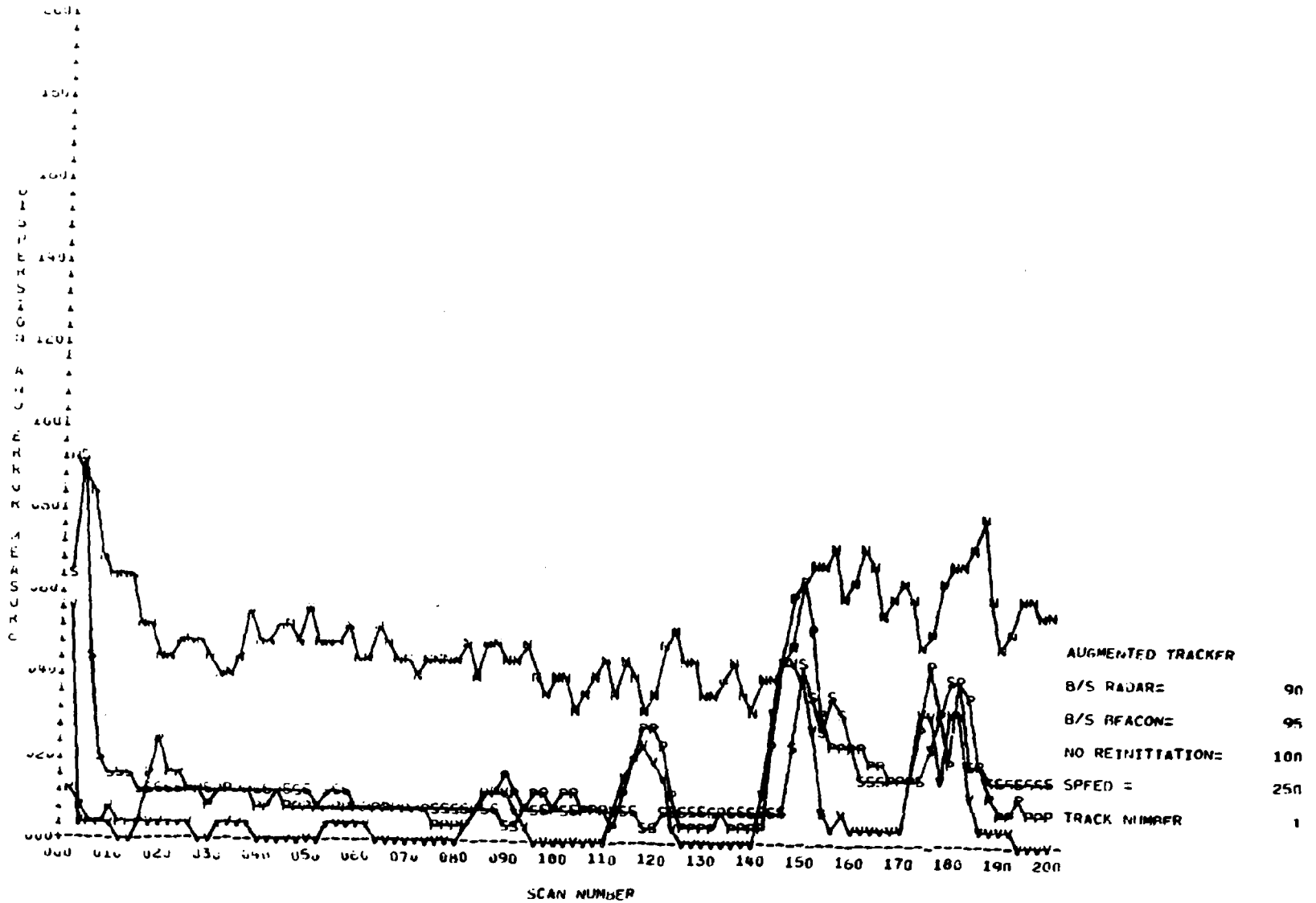

Figure D-3. Augmented Tracker - One Radar/Beacon Track

D.5 (continued)

V = Velocity error - the average error between the true and smoothed velocity vectors at each observation, normalized by the speed of the target.

N = Position dispersion - the standard deviation of the smoothed position at each observation, normalized by the standard deviation of the reported radar position.

S = Velocity dispersion - the standard deviation of the smoothed velocity estimate (translated into a position by multiplying by the sensor scan interval) at each observation, normalized by the standard deviation of the reported radar position.

Each of these performance items are accumulated over a number of equivalent runs to provide a statistical average.

D.5.1 Denormalization of Performance Measures

As stated previously, these performance measures are designed to eliminate, by normalization, the effect of as many target and sensor parameters as possible. This allows most attention to be directed upon the tracking algorithm itself. Since it may be desirable under certain circumstances to obtain exact (denormalized) values, we will present several exercises in denormalization. We will use the performance plot for the augmented tracking system shown in figure D-3 as the basis for these exercises.

The examples which are provided below show the dispersion measures along the steady state tracking segment at a range of 40 miles and the peak errors in following the 1/4 g turn. Each example considered is for a target traveling at 250 knots and a sensor scan interval of 4 seconds. However, as can be seen from the general form of the equations, the same plot can be used with any target speed and sensor scan interval to derive corresponding denormalized values. The parameters referenced within these equations are defined as follows:

S = target speed in knots

T = sensor scan interval in seconds

σ_{ap} = a priori standard deviation of the input data noise

X = normalized value read from the plot.

D.5.1.1 Peak Position Error in Following a ¼ g Turn

The position error measure is normalized by the distance the target travels in one scan interval. We see from figure D-3 that the peak position error for the ¼ g turn (scans 110 thru 120) is approximately .28. This corresponds to an actual distance in miles according to the following computation:

$$P_A = S \bullet T/3600 \bullet X$$

$$= 250 \bullet 4/3600 \bullet .28$$

$$= .078 \text{ miles.}$$

D.5.1.2 Peak Velocity Error in Following a ¼ g Turn.

The velocity error measure is normalized by the speed of the target. We see from figure D-3 that the peak normalized velocity error in following a ¼ g turn is approximately .24. Thus the acutal peak velocity error in miles per hour is computed as:

$$V_A = S \bullet X$$

$$= 250 \bullet .24$$

$$= 60 \text{ miles/hour.}$$

D.5.1.3 Average Steady State Position Dispersion.

We see from figure D-3 that the average normalized steady state position dispersion is approximately .48. The acutal position dispersion in miles may be obtained by multiplying this measure by the <u>a priori</u> standard deviation of the input data noise at that range. Assuming independent noise in range and azimuth, stationary in range, the <u>a priori</u> standard deviation of the input data noise is given by $\sigma_{ap} = \sqrt{\sigma_\rho^2 + \rho^2\sigma_\theta^2}$. For our example we are considering a sensor with error characteristics $\sigma_\rho = 0.05$ miles and $\sigma\theta = 0.25$ degrees. The <u>a priori</u> standard deviation of input noise at a range of 40 miles is then computed as .176. Thus the actual steady state position dispersion in miles, at a range of 40 miles, is derived as:

$$N_A = \sigma_{ap} \bullet X$$

$$= .176 \bullet .48$$

$$= .084 \text{ miles.}$$

D.5.1.4 Average Steady State Velocity Dispersion

The velocity dispersion measure is a velocity translated into a position by multiplying by the sensor scan interval, normalized by the standard deviation of the input data noise. We see from figure D-3 that the average steady state velocity dispersion measure is approximately .12. Again, for the example we are considering, the a priori standard deviation of the input noise at a range of 40 miles is .176 (as computed in section D.5.1.3 above). Thus the average steady state velocity dispersion in miles per hour, at a range of 40 miles, is computed as:

$$S_A = 3600/T \bullet \sigma_{ap} \bullet X$$

$$= 3600/4 \bullet .176 \bullet .12$$

$$= 19.0 \text{ miles/hour.}$$

D.6 USE OF THE TRACKING ANALYZER

Throughout the augmented tracking study effort, extensive use was made of the tracking analyzer for both qualifying and optimiizing those tracking methods which analytically showed promise. The flexibility in providing a variety of data situations within realistic environment conditions allowed us to recommend with confidence those tracking methods which show improved performance. In addition, this simulation tool was used to obtain performance statistics on the ARTS-III and Basic RBTL level of tracking to provide a baseline from which the augmented tracking improvements could be measured.

It is felt that this tool will continue to prove invaluable in obtaining system parameters which provide optimum performance during the augmented tracking design effort which follows.

APPENDIX E

TRACKING ALGORITHM EVALUATION

E.1 INTRODUCTION

This section examines several tracking algorithms which have been developed specifically for use in the terminal area. The tracking performance of each of these algorithms is statistically determined and recorded using the "tracking analyzer" described in the preceding appendix D.

Included in this section are the description and result of operation for the ARTS-III Beacon Tracking Level (BTL) system and the Basic Radar Beacon Tracking Level (RBTL) system. These are included as the first part of this section to show the improvements realized with the addition of radar tracking within ARTS-III to provide the Basic RBTL baseline system. The remaining algorithms which are examined in this section represent those recommended as improved tracking techniques. Each algorithm is introduced with a verbal description, followed by a list of selected performance measures. The detailed analysis governing each algorithm is not included in this section since it is available either in other sections of this study or in separate documents as referenced along with that description.

To limit the sheer size of this document, only selected performance graphs are included for each tracking algorithm. These performance measures in most cases represent the recommended or optimized approach. Results of precursory experiments in development of these optimum methods are, for the most part, not included. The following paragraphs present the evaluation results of these tracking algorithms. It is important to note that all graphs included in this section represent tracking performance following the "standard track" described in appendix D.

E.2 BASIC ARTS-III BEACON TRACKING LEVEL (BTL) SYSTEM

The ARTS-III tracker is a beacon only tracker which is completely dependent on cooperative airborne beacon equipment. It is a two dimensional tracker with bifurcation logic. All corrections or modifications made to a track's positional data, velocity data, or track classification, is a function of the track's firmness. The firmness is a parameter which reflects the history of the track. The larger the firmness, the more stable the track is considered to be.

Three basic processes (correlation, correction, and prediction) are performed for every track once each sensor scan.

The correlation process determines which new target report is associated with a tracked aircraft. Correlation is accomplished by building primary and secondary bins around the track's current (last predicted) position, the secondary bin being twice the size of the primary. In general, the primary

E.2 (continued)

bin decreases in size as the track becomes more stable. The new target reports are searched to find if any of them falls within the primary bin. In the ideal case, one, and only one, report is found, and unique correlation is achieved. Ambiguous situations (more than one report in the bin) are logically resolved by the tracking subprogram by comparison of the assigned and reported beacon codes.

As a result of correlation, either a track is associated with a unique target report or else unsuccessful correlation is indicated. If correlation is successful, the track is updated through a process called correction. Correction computes smoothed estimates of position and velocity, using an optimum weighting between the predicted and reported track coordinates. These weighting factors, Alpha and Beta, are referenced by the track's current firmness. The Alpha parameter is used to smooth the track's position and the Beta parameter is used to smooth the track's velocity. In general, as the track becomes more stable, more emphasis is placed upon predicted position, thereby filtering out the noise components in the data input.

If no report is found within the primary association bin, two turning tracks are established. These turning tracks are generated by using the last smoothed velocity to compute a point along the track which is three scans back from the straight-line prediction. From this point, turning tracks to the right and left of the parent (straight) track are computed, using standard turn rates of $1\frac{1}{2}^{\circ}$/second for target speeds above 220 knots and 3°/second for speeds less than or equal to 220 knots.

If a secondary report exists, bins are built around the turning tracks and are checked for best reports. If only one of the turning tracks correlates, its position is corrected, its class is changed to turning trial, and its associated turning track is dropped. If neither correlate, they will both be retained for a maximum of three scans. If both turning tracks correlate, they are both terminated. If no secondary report existed, bins are not checked on the current scan and the track is coasted.

A turning trial track requires successful correlation for two consecutive scans, at which time it becomes a normal track and both its position and velocity are corrected. During the time that turning tracks are out, the predicted position of the straight-line track and its associated velocity are used as smoothed parameters in the statistical routines.

After a track has been correlated and corrected, the new corrected position and velocity are used to predict its position for the next sensor scan. If a track fails to correlate during the current scan, no corrected data is calculated, and the track is extrapolated on the basis of the previous position and velocity information.

E.2 (continued)

A further description of this algorithm, along with specific parameter values, may be found in the document "System Design Data for the ARTS-III Modular Automated Terminal Air Traffic Control System Beacon Tracking Level," Volume 1 and 2, November 1, 1969.

Figures E-1 through E-3 contain the performance measures of the Operational ARTS-III tracker following a non-discrete beacon target under a variety of data conditions. These figures show the beacon only tracker to be quite noisy, especially the position dispersion (symbol N). Turns are well defined by the high peaks, showing that this tracker is geared to straight-line flight. As the data rates decrease there is a drastic loss in track following ability, as illustrated by the percentage of runs which do not reinitiate (parameter block labeled NO REINITIATIONS).

It must also be pointed out that the performance graphs shown here may represent somewhat idealistic data conditions in that beacon fade in the turns is inhibited. When runs were performed with realistic fades during the turns, tracking performance drastically deteriorated, resulting in a very noisy track requiring frequent reinitiation. This becomes less pronounced if the target contains discrete beacon, since the reacquisition logic tends to salvage the track before it is auto terminated for lack of correlation.

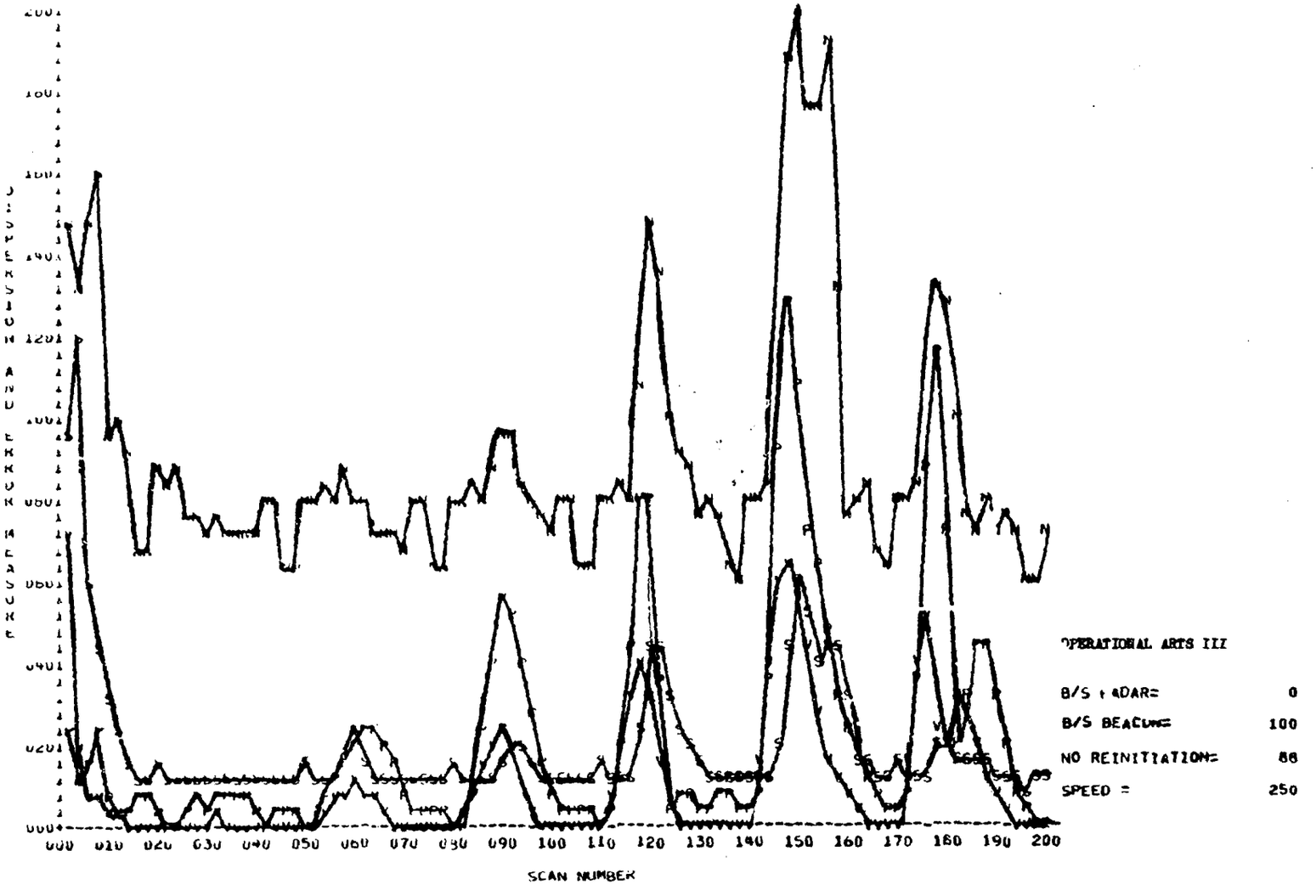

Figure E-1. Non-Discrete Beacon

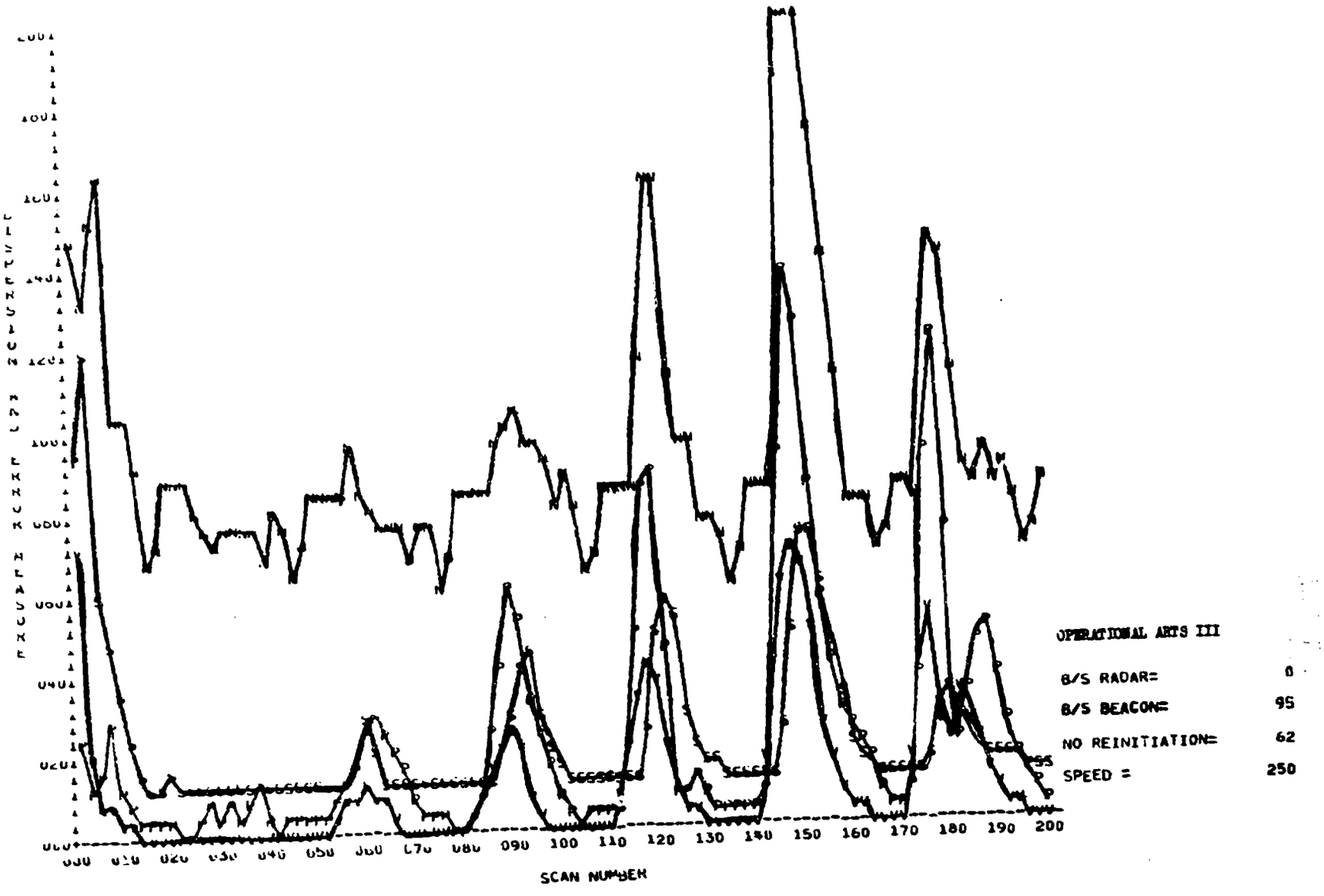

Figure E-2. Non-Discrete Beacon

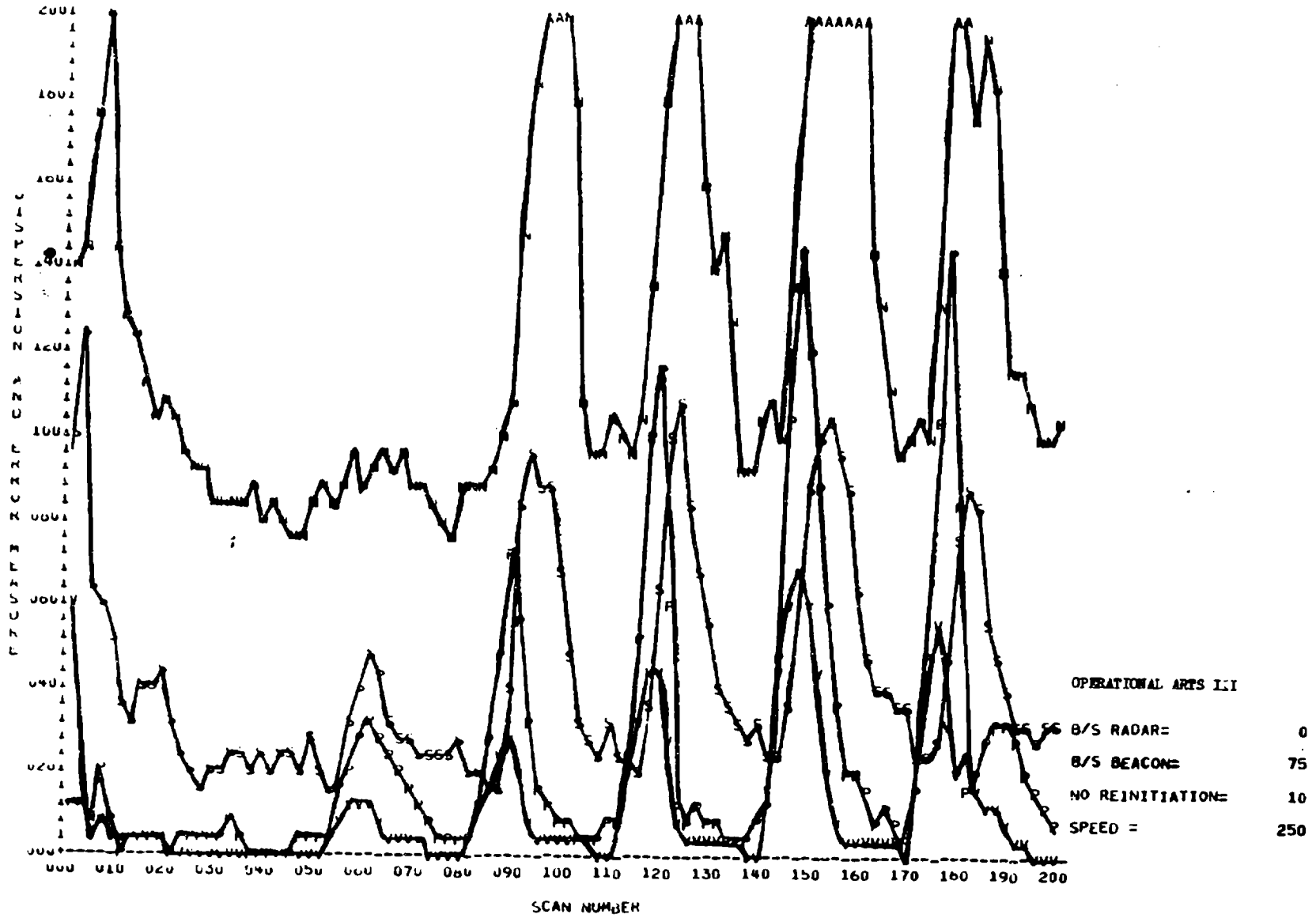

Figure E-3. Non-Discrete Beacon

E.3 BASIC RADAR BEACON TRACKING LEVEL (RBTL) SYSTEM

The Basic RBTL tracker is a first step which introduces radar data into the beacon tracking capabilities of the basic ARTS-III BTL system. The Basic RBTL tracker uses the same report-to-track correlation logic as the ARTS-III tracker augmented by the incorporation of a Radar Tracking Level (RTL) add-on package. The resultant is a tracker which is no longer totally dependent on cooperative, airborne beacon equipment.

The addition of radar tracking provides for automatic reporting and tracking of non-beacon equipped aircraft. For beacon equipped aircraft, it provides reporting backup in the event of beacon failure. In addition, our results have shown that the dual reporting capability (beacon and radar) permits improved reporting accuracy by optimally combining the two reports into a single, more accurate estimate.

To accomplish the above tasks, beacon and radar reports are processed within a beacon/radar correlation routine before being sent on to the report-to-track correlation logic. This routine attempts to correlate beacon and radar reports representing the same aircraft to derive a common position report. To achieve report-to-report correlation, a bin is centered on the beacon report and the radar report store is searched for reports lying within the bin. If a radar report is found, the beacon report is flagged as reinforced and the two reports are combined into a common position. In the baseline system, the bin consisted of a range gate of 1/16 nm and the azimuth gate of 1^0. Analytically, it can be shown that approximately 38% of the time when both a beacon and a radar report are present for the same target, they will not correlate with a range tolerance of 1/16 nm (assuming existing sensor error characteristics). We find that the errors in range and azimuth about the true position of the track are Gaussion random numbers. In our simulation, the reported ranges for both beacon and radar reports were generated using a mean of zero and a standard deviation of .05 nm. Therefore, the differences between the two ranges on a given scan have a mean of zero with a standard deviation equal to $2.(.05)$. By normalization, we find the probability of the range difference falling outside the 1/16 nm tolerance to be 38%.

By increasing the range tolerance to 1/8 nm, the probability of the reports not correlating falls to about 8%. In this way, more of the available data is used. Our simulation verified the above assumption with approximately 90% of the available radar/beacon pairs correlating.

After a radar/beacon pair has been designated, they are combined into a single report. In the baseline system, the two reports are merged using the radar report's azimuth and the beacon report's range. Another method of combining the two reports is through the use of minimum variance estimation. This process makes use of the range and azimuth of both reports to form the combined coordinates.

E.3 (continued)

This method applies an optimal weighting on each reported value. This weighting is inversely proportional to the respective noise variances of the sensors. Thus, the final product is biased toward the sensor with the smallest variance. As an example, our simulation generated beacon and radar reports having equal range variances of 0.0025 nm. The ranges are therefore weighted equally, and the final range is midway between the two. On the other hand, the variance in azimuth for reported radar positions is 0.0625^{o}, and the variance for beacon is 0.1089^{o}. Therefore, the final azimuth will be biased toward the reported radar azimuth.

Simulation results showed a significant reduction in position and velocity noise and error measures by using minimum variance estimation. This method is described further in section 3.2.2.2 of this document.

As we stated earlier, report-to-track correlation, correction, and smoothing were essentially unchanged from the concepts used in the ARTS-III BTL system. However, in an attempt to obtain better turn following, a number of options were tried, the results of which showed no improvement in tracking performance. In the generating of turning tracks, we make the assumption that the target went into a maneuver a number of scans before the report actually fell out of the primary bin. Therefore, turning tracks are generated from a point projected back three scans from the unsuccessful predicted position, using the last corrected velocity of the track. An alternative method would be to save the smoothed position from scan n-3 for the generation of turning tracks. Computer results showed no improvement, and, in fact, a loss of performance, when compared with the results from back projecting.

One other experiment involved the generation of the predicted position after a turning trial had become a new normal track. In the baseline system, this occurs after two consecutive correlations in the turn bin. At the time of the second successful correlation, both the position and velocity are corrected, and the track is predicted straight ahead using the new smoothed velocity. Assuming that the target is still in a maneuver, the next report may fall outside the primary bin, and turning tracks would again have to be established. With the above assumption in mind, we predicted the target along its turning path for one more scan after it had correlated on two consecutive turning trials. Our results again showed no improvement in tracking performance.

A further description of this algorithm may be found in the document titled, "Expansion of the ARTS-III System to the Basic Radar Beacon Tracking Level System" March, 1971.

Figures E-4 through E-6 contain the performance measures of the baseline RBTL tracker following a non-discrete beacon target.

Figures E-7 through E-9 contain the performance measures of the optimized RBTL tracker following the same non-discrete beacon target.

E.3 (continued)

In figures E-4 through E-6, it can be seen that the addition of radar data within the BTL system results in a drop in the dispersion (noise) and error measures. The improved track accuracy results in better track reliability. Turns, although still well defined, peak out at a lower level showing increased primary bin tracking. Track following ability has increased by 12% at the highest data rates, when compared to the BTL measures, and by 47% at the lowest data rates.

Figures E-7 through E-9 show the optimized version of the RBTL tracker. The major changes include the increase in the range dimension of the report-to-report correlation bin and the use of minimum variance estimation for combining reports. The graphs show an increase in tracking accuracy (lowering of the performance measures), as well as a steadying out of the dispersion measures for both position and velocity. The peak values on turns are also reduced.

In addition to the tracking performance described above, the effect of target speed and maneuverability was also evaluated. From the results obtained, it is concluded that the Basic RBTL is optimized to operate as a straight line tracker which frequently uses the emergency search mode (turning tracks) to maintain target tracking. This is true for a large percentage of the maneuvers which are performed in the terminal area. Statistics gathered on the frequency of turn calling while following the "standard track" show that even under ideal data conditions (B/S = 100), the RBTL tracker relies on this emergency search mode to re-establish normal tracking on the average of 2 times per run (200 scans). Closer analysis shows that this loss of primary bin correlation and the establishment of trial tracks is associated primarily with turns in which the accelerations are ¼ g and greater, and which are not uncommon in the terminal area.

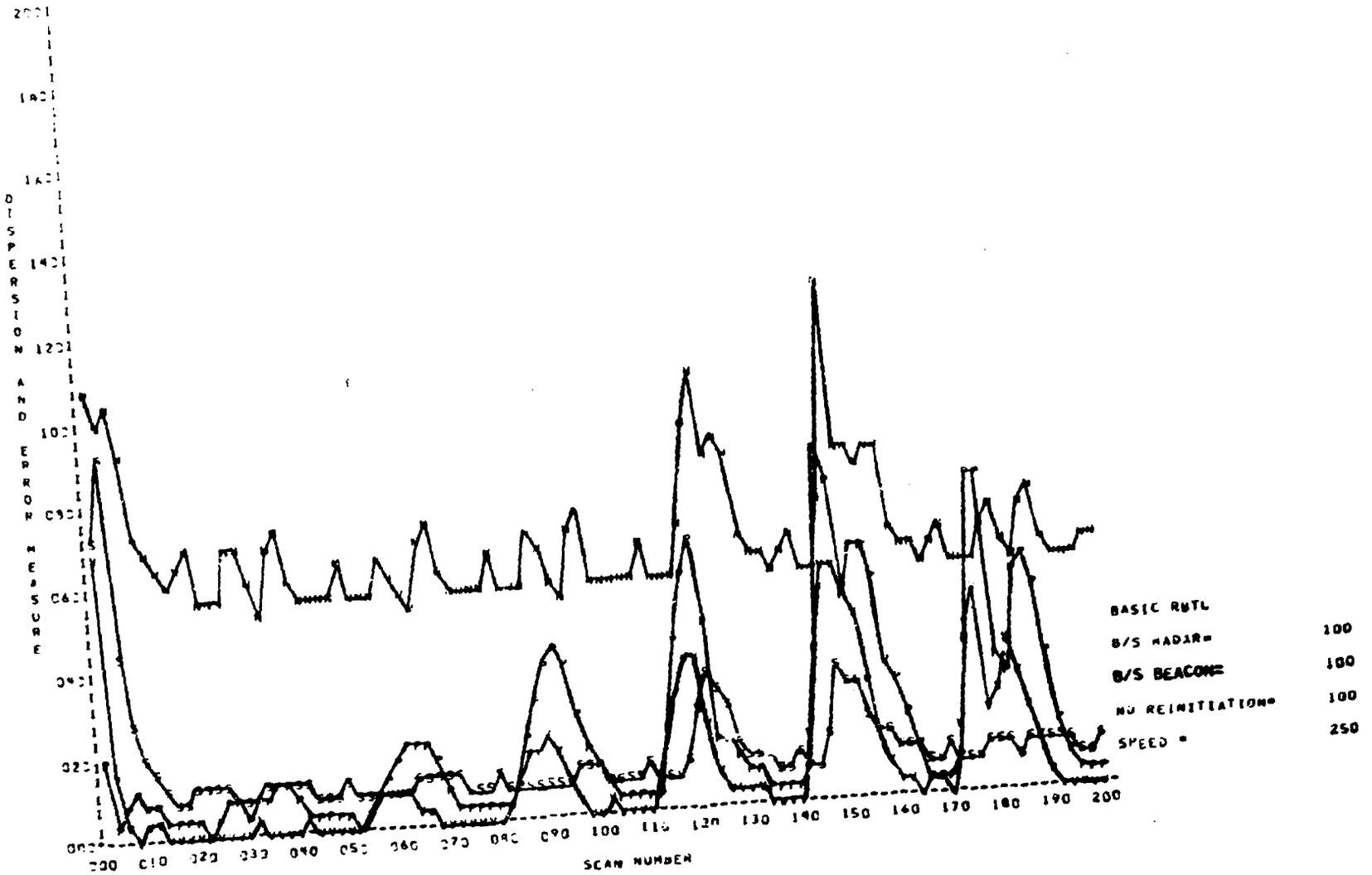

Figure E-4. Non-Discrete Beacon

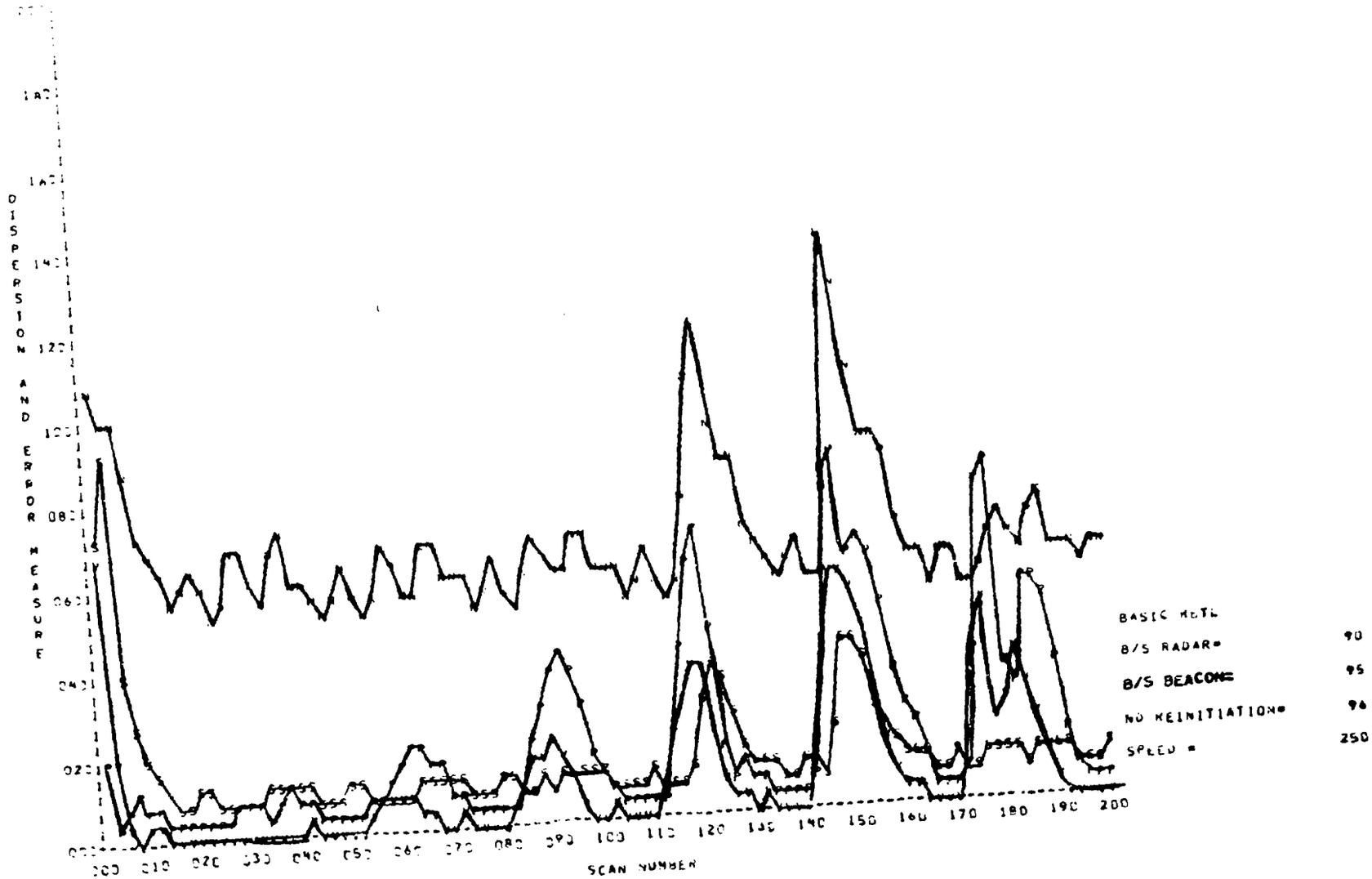

Figure E-5. Non-Discrete Beacon

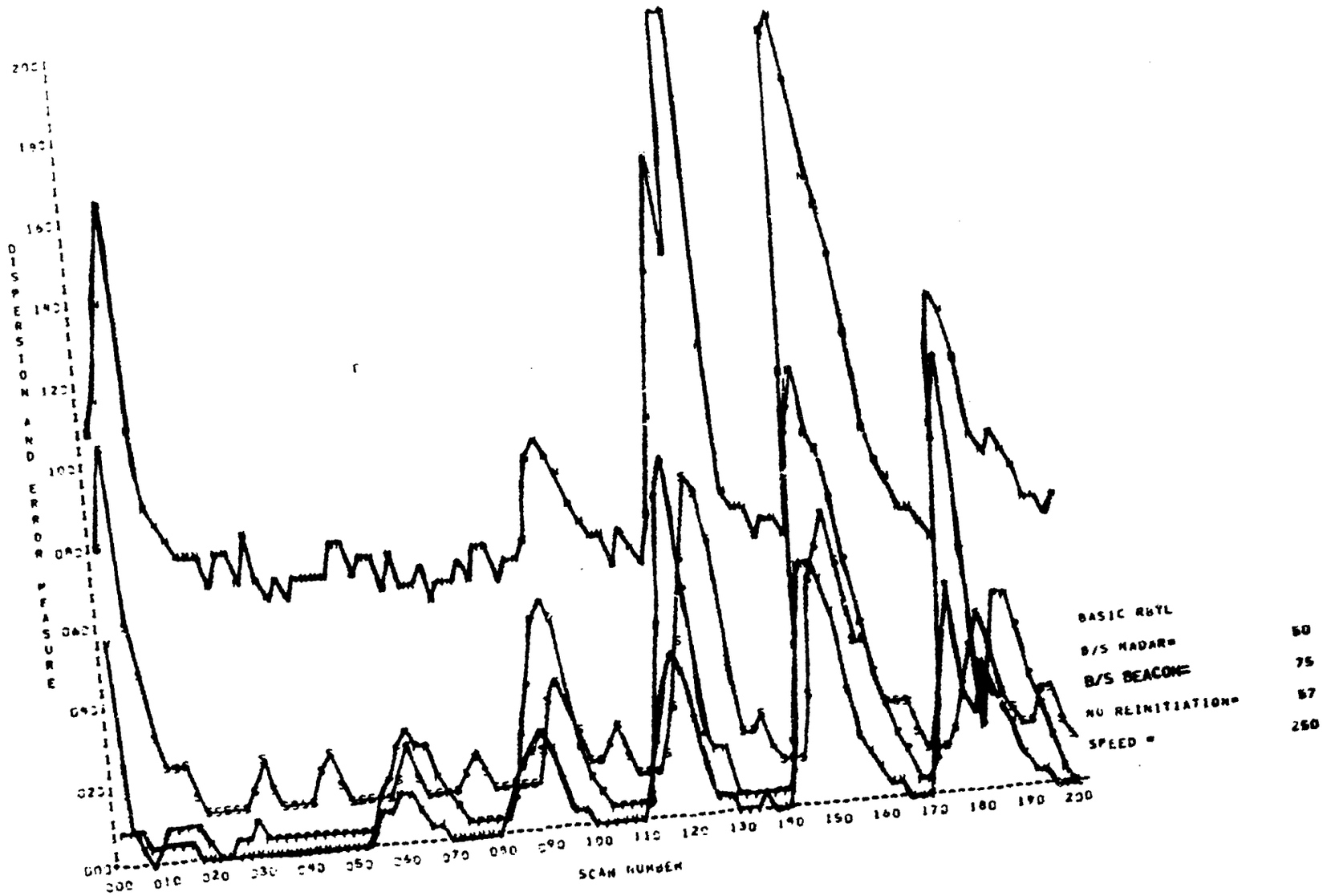

Figure E-6. Non-Discrete Beacon

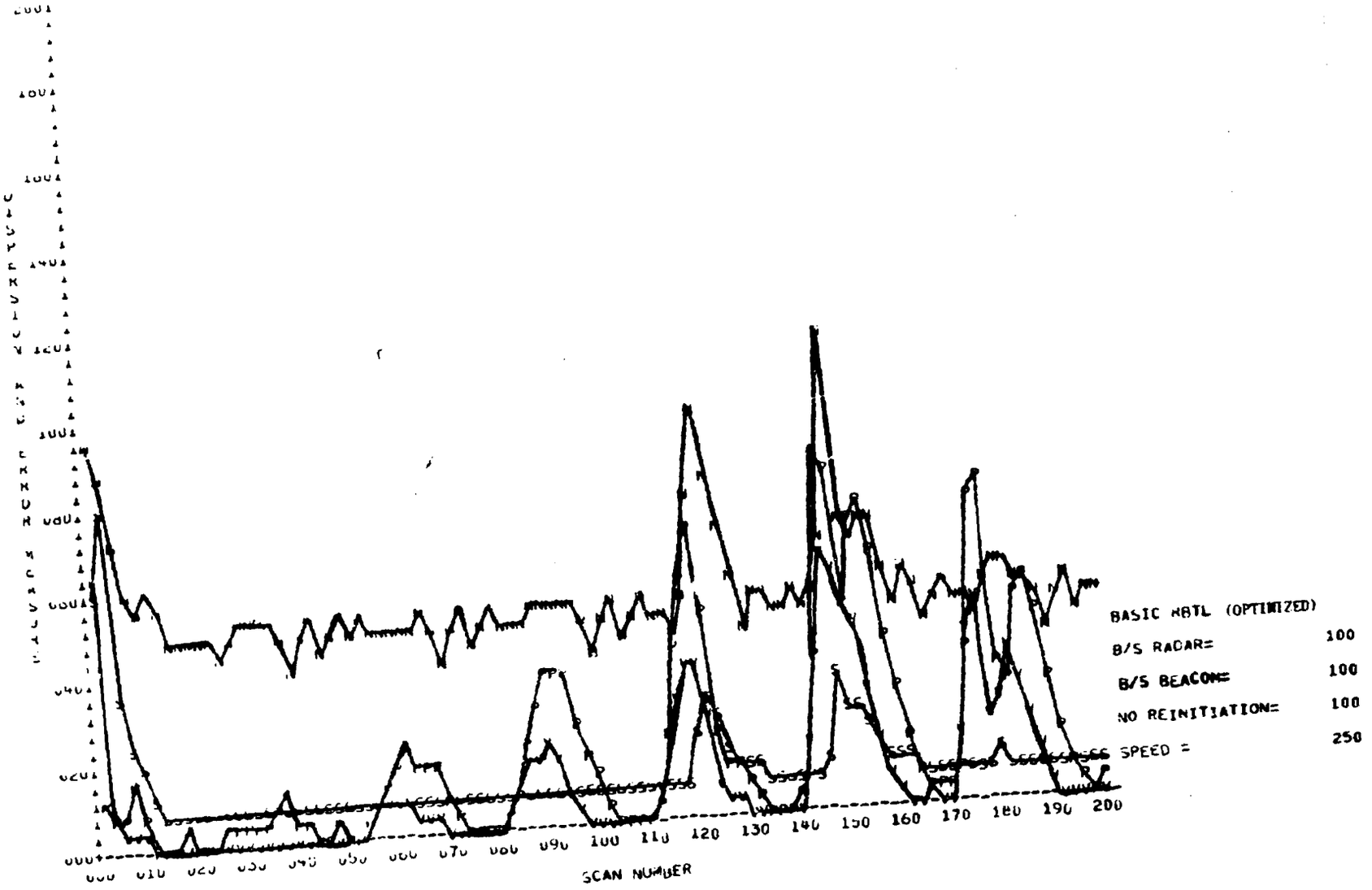

Figure E-7. Non-Discrete Beacon

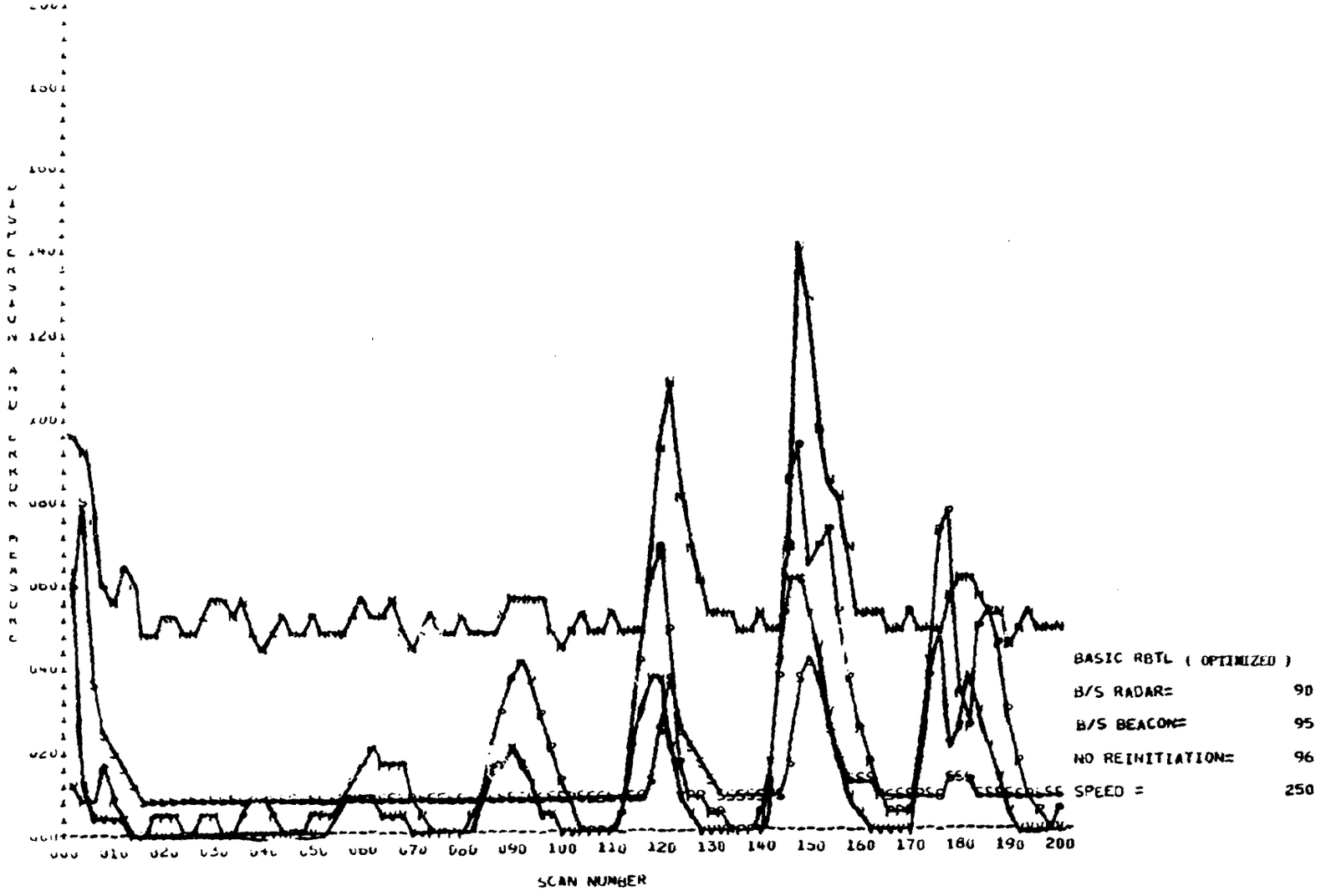

Figure E-8 . Non-Discrete Beacon

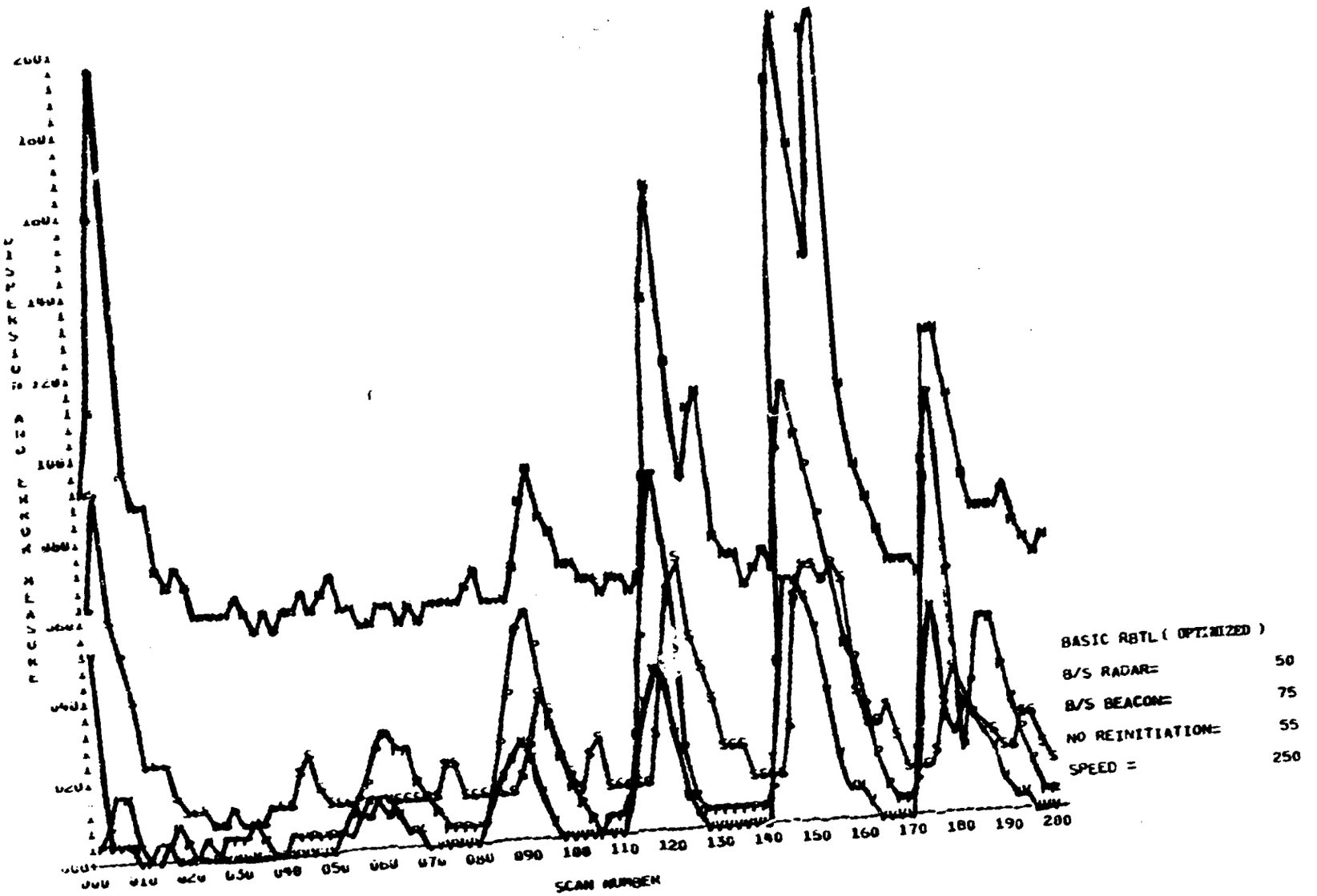

Figure E-9. Non-Discrete Beacon

E.4 AUGMENTED RADAR BEACON TRACKING LEVEL (RBTL) SYSTEM

The Augmented Tracking Level system is an expansion of the Basic RBTL system, incorporating those improved tracking techniques which the concept study showed to be most promising and which were verified by simulation. Perhaps the single most important feature of the augmented tracker is reflected in the concept of Track Oriented Smoothing (TOS). TOS basically involves smoothing in a rotated coordinate system, along the track's estimated direction, while preserving the use of ordinary X, Y coordinates for its implementation. The result is a tracker extremely adaptable to tracking in the terminal environment. Simulation analysis showed that by introducing track-oriented smoothing into the basic RBTL system, the need for secondary correlation logic was reduced, on the average, by 71%. This significant improvement in primary bin tracking results in the use of more of the available data and reduces the number of coasts and trial tracks to a minimum.

As the name implies, track-oriented smoothing orients the smoothing operations to the estimated track direction. This is motivated by the knowledge that aircraft normally move in such a way that transverse accelerations are larger than longitudinal accelerations, therefore inviting separate α, β smoothing along and across the track's direction. (See section 3.2.2.4 for a detailed description of the track-oriented smoothing equations.) Simulation showed that for track-oriented operations to function optimally, the firmness control, as described in the Basic RBTL Tracker, needed adjustment. This involved extending the maximum firmness to higher levels in order to provide somewhat smaller α, β values for longitudinal smoothing. The result was a separate running calculation of firmness in longitudinal and transverse directions for each track, with the limit on the longitudinal firmness higher than on the transverse firmness (computer results showed an optimum difference of +14). The result of the lower transverse firmness limit is a tracker that is more responsive to track maneuvers without having to rely on secondary turning logic.

In designing the augmented tracker, statistics were gathered for a number of methods of correlating radar and beacon reports representing the same target. As was stated earlier, the RBTL system performs report-to-report correlation by searching for a supporting radar report in a correlation bin centered on each beacon report prior to tracking. An alternative method which was tested did not perform pre-tracking report-to-report correlation, but rather passed along all radar and beacon reports to the tracking function. Each track was then checked for beacon reports in its primary bin and for each beacon report an intermediate smoothed position between the report and the predicted position was generated. The intermediate position was then used for centering the radar correlation bin. This method assumes the smoothed position to be the best estimate of the actual target position. A third option, and the one which we feel is most appropriate, makes use of pre-tracking report-to-report correlation followed by a second attempt in tracking to reinforce those beacons which failed to correlate initially, through the use of the intermediate radar search position. This process is recommended because the extra processing time

required to perform intermediate smoothing for each beacon to track pair has now been limited to those 8-10% of the beacon reports which failed pre-tracking report-to-report correlation. Also, no extra logic is needed to reinforce secondary reports or reports going through track initiation.

The table shown below lists the various options and their performance as measured via simulation.

Correlation Logic	Percent of time Beacon and Radar Reinforced
Pre-Tracking Report-to-Report 1/16 nm range gates	62%
Pre-Tracking Report-to-Report 1/8 nm range gate	90%
In-Tracking logic using an Intermediate Search Position	90.7%
Pre-Tracking Report-to-Report with an In-Track Intermediate Search for those not correlating initially	94.7%

In the area of report-to-track association, the augmented tracker has carried the decision process further than that found in the Basic RBTL tracker. The first step in maintaining successful primary bin association involves the use of quality scores. Each report in the primary bin of a given track is assigned a score based upon its RBC, code and altitude validity, report quality, radar reinforcement, and its relationship to the track's history data. During the first pass of a two pass system, tracking attempts to select the correct report for a given track on the qualifying score alone. If, on the first pass, the score alone cannot resolve an ambiguous situation (e.g., more than one valid report in the track's bin with equal scores), the track is flagged for second pass processing. If, after second pass processing, an ambiguous situation still exists, deviation scoring is used to select the correct report. The deviation score is the distance between the track's predicted position and the reported position of the beacon and/or radar report. Deviation scoring was incorporated under the assumption that the generalized nearest fit will produce near-optimum solutions to the associated problem. Simulation results have indicated that deviation scoring should be looked at more closely under live environment conditions. It is also recommended that deviation scoring be used only when:

1) The primary bin contains more than one valid report and none of them is in the primary bin of another track. (1 track and more than one report).

E.4 (continued)

2) The primary bin contains one valid report, and this report is the only valid report for one or more other tracks' (1 report and more than one track).

To increase the tracker's response to data changes, a form of deviation controlled smoothing was introduced into the simulation model. Deviation control calls for the immediate establishment of a trial track when primary correlation fails and it is determined that a report lying in the track's secondary bin is the report associated with the track. This report is smoothed using a higher α, β value during one update period. This allows for a faster response in tracking on turns and eliminates the need for establishing two turning tracks on the first scan if primary correlation fails. It should be noted that this immediate response results only in the establishment of a trial mode and does not effect the parent tracks' history data until the trial track has successfully correlated for two consecutive scans. Where the immediate detection of a possible turn cannot be made, turning tracks are created and processed as described in the Basic RBTL. Simulation results using deviation controlled smoothing have shown no loss of tracking performance when compared to the turning track method employed in the RBTL Tracker. However, results do indicate that a velocity filter may be needed to determine optimum smoothing parameters for various speeds of tracks (particularly high speed targets).

Simulation has also shown that although the Basic RBTL correlation bins may be too restrictive, the improved primary bin tracking obtained through the use of track-oriented smoothing works very well with the bin sizes specified in the Basic RBTL. In fact, a reduction in bin sizes, possibly as much as 10%, may be tolerated with little change in track performance. This would particularly apply to radar only tracks. It is important to note that the Basic RBTL tracker was designed for straight line tracking and to rely heavily on its turning logic for maintaining track on maneuvering aircraft.

Our simulation model was also used to look at a number of missing data sequences. In no case did we find any noticeable improvement in track performance.

Figures E-10 through E-12 contain the performance measures of TOS with Basic RBTL secondary logic for maneuver detection following a non-discrete beacon target. In this configuration, the complete RBTL correlation logic is retained and only the track smoothing algorithm is replaced. In comparing this with the performance of the Basic RBTL tracker (Figures E-4 through E-9), it can be seen immediately that both the dispersion and error measures are signficantly reduced. The position dispersion (N) and the velocity dispersion (S) are nearly constant, with no large increases during maneuvers. For runs with high data rates, tracking is almost entirely confined to the primary bin (98% of the runs did not require turning logic).

E.4 (continued)

The performance shown here represents a λ value in the range of 0.02 - 0.05, which corresponds to the class of targets most generally found in the terminal area. A number of runs were also performed using other λ values and a variety of track classes. This analysis showed that by assigning appropriate λ values to describe the maneuverability of various track classes, consistent tracking can be maintained. In addition, this analysis showed that the Basic RBTL tracker is designed to operate optimally on that track class described by a λ value of .005, which represents light maneuvers or basically straight line tracks. This agrees with the analysis described in the preceeding section E.3, which showed the RBTL tracker relying heavily on turn calling logic.

Figures E-13 through E-15 contain the performance measures of track-oriented smoothing with deviation control secondary logic following a non-discrete beacon target. In this configuration, the turning logic as described in section E.2 (two trial tracks) is completely replaced with the deviation control smoothing method. This method shows no loss in track accuracy at the higher data rates, and at low data rates, track reliability is actually improved by about 17% over the Basic RBTL type turning logic. In addition, the logic required to process a turning track is greatly reduced, as is the requirement for devoting computer memory to the extra trial track. A number of α and β values were evaluated to determine optimum deviation smoothing. A range of optimum values between .25 and .75 for α and β are recommended for various classes of tracks.

Figures E-16 through E-18 contain the performance measures of the Augmented Tracking system using Report-to-Track correlation (no pre-tracking report-to-report correlation) following a non-discrete beacon target. The Augmented Tracking system refers to that system configuration which combines track-oriented smoothing and deviation control secondary logic, as described above, while retaining the Basic RBTL method of turning logic when deviation control encounters ambiguity. These figures show that as data rates decrease, report-to-track correlation of beacon/radar pairs adversely affects both track accuracies and reliabilities when compared with the pre-tracking correlation methods used previously. This is especially true in the areas of initialization and higher maneuvers. In these areas, the accuracies of the predicted position are suspect and do not provide a reliable estimate (after the initial smoothing) for positioning the radar search bin. This is seen in the erratic behavior of the performance measures during start-up and the higher turn rates.

The final system configuration whose performance is shown in Figures E-19 through E-21 combines those features of Basic RBTL which have been proved effective with those features addressed in this section as improved

E.4 (continued)

techniques. The basic structure of this Augmented Tracking System includes the following methods:

1) Track-oriented smoothing.

2) Pre-tracking report-to-report correlation.

3) Report-to-track correlation for those beacon reports which are not radar reinforced following the initial correlation attempt.

4) Deviation controlled smoothing.

5) Turning trial tracks as defined for the Basic RBTL system when deviation controlled smoothing is unsuccessful.

6) Minimum variance estimation for combining beacon/radar pairs.

7) Quality scoring and deviation scoring to resolve correlation ambiguities.

8) Cross referencing of each eligible report and track combination.

These combined features show an improved tracking system which maintains a high degree of both accuracy and reliability even under extremely adverse data conditions. (93% tracking continuity at low blip/scan rates). It is recommeded that these features be further optimized and combined within the Augmented Radar Beacon Tracking Level system design, and evaluated as an operational system.

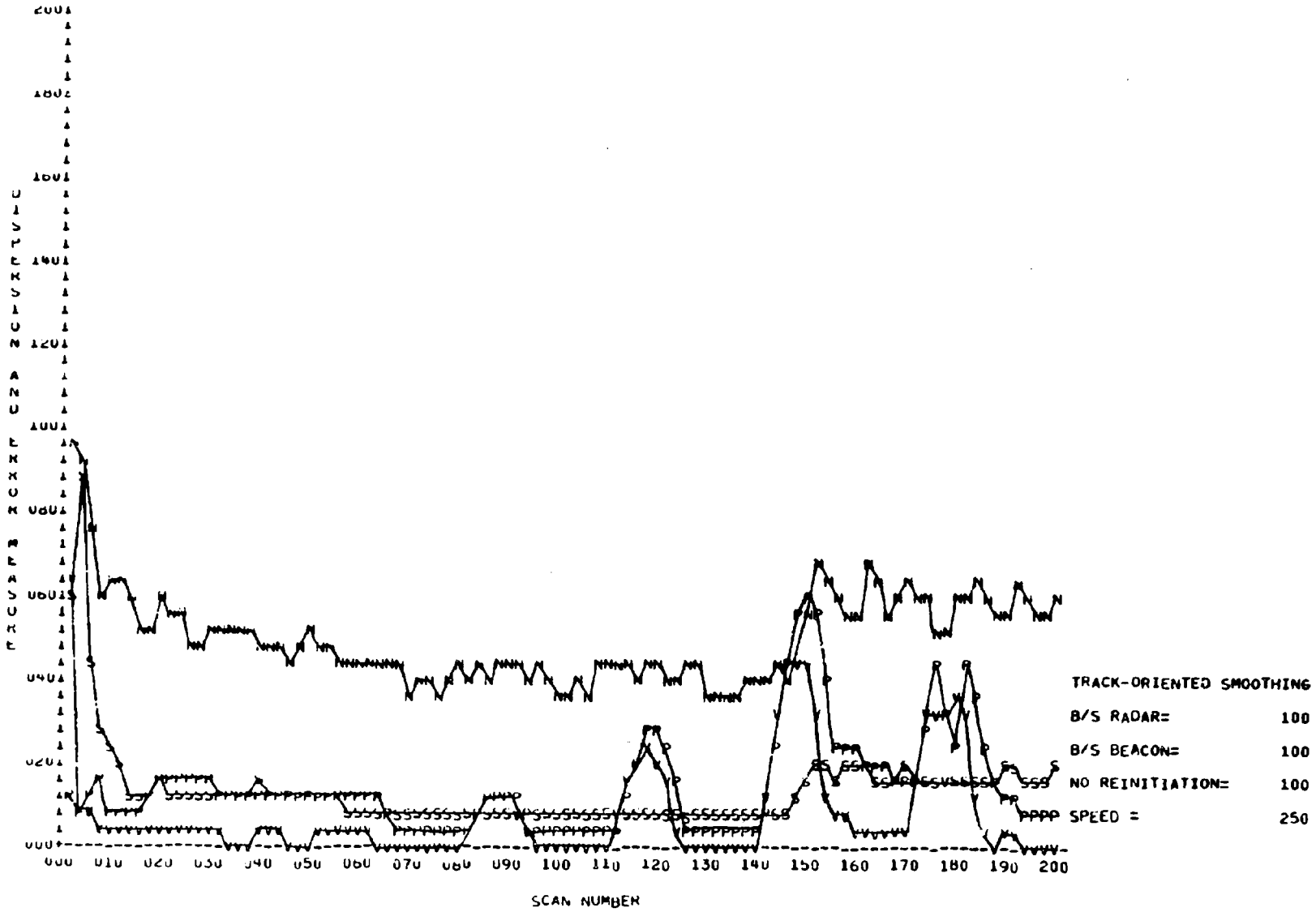

Figure E-10. Non-Discrete Beacon

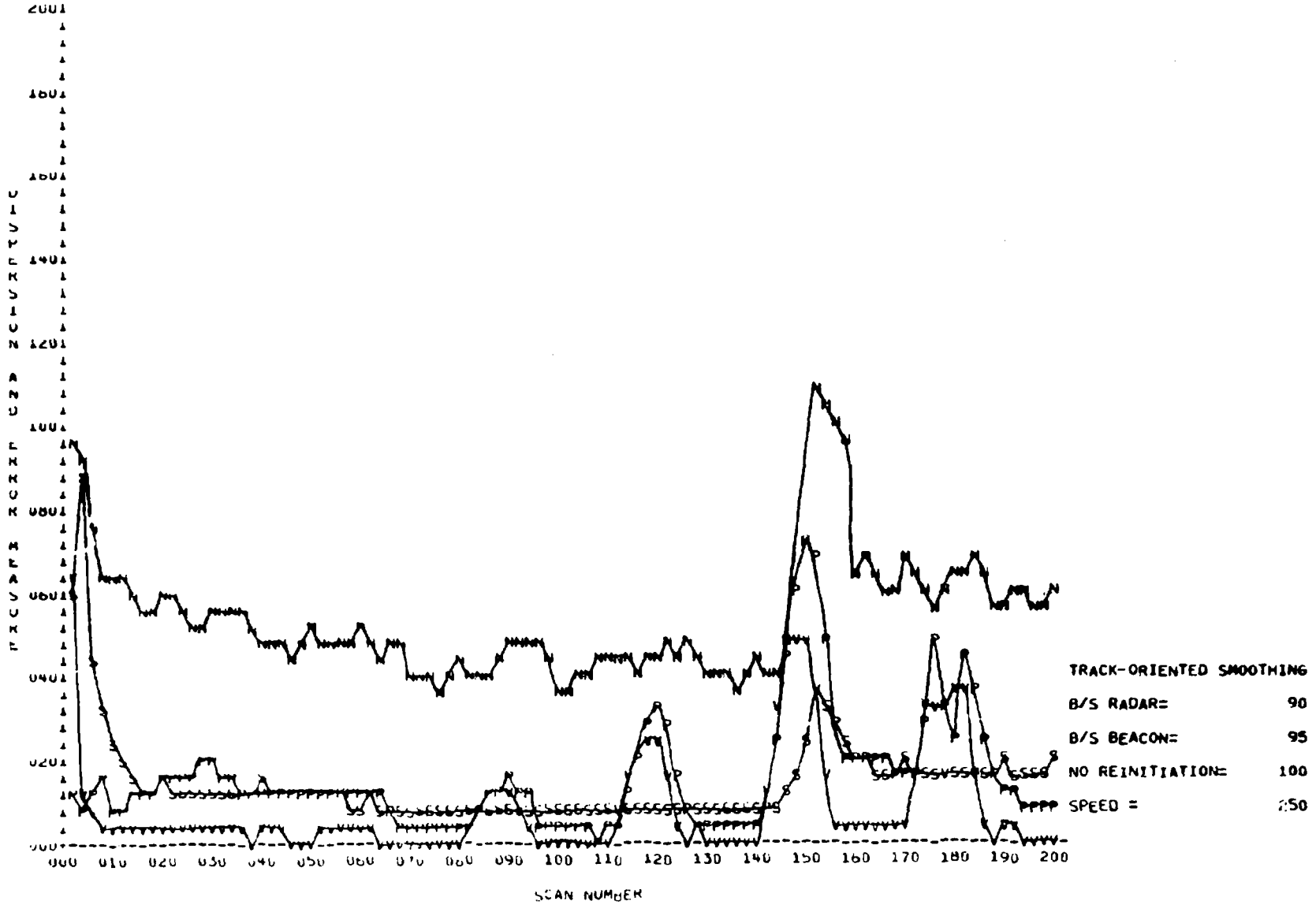

Figure E-11. Non-Discrete Beacon

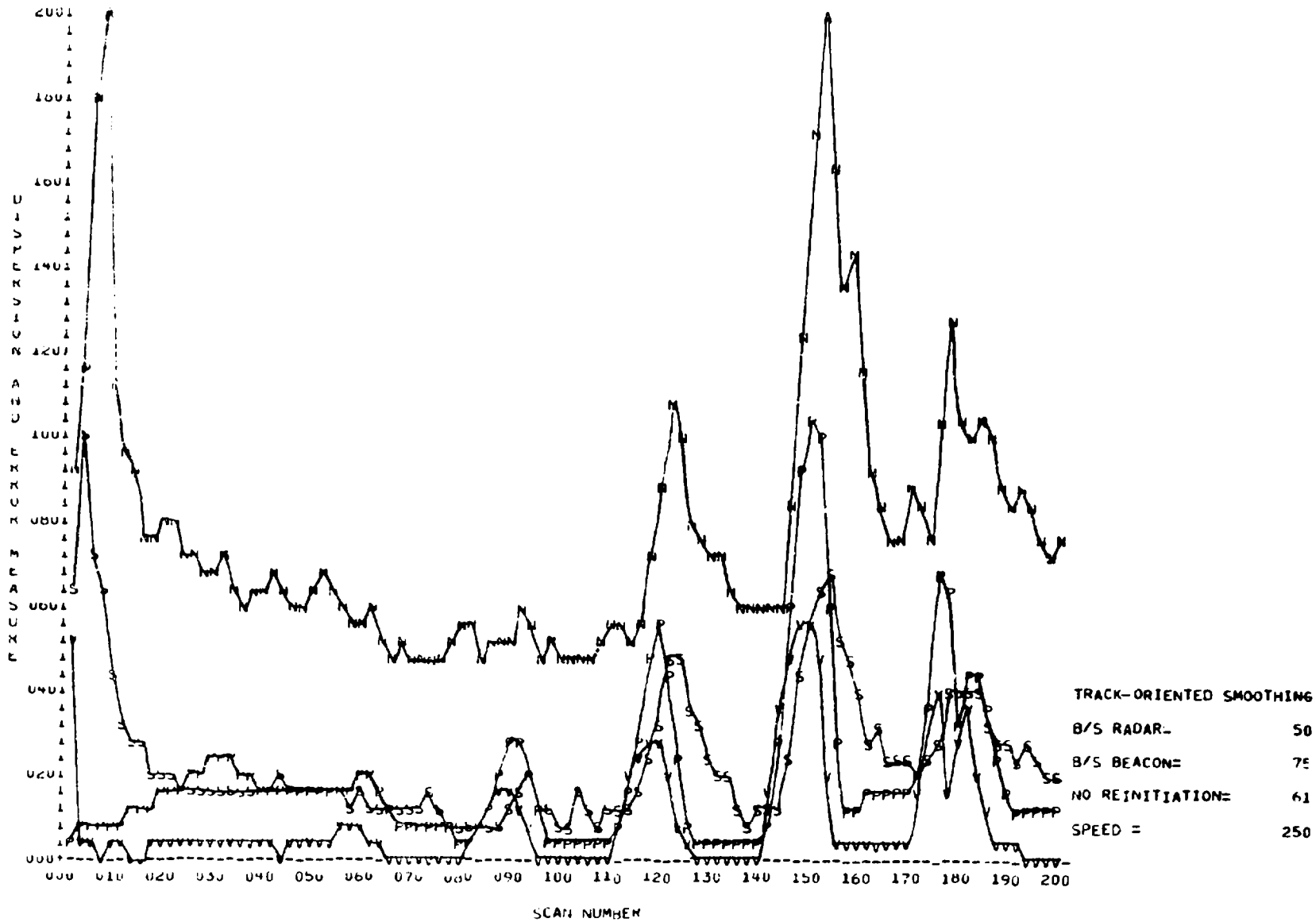

Figure E-12. Non-Discrete Beacon

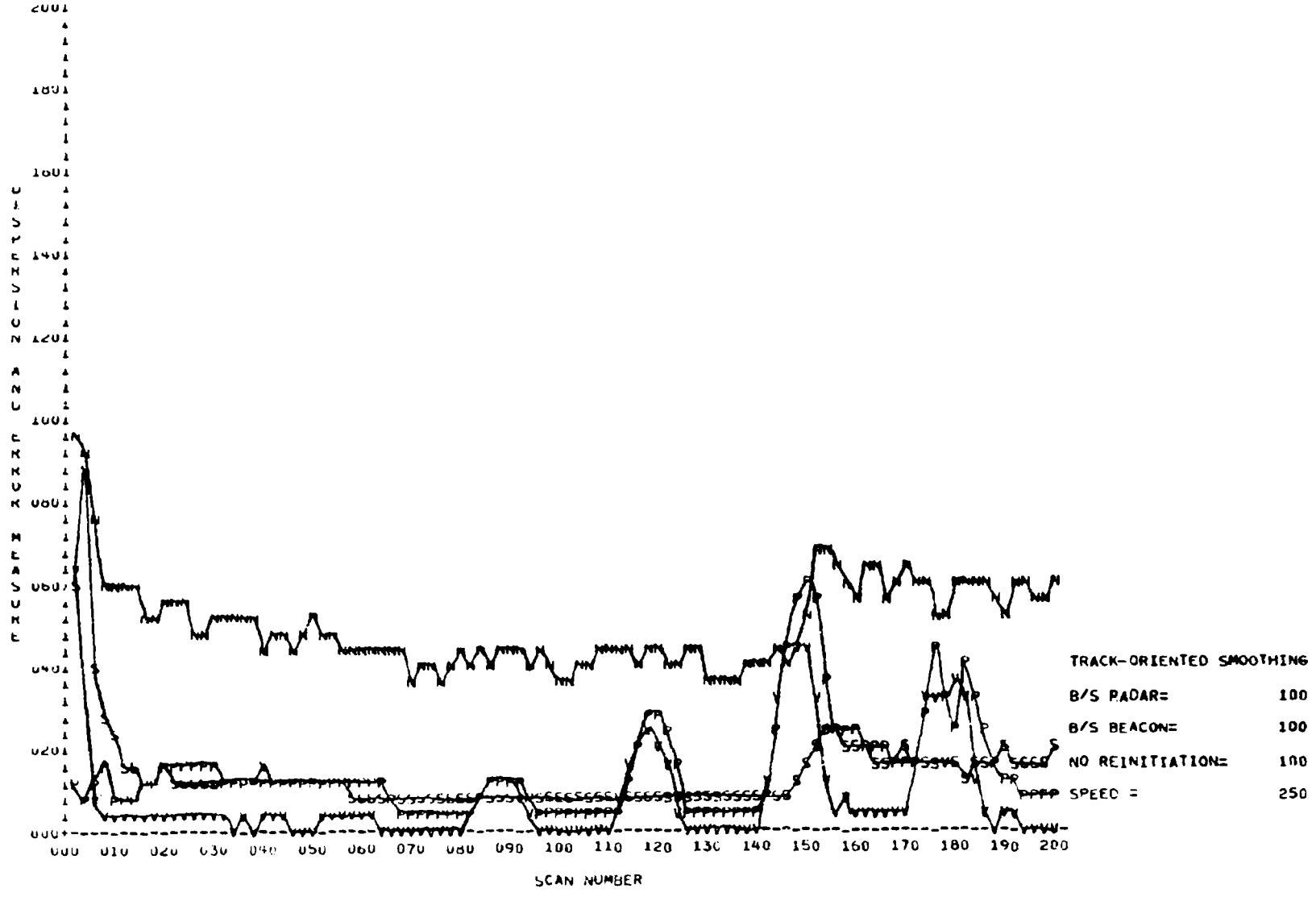

Figure E-13. Non-Discrete Beacon

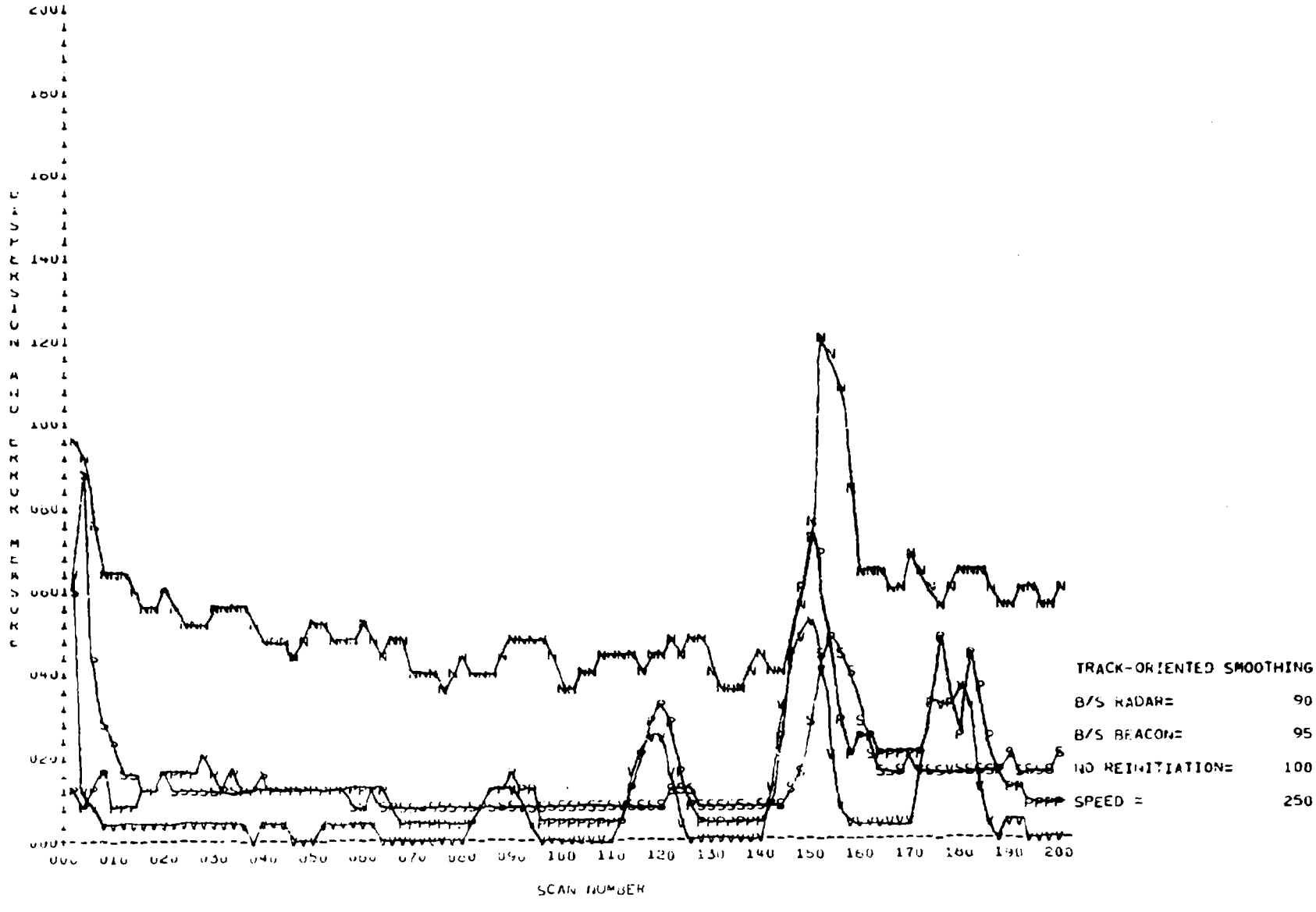

Figure E-14. Non-Discrete Beacon

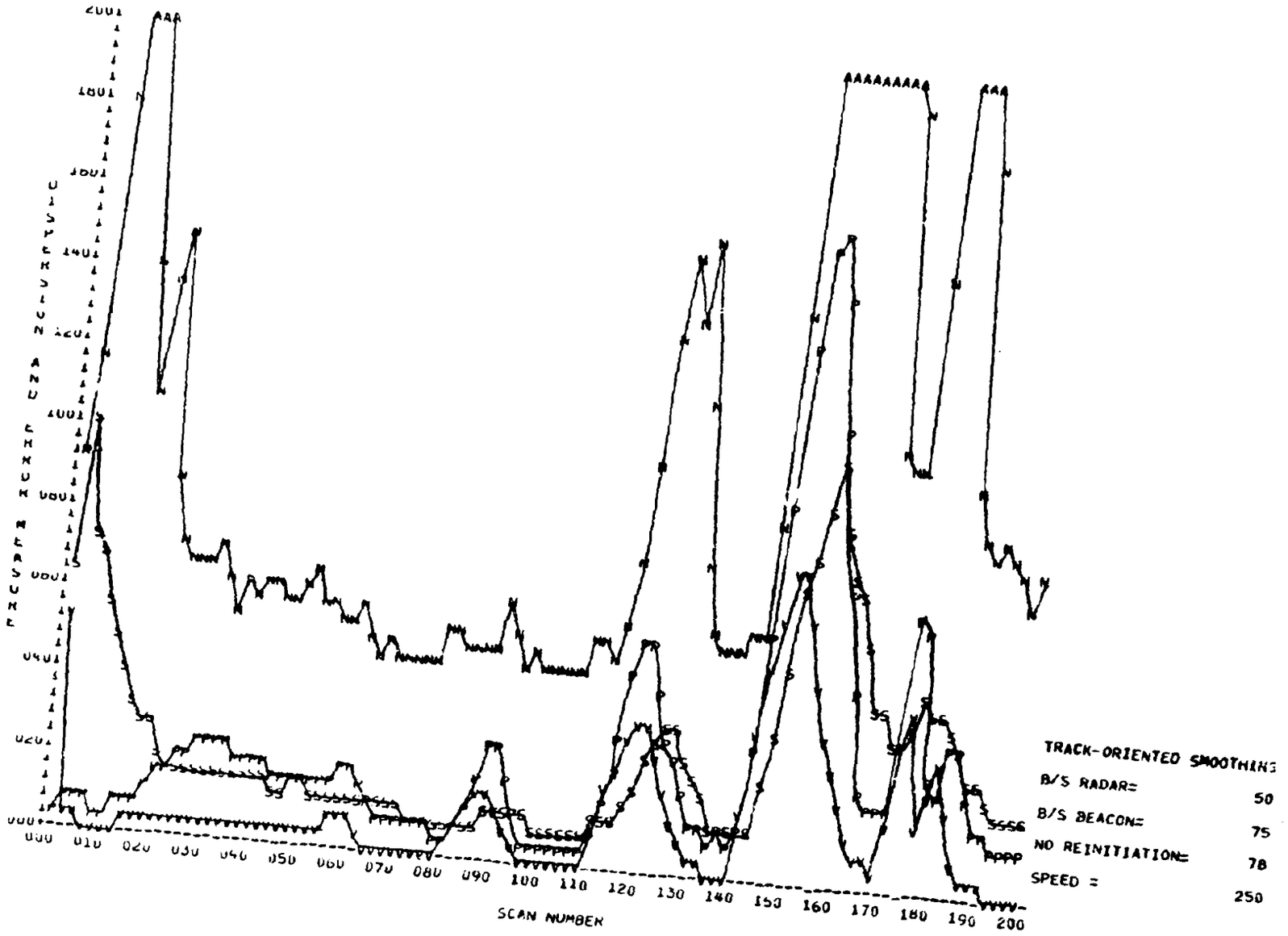

Figure E-15. Non-Discrete Beacon

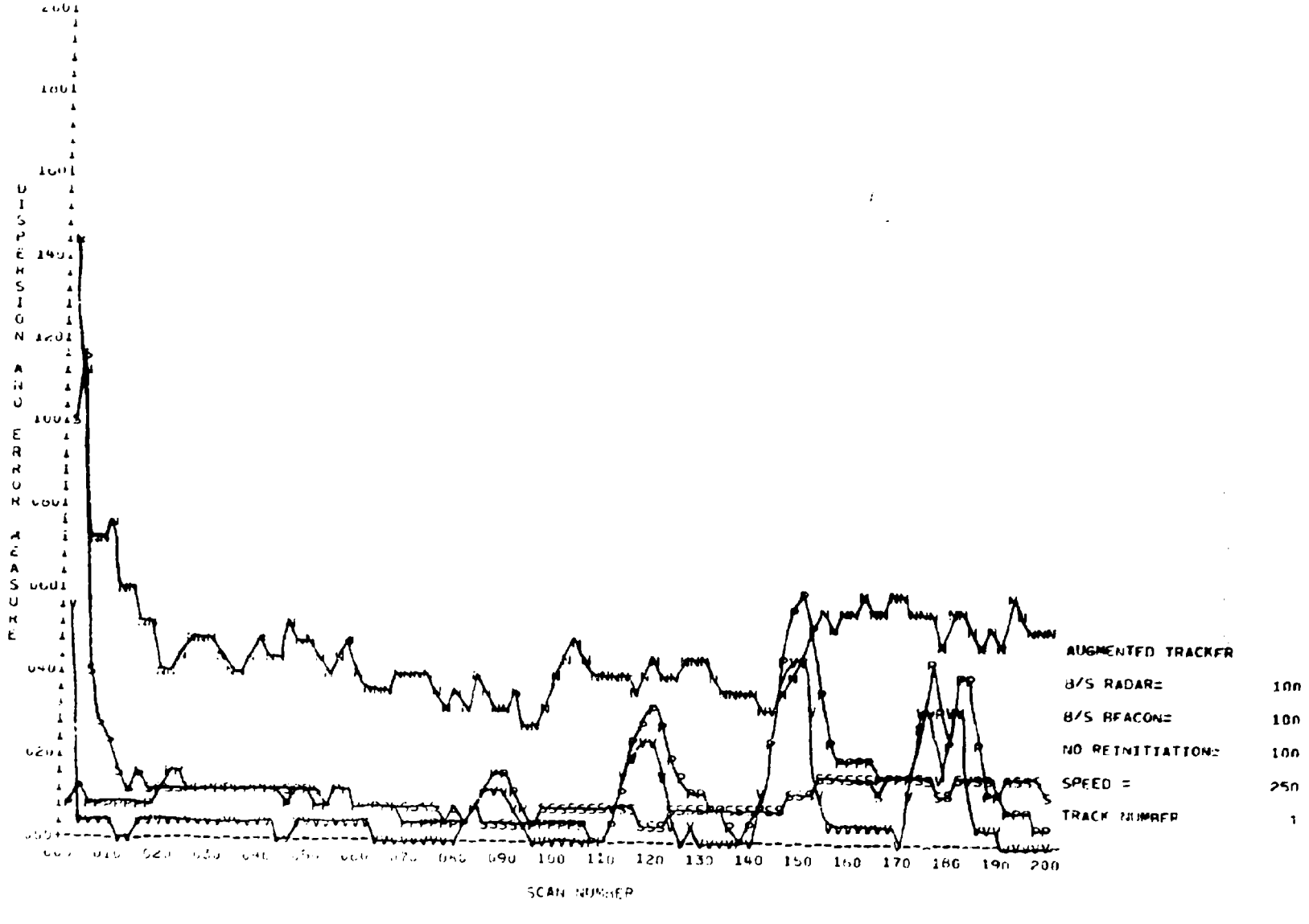

Figure E-16. Non-Discrete Beacon

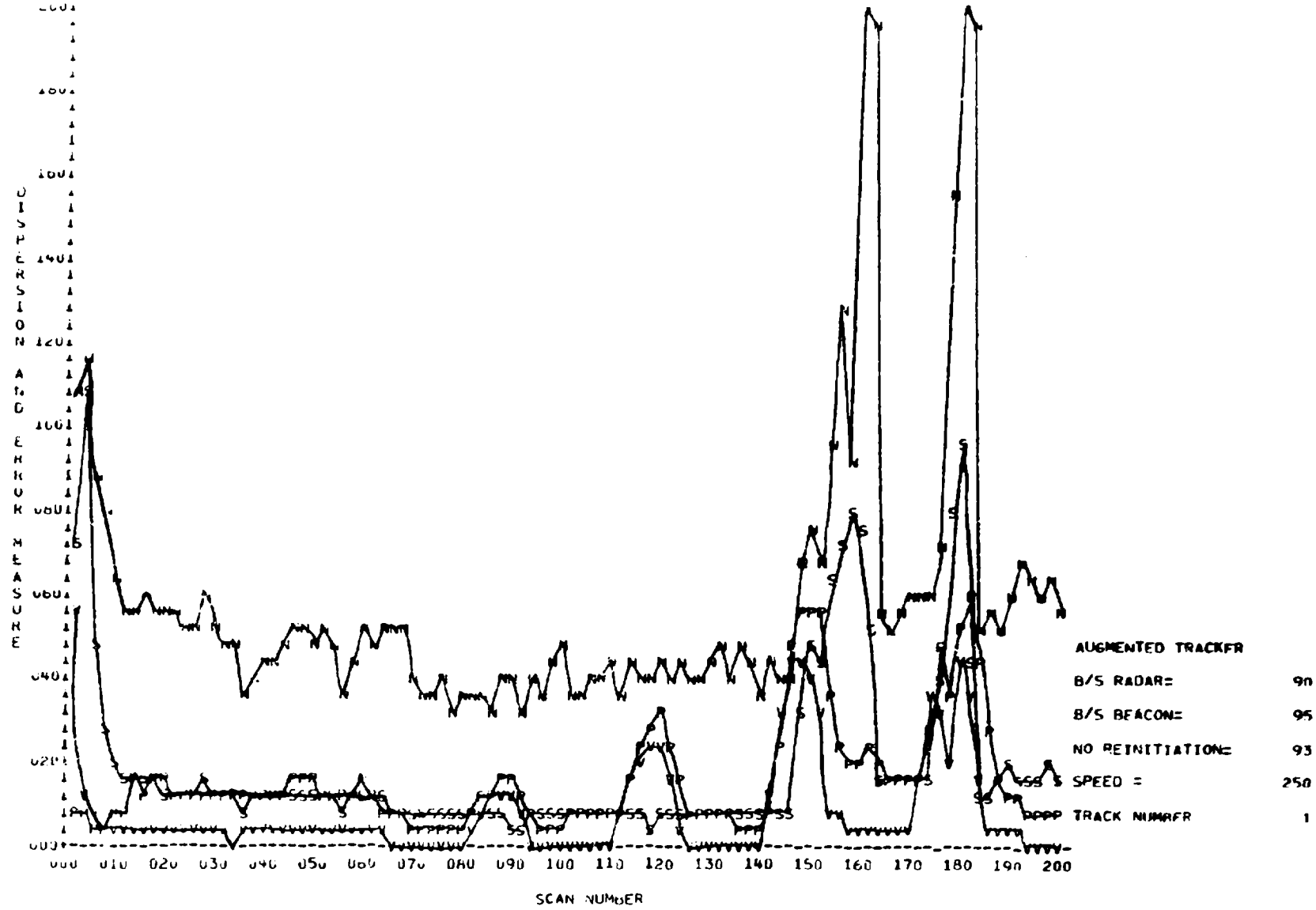

Figure E-17. Non-Discrete Beacon

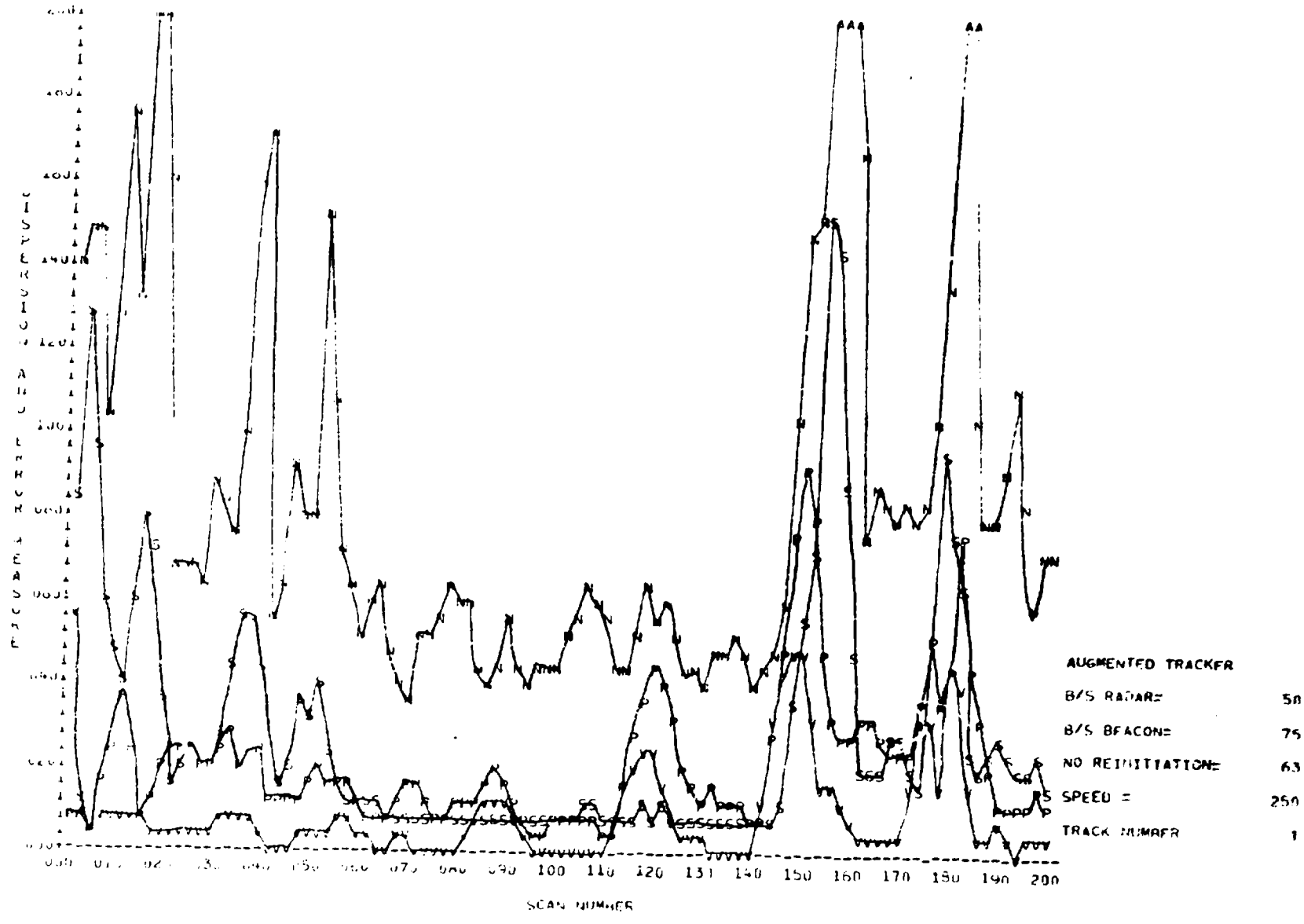

Figure E-18. Non-Discrete Beacon

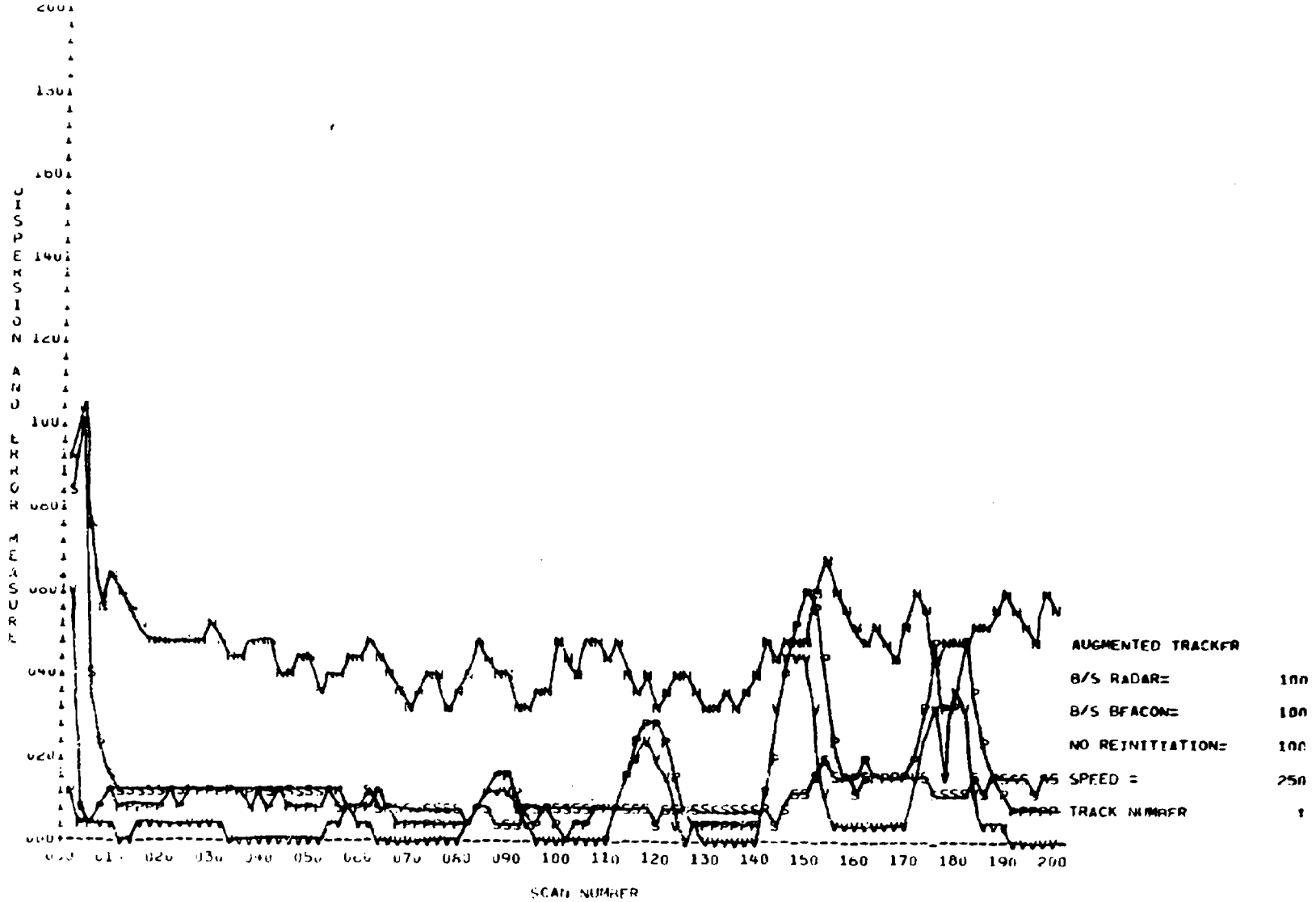

Figure E-19. Non-Discrete Beacon

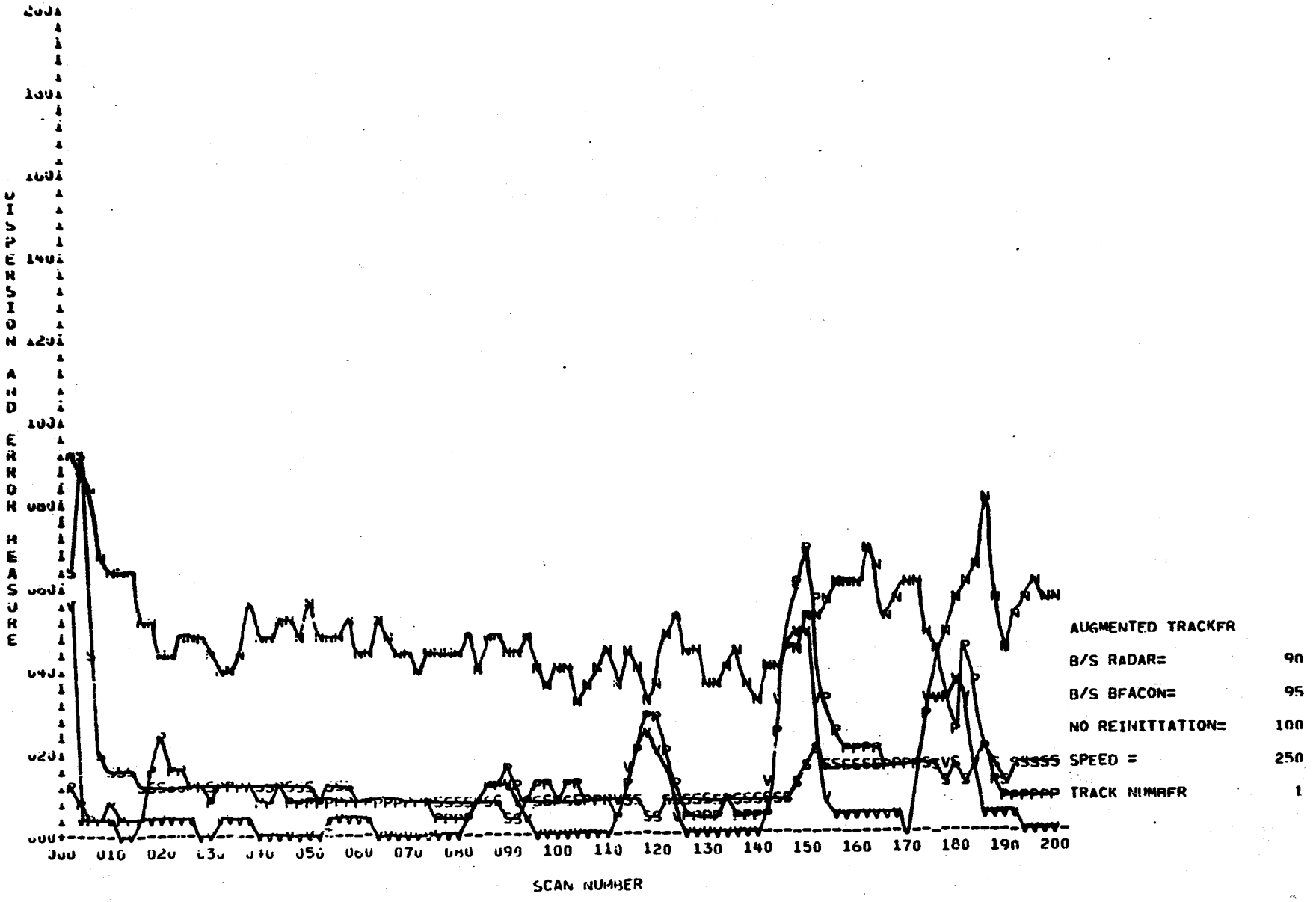

Figure E-20. Non-Discrete Beacon

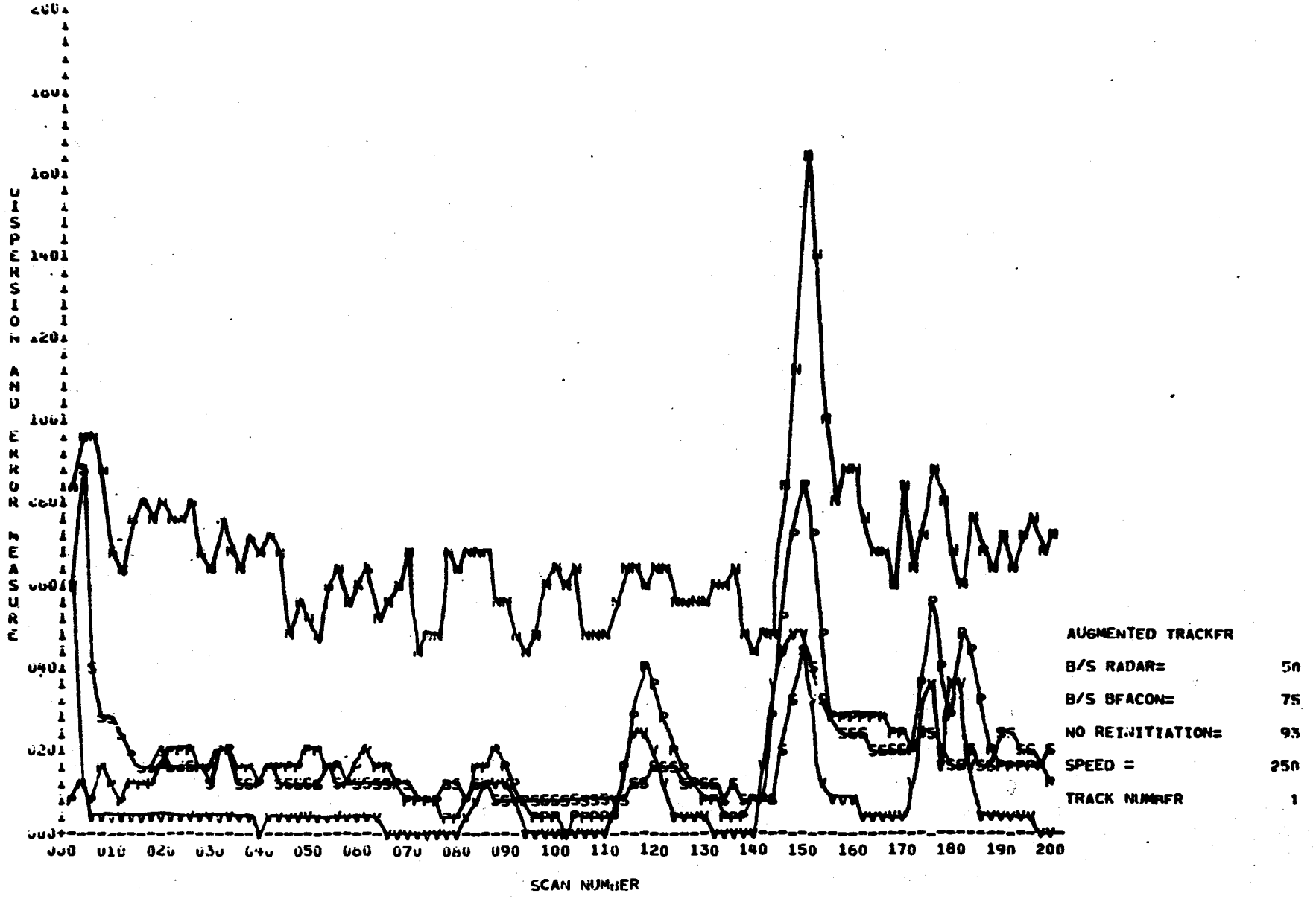

Figure E-21. Non-Discrete Beacon